Risk-Modeling Tools for Designing Resilient Micro Energy Grids

by

Yahya Koraz

A thesis submitted to the
School of Graduate and Postdoctoral Studies in partial
fulfillment of the requirements for the degree of

Doctor of Philosophy

In
Electrical and Computer Engineering
Faculty of Engineering and Applied Sciences
University of Ontario Institute of Technology
Oshawa, Ontario, Canada
March 2019

THESIS EXAMINATION INFORMATION

Submitted by: Yahya Koraz

Doctor of Philosophy in Electrical and Computer Engineering

Thesis title: Risk-Modeling Tools for Designing Resilient Micro Energy Grids

An oral defense of this thesis took place on January 14, 2019 in front of the following examining committee:

Examining Committee:

Chair of Examining Committee	Walid Morsi Ibrahim
Research Supervisor	Min Dong (Nominal)
Examining Committee Member	Tarlochan Sidhu
Examining Committee Member	Mohamed Youssef
University Examiner	Ibrahim Dincer
External Examiner	Kankar Bhattacharya, University of Waterloo

The above committee determined that the thesis is acceptable in form and content and that a satisfactory knowledge of the field covered by the thesis was demonstrated by the candidate during an oral examination. A signed copy of the Certificate of Approval is available from the School of Graduate and Postdoctoral Studies.

Abstract

Micro energy grid (MEG) is widely used to meet the combined electricity, heating, cooling and natural gas demands for numerous customers' types. Design of MEGs were extensively introduced in numerous articles, however safety analysis methods for MEG design are not existing so far. This study develops a hazard and operability (HAZOP) matrix for MEGs by proposing a resilience matrix (RM). In addition, it proposes two advanced risk-modeling approaches, namely fault tree and layer of resilience analysis (LORA), for risk and resilience analysis of MEG. Selected independent resilience layers (IRLs) were proposed to achieve a resilient MEG by increasing safety integrity level (SIL).

IRLs are applied using co-generation and thermal energy storage (TES) technologies to mitigate the hazards of system failure, increase efficiency, and minimize greenhouse gas emissions. The proposed risk assessment approach aims to design a resilient MEG that has the ability to deal with those potentials efficiently. In addition, an energy risk analysis has been applied to each MEG's physical domains such as electrical, thermal, mechanical and chemical. These concurrent objectives lead to achieving higher resilience, fewer greenhouse gases emissions, and greater sustains economy.

A multi-level hierarchical decision making (MLHDM) is one of the IRLs that are proposed in this study. It aims to boost the MEG's self-healing features on risks uncertainty of the system operation. The structural design of MLHDM consists of three concurrent levels functioning together to achieve a resilient operation. The simulation results of the proposed resilient MEG infrastructure that combine a selected group of IRLs, shows the ability to work with high level of self-healing capability under various hazardous scenarios as well as meeting the on-demand energy requirement.

On the other hand, intelligent reasoning algorithms using Bayesian belief network (BBN) are proposed to accurately and instantaneously estimate risks in MEG. The offered BBN based monitoring/alarm system is one of the IRLs that are proposed in this study for a resilient MEG design. This study introduces a hybrid-safety assessment approach for MEG diagnosis by using a combination of ANFIS and BBN techniques.

The approach enables measuring the MEG's condition using fault diagnosis assessment by means of a hybrid BBN and ANFIS based model. The BBN is capable to form a consistent function of MEG's uncertainty based on experts' contribution more than the data from measurement instruments (I&Cs). The proposed method shows a capability to predict the source(s) of failure by using fault-assessment computation process for the observed symptoms.

Finally, the methods and data that were proposed and used in this research are validated by using three main types of validation namely validation of MEG simulation, validation of LORA and validation of BBN. The validation results of the proposed safety analysis tools reveal promising solution for designing resilient MEG.

Keywords: Micro Energy Grid, Risk-modeling, Risk Analysis, Fault Diagnosis and Prognosis, Layer of Resilience Analysis

Declaration

This thesis is a demonstration of my own research work. All possible means and efforts were made to indicate contributions of others whenever involved in the context of this thesis. This was done by reference to the literature, and acknowledgment of collaborative research and discussions. The work was done under the guidance of the supervisory committee namely Prof. Tarlochan Sidhu, Prof. Min Dong and Prof. Mohamed Youssef, at the Faculty of Engineering and Applied Science, University of Ontario Institute of Technology, Oshawa, Canada.

Acknowledgments

I would like to express my sincere appreciation to my supervisory committee, Prof. Tarlochan Sidhu and Prof. Min Dong and Dr. Mohamed Youssef, for their encouragement, direction and support throughout my doctoral study. In addition, I would like to thank all my colleagues at the Faculty of Engineering and Applied Science (FEAS) for their support in many ways. Also, I take this opportunity to record my sincere thanks to all the faculty members and staff of the Department of Electrical and Computer Engineering - UOIT for providing me with resources. Above all, I would like to express my appreciation to my family and closest friends for their love, perpetual support and honorable commitment to my education.

Yahya Koraz

Table of Contents

List of Figures

List of Tables

Nomenclature

Symbol	Definition	Units
A_i	The ability for failure avoidance	N/A
A_{xs}	Tank cross-sectional area	m^2
C_i	Class hazard event likelihood	N/A
COP	*Coefficient of Performance*	N/A
C_p	Storage fluid heat capacity	J/K
C_{tp}	Specific heat of products of combustion	$Btu/lb_m{}^oF$
e	HRSG effectiveness	N/A
$E[x]$	Quantifying Risk	N/A
f	Fuel	m^3
F_i	Frequency	N/A
$F(t)$	The probability of failure on demand	*f/yr*
f_n	LOPA	*f/yr*
H_l	Hazard level	N/A
h_{saf}	Saturated liquid enthalpy in steam drum	kJ/kg
h_{sh}	Enthalpy of steam leaving superheater	kJ/kg
K	A constant for calibration purpose	N/A
L	A factor to account radiation and other losses= 0.985	N/A
N	Speed	rpm
P	Pressure	Pa
p_i	Probability density	N/A
$p(v,w)$	Joint probability	*f/yr*
P_{in}	Power input to MEG	kW
ρ	Density	kgm-3
P	Tanks perimeter	m
p(v|w)	Conditional probability	*f/yr*
pow	Power	*kW*
r	A constant variable	N/A
R	Reliability	N/A
S_i	The consequence severity of the hazard event	N/A
τ	Torque	Nm
T	Time	s
T_m	Temperature	K
T_1	Gas temperature afterburner	^oF
T_3	Saturation temperature in steam drum	^oF
U	Tank fluid to ambient overall heat transfer coefficient	$Btu/(ft^2\ h\ {}^oF)$
V	Random event	N/A

W	Random event	N/A
W_m	Mass flow rate	kgs-1
w_i	Weight of importance (0-1)	N/A
W_s	Steam flow rate	lb/hr
W_g	Exhaust flow rate to HRSG	lb/hr
x_i	Random variable for severity consequence	N/A
σ	Pressure loss coefficient	N/A
η	Efficiency	N/A
ρ	Storage fluid density	kg/m^3
Δx	Length of node	m
$\dot{m}$	Mass flow rate	Kg/s
$\lambda(t)$	Failure Rate	*f/yr*

List of Abbreviations

AC	Alternating current, an electric current that reverses its direction many times a second at regular intervals
Availability	The likelihood that a system or equipment will operate satisfactorily and effectively at any given point in time.
ANFIS	Adaptive Neuro-Fuzzy Inference System
ANN	Artificial Neural Network is an information processing paradigm that emulates the biological nervous systems
BBN	Bayesian Belief Network is a probabilistic graphical model that illustrates a set of random variables with their conditional dependencies using a directed acyclic graph (DAG).
CC	The combined-cycle power station, In electric power generation a combined cycle is an assembly of heat engines that work in tandem off the same source of heat, converting it into mechanical energy, which in turn usually drives electrical generators. The principle is that the exhaust of one heat engine is used as the heat source for another, thus extracting more useful energy from the heat, increasing the system's overall efficiency
CG	Co-generation is a power plant that produces electricity but does not waste the by-product of heat. The heat is used for district heating or other purposes, and thus the overall energy production efficiency is improved.
DAG	Directed Acyclic Graph

DER	Distributed energy resources are smaller energy sources that can be aggregated to provide the required energy to meet regular demand.
DG	Distributed generation, is generated or stored by a variety of small, grid-connected devices referred to as distributed energy resources (DER)
DNS	Demand not served, is the failure to provide a sufficient energy to cover the end users consumption requirements.
Fault tolerant control system	A fault tolerant system where faults are explicitly detected and accommodated.
FPGA	A field-programmable gate array (FPGA) is an integrated circuit has the capability to be configured by a customer after manufacturing
FTA	Fault tree analysis (FTA) is a hierarchical failure analysis using Boolean logic to combine a series of basic fault events to define the probability of top even failure
HRSG	Heat recovery steam generator, an energy recovery heat exchanger that recaptures heat from a hot gas stream produced by the prime mover engine.
IPL	Independent protection layer, A device, system, or action that is capable of preventing a scenario from proceeding to the undesired consequence without being adversely affected by the initiating event or the action of any other protection layer associated with the scenario.
IRL	independent resilience layer a modification of the IPL for enhancing the systems resiliency

Islanded Mode	Refers to the condition in which a distributed generator (DG) continues to power a location even though electrical grid power from the electric utility is no longer present.
LOPA	A layer of protection analysis is a method of analyzing the likelihood (frequency) of a harmful outcome event based on an initiating event frequency and on the probability of failure of a series of independent layers of protection capable of preventing the harmful outcome.
LORA	A layer of resilience analysis is a method of analyzing the likelihood (frequency) of a harmful outcome event based on an initiating event frequency and on the probability of failure of a series of independent layers of resilience able to prevent the harmful outcome.
MEG	Micro energy grid, a system that comprises intelligent energy sources and distribution systems, automated metering, and a specialized computing system.
MG	A microgrid is a district energy system comprising of distributed energy sources, energy storage and loads. It has the capability to operate with or independently from the utility grid.
MLHDM	A multi-level hierarchical decision making. It enhances the self-healing characteristics of MEG against uncertainty hazards during the system operation.
MTTF	Mean time to failure, is the predicted elapsed time between inherent failures of a system during operation.
PFD	Probability Failure on Demand, the probability that a system will fail dangerously, and not be able to perform its safety function when required.

PMU	Phasor measurement unit (PMU) or synchro-phasor is a device which measures the electrical waves on an electricity grid, using a common time source for synchronization. Time synchronization allows synchronized real-time measurements of multiple remote measurement points on the grid.
Power-System Protection	Power-system protection is a branch of electrical power engineering that deals with the protection of electrical power systems from faults through the isolation of faulted parts from the rest of the electrical network. The objective of a protection scheme is to keep the power system stable by isolating only the components that are under fault, whilst leaving as much of the network as possible still in operation. Thus, protection schemes must apply with very pragmatic and pessimistic approach to clearing system faults. The devices that are used to protect the power systems from faults are called protection devices.
protection devices	The devices that are used to protect the power systems from faults
PV	Photovoltaic, solar power technology that turns sunlight directly into electricity.
PVC	A photovoltaic cell, often used interchangeably with PV module (especially in one-module systems), but more accurately used to refer to a physically connected collection of modules (i.e., a laminate string of modules used to achieve a required voltage and current).
PVs	Process variables, the measurements variables for monitoring and control the system during the process time.

Reliability	The probability of a system to perform a required function under normal conditions and during a given period of time.
Renewable energy sources (RES)	Renewable energy sources are naturally replenishable but flow-limited. They are virtually inexhaustible in duration but limited in the amount of energy that is available per unit of time. Such as biomass, hydro, geothermal, solar and the wind. In the future, they could also include the use of ocean thermal, wave, and tidal action technologies.
Risk assessment	Risk assessment A systematic process of evaluating the potential risks that may be involved in a projected activity or undertaking.
Risk Management	Risk Management, The systematic application of management policies, procedures and practices to the tasks of establishing the context, identifying, analyzing, assessing, treating, monitoring and communicating.
RM	Resilience Matrix is a proposed matrix that is used for risk and resilience assessment to define the level of risk by considering the category of probability or likelihood against the category of consequence severity and the ecological risk index.
ROI	Return on investment, the amount of profit, before tax and after depreciation, from an investment made, usually expressed as a percentage of the original total cost invested.
Safety	The safe state is a freedom from the risk of injury, danger, or loss. It is the condition of being protected from harm or other non-desirable consequences. Safety can also refer to the control of recognized hazards in order to achieve an acceptable level of risk.

Safety Design	Safety design is the concept of minimizing hazards and eliminating danger level through applying detailed planning of the necessary safeguards plus the selection of appropriate technologies. It is essential to integrate a detailed safety design before the concrete implementation, in order to avoid subsequent costs, increase the system's availability and reduce downtime.
SAIFI	System average interruption frequency index, An index of average power interruption frequency within electricity distribution. Measured in terms of the number of power interruptions per customer and year.
Severity	A measure of the seriousness of fault effects using verbal characterization. Severity considers the worst case damage to equipment, damage to the environment, or degradation of a system’s operation.
SIF	Safety Instrumented Functions are the specific control functions performed by a SIS. They are implemented as part of an overall risk reduction strategy which is intended to eliminate the likelihood of a previously identified failure event that could range from minor equipment damage up to an event involving an uncontrolled catastrophic release of energy and/or materials.
SIL	Safety integrity level is a measurement of performance required for a safety instrumented function (SIF).
SIS	Safety instrumented system, an instrumented system used to implement one or more safety instrumented functions. It is a combination of sensor(s), logic solver(s), and final element(s). IEC 61508 uses the term "safety-related system" instead of uses the term SIS.

SPI	Safety performance indicators, is a high-level measure of system's safety output, traffic or another usage, simplified for gathering and review on a weekly, monthly or quarterly basis.
TES	Thermal energy storage refers to the technology that allows the transfer and storage of heat energy or, alternatively, energy from ice or cold air or water. The storage of thermal energy (heat or cool) during power provider off-peak times at night, for use during the next day without incurring daytime peak electric rates.
WT	Wind turbine, A device that captures the force of the wind to provide rotational motion to produce power with an alternator or generator.

CHAPTER 1 Introduction

1.1 Background

The beginning of micro-grids (MGs) were started as early as the beginning of using distributed generations (DGs) to supply small towns with electric power in the late 19th century. MG is an expression for small-scale, i.e. low and medium voltage distribution grids consists of DGs and loads. The last two decades show a significant increase of using interconnected DGs into the distribution grids due to the rapid development of the renewable energy technologies namely fuel cell (FC), solar energy (PV) and wind energy (WT). The main advantages of using renewable energy sources (RES) can be summarized as follows: the capability to reduce greenhouse gas emissions, the natural alternative energy source for fossil fuel that is dramatically depleted and a solution for the rapid increase on power demand and transmission losses [1].

Many benefits were alleged for using MGs in the 21st-century grids such as MGs are cheaper, more reliable and cleaner than legacy-grids [2]. Nevertheless, these are not true for every MG as several factors are influencing each entity. Eventually, most of the existing MGs are unable to concurrently achieve all the above mentioned benefits. Using MG has proven that it cannot be a cheaper option as two-thirds of all fuel used to produce power electricity is mostly wasted by emitting unused thermal energy from power generation system into the air or into water streams (e.g. sea and river). The average efficiency of power generation has remained around 33 percent since 1960. Therefore, with the increasing concerns regarding energy reliability and emissions, the claim on a combination of distributed energy resources (DERs), district cooling/heating units, energy storage devices, and renewable energy sources (RES) are increasing accordingly. The combination is widely deployed to meet the energy demands of electricity, cooling and heating for numerous types of buildings [3]. This combination is commonly named micro energy grids (MEGs).

MEGs defined as a system comprises intelligent energy sources, distribution systems, automated metering, and a specialized computing system [4]. The MEG can increase the

overall energy efficiency of the energy system, as well as to provide environmental benefits by reducing primary energy consumption and related greenhouse gas emissions [5].

The MEG has become a key point in the energy system for several reasons. Firstly, these systems can upsurge the energy efficiency up to 90 percent by utilizing thermal energy by-product of power generation for cooling, heating, and humidity control systems [6]. Secondly, with the rapid development of MEG technologies, the renewable energy industry has become one of the fastest growing industries in the last two decades [7]. The integration of renewable energy systems (RES), such as photovoltaic (PV), wind turbine (WT), small hydro, geothermal, waste-to-energy, and combined heat and power systems (CHPs), into the conventional energy grids improves the energy efficiency, increases the system's reliability and reduces the greenhouse gas emissions. Thus, the MEG is considered an integrated energy system, which contributes a high dynamic distribution system for different types of energy such as electricity, cooling, heating and natural gas [8].

1.2 Problem Definition

Till date, the studies on risk analysis of MEGs are rare and incomplete, despite it is paramount for designing resilient MEG. Failure in any components such as DERs may increase the hazard(s) of demand not served (DNS) and/or general blackout/brownout. In addition, utilizes of on-site renewable sources (RES) that have accompanying unpredictability and variability may affect the integrity of MEGs. Thus, MEGs require a high adaptive performance from the distributed energy systems [9].

Boosting the MEGs' resiliency improves the grids' reliability, increases fuel source variety and enhances national security [10]. The reliability idiom defines the capability of the energy system to offer the energy service to all customers at an affordable price [11]. However, the utility's grid reliability is decreased dramatically as much as the number of customers (i.e. residential, commercial and industrial) increases [12].

Basically, MEG reduces energy squandering and increases self-healing capability [13]. Whilst the conventional energy system generates these different types of energy independently, which causes low energy efficiency and high operational costs [14]. MEG structure may include the following: distributed generators, energy storage devices, and

energy management controller to reduce electricity costs and emissions, as well as to improve energy reliability and efficiency [8].

The North American Electric Reliability Corporation (NERC) definition of the power reliability can be extended to define the energy grid reliability as an integration of grid sufficiency (energy production meets demand) and grid security (capability to adapt disturbances). However, the 21st-century energy systems require grids that have the ability to continuously operate during various topologies conditions and to withstand in abnormal events by eliminating hazardous consequences that influence life quality, economic activity, and environmental sustainability. Therefore, the reliability, as a definition, is not enough for MEG's sustainability that needs to be enhanced by resilient method(s).

MEG analysis should have a wider perspective of the energy grids, not only as energy flow but also as grids that serve and influence people and societies. Hence, it requires studying the consequences of each component failure within MEG infrastructure.

Several advantages can be gained by utilizing resilient MEGs, as listed below [15]:

1. Enhance the reliability of system's performance,
2. Enhance customers' awareness and choices,
3. Encourage efficient decisions to be taken by the utility provider,
4. Provide a closer proximity between energy generation and energy use. Thus, lower costs and losses.

When resilient MEG technology is applied to a city, the city is called a "Smart Green City", such as Canada's Dockside or the UAE's Masdar.

From a systems perspective, the MEG as one controllable unit that combines energy sources, loads, and storage units, has the ability to supply electricity, cooling, heating and natural gas energy to the end users independently [16]. Thus, during the peak demand period, or at energy failure occurrence, the MEG can operate independently out of the utility grids by isolating its energy nodes (generation and load) from disturbance without affecting the larger grid's integrity. On the other hand, integrating multi-DERs, particularly renewable energy sources (RES), into existing energy grids offers significant challenges

due to the intermittent and varied characteristics of the environment. further to the uncertainty of dealing with indefinite system's behavior, which means constructing such a large complex system, MEG, with the uncertainty of dealing with various unknown parameters, which increase the hazardous condition [17]. Thus, there is an increased demand to design MEGs with higher safety fault tolerance of numerous types of risks compared with classical discrete systems [18]. Therefore, quantitative and qualitative terms of risks that threaten the MEG are mandatory for design of resilient MEG with high fault-tolerant capability. Hereby, the risk analysis becomes a fundamental part of practical MEGs.

Faults in MEGs, if not controlled properly, might propagate and cause blackouts and/or energy outages. However, faults detection and toleration action in MEGs are still open research areas. The existing studies about hazard estimation are on a case-by-case basis [19]. Estimating the fault propagation and analyzing the consequences are major challenges for safety design verification. To implement a precise safety verification approach, it is vital to analyze and diagnose all hazard and fault events of the MEG and to study fault propagation scenarios.

Faults in MEG causes abnormal operating occurrence that leads to degradation in performance. Therefore, fault analysis of the MEG is important at design and operation stages. Fault prognosis and diagnosis respectively, have direct benefits on energy optimization and operating cost savings. Different fault prognosis and diagnosis approaches have been developed for several types of complex systems. Nowadays, the fault detection, diagnosis and prognosis methodologies has become engaged in various system analysis, from univariate statistical process control to multivariate control systems [20]. In general, control charts are created based on critical quality attributes of the process, e.g. CUSUM chart. The control chart helps to identify the cause of the failure once indicated by operator [21]. However, it is difficult to identify the failure root without expert's contribution as there are many factors that may cause a certain failure mode [22]. Moreover, different control charts are necessary for identifying different problem types. Nevertheless, as the number of control charts increased it becomes hard to monitor them

simultaneously. Several fault diagnosis and prognosis methods were presented in many articles toward providing practical solutions as discussed in Section 2.11.

Although, Bayesian belief networks (BBN) have been extensively developed for fault prognosis and diagnosis in several fields, as shown in Section 2.12. It can be concluded that BBN has not been applied yet to MEG diagnosis and prognosis. Therefore, this study offers the application of BBN for fault diagnosis and prognosis in MEG by implementing the BBN model for a concerned MEG, the uncertainty between control parameters and their impact on energy performance can be qualitatively interpreted to a unique BBN structure and quantitatively presented by determining the conditional probability table (CPT) for each node in the BBN structure.

The performance of the proposed resilient MEG, that guarded by selected independent resilience layers (IRLs) can be validated by implementing a model for the MEG case study in Matlab-Simulink platform. The mathematical equations of the model performance can be converted into a more tangible model by using interactive graphical shapes in the Simulink environment.

1.3 Objectives

The work addresses one of the most challenging problems on our society as it focuses on the transition from a centralized energy production to a distributed ones. The thesis outlines the advantages of this process and deals with its most critical issue namely the resiliency of the new energy paradigm. MEGs are efficiently exploited the primary fuels but due to its innovative structure and limited hardware capabilities, many critical points to be studied in its response to fault conditions. In order to assess MEG's resiliency, many aspects must be considered namely society, economy and environment.

The main objective of this study is to propose a practical methodology using safety design/analysis tools to attain resilient MEGs. This can be achieved by developing the hazard analysis and the risk assessment methods for MEGs, this can be implemented by Study hazards and estimate risks of MEG such as hazards in electricity, heating, cooling, transportation and natural gas sectors. In addition to the hazards of natural phenomena. The proposed method should evaluate the MEG's performance under several hazard scenarios

and prioritize the risks according to its associated risk rank. Therefore this research should focus on defining and developing numerous independent resilience layers (IRLs) for MEG safety design in order to increase SIL and reduce the risk. The MEG's risk level can be evaluated by using two advanced approaches, i.e. developed fault tree analysis (FTA) and advanced layer of resilience analysis (LORA) to estimate changes in safety integrity level (SIL) due to integrating selected independent resilience layers (IRLs) to the MEG entity. The development of risk analysis tools for resiliency is leading to define a new performance indicators named resilience risk performance indicator (RRPIs).

In addition, this research is focusing on proposing a non SIF IRL and a SIF IRL successively a hierarchical decision making structure for MEG and a MEG alarm system.

A smart fault prognosis system able to predict risk-roots is proposed using Bayesian belief network (BBN) and Adaptive Neuro-Fuzzy interference system (ANFIS). The strategy is to develop advanced and more robust predictive techniques to improve the resiliency of MEG condition monitoring systems.

The specific objectives of the thesis can be summarized as follows:

1- Study hazard scenarios for MEG by proposing a resilience matrix and developing a resilience risk performance indicator (RRPI) to measure the MEG resiliency
2- Define, develop and propose independent resilience layers (IRLs) for resilient MEG
3- Propose layer of resilience analysis (LORA) for safety analysis tools for resilient MEG design and utilize the fault tree analysis (FTA) for resiliency assessment
4- Study and implement an intelligent reasoning algorithm by using BBN and ANFIS techniques for resilience design and verification of MEG.

1.4 Methodology Framework

This research concerns in proposing a methodology of safety design and evaluation to achieve resilient micro energy grid (MEG). This method pursues to offer a tool to achieve an accurate design of resilient MEG, by proposing safety design tools namely developed hazard analysis and advanced risk assessment evaluation methods, then implement the

required independent resilience layers (IRLs), consist of SIF and non-SIF components, to achieve an acceptable safety tolerance margin.

Specialised intelligent reasoning algorithm like Bayesian inference, Neural Networks and Fuzzy Logic are employed in forecasting the behavior of the MEG under different working scenarios. The proposed algorithm offers a tool for MEGs safety design analysis (prognosis) and for MEGs fault identification (diagnosis) as well. Several hazards scenarios were studied in order to examine the MEG self-healing and resilience performance. ***Fig. 1.1*** shows the steps followed to achieve the objective of the research study.

The framework shown below begins with the study of a theoretical model of a MEG design case study that is presented in CHAPTER 3 and implements a static and dynamic simulation models by using the Simulink platform in order to study and validate the proposed safety design techniques for a resilient MEG structure. Different levels of the simulation are used from the models of the components to one of their interactions as shown in Section 3.3.

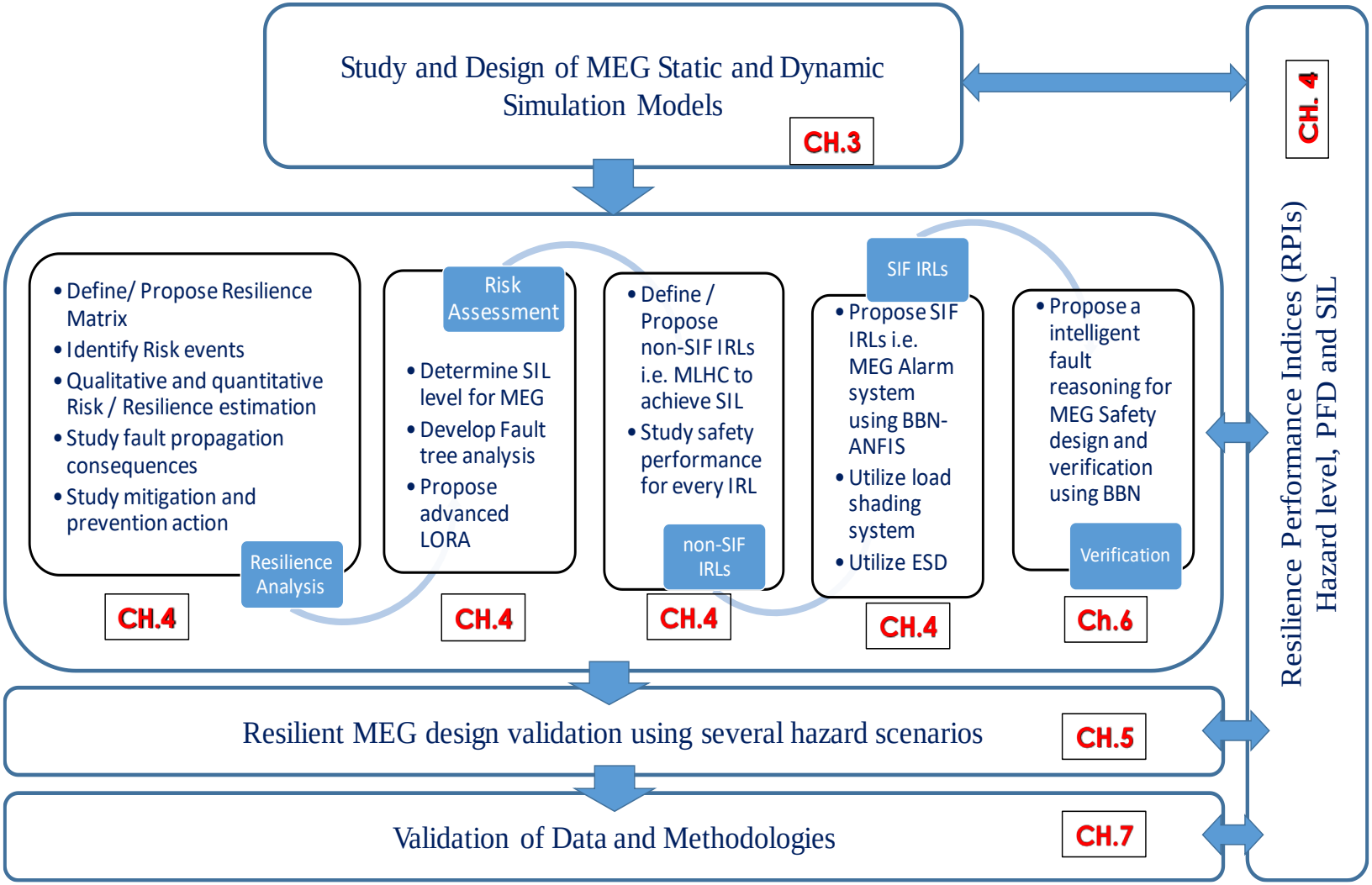

Fig. 1.1: *Methodology framework for this thesis*

The next step is the hazard analysis by studying risks that threaten the MEGs' resiliency. The resilience matrix (RM) is proposed in Section 4.2. The RM consists information about quantitative and qualitative risk estimation. In addition, it shows forecasted risk consequences and offers the available mitigation and prevention actions. The resilience risk performance indicator (RRPI) is used as KPI to evaluate the MEG's performance.

The third step is the risk assessment that illustrated in CHAPTER 4. Where the safety integrity level (SIL) for a MEG was determined and two risk assessment tools were proposed namely a developed fault tree analysis (FTA) and an advanced layer of resilience analysis (LORA) to evaluate/improve the resilience of MEG. The probability failure on demand (PFD) and the safety integrity level (SIL).

A study of the safety performance for selected IRLs was attained in order to be utilized in a MEG to improve the RRPI value and the resilience of a MEG. Different types of safety instrumented systems (SIF) such as MEG alarm system, load shading system and emergency shutdown system (ESD) were utilized for additional improve the resiliency.

A non-SIF IRL is proposed in CHAPTER 5 by implementing a multi-level hierarchical decision making structure and validate the new resilient MEG through numerous hazard scenarios were simulated for design validation of the proposed resilient MEG.

A SIF IRL MEG's alarm system was proposed in CHAPTER 6 by using a BBN-ANFIS based intelligent fault reasoning for MEG. The proposed fault reasoning tool has the ability to predict risks and diagnose faults to improve the MEG condition monitoring systems that have a direct positive impact on the MEGs' resiliency.

Finally, three validation process were proposed to verify the data and methods that offered in this study, i.e. the MEG simulation model, LORA and BBN.

Hence, the risk analysis techniques that proposed in this study can be projected on different MEG entities by minor tune-ups to fit the new MEG configuration.

1.5 Thesis Organization

The main outlines of this work are organized as follows:

The next chapter, CHAPTER 2, presents a review of ultimate literature associated with this study. Fundamental of the micro energy grid, the definition of risk concepts of fault detection and diagnosis are briefly explained. In addition, a review of hazard and risk analysis, safety and protection were presented.

CHAPTER 3 is devoted to describe a selected case study of MEG's infrastructure and extensively discuss the mathematical formula of its components. In addition, modeling and simulation of a selected MEG are presented in this chapter. Additionally, three baseline operational scenarios are studied to evaluate the MEG's performance.

CHAPTER 4 defines the hazard and risk in MEGs, proposes resilience matrix and defines/propose resilience risk performance indicator (RRPI). Then demonstrates problems associated with the MEG design and operation process. In addition, it determines the definition of MEGs' resilience design. It proposes methodologies for MEG fault analysis namely fault tree analysis and layer of resilience analysis (LORA) and finally, discusses the self-healing mechanism for MEGs.

CHAPTER 5 three control types of MEG's are presented in brief. Then a hierarchical decision making structure is proposed by using a neuro-fuzzy decision-making method. Finally, a selected operational scenarios are studied to evaluate the MEG's performance.

CHAPTER 6 devotes for discussing and developing MEG's fault detection and diagnosis approaches by proposing Bayesian belief network (BBN) and Adaptive Neuro-Fuzzy interference system (ANFIS) technologies.

CHAPTER 7 validates the data and methods used/proposed in this research. Three main items will be validated namely the simulation of MEG operation, LORA and BBN.

CHAPTER 8 conclusion, contribution and future works for the research are presented and discussed

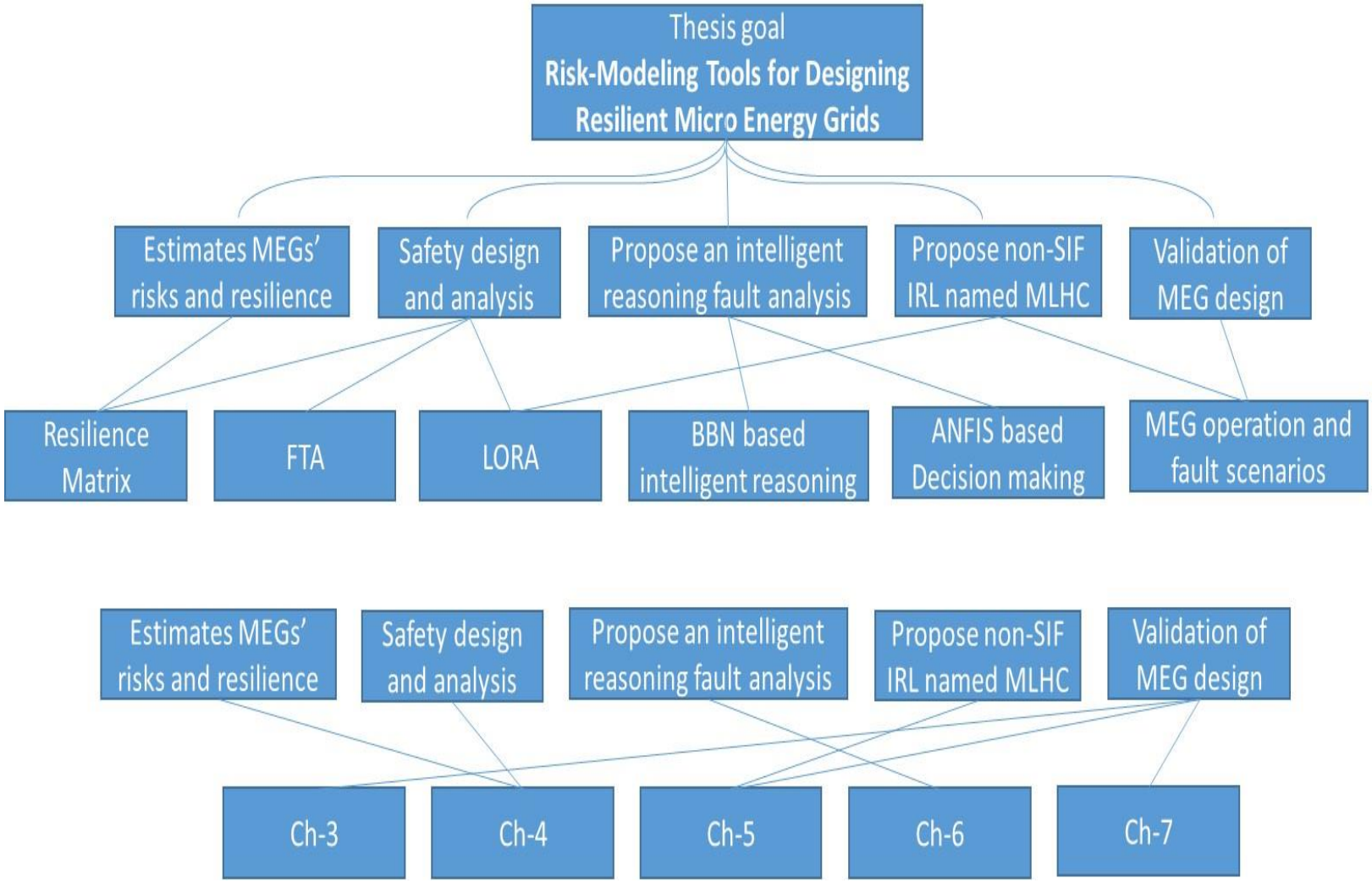

Fig. 1.2: *Thesis structure*

CHAPTER 2 Literature Review

This chapter provides a comprehensive review of existing literature related to the research study. The flow of the chapter will start by introducing ultimate references in the basic concepts of micro energy grids (MEGs) and its main distributed energy resources (DERs). The recent citation in fault detection techniques and fault tolerant control methodologies for MEG are studied in order to have sufficient knowledge before going through the hazards and risk analysis discussion, which is the key point for safety and self-healing methods. Also, references in protection and energy management are justified for system reliability and energy optimization. Numerous techniques for MEGs management and optimization are discussed to illustrate benefits on economic, sustainability and environment. Different fault diagnosis and prognosis methods for several applications are illustrated then Bayesian belief networks methods and implementation for online fault detection and diagnosis of different application are discussed.

2.1 Micro Energy Grid

Micro energy grid is an entity consists energy sources and loads that are in a capacity of 50MW and less [23], which typically operates in connection with traditional utility grid nevertheless it can be disconnected to island mode. In [24] a coupled microgrids were proposed by utilizing the waste heat that is co-produced by the combined heat and power (CHP), and gas generators in the MG. the new configuration enhance the reliability, self-healing and increase the generation efficiency. The articles in [15] and [17] illustrate a physical case-study for distributed energy plant at University of California - Irvine campus, to provide effective control methodology to cover the energy demand of electricity, cooling and hot water, eliminate gases emission and reduce cost. To achieve the simultaneous goals, the following techniques were used: load-following generators, energy storage devices, and predictive energy management. Promising results were found where the annual utility bill costs reduced by 12.0%, net energy costs by 3.61%, and improve energy efficiency by 1.56%. A hybrid poly-generation management methodology was proposed in [25] to achieve an optimal operation cost, energy usage and gases emission. The model was implemented in Simulink platform to validate the proposed optimization method. A

battery energy storage (BES) was proposed in [26] to improve the reliability of power system in the MG. An enhanced control methodology was used to mitigate the impact of the intermittency on MG and a genetic algorithm (GA) was used to define the optimal size of the BES. The validation was done using PSCAD/EMTDC software platform. In [27] a MG combing a gas and renewable energy generation were proposed to improve the reliability and resiliency of the system performance. Distinct key performance indicators (KPI) were proposed to evaluate and optimize the system performance. The MEG model was validated in Matlab platform. In [28], an experimental study for utilizing a CHP in a commercial building was conducted. Validation for both operating modes of the CHP, namely following thermal and electrical loads (FTL and FEL), were realized. The results show the advantages and disadvantages of each mode.

This thesis study proposes risk modeling techniques to design a resilient MEG that consists electricity, cooling and heating energy. The MEG analysis should have a wider perspective of the energy grids, not only as energy flow but also as grid that serve and influence people and societies. Hence, it requires studying the consequences of each component failure within MEG infrastructure. The socio-econo-ecological method is proposed to design resilient MEG by improving MEG's stability characteristics.

2.2 Risk Management Approaches

Risk is an essential factor in any system's safety design, where risk can be defined by the potential harm or loss correlated with an activity performed in an uncertain circumstance. The first use of "Risk" was in 1667, by Arnauld and Nicole, who assumed it consists of at least two components. "Fear of some harm ought to be proportional not only to the magnitude of the harm but also to the probability of the event" [29]. Knight defines risk as a situation of being exposed to danger where the uncertainty of injury or loss is high [30]. Thus, Knight's definition associated the risk with the uncertainty which can be reduced to a single probability [31]. Therefore, risk management can be defined based on knight's standpoint as an expert knowledge analysis of the uncertainties. Ellsberg distinguished between the uncertainty and the risk, where the uncertainty has impacts on the decisions due to known and unknown causes probabilities, whereas risks are a small

portion of the ambiguity [32]. Adams describes risk as an interactive event that has a significant level of uncertainty tied to varying reactions of different risk judgment [33]. Resilient model of a health care system was presented in [34] to mitigate risks consequences by monitoring the system's states parameters, analyzing its safety measurements and predicting the risk level before the consequences such as failure and harm take place, this model can be utilized for any complex systems.

The risk modeling techniques are extended in this thesis to be utilized for MEG design and to measure the resilience parameters of the MEG. Whereas the existing studies about hazard estimation are on a case-by-case basis. Estimating the fault propagation and analyzing the consequences are major challenges for safety design verification. To implement a precise safety verification approach, it is vital to analyze and diagnose all hazard and fault events of the MEG and to study fault propagation scenarios.

2.3 Risk Matrix

It has different names as a "risk assessment matrix", "risk management matrix," "risk rating matrix," or "risk analysis matrix". Risk matrix consists of two main features that will be discussed in detail in Section 2.4:

- Severity: The impact of a risk and the negative consequences that would result
- Likelihood: The probability of the risk occurring

A historical review of risk matrices types was presented in [35] by discussing the probability consequence diagrams and the factors that may affect the risk analysis. The article [36] presents methods for risk ranking and risk analysis that takes in consideration various risks factors due to different stakeholders perspectives. Three Main perspectives are formulating the proposed method namely the expected value, uncertainty and moral perspective. A logarithmical scale risk assessment matrix was proposed in [37] to mitigate the inherent limitations of using linear scale risk matrices. The linear scale risk matrices have a deficiency in dealing with assessment and management analysis. In article [38] develops the multiple criteria decision analysis for implementing risk matrix structures for health and safety risks assessment at the occupational health and safety unit (OHSU) of the regional health administration of Lisbon and Tagus valley. The proposed method focuses

on the risk control level to reduce the importance of the risk assessment level in the hazard management process to achieve higher uses of resources and improves the decision making process time.

The risk matrix is developed in this thesis to produce a resilience matrix. The resilience matrix presents important information of socio-econo-ecological parameters in a form of resilience risk performance indicator (RRPI). The RRPI is an indicator for the system performance that evaluate the society, economy and environment risk levels for every hazard event to assist the engineers in both design and operation process.

2.4 Risk Assessment Techniques

There are different methods to identify and quantify risks. Here below are illustrated discussions of the existing quantifying risk methods:

1- Haimes in [39] uses accumulate summation of the probability density function of the severity of consequences and a random variable of the severity of consequences, as illustrated by the following equation:

$$E[x] = \sum p_i x_i \tag{2-1}$$

where p is the probability density function of x and x is a random variable representing the severity of consequences; thus, the frequency of occurrence of the hazard is latent.

2- Bahill in [40], uses a different method for quantifying the risk by combining the frequency of occurrence with the severity of failure consequences., the function can be presented as follows:

$$Risk = relative\ likelihood\ (frequency\ of\ occurrence) \\ X\ severity\ of\ failure\ consequences \tag{2-2}$$

Bahill's method is commonly used in North America industries.

3- In [41], two combining functions were illustrated:

a. Linear combining function that accumulates the summation of the combined products of the weight of importance with the score variable. The weight of importance is a random variable between 0 and 1.0:

$$E = \sum_{i=1}^{n} w_i . x_i \quad (2\text{-}3)$$

where *w* is weight of importance (0-1) and *x* is the score

b. Product combining function that accumulates the products of the score variable to the power of the weight of importance:

$$E = \prod_{i=1}^{n} x_i^{w_i} \quad (2\text{-}4)$$

4- Exponential combining function [42], that utilizes an exponent of the summation of a linear combining function between the weight of importance and score variable. Hence, a constant variable can be used for calibration purpose:

$$E = 1 - e^{-\sum_{i=1}^{n} k w_i x_i} \quad (2\text{-}5)$$

where k is a constant for calibration purpose

5- Summation minus product combining function [43], which derived from the probability of unions between independent variables. However, this function is lacking when used to qualify the risk, where if severity or likelihood is 0 then the risk should be 0, which is not the case by using this equation

$$E = w_1 x + w_2 y - w_1 x y \quad 2\text{-}6)$$

Which derived from the probability of unions between independent variables. However, this function has obstacle when used to qualifying the risk, where if severity or likelihood is 0 then the risk should be 0, which is not the case by using this equation

6- Compromise combining function [44]:

$$E = [\,(w_1 x)^r + (w_2 y)^r]^{1/r} \quad (2\text{-}7)$$

where *r* is constant factor

7- [45] presents risk by doubling the severity weight

$$Risk = relative\ likelihood\ (frequency\ of\ occurrence) \times (severity\ of\ failure\ consequences)^2 \quad (2\text{-}8)$$

8- In [46] the failure modes and effects analysis (FEMA) comprises the difficulty of detection

$$Risk = relative\ likelihood\ (frequency\ of\ occurrence) \times severity\ of\ failure\ consequences \times difficulty\ of\ detection \quad (2\text{-}9)$$

9- The hazard level can be calculated by the following formula [47] [48]:

$$Hazard\ Level\ (H_L) = S_i * C_i \quad (2\text{-}10)$$

where, $C_i = (P_i + F_i + A_i)$ and S_i is the consequence severity of the hazard event, C_i is the class hazard event likelihood, P_i is the probability, F_i is the frequency, and A_i the ability for failure avoidance.

In this thesis Bahill's risk assessment equation (2-2), was used as a base for developing resilience risk performance indicator (RRPI) to assess the socio-econo-ecological parameters of the MEG. The RRPI is capable to assess the resilience of MEG, which is a paramount tool in risk analysis and decision-making process.

2.5 Micro Grid Fault Detection

The resiliency of Micro energy grids is under threat of imperceptible faults. Therefore, development of efficient fault detection methodologies are highly important to improve the systems' operation security. Numerous researches and articles were presented, in the last two decades, to solve this dilemma. In [49] a fault detection approach was proposed to secure the microgrid (MG) against faults risks. The approach focuses on the faults that can be defined by changes in the state space matrices model. The numerical results show that this approach is efficient mainly with the small changes. In [50] numerous heterogeneous features were utilized to modeled localized faults in the smart grid. The proposed classifier model is mainly depending on two features, the interaction between the clusters and the dissimilarity measures learning techniques, based on genetic weighting parameters

optimization. Paper [51] study fault detection and localization methods in both transmission and distribution system within smart grids. Then it proposed a methodology to enhance the accuracy of fault location. Wavelet multiresolution analysis (MRA) was utilized with GPS and intelligent computation technologies in the article [52] to provide an efficient algorithm able to detect the fault in the transmission line of smart grid and define its location. The adaptive neuro-fuzzy inference system (ANFIS) and artificial neural network (ANN) were used to improve the fault location accuracy. Monte-Carlo simulation was used to validate the proposed algorithm. An active fault detection and isolation scheme for islanded faults in the MG was presented in [53]. Utilizing a set-membership filter and Kalman filter gave the ability to achieve the proposed approach. The article in [54] presents a fault detection, isolation, and service restoration (FDIR) for an outage event in an electrical distribution grid.

Many studies were done in fault detection of MG however up to date, there are none of the studies conducted on fault detection of MEG. In this study an alarm/monitoring system is proposed for a MEG by using SIF-IRL based BBN-ANFIS techniques for fault detection and diagnosis.

2.6 Protection Systems

The general purpose of utilizing protection systems is to isolate rapidly and narrowly disturbance area(s) in order to protect the system's assets and to maintain operational status of the rest of the system entity. Therefore, protection systems detect and eliminate faults to prevent dragging the system to undesired consequence conditions due to faults propagation.

2.6.1 Micro Grid Protection Systems

Microgrid (MG) has various unique structures and combining of numerous components that make protection strategies more complicated and challenging. The dynamic non-radial topology accompanying with different types of DERs in addition to the altering connection mode between utility grid connected and islanded modes have originated new problems that does not exist in the legacy distribution systems. Those new problems are preventing the MG to be widely spread, therefore many ultimate researches are addressing those

problems and proposing different methodologies for fault detecting, preventing and mitigating processes.

Line ratings are the main limiting factor for MGs in grid-connected mode. However, it is not the case for MGs in the islanded mode as DERs capacities are much less than the utility's electricity supply. Therefore the limiting factors become DERs' maximum output. On the other hand, the fault currents are varies as the DER's type are varies, where the fault currents of rotating machines, such as co-generator and wind turbines, are extremely higher than their maximum rated current, whereas inverter based DERs has low fault current adjacent to the rating currents, between 110-200% [55]. Subsequently, many research studies aim to achieve intelligent protection schemes are currently in process.

Papers [56] proposed adaptive protection schemes for MG in both islanded and grid-connected modes. Validation of the offered method was conducted and concluded that still more efforts are required to achieve a robust protection scheme. New indices for metering digital protection algorithms were proposed in [57] in order to assess its performance, within islanded MG, in presence of harmonics, frequency deviation and time-varying loads. Numerous actual field data for a wind farm substation and electric arc furnace were applied to validate the proposed metering algorithm. A review of recent MG protection studies was illustrated in [58] and a proposal for a new adaptive protection method was justified in order to achieve global decisions multi-agent protective plans. Paper [59] proposes a controller area network (CAN) based smart protection scheme for MG system. Where the dynamic state of DERs are monitored by measuring the operational performance attributes and environmental data. The proposed scheme has the ability to recognize the type and location of a fault in order to isolate a minimal faulted section. An intelligent power switch with integrated protection and self-diagnostic was proposed in [60], by using HV-CMOS technology to safely handle the ordinary and extraordinary automotive electrical and environmental conditions. Zero sequence components were offered in [61] for microgrid protection of single line to ground faults by utilizing coordinated neutral point of the generation units. The reference [62] utilizes negative sequence components of the line current for the protection of line to line faults. Plug and play function was proposed

in [63] by creating IEC 61850 information structure of a micro energy grid. The proposal aims to create standards for design, operation and protection of microgrids.

MG protection systems should consider the following requirements [64]:

1. Dynamic configuration capability

2. High-speed standard-based communication namely IEC 61850 should be utilized

3. Prompt reaction operation in the case of deep voltage dips in order to maintain stability of the other healthy part of the grid and to ensure high protection for the assets and the public

4. Selective operation in all kinds of faults

5. Avoid unnecessary activation of protection devices

2.6.2 CHP Protection Systems

A static model was proposed in [65] by using conventional SPC charts to monitor the heat exchanger operation condition. The model capable to discover fouling of a heat exchanger. A method of early detection of fouling build-up of the coolant system of CHP units has been presented in [66]. By using the net transfer coefficient charts to assist engineers to distinguish between a pump failure and heat exchanger fouling remotely, saving maintenance engineer hours. Fouling of the heat transfer surfaces greatly reduces the heat recovery and severely affects the whole efficiency of the unit, as it reduces the overall efficiency of the CHP unit by about 25%. The article [67], proposes thermoeconomic and exergetic cost tools to detect faults and malfunctions in a combined heat and power plant (CHP). The results by using the proposed approach show promising solution for determining the location of malfunctions

2.6.3 Cooling Protection Systems

The article [68] offers a fuzzy logic based smart fault detection system for a cogeneration and cooling plant. The proposed system was tested in a case studies consists of gas turbine generator (GTG), heat recovery steam generator (HRSG) and a steam absorption chiller. The results show 95 to 100% accuracy for true fault detection for inlet temperatures in the range of 24 to 34 °C. The article [69] proposes a fault detection tool named air handling

unit performance assessment rules (APAR). The proposed tool consists experts' knowledge-based set of rules for mapping the balance of mass and energy. APAR relies on the measurement data from I&C sensors and from control signals. The proposed fault detection tool was tested and validated in a commercial AHU. A proposed method in the article [70] is a combination of principal component analysis (PCA) and support vector data description (SVDD) methods named PCA-R-SVDD. These two methods individually are insensitive to faults of condenser fouling (CdF) and refrigerant leakage (RfL). The proposed method shows strength in detecting six of the common faults. For validation, the author utilized the experimental data for the centrifugal chiller that is presented in ASHRAE Research Project 1043 (RP-1043).

In this study, the protection idiom is extended to prevent / mitigate the top event of blackout and brownout of the MEG. Numerous independent resilience layers (IRLs) for MEG are proposed in this study namely non-SIF and SIF IRLs. The proposed independent resilience layer (IRL) is derived from the independent protection layer (IPL), these layers are utilized to prevent and mitigate the occurrence of energy blackout and brownout.

2.7 Micro Grid Fault Tolerant Control

The interest on integrating renewable energy sources (RESs) in power system is significantly increase worldwide. This has a magnified negative impact on power quality and reliability if improper control strategy is used. Many researches offer solutions on these challenges. A brief survey on the existing challenges and recent developments of power reliability are discussed in the following paragraph. The reference [71] proposed a fault tolerant control scheme for a wind turbine connected to a MG. it uses adaptive filters based on nonlinear geometric approach in order to instantaneously estimate faults in the hydraulic pitch actuator. The approach was examined on a known wind turbine model. Paper [72] demonstrates a fault detection and isolation approach in MG. The proposed flexible structure has the ability to adjust itself based on the grid changes by changing the analytic redundancy relations (ARR). The approach scheme was implemented using power factory simulation platform. The article [73] demonstrates major issues of connecting renewable energy sources (RES) in the MG. It focuses on frequency control problems and commented

on the use of $\frac{df}{dt}$ protective relay performance. In [74], a supervisory control scheme was illustrated to adopt the distributed generators power production and frequency set points in the MG. in order to accommodate the unexpected load variation and faults. The scheme was examined on a four-areas microgrids.

In this thesis, a multi-level hierarchical decision making (MLHDM) is proposed as a non-SIF IRL. It is proposed to enhance the self-healing characteristics of MEG against uncertainty hazards during the system operation. The structural design of MLHDM consists of three simultaneous levels functioning together to attain resilient operation.

2.8 Micro Energy Grid Security and Safety

The energy grid security is defined as the capability of the energy grid to provide sufficient energy that meet the demand at reasonable price rates in addition to its capability to adapt disturbances [75]. The concept was extended to address the critical affection of energy supply interruption in economic as declared in [76]. Recently the concept was extended to include eco-friendly requirements as discussed in [77].

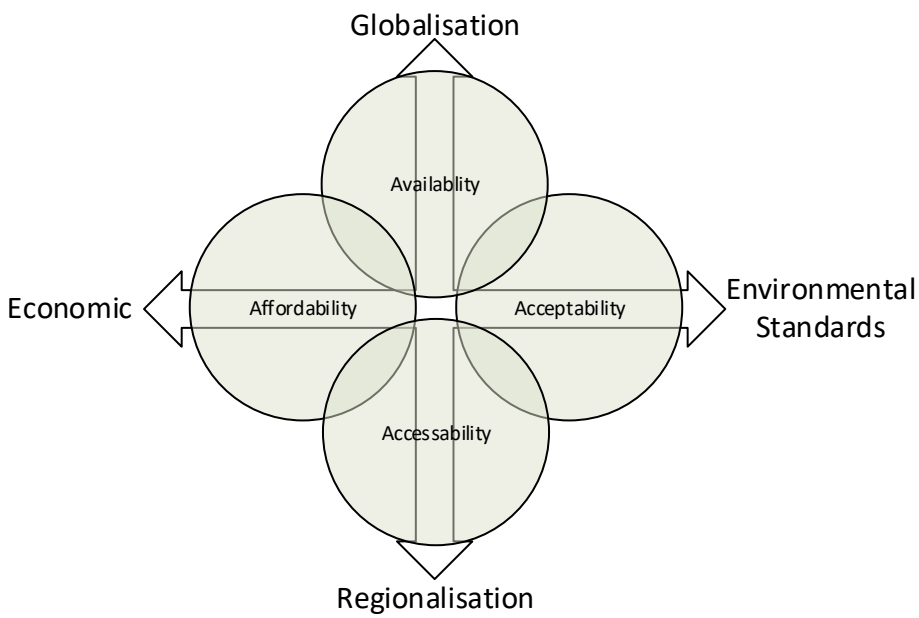

Fig. 2.1: *The main elements of energy grids security*

The energy grids security is presented in **Fig. 2.1**. The grids security consists the following essential elements [78]:

1. Availability: means the energy grid service to the public is ready to be used immediately
2. Accessibility: means easy to approach the energy grids service.
3. Acceptability: it refers to the agreement relation between the facility providers and the society to address environmental consequences in order to ensure sustainability.
4. Affordable: to ensure the end-users pay reasonable rate for the energy services in order to ensure smooth economic performance.

The ANSI/ISA-84.00.01-2004 (IEC 61511) standard defines a safety instrumented system (SIS) as an instrumented system used to implement one or more safety instrumented functions (SIF). A SIS is a combination of sensor(s), logic solver(s), and final element(s). IEC 61508 uses the term "safety-related system" instead of uses the term SIS. This term describes the same principle but with different language context that can be broadly applied to many industries [79]. The main purpose of the control loop in the basic process control system (BPCS) is to maintain the process parameters within their prescribed limits. A SIS monitors process parameters and interferes when required [80]. The safety design is an essential process for resilient MEGs implementation, where based on the hazard level of the MEG a selected safety procedure should take place. Six parameters have to be considered in hazard analysis as follows [81]:

1. Sensitivity: the nominal threshold value for protection system should identify the faults taking into consideration the MEG safety level.
2. Selectivity: determine the zone where the fault occurred. In order to isolate the faulted area.
3. Speed: the faster respond of the protection system to the fault, the minimal impacts on the MEG stability
4. Security: the protection system should recognize both faults and abnormal condition but to act in the event of fault only.
5. Redundancy: is required to increase the reliability of the protection system
6. Reliability: high-reliability level is required in both control and protection systems

This study proposes a methodology of safety design and evaluation tools to achieve resilient micro energy grid (MEG). This method pursues to offer a tool to achieve an accurate design of resilient MEG, by proposing safety design tools namely developed hazard analysis and advanced risk assessment evaluation methods, then implement the required independent resilience layers (IRLs), consist of SIF and non-SIF components, to achieve an acceptable safety risk tolerance margin.

2.9 Resilient Energy System

The resilience term is a firmly associated with sustainability, where the sustainability is defined as the ability to maintain social, economic and environment at a certain desired levels over time. Therefore, it can be concluded that any sustainable system must be resilient as well [82]. Literature review illustrates three most acceptable definitions of the resilience that are engineering resilience, ecological resilience and adaptive resilience [83]. The engineering method perspective defines resilience as system's robustness and immunity of external disturbances further to its self-healing capability to return the system to the stability region. The ecological approach identifies the uncertainties of the system and assures its ability to cope the disruption to keep functioning as designed. The adaptive or socio-ecological method describes resilience as autonomous learning capability to adapt the system's characteristics for optimum operational performance and risk immunity.

This study develops the resilience definition as an approach aimed to eliminate hazardous consequences on socio-econo-ecological parameters that influence respectively the life quality, economic activity, and environmental sustainability. Resilience guards ensure maintaining the system operates as designed.

2.10 Hazard Analysis

A layered fault tree model was modified in [84] in order to differentiate between islanded and grid-connected modes for the microgrid (MG). By considering the load priority measures the model is capable of defining the weak part of the system in order to enhance the design concepts. The hierarchical Monte Carlo simulation method was utilized to examine the system reliability, by combined power sufficiency assessment with system

failure insights. The design concept was enhanced based on the assumption that the load priority measures are sufficient to define the weak part of the system. In [85] a comparison study between Bahill and Haimes risk analysis approaches was justified and a case study of the risk of incorporating solar photovoltaic systems into a commercial electric power grid. The study shows the strength and the weak points of each approach. A new design for a process named Diogenes was revealed in [86]. Diogenes helps systems' engineers to identify the unintended, but predictable, consequences of fault propagation for new systems under design. An efficient multiplayer collaboration framework was presented in [87] to characterize sources of system risk from various expert opinions. It can be considered as a key solution for unstructured, multidimensional problems. Paper [88] introduces risk analyses for pinewood derbies, also it shows several risk analysis techniques and presents the accompanying problems.

This study proposes a framework that addresses the demand of resilient MEG by using safety analysis tools for greater clarity decision making. The socio-econo-ecological method is proposed to design a resilient MEG by modifying MEG's stability characteristics.

2.11 Fault Diagnosis and Prognosis

In [89] a fault diagnosis approach was proposed, for a building air-conditioning systems, based on the exponentially-weighted moving average control charts for centrifugal chillers.

In [90] a fault detection method was presented, for air-source heat pump water chiller/heaters, based on principal component analysis model. Reference [91] implements a diagnostic Bayesian network of three layers in order to utilize more feature information of the chiller unit along with expert knowledge. The article in [92], proposes and implements a real-time distributed measuring nodes network to diagnose faults in uninterruptible high-power supply systems and high-power transformers of MG used for railway interlocking signaling installations. The proposed methodology is based on the thermal and electrical symptoms analysis and the mechanical degradation index by measuring the vibration. A failure mode and effect analysis (FMEA) approach was presented in [93], for fault diagnosis of energy storage unit, Valve-Regulated Lead-Acid

(VRLA) batteries, and 3-phase high power transformers, utilized in switching converters and power isolation. The FMEA approach utilizes a distributed measuring nodes network, described in [92], based on electrical (voltage, current, impedance) and thermal degradation analysis and vibration-based mechanical stress diagnosis.

In this study a hybrid technique was proposed by using BBN and ANFIS based technologies. The hybrid technique contributes an efficient tool for MEGs fault diagnosis. The results demonstrate that the hybrid BBN-ANFIS can perform fault diagnosis with complete or incomplete symptoms. The main strength of the proposed approach is due to its dependency on experts' knowledge than the data from measurement instrumentation (I&C) in its decision-making process.

2.12 Bayesian Belief Networks

Bayesian belief networks (BBN) is an expression for a probabilistic inference network that comprises the decision-making process based on Bayesian probability theory [94]. BBN was coined by J. Pearl in 1988, and it shows promises result in many different topics [95]. BBN is extensively used in safety assessment for systems with uncertainty and incomplete knowledge. Therefore, BBN is the base of different types of expert diagnosis systems in numerous fields such as nuclear power systems operation monitoring [96], oil and gas pipelines safety assessment [97], wind turbine fault diagnosis [98] and risk assessment of complex systems [99]. In [100], a comparison between BBN and the rule-based expert system was performed for fault detection. The study shows that BBN has more reliability than the rule-based system. In [101], a software prototype was developed for online fault detection and diagnosis for a turbine engine. This software has the ability for monitoring and classifying the faults based on its source, type and components. Another case study on a gas turbine was studied in [102] using BBN and it shows an impressive accuracy of 96%, with high reliability in fault detection and diagnosis. Other developed BBNs were presented in [103], to provide a probabilistic framework for accurate faults prediction and diagnosis. BBN was developed by several researchers that focused on fault diagnosis of a solar assisted heat pump system, in order to achieve an accurate fault identification for the heat pump[104]. BBN is a powerful tool to illustrate and to understand

complex systems with uncertainty and incomplete information [105]. Compared to the neural network, BBN provides superior performance information, which made BBN the most important research topic in the field of artificial intelligence [106]. There are several applications for BBN in fault diagnosis. In [107], a BBN was constructed, for industrial process, by tabulating the probabilities for each node based on expertise contribution. In [108], they implement a BBN by extracting statistic features of different time domains, for rotation gearbox. In [109], BBN offered fault diagnosis of wind turbine gearbox by using time-frequency domain. The results of the ultimate articles show promising achievements.

This thesis offers online fault analysis of MEG that predict risks and diagnose faults based on Bayesian belief network (BBN). The main objective is to develop an advanced and more robust predictive/diagnosis techniques to improve the MEG condition monitoring and alarming systems.

2.13 Energy Management and Optimization

Paper [110] proposed an architecture for resources management protocol for the microgrid (MG), based on DERs computational environment to achieve optimal scheduling for the electrical loads by using a genetic algorithm take in consideration tariff prices and forecasted power generation by renewable resources. The demonstration of the proposed architecture was validated on a multi-agent simulator platform. In [111] six different cases in MG system were studied to manage the MG consumption and generation further to control the utility connection in order to achieve optimal operation cost and minimal pollutant emission. A simple structure of MOPSO method using fuzzy logic was implemented and a promises results were shown using Matlab platform environment.Paper [112] classifies MG control strategies into three levels: primary, secondary, and tertiary, where primary and secondary levels are related to the operation of the MG itself, and tertiary level concerns to the coordinated operation of the MG and the host grid. ESS is recognized as a key technology for the combination of intermittent renewable energy sources. GA was utilized in [16] to achieve energy saving management for four buildings in Sejong, smart grid. The experimental results show a major saving on energy consumption which has a direct positive impact on cost and environment as well. Paper

[113] proposed A new class of MG, called provisional MG, to address prevailing challenges in MG deployments associated with islanding requirements. An uncertainty-constrained optimal scheduling model was proposed to efficiently model the day-ahead operation of provisional MG considering usual operational uncertainties. The robust optimization was employed, where the original problem was decomposed into smaller and coordinated problems for uncertainty consideration. The proposed model was analyzed through numerical simulations, and it was shown that provisional MG offers economic benefits, ensure reliability, and prevent underutilization of deployed capital-intensive DERs. An intelligent distribution over the grid was proposed in [114] to balance the supply and demand of the MG. Where a distributed energy management approach based on the consensus and innovations method is presented and used to coordinate local generation, flexible load, and storage devices within the MEG. Takes advantage of the fact that, at the optimal allocation settings, the marginal costs given as a function of the power output/consumption need to be equal for all nonbinding network resources. Paper [115] proposed an extended distributed model predictive control (DMPC) framework specifically for a combined environmental and economic dispatch (EED) problem which is a non-trivial multi-objective optimization problem at large scale smart grid case study. The DMPC is applied to a smart grid composed of 11 consumer centers, 6 energy storage, 11 generation systems and 31 transmission lines. Simulation results show reductions of generation costs up to 40% when predictions are included in the formulation. Furthermore, the simulation of forecast errors results in up to 8% generation over cost. Paper [116] presents a two-stage stochastic model with fuzzy chance-constrained programming for MG operation. The model is aimed to optimize the generation schedule for the dis-patchable DERs based on day ahead generation schedule and the real-time emission control criteria. A mixed integer linear programming (MILP) model was presented in [117] to define the optimal size and operation for seven CCHP units serving heating, cooling and electricity demands. Experimental results for optimal operation cost and minimal emission generation was conducted for a residential district in the east of Tehran. Paper [118] presents an optimization algorithm in order to determine the optimal arrangement of DERs operation in a microgrid. The proposed algorithm intended to minimize the fuel consumption only without taking in consideration the operational cost and gases emission.

In this study a MILP optimization technique was utilized to predict the MEG operation by using static MEG model. This static model is used to validate the dynamic MEG model that implemented using the Simulink platform. The comparison between MEG's models verify the effectiveness of the proposed approaches.

CHAPTER 3 Design and Simulation of a MEG Case Study

This chapter is aimed to build a MEG case study model that emulate existing MEG infrastructures and operation. This case study is implemented by using dynamic models for the main components of the MEG namely co-generator, TESs and chillers. The MEG dynamic model is implemented using Simulink and Matlab platform. The MEG dynamic model will be used throughout this thesis as a case study to assess the proposed risk analysis methodologies that are proposed in this thesis

3.1 System Description

MEGs consist of localized energy generation equipment. It may consist of microturbines, solar panels, wind turbines, fuel cells, etc., which can provide energy to a local area in a cleaner way. MEGs operate either in a main grid-connected mode or in an islanded mode [119]. In a main grid-connected mode, MEGs exchange energy generated by renewable sources with the utilities grid. In the case of energy outage on the main grid, MEGs can take charge and provide the required energy to the end users. However, the islanded mode has accompanying intermittency in the energy flow. The simulation results illustrate that the dynamic performance of the MEG during and after islanded-mode is better when supplementary storage devices supported the MEGs, as compared to those without energy storage. Therefore, it is a better option to have MEGs equipped with storage devices for better overall dynamic performance.

In-depth, detailed models of MEG components dynamic performance are extensively available [120]. Nevertheless, integration of such detailed models for complete MEG optimization would eventually result in undesirably massive computation times and other associated challenges [15]. Therefore, reduced order models are necessary. Without losing important dependencies expressed by detailed models.

A selected MEG shown in [15][17] is presented in this research as a case study for safety implementation of a resilient MEG. Different MEG's configuration can be utilized for the same purpose, which is not the aim of this study.

The MEG model is shown in *Fig. 3.1* has the ability for self-sufficiency in its electricity, cooling and heating demands most of the year by utilizing DG, PV, WT, and district heating/cooling units with TES and supercapacitor bank for swift and dynamic power backup. Despite that the MEG has the ability to operate in islanded mode, it is interconnected with the capital grid to ensure resilient operation in case of hazard scenarios, and offers backup source for uncertain increasing demands. A set of six electric thermal cooling units of varied size and performance characteristics, shown in ***Table 3-1***, produces cold water to supply the cooling demand, and/or is stored in a 400 MWh TES tank for future use. An on-site 15 MW cogeneration gas turbine (CG) is the prime mover source of electrical power for the facility. Furthermore, exhaust gas from the CG is used to provide steam to a heat recovery steam generator. Where the steam is used for driving a 3 MW steam turbine in order to produce additional electrical power and to produce heat energy in order to meet the majority of the facility-heating load shown in *Fig. 3.2*.

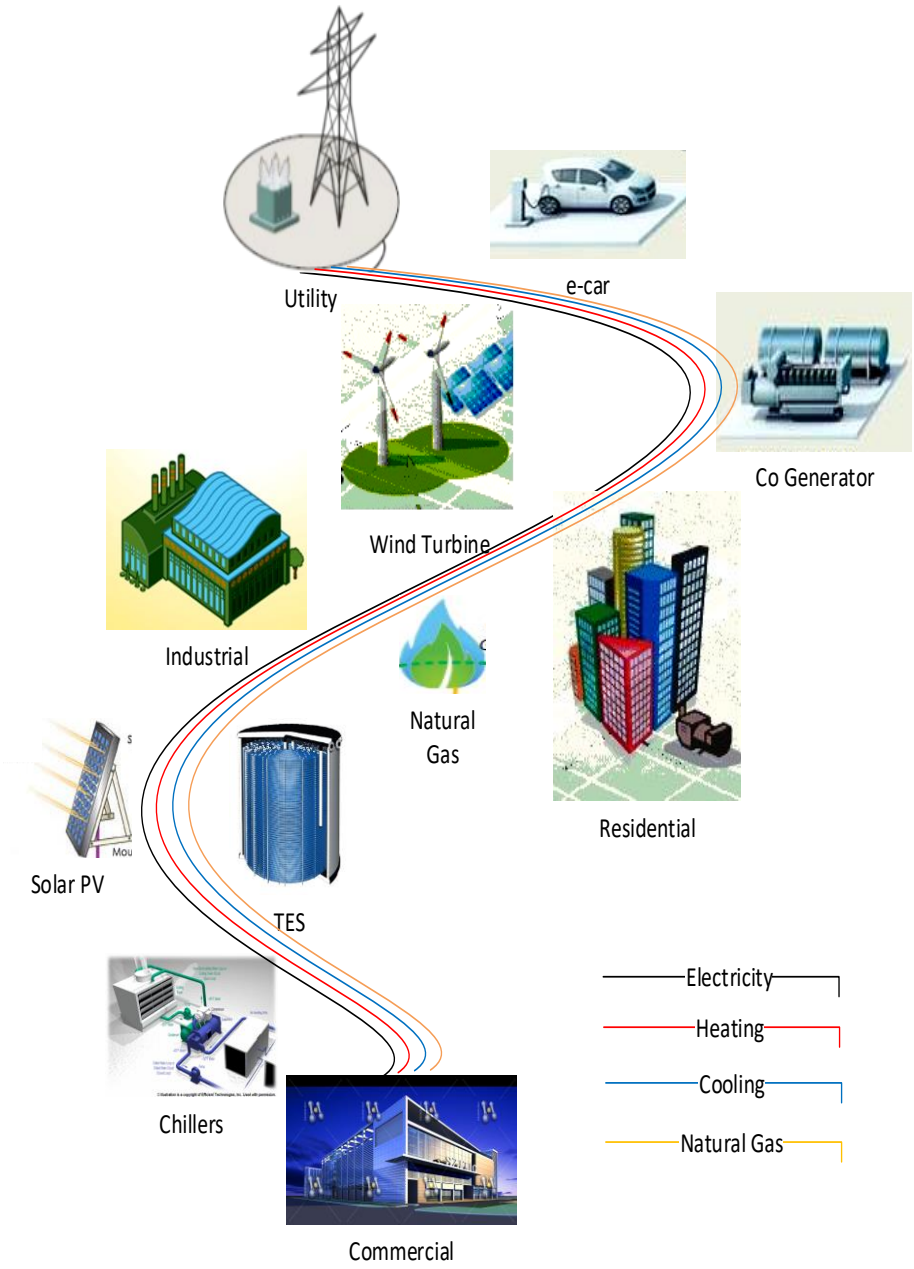

Fig. 3.1: *Proposed MEG case study model*

Table 3-1: *Thermal cooling units rated size and coefficient of performance (COP).*

Thermal cooling	**Thermal Cooling Unit-1**	**Thermal Cooling Unit-2**	**Thermal Cooling Unit-3**	**Thermal Cooling Units 4, 5 & 6**
Size (Tons)	900	1000	2800	3500

Size (kWe)	600	620	2000	2100
COP	5.0	5.5	4.5	6.0

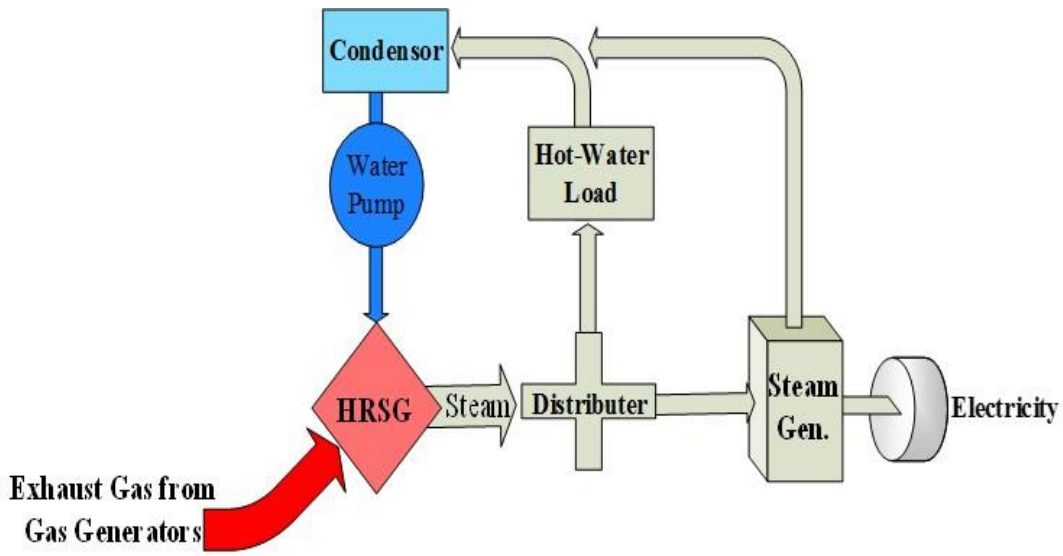

Fig. 3.2: *Steam loop schematic diagram* [15]

3.2 Detailed Model of MEG Components

3.2.1 Co-Generator Gas Turbine

The gas turbine is one of the effective power generation technology, which operates on the thermodynamic cycle or Brayton cycle. This turbine is mainly composed of three stages: a compressor, a combustor and a turbine. The compressor increases atmospheric pressure into the combustor. The combustor merges this air with fuel then burns the mixture. Then the exhaust hot gases sent into the turbine, to convert the energy into mechanical work [121]. Fig. 3.3 shows the principal components of a simple-cycle gas turbine. The gas turbine is used in the MEG to produce electrical power as a conversion of the turbine mechanical work with an electrical efficiencies range from about 20 to 25%, as well as produces hot exhausted gases which can be 700K to 866K, depending on the type of turbine. These high exhaust temperatures are a ground for several studies and researches for restoring this wasted thermal energy [122].

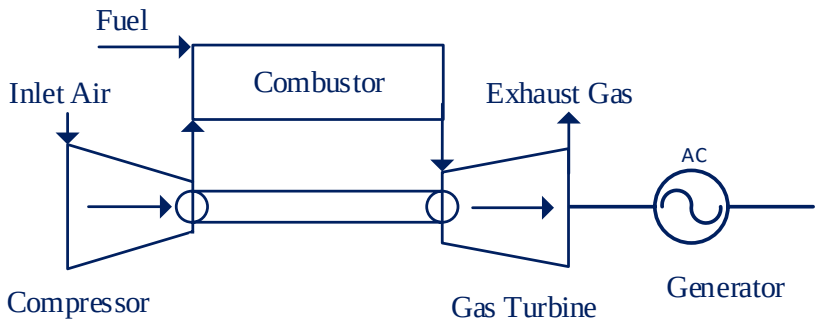

Fig. 3.3: *Gas turbine model*

The dynamic behavior of the gas generator can be simulated by identifying the nonlinear form of mass and energy conservation equations for each component. In addition, applying some static equations to complete the linear model. Schematic of the gas turbine is shown in Fig. 3.4.

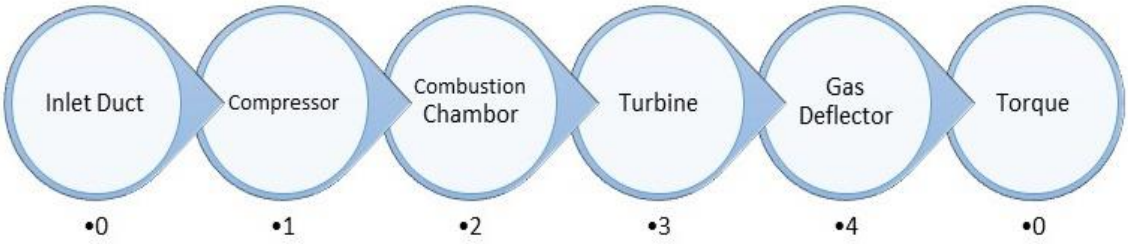

Fig. 3.4: *Schematic diagram for gas turbine*

The static model of a Co-Generator (CG) can be obtained by using thermodynamic equations and map the components in order to determine the off-design performance of the CG with constant output power [123]. There are three types that modeling the CG namely static, dynamic nonlinear and linearizing of dynamic nonlinear equations. The static model is the simplest one of the three models however it is the lowest accuracy among them as it cannot emulate the transient condition of the CG behaviour. On the other hand, the dynamic nonlinear model is the most accurate mimic, however it has more complicated mathematical computation and consequently lead to longer process time consumption. In this study the linearization model of dynamic nonlinear equations is utilized to have an accurate performance emulation and a reasonable computation time duration [123].

The efficiency of the prime mover such as steam turbine, gas turbine and diesel engine can be presented as:

$$\eta_m = \frac{W_s}{H_f} = \frac{W_s}{m_f H_u} \tag{3-1}$$

where

$\dot{W}_s$ prime mover shaft power

$\dot{H}_f$ the fuel power consumed by the system

$$\dot{H}_f = \dot{m}_f H_u \tag{3-2}$$

$\dot{m}_f$ flow rate of the fuel mass

H_u the lower heating value of the fuel

The electrical efficiency is presented using this equation:

$$\eta_e = \frac{\dot{W}_e}{\dot{H}_f} = \frac{\dot{W}_e}{\dot{m}_f H_u} \tag{3-3}$$

where $\dot{W}_e$ is the useful electric power generated by the cogen.

The thermal efficiency is presented using this equation:

$$\eta_{th} = \frac{\dot{Q}}{\dot{H}_f} = \frac{\dot{Q}}{\dot{m}_f H_u} \tag{3-4}$$

where $\dot{Q}$ is the useful thermal power generated by the cogen.

Therefore, the total efficiency of the cogenerator

$$\eta = \eta_e + \eta_{th} = \frac{\dot{W}_e + \dot{Q}}{\dot{H}_f} \tag{3-5}$$

3.2.2 Heat Recovery Steam Generator

The heat recovery steam generator (HRSG) is defined as an energy recovery heat exchanger that recaptures heat from a hot gas stream. The steam is generated to drive a steam turbine. A combined-cycle power station (CC) is a common application for an HRSG, where the hot exhaust gas produced from a gas turbine is fed to an HRSG to produce steam to drive a steam turbine *Fig. 3.5*. The CC produces electricity more efficiently than either the gas turbine or steam turbine individually, where the electrical efficiency range from about 25 to 45% and overall CC efficiency of 65 to 80% for

combined electrical and heat energies [122]. The HRSG consists of four major components: Evaporator, Superheater, Economizer, and Drum. The different components are combined to meet the operating requirements of the unit [124]. The high quality heat from the gas turbine exhaust allows to utilize the thermal energy to generate electricity by a steam turbine along with the gas turbine in a combined cycle system process also allowing the thermal energy to be restored and used for heating or cooling of the premises and used to provide domestic hot water [125].

The following equation evaluates the volume of steam that HRSG is able to generate [126]:

$$W_s = \frac{W_g C_p (T_1 - T_3) eLf}{h_{sh} - h_{saf}} \tag{3-6}$$

Where: W_S = steam flow rate; W_g=exhaust flowrate to HRSG; C_p = specific heat of products of combustion; T_1 = gas temperature after burner; T_3 = saturation temperature in steam drum; L = a factor to account radiation and other losses= 0.985; h_{sh} = enthalpy of steam leaving super heater; h_{saf} = saturated liquid enthalpy in steam drum; e = HRSG effectiveness = $\frac{(T_1 - T_2)}{(T_1 - T_3)}$; f = fuel factor, 1.0 for fuel oil, 1.015 for gas.

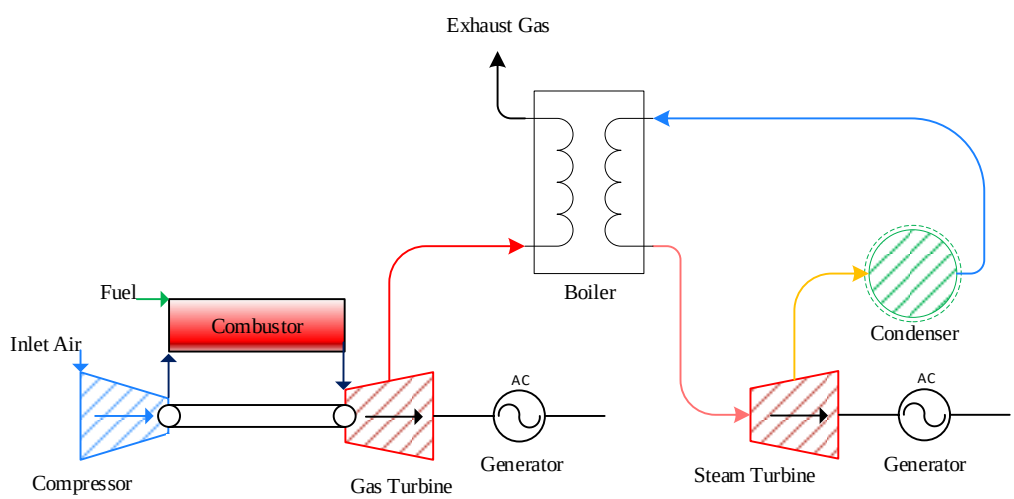

Fig. 3.5: *Combined cycle power plant*

In order to simplify the model, the CHP unit is compacted in a single block that has fuel as input and the outputs are electrical and thermal energy. The fuel power (P_{fuel}) in kW

proportion to the fuel flow ($\dot{V}_{fuel}$) in m^3/s times the constant fuel heating value (H_i) kJ/m^3, as given below [127].

$$P_{fuel} = \dot{V}_{fuel} x H_i \tag{3-7}$$

The above equation is used in this study to calcualte the fule volume that is required to operate the CHP unit.

The transfer function of the thermal energy is shown in the equation below.

$$G_{thermal} = \frac{k_1}{(1 + k_2.s + (k_3.s)^2)(1 + k_4)} \tag{3-8}$$

where the constants used are as follows $k_1 = 0.43472$, k_2= 2.5774, k_3= 1.7472, k_4= 7.409.

And the transfer function of the electrical energy is shown in eq. 3-9.

$$G_{electricity} = \frac{k_1}{(1 + k_2.s)} \tag{3-9}$$

where the constants are as follows: $k_1 = 0.4386$, k_2= 0.61823.

These two transfer functions are presenting a compact block of the CHP dynamic performance that will be used in this study in the Simulink case study Section 3.3.

3.2.3 Thermal Energy Storage

The principle idea behind using thermal energy storage (TES) is to provide a buffer to balance fluctuations in supply and demand of energy [128]. Energy demand in the residential, commercial and industrial regions fluctuates in course of day periods, intermediate periods (e.g. seven days) and seasons (spring, summer, autumn, winter). Consequently, various TES systems are utilized to match the demand as well as to reshape the actual demand on the energy sources. TES has been used for decades in different forms for space and process heating/ cooling applications. Different types of materials such as latent or phase change materials (PCM) and sensible heat materials have been applied to be used as prospective heat transfer medium for the energy storage application. For the

latent, the thermal energy is absorbed and released by a phase change of the storage media by fusion. However, the sensible heat storage materials were utilized based on its ability to raise or lower the temperature of storage media without a phase change [129].

A stratified cylindrical tank operates either on transfer and retrieval mode consequently the concluded model is a hybrid. The relationship between the number of nodes used in simulation and the degree of stratification which the model predicts are shown in ***Fig. 3.6***. Tank operates either in charging or discharging modes; therefore, the resulting model is a hybrid. The TES can be modeled using dynamic finite element based, which divides the tank into 100 control volumes along its height. Energy and mass conservation laws are applied to each control volume [123][130].

The approximate dynamic temperature profile of a TES system can be simplified as follows:

$$\rho C_p A_{xs} \Delta x \frac{dT_i}{dt} = C_p \dot{m}_{sink}(T_{i-1} - T_i) + C_p \dot{m}_{source}(T_{i+1} - T_i) - UP\Delta x(T_i - T_{amb}) + \frac{\varepsilon A_{xs}}{\Delta x}(T_{i+1} - 2T_i + T_{i-1}) \quad (3\text{-}10)$$

Where: ρ: storage fluid density, C_p: storage fluid heat capacity, Δx: length of node, $\dot{m}$: mass flow rate, T: time, U: tank fluid to ambient overall heat transfer coefficient, P: tanks perimeter, A_{xs}: tank cross sectional area.

The basic function of thermal energy storage is to accumulate the surplus thermal energy in order to be utilized when it is needed. In this study the thermal energy storage model is not consider internal losses of the TES, therefore it is represented by an integration operation with a limited capacity as shown in 3-11 [131].

$$S(t) = \begin{cases} S_{max} & if\ S(t-1) \geq S_{max} \\ S_0 + \int_{t_0}^{t} P_{th}(t) - D_{th}(t) & if\ P_{th}(t) > D_{th}(t) \\ S(t-1) & Otherwise \end{cases} \quad (3\text{-}11)$$

Where S_0 is the thermal energy in kJ that stored initially in the TES, S_{max} is the maximum thermal storage capacity that the TES can reserve in kJ, P_{th} is the input thermal power kW and D_{th} is the thermal power demand kW. Hence the *kJ= 3600*kWh*

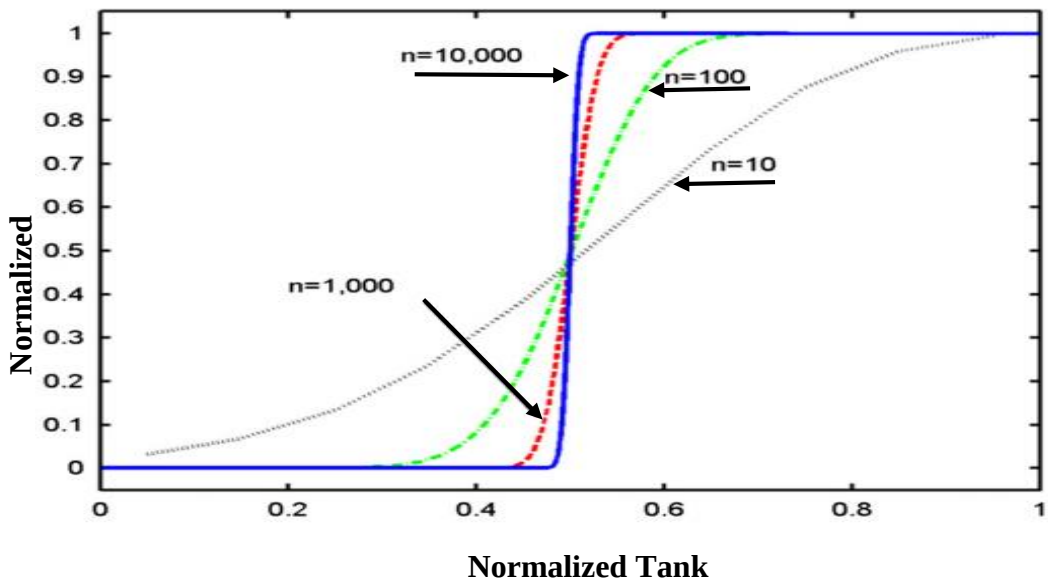

Fig. 3.6: *Simulated TES profile*

3.2.4 District Thermal Cooling Unit

The district thermal cooling unit is modeled using the standard approach for an integration of static models for essential components, such as evaporators, condensers, compressors, cooling towers, and pumps [132]. where the ideal compressor equation:

$$W_{comp-s} = \left(\frac{n}{n-1}\right) \dot{m}_{ref} P_2 V_2 \left[\left(\frac{P_2}{P_1}\right)^{\left(\frac{n-1}{n}\right)} - 1\right] \tag{3-12}$$

The compressor polytrophic efficiency is evaluated by:

$$\eta_{pol} = \frac{1}{CPR}\left[\frac{W_{comp-s}}{\eta_m W_{comp-design}}\right] \tag{3-13}$$

and the actual compressor work is defined by:

$$W_{comp} = \frac{W_{comp-s}}{\eta_m \eta_{pol}} \tag{3-14}$$

The thermal cooling model in this study can be presented as a constant amplifier of the COP value as the chiller units are conventional type which mean the operation status either ON full load or OFF and the transient period is not important in long operations studies.

3.3 A MEG Modeling and Simulation

The performance of the proposed resilient MEG, which guarded by selected independent resilience layers (IRLs) can be validated by implementing a model of MEG case study in Simulink and Matlab programming platforms. The mathematical equations of the model performance can be converted into more tangible models by using interactive graphical shapes in the Simulink environment

In this chapter, a MEG with adaptive control/scheduling algorithms for its local energy sources is implemented to study the MEG operation performance during normal and/or peak demands. Moreover, those adaptive algorithms facilitate self-healing capability during main/upstream grid failure. This is because the MEG can operate independently in isolated mode by using its generation sources and energy storage units to meet the local demand.

3.3.1 Simulation of a MEG Case Study

In order to demonstrate and validate the dynamic behavior of MEGs integrated with different combinations of IRLs that will be illustrated in Section 4.6, a MEG case study shown in ***Fig. 3.1*** is implemented in the Simulink environment. Dynamic systems that have time-varying characteristics can be modeled and simulated accurately by using the Simulink platform and Matlab programming environments. Simulink has the ability to convert mathematical equations that describe the model behavior into interactive graphical shapes, which are more understandable models.

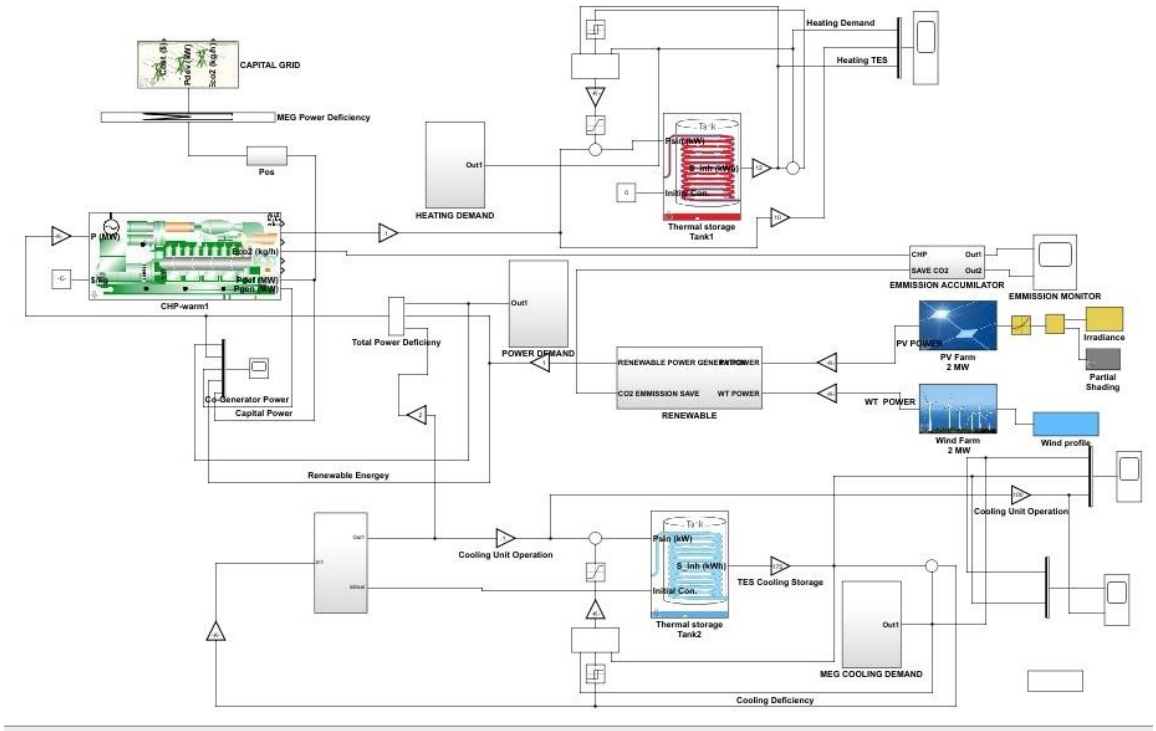

Fig. 3.7: *Simulink model for proposed MEG system*

The proposed MEG structure is implemented in the Simulink environment shown in ***Fig. 3.7***, to study the system performance in different operational scenarios to examine the MEG resiliency for prescribed cooling, heating and electricity energy demands.

3.3.2 Operational Scenarios of MEG Simulation

Data for a one week in summer with two-hours sampling time has been analyzed to evaluate and improve the MEG system operation. The interaction between Co-generators, thermal cooling units (TES) and the utility's grid are explored to increase MEG's safety level, resilience, and self-healing.

Four baseline strategies are explored in this section as follows:

1. <u>In the first baseline strategy</u>, one IRL was utilized, i.e. Co-generator.
2. <u>In the second baseline strategy</u>, two potentially valuable structures, namely TES and Co-generator, are used.

3. In the third baseline strategy, a heuristic rule-based methodology using physical anticipation model is used to determine the operating attributes of the MEG without installing additional MEG's hardware.

The proposed IRLs integration are aiming to reduce the MEG's failure hazard by optimizing DERs operation and TES energy storage.

First Scenario Strategy:

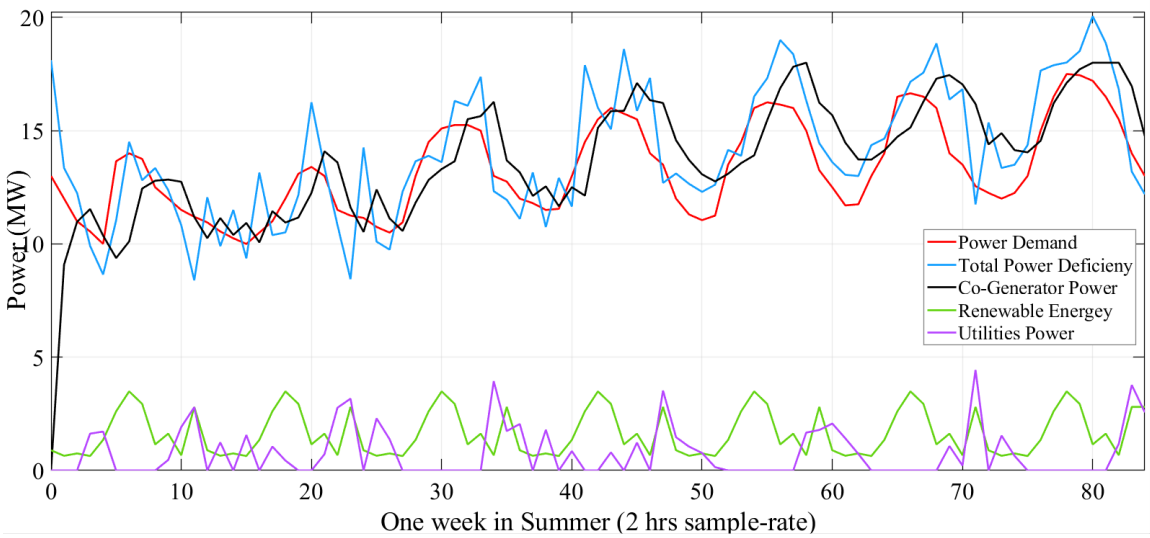

Fig. 3.8: *Power profile for foundation MEG (2hrs rate sample)*

Fig. 3.8 illustrates the power demand profile for a one week in summer for the original MEG integrated with one IRL, i.e. Co-generator. The figure defines that the combination of Co-generator and renewable sources are unable to handle the electricity demand. Thus, the electricity-utility grid must interfere to cover the power deficiency caused by a sudden rise in the electricity demand. The power deficiency caused by two reasons, first due to the limited capacity of DERs and secondly due to the dynamic behavior of the co-generator that lead to a delayed response to the rapid change in the demand profile.

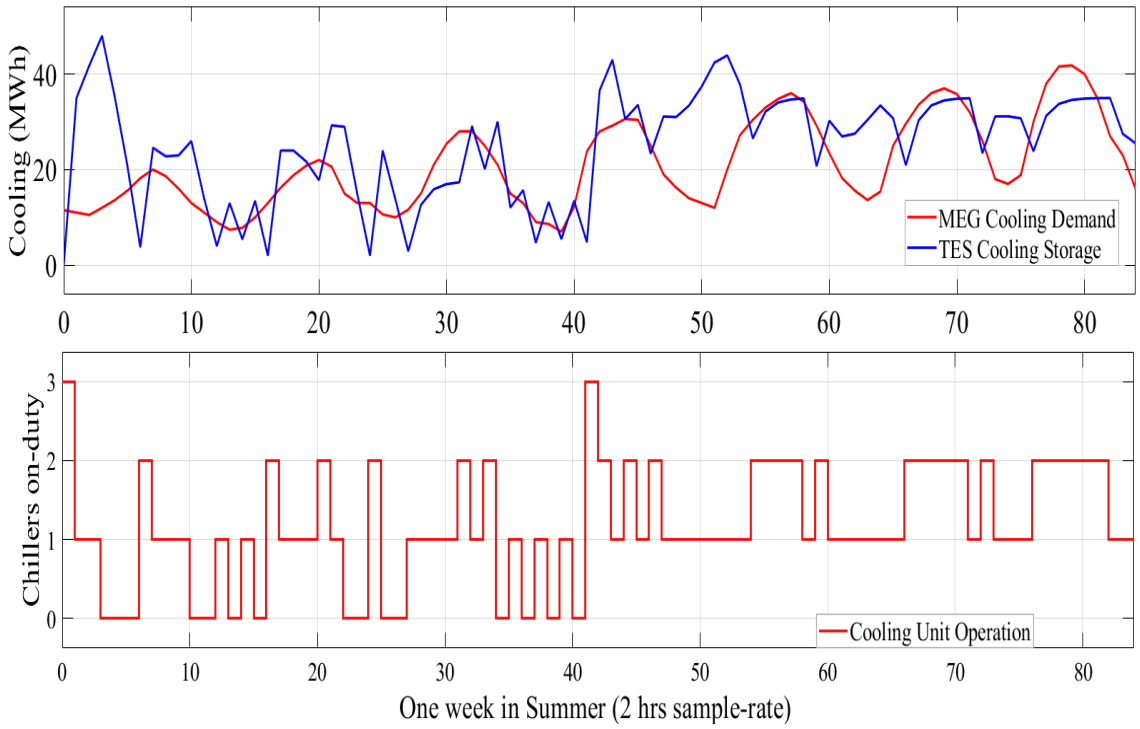

Fig. 3.9: *Cooling profile for foundation MEG(2hrs rate sample)*

Cooling profile in **Fig. 3.9** shows the MEG cooling demand of a one week in summer without utilizing TES, the figure illustrates a high frequency of on-off operation of the district cooling units (DCU) during the course of the day. The more on-off operations lead to a high dramatical reduction in the DCU performance. Where during the DCU's start-up the inrush current is more than double of rated current values. On the other hand, it can be noticed that all the DCUs are on duty most of the day with an increasing number of operating units during the on-demand period. In addition, the high correlation of cooling demand with electricity demand increases the operation complexity and increases the total on-peak electricity demand.

Second Scenario Strategy:

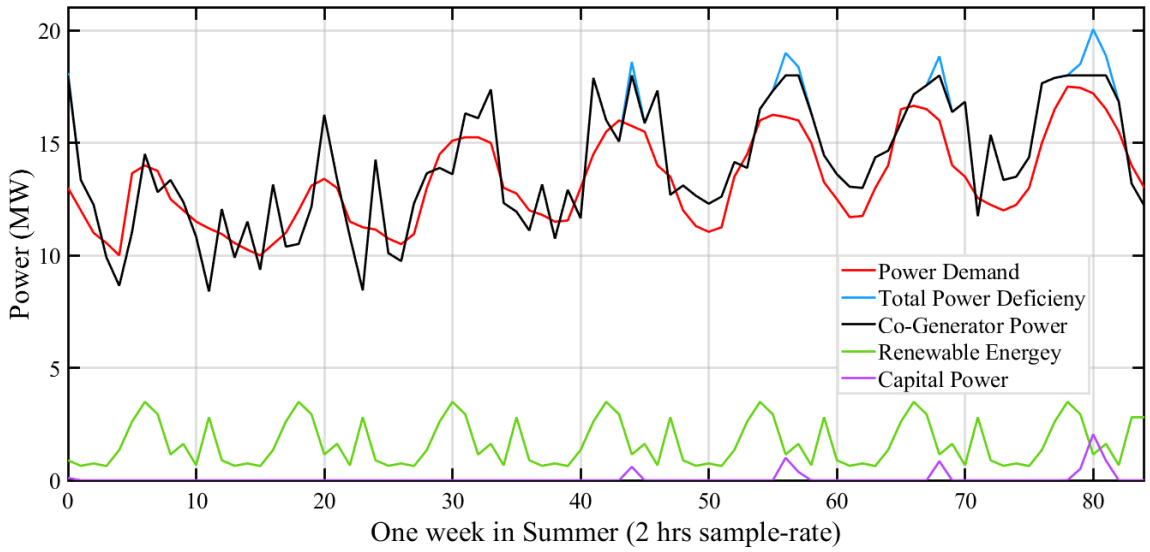

Fig. 3.10: *MEG power profile by utilizing co-generation and TES IRLs (2hrs rate sample)*

Fig. 3.10 presents the electricity demand profile of a one week in summer for a MEG consists two IRLs i.e. Co-generator and TES. The figure above illustrates that the co-generator was capable to cover the electricity demand in the first four days by the support of RES. Whilst, in the last three days of the same week, the utility grid was interfered partially to cover the power deficiency caused by a sudden rise in the demand. The power deficiency occurred two times a day with a maximum capacity of 4 MW for an interval of two hours, while the Co-generator serves an average of 14 MW with a maximum production of 18 MW.

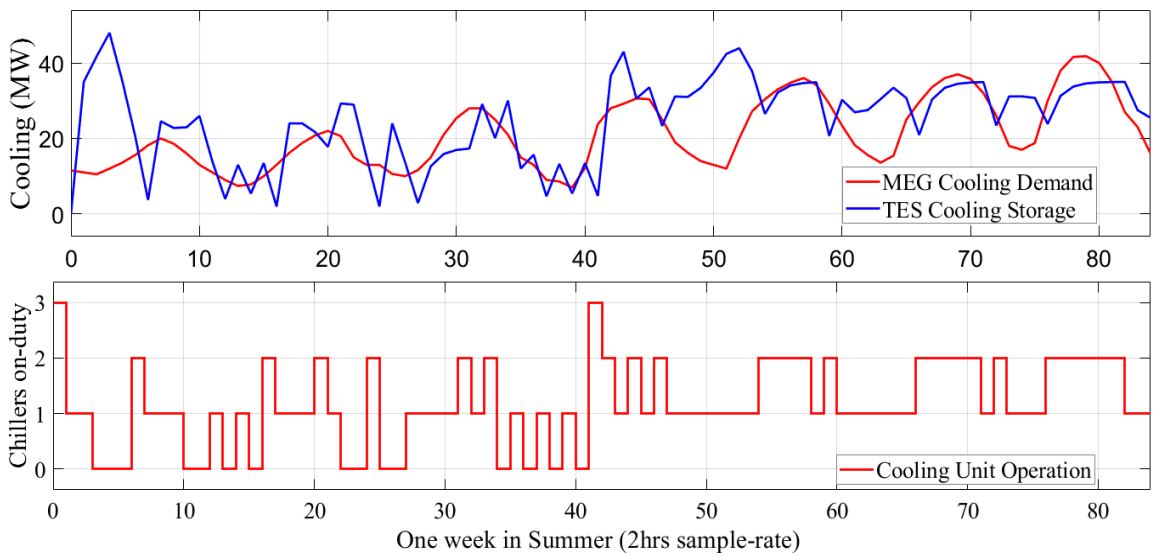

Fig. 3.11: *MEG cooling profile by utilizing co-generation and TES IRLs(2hrs rate sample)*

Cooling profile in ***Fig. 3.11*** shows the MEG cooling demand within a one week in summer under the second scenario conditions. The figure illustrates that despite the high correlation between cooling demand and electricity demand the use of TES improves the cooling imports with less operational hours of DCUs.

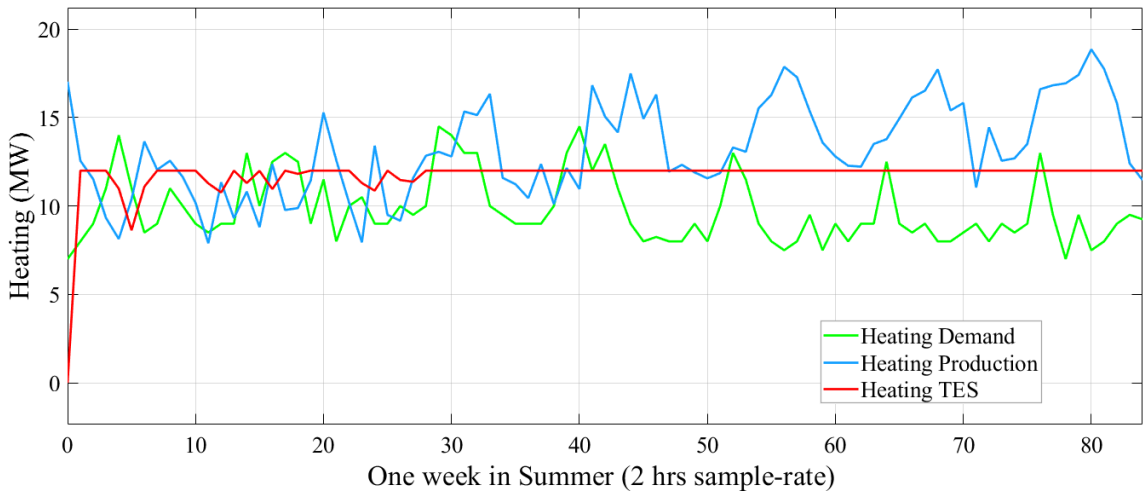

Fig. 3.12: *MEG heating profile by utilizing co-generation and TES IRLs*

Fig. 3.12 presents a sample of heating demand profile for one week in summer. The figure shows extensive coverage of heating demand by the heating energy generated by the

Co-generator. In addition, it can be noticed the Co-generator produces a surplus heating energy than needed. In addition, there is a low correlation between electricity demand and heating demand during the summer season.

Third Scenario Strategy:

The integration of the three IRLs into the original MEG promotes its operation to an islanded mode under most of the operating conditions without the need for utility grids interference.

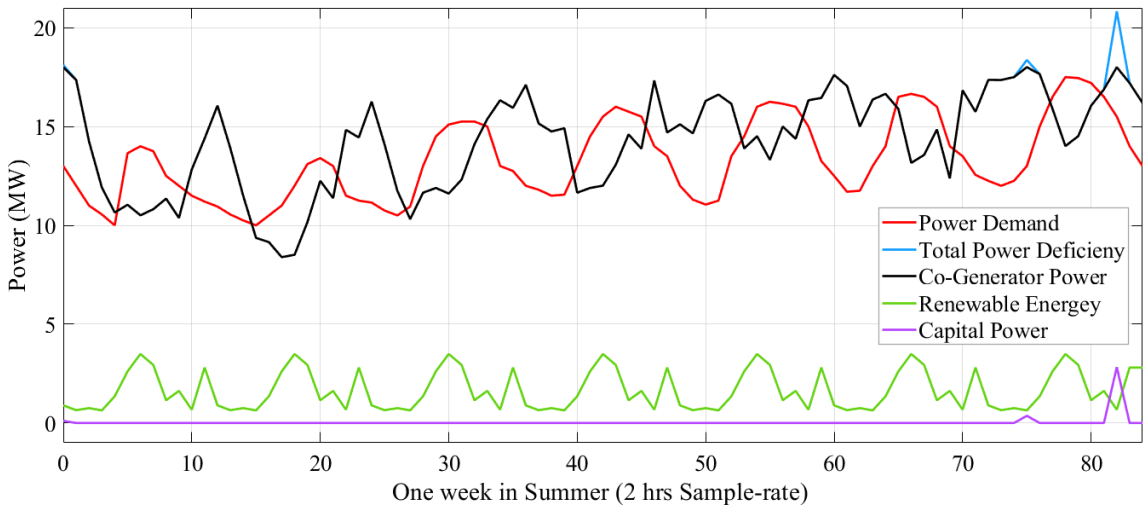

Fig. 3.13: *MEG power profile by utilizing IRL-1, IRL-2 and IRL-3*

Fig. 3.13 shows the Co-generator ability to cover the power demand in the first five days with the support of RES, while in the last two days the utility grid interferes was lightly required to cover the deficiency of sudden rise in the power demand. The power deficiency occurred twice within the tested week, for a period of two hours in each, with maximum 3 MW while co-generator serves an average of 12 MW with a maximum production of 18 MW.

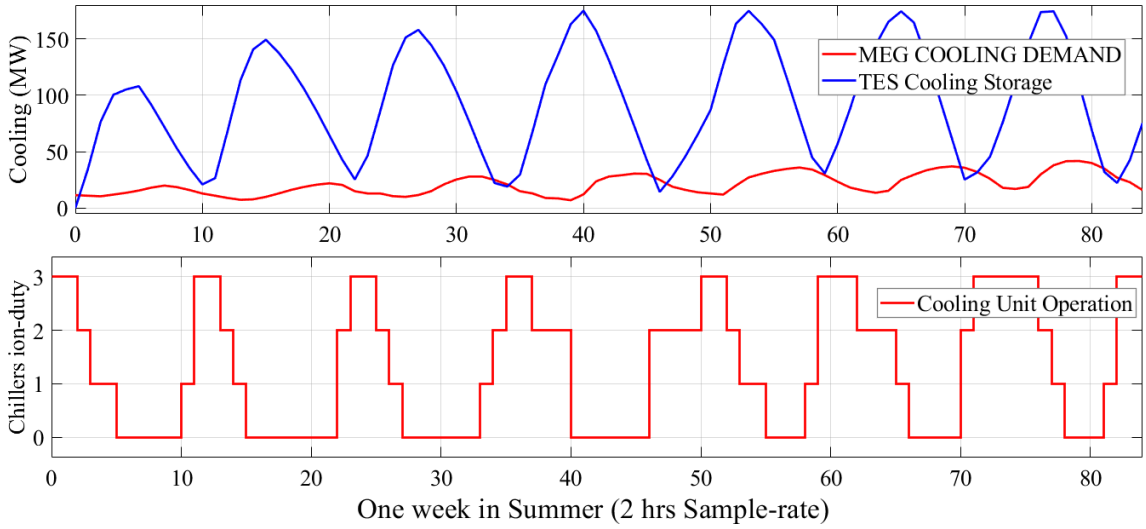

Fig. 3.14: *MEG cooling profile by utilizing IRL-1, IRL-2 and IRL-3*

The cooling profile in ***Fig. 3.14*** shows an improvement in the thermal cooling unit operations, where cooling on demand was shifted completely to the off demand period, by rescheduling the operation of the DCUs. The reframing of the cooling profile has major advantages on electricity and cooling production industry, where reshaping the cooling demand is increasing the MEG's capability without the need for additional physical hardware upgradation. In addition, it improves the MEG resilience and self-healing competence.

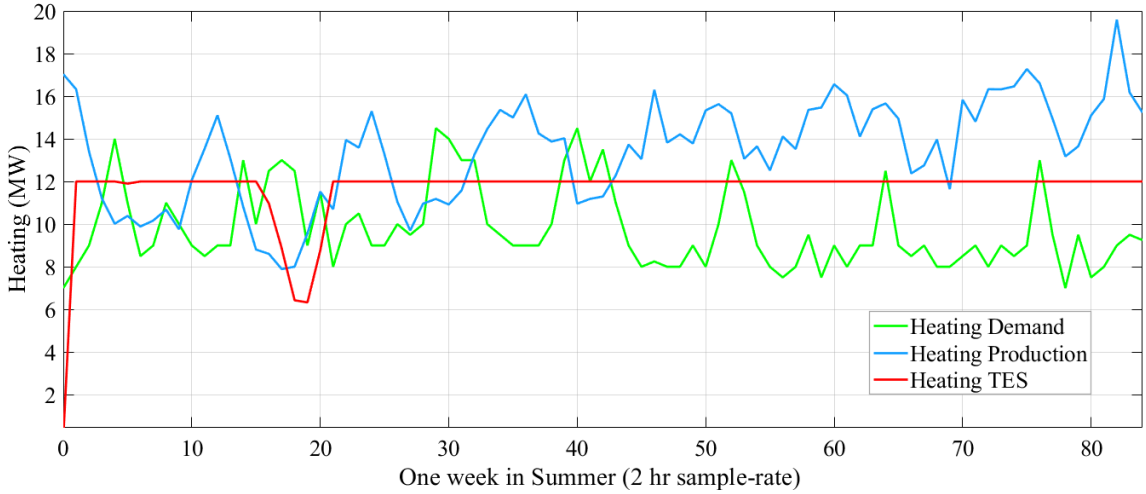

Fig. 3.15: *MEG heating profile by utilizing IRL-1, IRL-2 and IRL-3*

The heating demand profile for a one week in summer was illustrated in ***Fig. 3.15***. Wide coverage of the heating demand can be achieved by the heating generated from the co-generator. However, the low correlation of electricity demand and heating demand particularly during the summer season makes asynchronous between the heating demand and the heating generated by co-generator. The comparison between ***Fig. 3.12*** and ***Fig. 3.15*** shows that still there is squandering in the heating production.

3.4 Resiliency Requirements Analysis for MEG

The most global threats such as climate change, civilization and depletion of natural resources are the main challenges of the energy industry. The resiliency and sustainability of energy industry in cities is affected by numerous threats that can be categorized as follows, see ***Fig. 3.16***:

1- Generation fluctuation
2- Load demand fluctuation
3- Weather volatility and climate change
4- Cyber attacks and terrorism
5- Technical malfunction such as technology, component

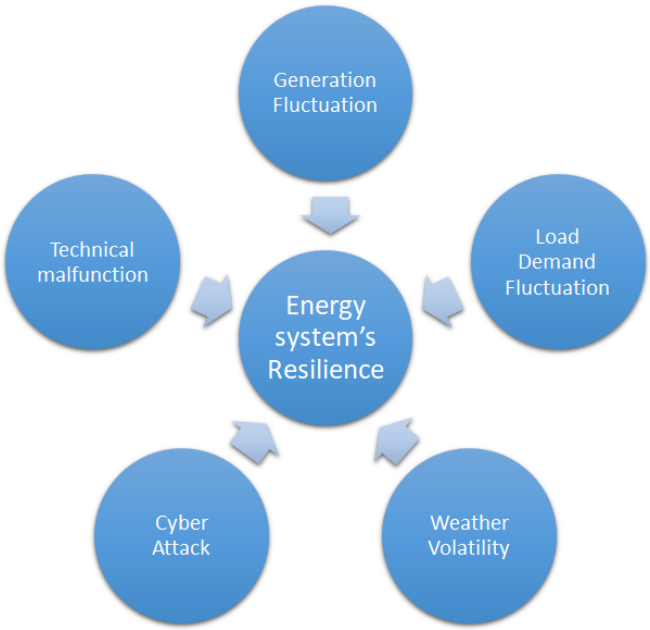

Fig. 3.16: *Threats types on energy system resiliency*

To determine the threats impact on the energy entity is paramount to avoid interruption in energy supply [83]. The resilience is an approach aimed to eliminate hazardous consequences in socio-econo-ecological parameters that influence respectively the life quality, economic activity, and environmental sustainability. Resilient guards ensure maintaining the system operates as designed.

The resilient MEG should be enhanced at the design stage to guarantee the availability, accessibility, affordability, and acceptability of the energy service under different circumstances in order to achieve resilient MEG. Thus, resilient MEG must consist the following characteristics to ensure a resilient performance: robustness, stability, flexibility, resourcefulness, coordination capacity, redundancy, diversity, foresight capacity, independence, interdependence, collaboration, agility, adaptability, self-organization, creativity and efficiency [133].

The literature on MEG resilience still limited. The core innovation of this study is the proposal of design a resilient MEG from a safety perspective. Where this study is an attempt to cope the gap between the requirements for a resilient MEG design and the safety analysis tools.

A resilience risk performance indicator (RRPI) is proposed in this study to evaluate the MEG resilience. The RRPI is derived from safety analysis concepts in order to identify the MEG safety design criteria that are required for resilient MEG. In addition, RRPI is able to link this criterion with the essential components of the independent resilience layers (IRLs). IRLs are proposed in Section 4.6 to improve the resiliency of MEG at numerous hazardous events.

3.5 Chapter's Conclusions

A safety design of a MEG is proposed in this study in order to mitigate major hazards that threaten the original MEG, by increasing the energy grids resilience by using three IRLs. The Co-generator, TES, and a heuristic rule-based methodology controller are used as IRLs to enable the MEG working in an islanded mode for normal energy demands during different seasons. Those IRLs increase the MEG reliability to more than double its normal capacity, while the co-generator, TES, and heuristic rule-based methodology controller

offer a significant reduction in the utility grid risk severity. Subsequently, the IRLs enable the improvement of MEG performance with practical everyday considerations, such as equipment maintenance and variation in energy demand, that affect MEG operation and load distribution. Predicting future load profiles from historical data can provide a tolerable approximate tool for scheduling the dispatch of MEG resources. The optimal energy imports can be achieved by using real-time energy dispatch control for effective management of MEG resources and energy flow mapping.

CHAPTER 4 Safety Design, Risk Assessment and Proposed Resilience Layers for MEG

4.1 Design of Resilient Micro Energy Grid

The current reliability, resiliency and sustainability methods are dealing with these hazards separately [134]. This study aims to propose a framework that addresses the demand of a resilient MEG by using safety analysis tools in order to offer a greater clarity to the decision makers. The socio-econo-ecological method that declared in Section 3.4 is proposed to design a resilient MEG by modifying MEG's stability characteristics using the framework illustrated in **Fig. 4.1** and described in the following points:

1. Initiate the design process based on the available information of MEG's hazard scenarios that need to be eliminated.
2. Monitor the system's resilience risk performance indicator (RRPI) during the hazard scenarios. (will be discussed in section 4.2)
3. Eliminate fault consequences in order to keep the system functioning by adding non-SIF independent resilience layers (IRLs). (will be discussed in section 4.6)
4. Adapt system's characteristics, based on internal learning reasoning and expert knowledge on the learned lesson, by adding SIF IRLs to improve the system's RRPI and to cope future hazard events. (will be discussed in section 4.6)

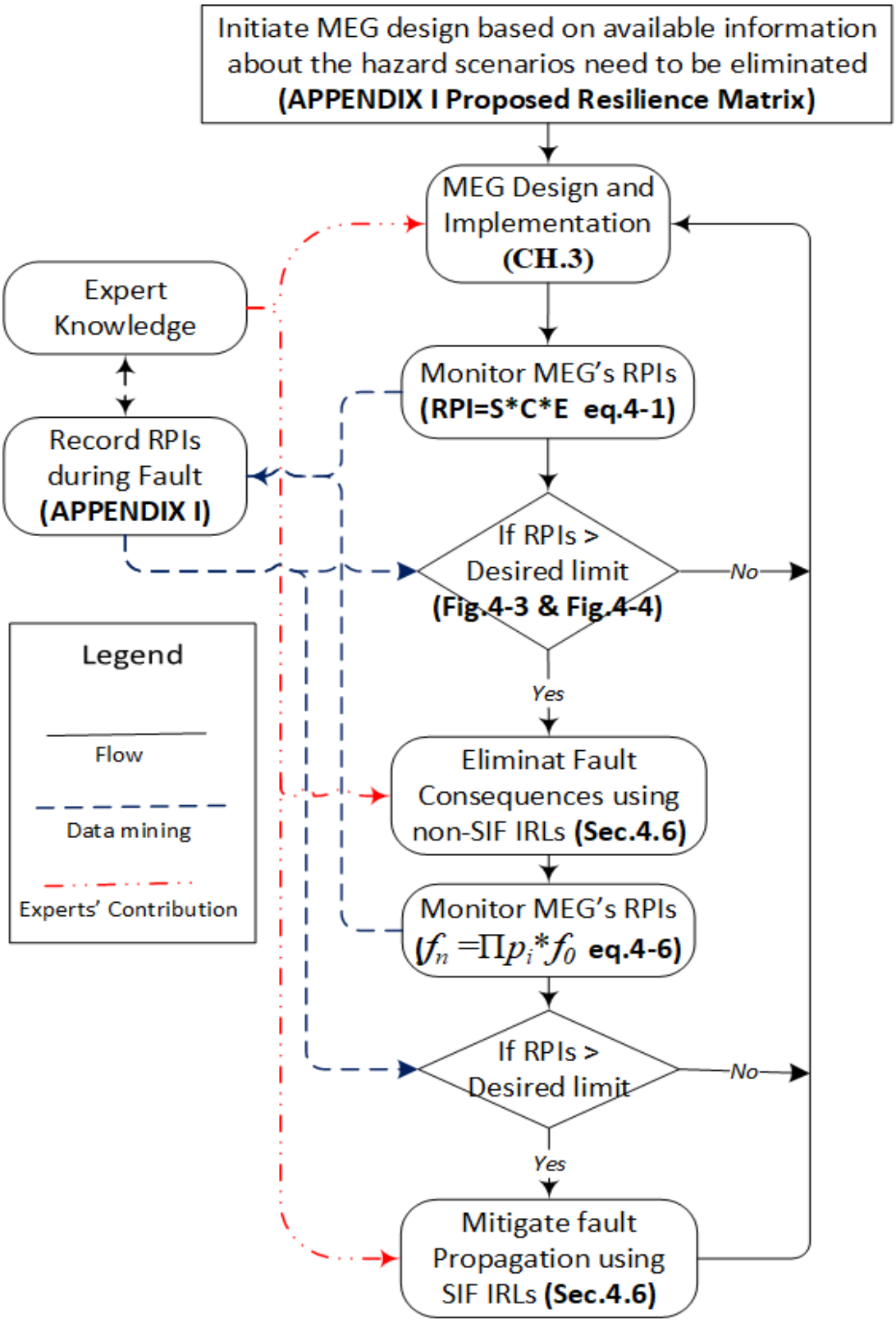

Fig. 4.1: *Proposed resilient micro energy grid implementation framework*

4.2 Proposed Resilience Matrix for MEGs

Risks are generally measured based on probabilities theory. Risk assessment methodologies are based on the historical statistical information of similar systems' characteristics that give the risk management team the ability to assure certainty of risk measurement in numeral values [135].

The safety design toward resilience of complex systems, such as MEG, requires extending MEG's flexibility to cope with unknown variations, in addition, to deal with known variations

The first use of risk matrix was in 1973 [136]. The risk matrix is an effective methodology used in risk analysis. The proposed resilience matrix (RM) is derived from the hazard matrix by adding a socio-econo-ecological attributes named resilience risk performance indicator (RRPI). The RM has the ability to visualize and rank the hazard event of a MEG based on its RRPI. The RRPI is a proposed indicator for system performance that assesses the society, economy and environment risk level for every hazard event. Therefore, RRPI is capable to assess the resilience of MEG design, which it is a paramount tool in risk analysis and decision-making process.

The MEG foundation design in this research does not use inherent safeguard resilience layers. The proposed resilience table is shown in **Appendix-I** illustrates the major hazards that threaten the MEG system in electricity, cooling, heating and natural gas grids, and the possible remedial action for overcoming the related consequences, and for avoiding the risk of failure or blackout.

Each row in the resilience matrix, **Appendix-I**, defines hazards that threating the MEG, also it shows relative statistical attributes such as the consequence severity of hazard event, risk occurrences (i.e. frequency, probability and avoidance), ecological risk index and RRPI. Furthermore, fault consequences and, suggested remedy actions are presented [137]. The RRPI value can be defined by using (4-1 that derived from eq.2 10.

The hazard events information were collected from historical data presented in numerous professional studies illustrated in CHAPTER 2 Literature Review. In addition to experts contribution and field engineers feedback.

Base on (2-10 the RRPI was developed and expressed in the following formula:

$$Resilience\ risk\ performance\ indicator\ (\text{RRPI}) = S_i\ x\ C_i\ x\ E_i \tag{4-1}$$

Where:

1. S_i is an indicator of the consequence severity of the hazard event. The severity has four categories namely negligible, marginal, critical and catastrophic
2. The C_i is the likelihood class of hazard event, which is a combination of three important parameters measuring the intensity of the hazard. This combination is illustrated in:

$$C_i = (P_i + F_i + A_i) \tag{4-2}$$

The likelihood class has five categories i.e. very low, low, moderate, high and extremely high

3. P_i is a probability factor that implies how likely a hazard event will occur. The probability has five categories namely negligible (1/3), rarely (2/3), possible (3/3), likely (4/3) and common (5/3).
4. F_i is the frequency, which is the number of occurrences of a repeating hazard event per time. Frequency has five categories ie. Less (1/3), yearly (2/3), monthly (3/3), weekly (4/3) and daily (5/3).
5. A_i is the possibility of avoiding failure occurrence. Avoidance has three categories namely likely (1/3), possible (3/3) and impossible (5/3).
6. E_i *is* the ecological risk index that measures failure's impact on the environment due to the failure consequence, such as greenhouse gases emission and squandering natural resources.

The proposed RM has information about the expected hazard event consequences in the society, economy and environment. It also offers the available remedial / mitigation actions and the required RPLs for these actions.

4.3 Hazard Analysis for Resilient MEG

The safety design for the MEG aims to improve the stability of the energy system during abnormal conditions and to seize the fault/damage propagation. This can be achieved by interrupting and isolating faulted or failed components from the system, as well as providing resilience methods for properties, public and environment safeguards.

The dynamic structure of MEGs and their various operating conditions require the development of resilience method by using intelligent control and monitoring units that based on safety design criteria.

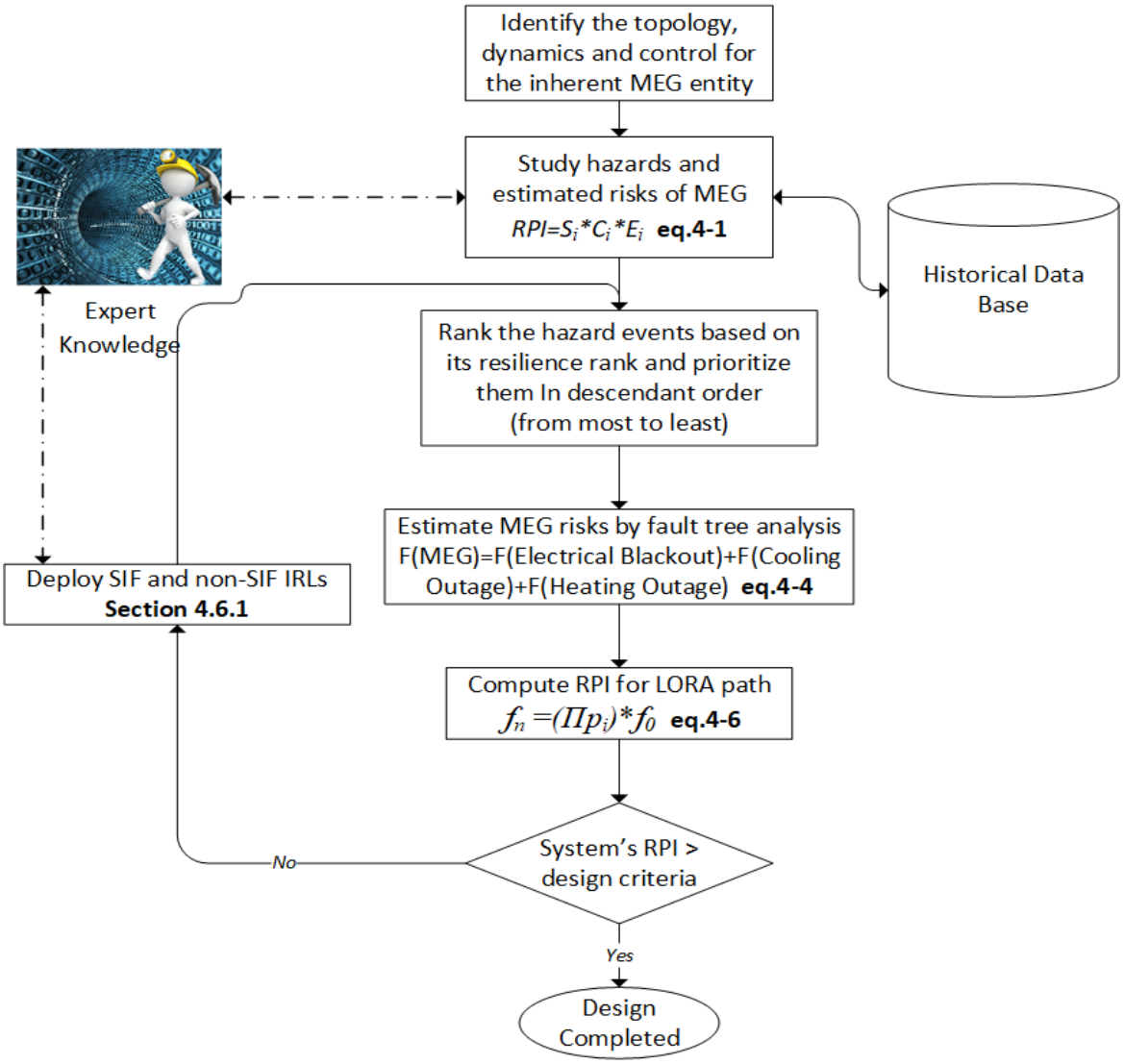

Fig. 4.2: *Proposed resilience analysis algorithm of MEG*

The resilience analysis algorithm for MEG illustrates in ***Fig. 4.2*** can be demonstrated in the following steps:

1- Study hazards and estimate risks of a MEG such as hazards in electricity, heating, cooling, transportation sectors and hazards due to natural phenomena by implementing MEG's resilience matrix and estimating RRPI (4-1.
2- Rank the hazard events based on its RRPI value in a descendant order.
3- Eliminate hazards that have low severity and low ecological risk with high class, hazards have high severity with low class and low ecological risk, and hazards have low severity and low class with high ecological risk
4- Prioritize the filtered hazard events based on RRPI level
5- Study prevention and mitigation solutions to deploy the necessary IRL(s) shown in Section 4.6.

In general, risk analysis idiom measures the hazardous conditions that appear during operation intervals. Where the average time period between successive hazardous events is estimated to be over 10 years if safety attributes are considered during the design process [11]. Accordingly, the SIS is passive during normal operation, and it may probably be only activated once during the ten-year interval or more. ***Table 4-1*** Illustrates the SIS operating conditions [138]. Fail-danger mode is the major hazard in the system. Where despite the system operating ordinarily in this circumstance, the automatic protection of the SIS is not guarded and there is no indication of that failure [139].

Table 4-1: *SIS operating condition*

SIS Operating Condition	Process	Protection Available	Failure Indication
Normal	Operating Normally	Yes	N/A
Fail-Safe	Falsely Operating	N/A	Yes
Fail-Danger	Operating Normally	No	Without Diagnosis

It is clearly defined that hazard analysis alone is not sufficient for the right decision. Where the hazards should be prioritized and discussed with the decision-making team in light of the affordable level of RRPI, tolerant rate of fault consequences losses and the available budget / components that can be utilized for remedial actions. ***Fig. 4.3*** illustrates MEG hazards based on the RRPI level shown in **Appendix-I**. The hazard events, shown in ***Table 4-2***, have the highest risk ranks, where they are allocated in the high catastrophic range; those hazards must have priority in resilience actions.

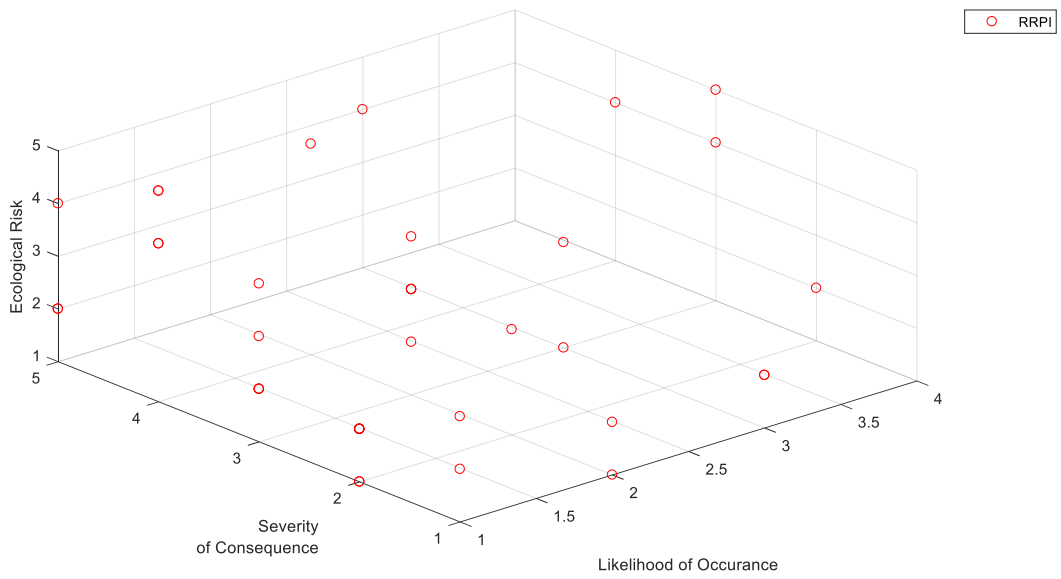

Fig. 4.3: *Proposed resilience chart for a MEG*

While ***Table 4-3*** illustrates the hazard events that allocated in the medium catastrophic range, which have less priority in the resilience actions.

The comparison between the MEG resilience chart ***Fig. 4.3*** and the MEG hazard chart ***Fig. 4.4*** that introduced in [137] shows that the resilience chart has visualized the ecological risk index for every hazard events whereas it can be noticed that ***Fig. 4.4*** is the virtical perspective of ***Fig. 4.3*** for the domain of class likelihood and severity.

In order to mitigate the consequences of the group of hazards depicted in ***Table 4-2*** and ***Table 4-3*** the following systems / devices are proposed to be added to the MEG entity namely Co-gen, TES, and management control, Alarm system and emergency shutdown system (ESD).

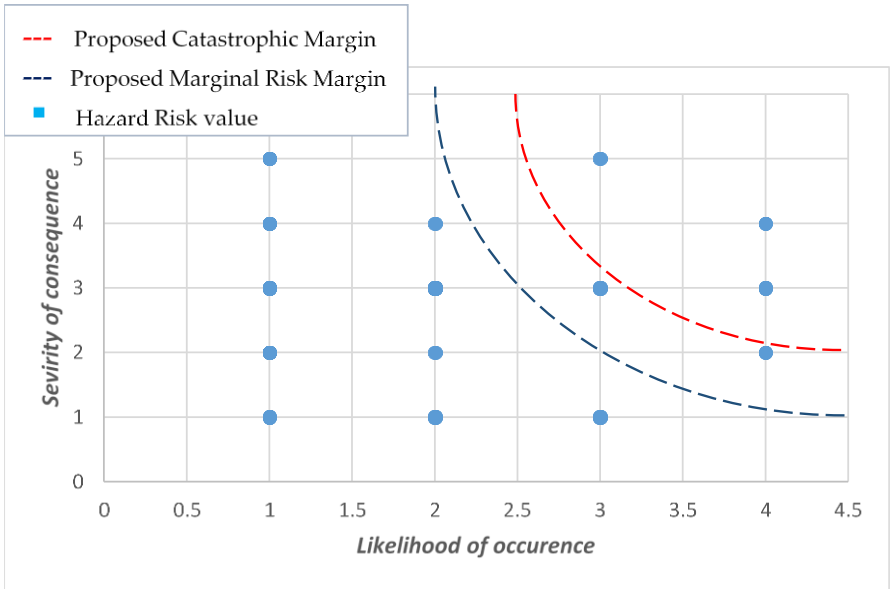

Fig. 4.4: *MEG hazards chart*

Table 4-2: *Hazard events in the high catastrophic range*

#	Hazard Mode	Hazard Events
1	Power blackout mode	Faults in the power systems (generation, transmission or distribution)
2		MEG has lack of DERs
3	Cooling outage	High correlation of cooling demand with electricity demand

Table 4-3: *Hazard events in medium catastrophic range*

#	Hazard Mode	Hazard Events
1	Power blackout mode	Intermittency of on-site renewable sources
2	Transportation Breakdown	Transportation energy demand contingency

It can be noticed that all the above proposed systems / devices have direct positive impact on mitigating the consequences of the catastrophic and medium hazard events. Therefore, this five systems / components are used in this study to improve the MEG resilience.

4.4 Safety Instrumented System Engineering Requirements

Nevertheless, a Safety Instrumented System (SIS) is similar to a process control system (BPCS) in numerous ways; the differences are found in the unique design, maintenance, and automated integrity requirements. Thus, in addition to the functional requirements of normal performance that are correlated with control system design, the requirements shown in ***Fig. 4.5*** must be considered for SIS design [79].

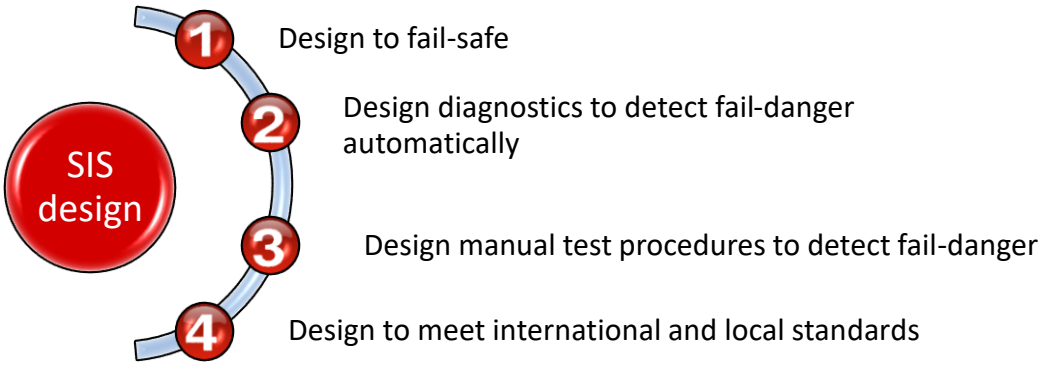

Fig. 4.5: *SIS design requirement*

4.4.1 Safety Integrity Level

Safety integrity level (SIL) is an expression for the relative level of risk-reduction offered by a certain SIF, where SIL is an indication of system safety performance. IEC EN 61508 has defined the relation of PFD (probability of failure on demand) and RRF (risk reduction factor) of low demand operation with SILs, as shown in ***Table 4-4*** [79].

4.4.2 Safety Instrumented Function

Safety instrumented function (SIF) is defined, in ANSI/ISA-84.00.01-2004 (IEC 61511 Mod), 3.2.71, as "safety function with a specified safety integrity level which is necessary to achieve functional safety" [140]. Safety function can be defined as a "function to be implemented by a SIS, other technology safety-related system or external risk reduction facilities, which is intended to achieve or maintain a safe state for the process, with respect to a specific hazardous event." [121].

Table 4-4: *Relationship between average probabilities of failure on demand to safety integrity levels (SIL)* [79]

SIL	General Description	PFD avg.	Risk Reduction Factor (RRF)	Availability (%)
4	Catastrophic community impact	10^{-4} to 10^{-5}	10,000 to 100,000	99.99 to 99.999
3	Employee and community impact	10^{-3} to 10^{-4}	1,000 to 10,000	99.9 to 99.99
2	Major property and production impact; Possible injury to employee	10^{-2} to 10^{-3}	100 to 1,000	99 to 99.9
1	Minor property and production impact	10^{-1} to 10^{-2}	10 to 100	90 to 99

4.5 Fault Tree Analysis for MEG

Mean time to failure (MTTF) is one of the most important static parameters in safety engineering. It can be used to derive another important measurement, known as failure rate. The real-time failure rate is generally obtained by counting the number of failures during a certain time period for a selected quantity of identical components exposed to failure.

$$\lambda(t) = Failure\ Rate = \frac{Failures\ Quantity\ during\ time\ period(0\ to\ t)}{Quantity\ \text{of}\ Exposed\ Components} \qquad ,\forall\, T > t \geq 0 \tag{4-3}$$

where t refers to the operation timeline, reliability is obtained by $R(t) = e^{-\lambda t}$, the probability of failure on demand is obtained by $F(t) = 1 - e^{-\lambda t} \approx \lambda t$ and the mean time to fail is obtained by $MTTF = 1/\lambda$.

The fault tree method is widely used to illustrate probability combinations. This technique begins with the definition of an "undesirable event," usually a system failure of some type. The analyst continues by identifying all events and combinations of events that result in the undesirable event. The fault tree is therefore quite useful when modeling

failures of a specific failure mode. These different failure modes can be identified as different undesirable events in different fault trees. A developed fault tree analysis shown in **Fig. 4.6** defines the top event probability of failure on demand (PFD) for a selected MEG. The developed method provides an effective tool to interconnect multiple failure modes in one entity. The PFD for a MEG can be estimated by using following equations:

$$F(MEG) = F(Electrical\ Blackout) + F(Cooling\ Outage) + F(Heating\ Outage) \tag{4-4}$$

where:

- $F(Electrical\ Blackout) = F(Utilities\ Grid) * F(Renewable) * F(Co - gen) * F(TES) * F(Manag.)$
- $F(Cooling\ Outage) = (6 * F(Chiller) * F(Co - gen) * F(TES) * F(Manag.)$
- $F(Heating\ Outage) = F(Co - gen) * F(Boiler) * F(TES) * F(Manag.)$
- $F(Utilities\ Grid) = F(Feeders) + F(Transformer) + F(Main\ feeders) + F(Fuses) + F(Substation) + F(Switches)$
- $F(Renew) = F(PV) + F(WT)$
- *F(PV)=F(Inverter)+F(Panels)+F(Hub)+F(C.B) + F(Ctrl)*
- $F(WT) = F(Saw) + F(Pitches) + F(Brake) + F(Ctrl.) + F(Hub) + F(C.B.) + F(Generator) + F(Hydraulic)$
- *F(Co-Gen.)=F(Fuel pump)+F(Alternative)+F(Cooling Radiator)+F(AVR)*

The PFD associated with each individual system in MEG can be illustrated from historical database and expert's knowledge [87]. PFDs for selected individual components are demonstrated in ***Table 4-5***, ***Table 4-6*** , ***Table 4-7*** and ***Table 4-8***.

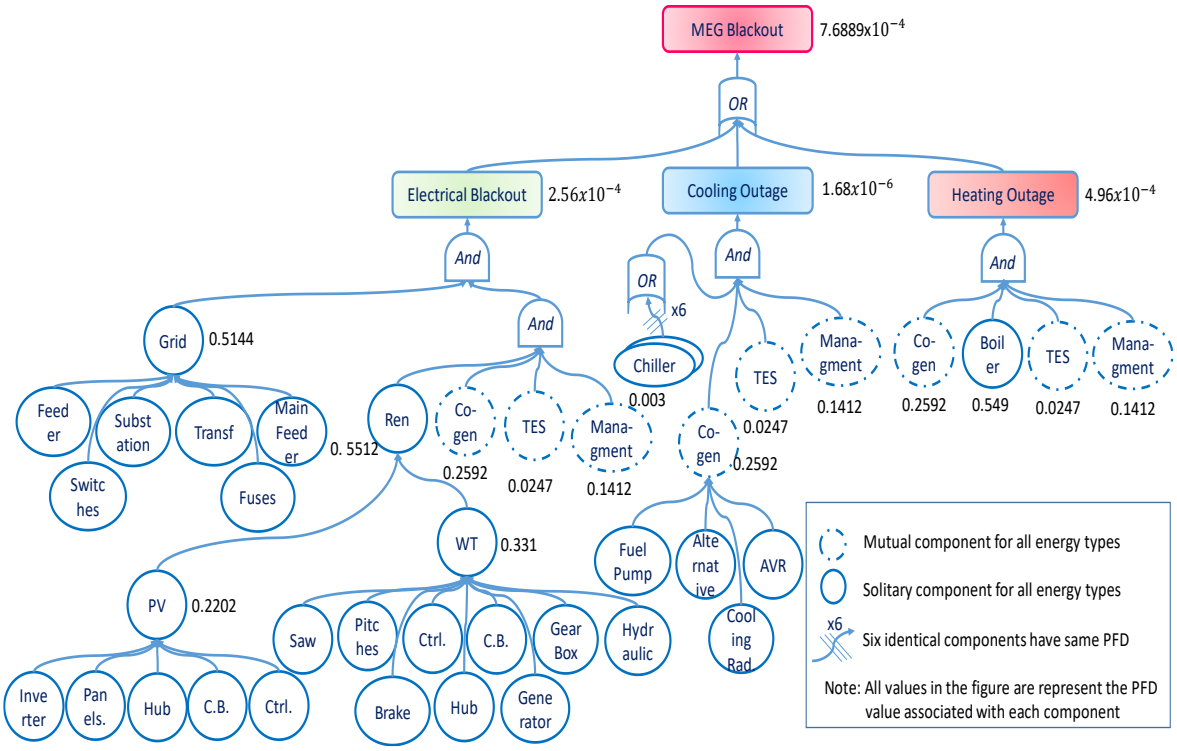

Fig. 4.6: *Fault tree for a selected MEG*

Table 4-5: *Reliability data for utilities' transmission and distribution components*

Components	Failure Rate (*f/yr.*)	Repair rate (*h*)	Reference
Substation	0.006	24	[141]
Feeder line section	0.065	6	[141]
Switches	0.006	4	[141]
Fuses	0.006	4	[141]
Transformer	0.015	10	[141]
Main Feeder	0.04/km	30	[141]

Table 4-6: *Reliability data for DERs*

Type	Failure rate (*f/yr.*)	Reliability $e^{-\lambda T}$	PFD $1 - e^{-\lambda T}$	Repair rate (*h*)	Reference
Solar system (PV)	0.2487	0.7798	0.2202	41.473	[142][143]
Wind Turbine (WT)	0.402	0.6690	0.3310	130	[144]
Co-generator (CG) Gas turbine	0.3	0.7408	0.2592	111.6	[145]
Utility grid	0.7224	0.4856	0.5144	7.655	[146]
Diesel generator (electrical + mechanical)	0.9	0.4066	0.5934	3.9	[145]
Chiller Unit	0.003	0.997	0.003	-	[147]
TES	0.0250	0.9753	0.0247	-	[148]
Boiler	0.7964	0.4509	0.5491	-	[149]
Fuel Cell (FC)	0.876	0.4164	0.5836	-	[150]
Battery (including controller and inverter)	0.2992	0.74141	0.25858	48.9	[142][143]
Micro Turbine	0.6257	0.5349	0.4651	-	[151]
Control computer and sensor system (Alarm)	0.1522	0.8588	0.1412	-	[152]
Power management system	0.1522	0.8588	0.1412	-	[152]
Protection Panel	0.02	0.9802	0.0198	8	[153]

Table 4-7: *Failure distribution and failure rate of wind turbine*

Type	Distribution of failure %	Failure rate *(f/yr.)*	Reference
Hub	0.3	0.001	[144]
Blades / Pitch	13.4	0.052	[144] [154]
Generator	5.5	0.021	[144] [154]
Electric system	17.5	0.067	[144]
Control system	12.9	0.05	[144]
Drive train	1.1	0.004	[144]
Sensors	14.1	0.054	[144]
Gear box	9.8	0.045	[144] [154]
Mechanical breaks	1.2	0.005	[144] [154]
Hydraulics	13.3	0.061	[144]
Yaw system	6.7	0.026	[144] [154]
Structure	1.5	0.006	[144]
Entire unit	2.7	0.011	[144]

The probability of the energy blackout of a MEG can be determined by compensating the failure rates of MEG's individual components into eq. (4-4). It shows that the top event risk reduced by 1400 times when utilizing the proposed combination of IRLs, details will be discussed in Section 4.6. The PFD became $7.688e^{-4}$ while it was 1.0814 for the conventional energy grid that consist utility grid, chillers and boiler.

Table 4-8: *Reliability data of PV components*

Type	Failure rate (*f/yr.*)	PFD 1-e^(-λT)	Repair rate *(h)*	Reference
PV Panel	0.04	0.0392	18.25	[142][143]
DC/AC inverter	0.143	0.1332	52.143	[142][143]
Boost DC/DC converter	0.0657	0.0636	62.5	[142][143]

4.6 Proposed Independent Resilience Layers and Layer of Resilience Analysis

The proposed independent resilience layer (IRL) is derived from the independent protection layer (IPL) that illustrated in [155]. The IRL can be defined as a device, system, or action that has the capability to maintain the process operate as designed without proceeding to undesired consequence scenarios. It must be independent from the initiating event or the action of any other layers of protection associated with the scenario. The fundamental characteristics of IRLs can be summarized as follows:

- Potential ability on suppressing the propagation of fault consequence, if the IRL functions as intended
- Auditable capability, where it assumed effective in terms of statistical validation of risk indices (by documentation, review or testing)

LORA used to determine whether the selected IRL(s) is (are) sufficient in tolerating certain risk and suppressing the hazard of consequence scenarios. Where every IRL has its own PFD.

$PFD = p_n$, where n indicates the layer level (4-5)

The PFD value has a direct impact on the system's resilience, as declared in LORA path equation:

LORA path= $f_n = (\prod_{i=1}^{i=n-1} p_i) x f_0$ (4-6)

where f_0 is the probability of the initiating event

LORA's formula can be extended to cover multi path resilience assessment for namely electricity, heating and cooling energy, as shown in ***Fig. 4.7***, by using the following equation.

LORA Multi-path= $f_{Multi\text{-}n} = 1 - [(1 - f_{Electricity}) x (1 - f_{Heating}) x (1 - f_{Cooling})]$ **(**4-7)

where f_n is the LORA path in (4-6) for Electricity, Heating and Cooling respectively

4.6.1 Proposed Layer of Resilience Analysis for MEG

IRLs combination shown in ***Fig. 4.7*** was proposed to mitigate the hazardous events that mentioned in ***Table 4-2*** and ***Table 4-3*** for a MEG. These IRLs are required to tolerate the hazard of losing energy in the MEG, by utilizing co-generators, TES and supervisory fault-tolerant predictive energy management control. Consequently, adding IRLs into a MEG realizes the concurrent goals of increasing the energy availability, improving the production quality/cost and reducing greenhouse gases emission, in other words it improves the MEG resilience. Details of the proposed IRLs in this study are as follows:

I. *IRL-1* co-generators, such as fuel cells, micro gas turbines, and hybrid turbine, to overcome the lack of power production during on-peak hours and to cope the intermittency of renewable energy resources (RESs).

II. *IRL-2* Thermal energy storage is an effective solution for MEG operation due to the following advantages:

A- Centralized infrastructure, where large thermal reservoirs provide flexibility to manage cooling dynamics, reduction of greenhouse gases emission and mitigation of energy failure risks.

B- Reshape the energy profile by reserving the off-peak production to be used at on-peak demand hours.

III. *IRL-3* Supervisory fault-tolerant energy management (FTEM) controller plays an essential role on MEG's resilience, where management of distributed resources near to RESs is the most effective means for increasing penetration of renewable sources. CHAPTER 5 proposes a multi-level hierarchical decision making as a non-SIF IRL for resilient MEG.

IV. *IRL-4 i*ntelligent alarm system is an important SIF layer, where its main role is to monitor the health status of the MEG and provide a real-time information about the correspondent fault type and location. Numerous types and techniques of alarm systems can be utilized such as Bayesian belief network based fault diagnosis system that proposed in CHAPTER 6.

V. *IRL-5* Emergency shutdown system (ESD) is an essential SIF layer due to its ability in suppressing the consequences of fault propagation.

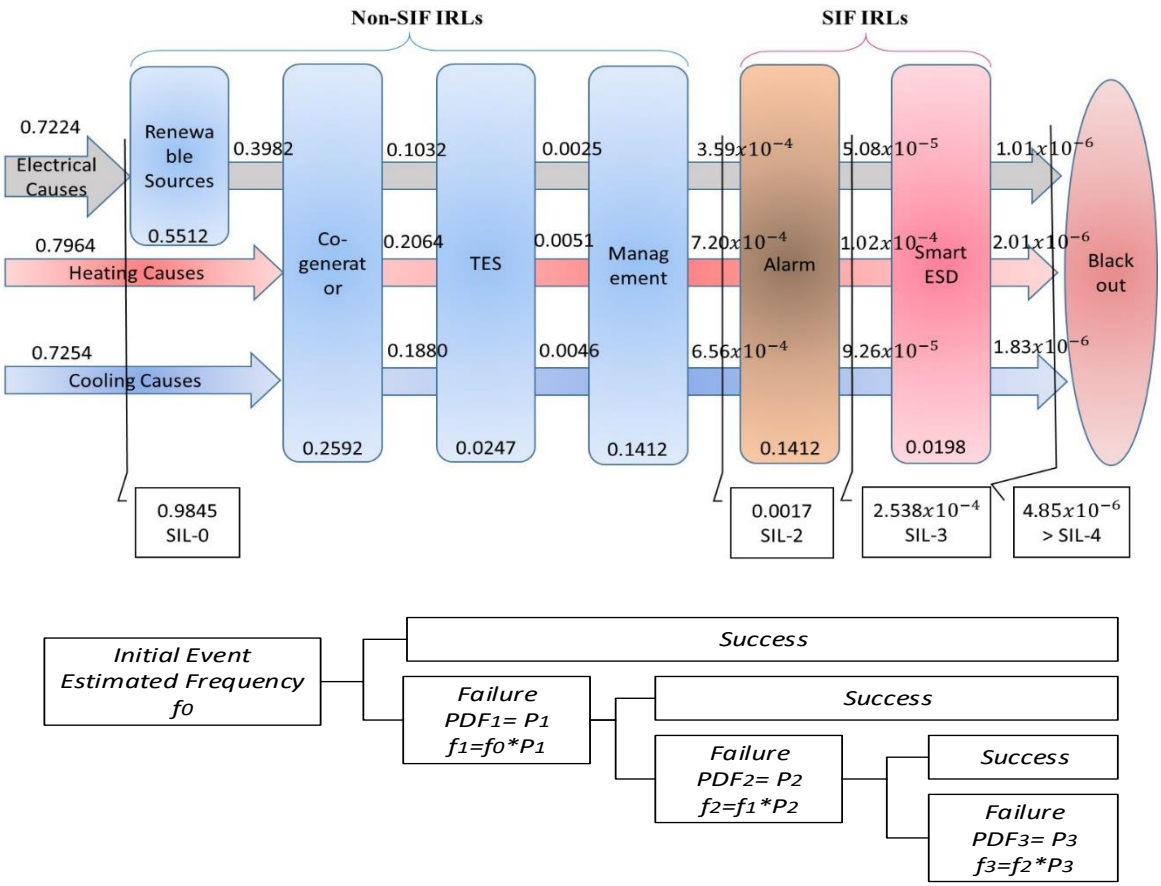

Fig. 4.7: *LORA path diagram for MEG system*

Table 4-9: *Examples of independent resilience layers (IRLs)*

No.	IRL	Examples
1	MEG Storage system (E/T/C):	Energy storage units are classified based on their technology, the following are the most popular energy storages: batteries, supercapacitors, flywheels, hydro tanks, thermal energy storage and superconducting magnetic energy storage
2	Prime mover	Co-generators, fuel cells, micro gas turbines, geothermal resources and hybrid turbine systems
3	Intelligent control systems for normal operation to ensure rigid performance	Various models based on individual units and systems within the MEG
4	Smart energy asset management for both sources and load within the MEG boundary	By using management and optimization methods
5	Emergency control of resilient systems during abnormal conditions	The proposed hierarchical decision making of three control level
6	Risk assessment platform and alarm systems	Fault diagnosis system i.e. the proposed BBN-ANFIS based risk analysis
7	MEG safety shutdown and restoration systems	Various models based on individual units and systems within the MEG
8	Upper-level centralized/decentralized MEG management with utility grids.	Management and control centre (MCC)

Several combinations of different IRLs can be implemented to augment the MEG resiliency. ***Table 4-9*** shows examples of IRLs that can be used for designing a resilient MEG

Some of these IRLs were used and discussed in this thesis, the reset can be implemented and studied in future researches to explore different techniques and compare their performances on MEGs resilience.

LORA shows a reduction on system risk level from 0.9845, SIL- 0, for the conventional energy grid to 0.0017, SIL-2, with a selected non-SIF-IRLs, i.e. Co-gen, TES and management control. ***Fig. 4.8*** shows LORA diagram and calculation for a MEG integrated with selected non-SIF-IRLs.

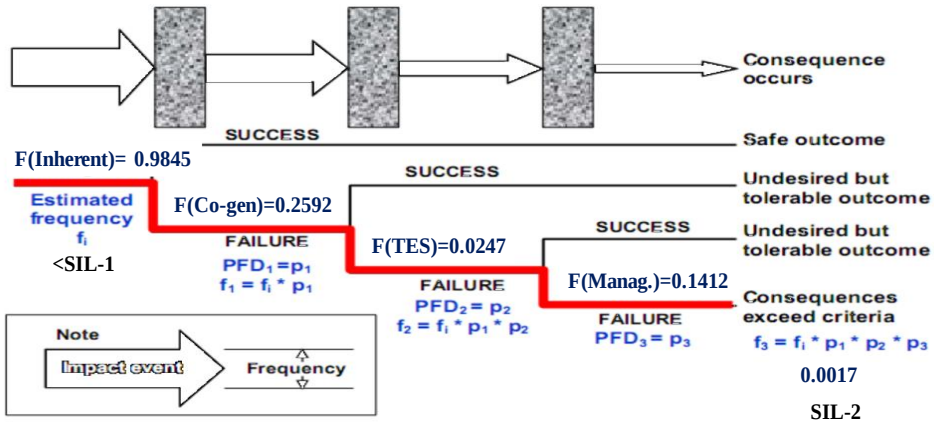

Fig. 4.8: *LORA diagram for the incorporating the selected non-SIF IRLs into a MEG*

Adding the selected SIF-IRLs, shown in ***Fig. 4.7***, into the MEG entity reduces LORA path value by a factor of $2.85x10^{-3}$. The new LORA value is defined by compensating the associated PFD values in (4-6 and 4-7as shown:

$$LORA = f_5 = 1-[(1-1.01\ x10^{-6})x(1-2.01\ x10^{-6})x(1-1.83\ x10^{-6}) = 4.85x10^{-6}$$

Thus, SIL margin increases to a range beyond SIL- 4 level.

4.6.2 Sensitivity Analysis

Successful self-sufficiency operation of MEG increases the energy resilience toward upstream failure. The energy upstream failure, Utilities failure rate, has a higher probability

of failure than the resilience MEG. The previous scenario that depicted in ***Fig. 4.7*** of a MEG assumes every DERs in the MEG able to supply the full energy demand individually; in other words, the MEG has a full sufficiency to operate in islanded mode if any DER is available. To evaluate the impact of partial switching to islanded mode for the MEG described in ***Fig. 4.7***, the probability of successful islanded is tested in five steps between 0% and 100% for every IRLs namely Renewable energy, Co-generator, TES, management control, Alarm system and ESD. Results for 15,625 cases that listed in Appendix II Sensitivity analysis for LORA and illustrated. ***Fig. 4.9*** shows the effect of utilizing the IRLs on the failure rate of MEG. The contribution of each IRLs are varied from 0 to 100% in five steps that created 15,625 different cases. The figure demonstrated that the higher contribution of every IRLs the lower failure rate the MEG has.

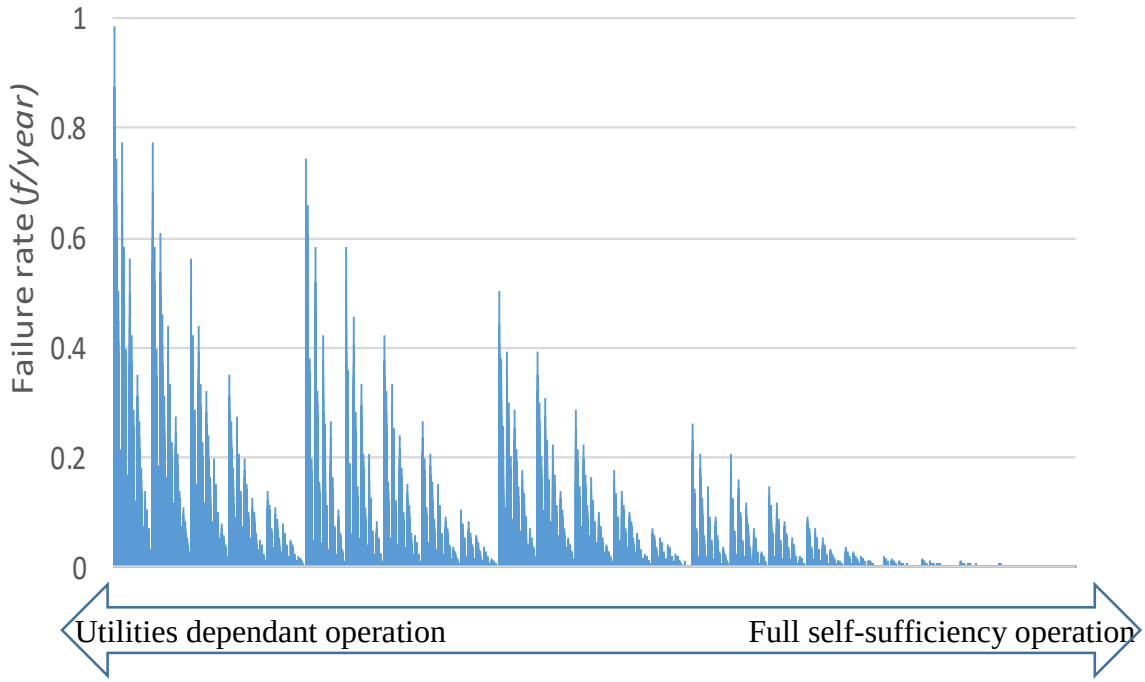

Fig. 4.9: *Sensitivity analysis for the resiliency of a MEG*

The failure rate varies from 0.9845 *f/year* for utility's dependent to 4.85021×10^{-06} for a self-sufficiency resilient MEG. The individual contribution of every IRLs on MEG failure rate are illustrated in ***Table 4-10***.

Table 4-10: *MEG's risk level by using the selected IRLs individually*

IRL	Renewable	Co-gen	TES	Management	Alarm	ESD
Risk level	0.966	0.476	0.054	0.102	0.091	0.0143

On the other hand, it is important to mention that the contribution of each IRL on LORA depends on the ratio of IRL capacity to the daily energy demand therefore this ratio should take place in the MEG risk level calculation. ***Table 4-11*** provides the calculation of LORA for the MEG case study by taking in consideration the contribution ratio of every IRLs. Consequently, the PFD of the MEG is 7.15996×10^{-05} and SIL-4 category.

Table 4-11: *Risk level for a MEG with a shared contribution ratio of every IRLs*

IRLs	Renewable	Co-gen	TES	Management	Alarm	ESD	MEG
Capacity	4 MW	16 MW	400 MWh	N/A	N/A	N/A	N/A
Peak power demand / Total energy	19.42MW	19.42MW	3,474.8 MWh (wk)	N/A	N/A	N/A	N/A
Contribution %	20.6%	82.4%	80.6%	100%	100%	100%	-
Failure rate (*f/yr.*) Electricity	0.656	0.255	0.055	0.008	0.001	2.16E-05	-
Failure rate (*f/yr.*) Heating	0.796	0.310	0.066	0.009	0.001	2.62E-05	-
Failure rate (*f/yr.*) Cooling	0.725	0.282	0.060	0.008	0.001	2.38E-05	-
Risk level	0.981	0.631	0.171	0.025	0.004	7.16E-05	7.16E-05

4.7 LORA-ISA Optimization Base for Resilient MEG Design

In this section, the interior search algorithm (ISA) is introduced to support engineers on finding an optimal design for MEG's components. The novel methodology uses ISA in optimizing MEG's components capacities that form IRLs into the proposed LORA that

described in Section 4.6. The proposed ISA structure takes in consideration the main constrains that facing resilient MEG design namely operation costs, greenhouse gases emission, capital cost and the system reliability. In such complex and nonlinear problems the local search algorithms, i.e. Nelder-Mead simplex method, is not an appropriate choice. Therefore, a global optimization algorithm is required [156].

4.7.1 Interior Search Algorithm

The elements are divided into two simultaneous optimization groups. Composition group is one group that changes the composition of elements to find better finesses and the other is the mirror group that produces more decorative environment. The following is describe the detailed ISA algorithm [157]:

1- Arbitrarily select the locations of elements within lower bounds (LB) and upper bounds (UB), then evaluate their fitness values.
2- Find the global best element, x_{gb}^{j}. This element has the minimum objective function among the jth iteration.
3- Divide the rest of elements arbitrarily into two groups named a composition group and a mirror group by using a threshold value α and arbitrary variables r1 (ranging from 0 to 1 for each element). Elements with $r_1 \geq \alpha$ go to the composition group and the rest go to the mirror group.
4- To optimize the global best, it is recommended to shift its location slightly by using a random walk for local search around the global best:

$$x_{gb}^{j} = x_{gb}^{j-1} + r_n \times \lambda \tag{4-8}$$

where r_n: a vector of normally distributed random numbers,

λ: a scale factor equal to 0.01×(UB-LB).

5- Each element in the composition group and its boundary conditions, upper and lower bounds, are arbitrarily changed :

$$x_i^j = LB^j + \left(UB^j - LB^j\right) \times r_2 \tag{4-9}$$

where r_2: a random value between 0 and 1;

x_i^j is the ith element in the jth iteration;

LB_j and UB_j: lower and upper bounds of the elements in jth iteration and they are, respectively, the minimum and maximum values of all elements in the (j-1) iteration.

6- The elements of the mirror group, a mirror is randomly placed between each element and the fittest element (global best). The location of a mirror for the ith element in the jth iteration is formulated as follows:

$$x_{m,i}^j = r_3 x_i^{j-1} + (1 - r_3) x_{gb}^j \tag{4-10}$$

where r3: a random value between 0 and 1. The location of the image or virtual location of the element depends on the mirror location, and can be formulated as follows:

$$x_i^j = 2x_{m,i}^{j-1} \tag{4-11}$$

7- Determine the fitness values of the new updated locations of the elements and images. Then update each location if its fitness is enhanced for revival design. For a minimization problem, this can be expressed as

$$x_i^j = \begin{cases} x_i^j & f(x_i^j) < f(x_i^{j-1}) \\ x_i^{j-1} & else \end{cases} \tag{4-12}$$

8- If any of the stop criteria is not satisfied, repeat the above steps from step 2.

4.7.2 Cost Function Optimization for Resilient MEG Design

The optimal resilient design for MEG's components can be achieved by using the proposed optimization methodology that illustrated in ***Fig. 4.10***. The proposed methodology is aimed to provide an effective design tool for resilient MEG that considers minimizing the risk level of MEG, operation / maintenance cost, greenhouse gases emissions and capital cost of MEG infrastructure. These optimization elements are presenting the resiliency parameters, namely socio-econo-ecological attributes, which were illustrated in detail in sections 3.4 and 4.1. ISA was proposed to minimize the proposed cost function:

$$Min\ (f_{Cost}) = Min\ (\mu_{risk} \times f_{Risk} + \mu_{Co2} \times f_{Co2} + \mu_{OC} \times f_{OC} + \mu_{CC} \times f_{CC}) \quad (4\text{-}13)$$

Where: f_{Risk} is LORA Multi-path risk level derived from 4-7 by adding the contribution factor of each IRL

$$f_{Risk} = 1-[(1- f_{Electricity}) \times (1- f_{Heating}) \times (1- f_{Cooling})] \quad (4\text{-}14)$$

$$f_{Electricity} = \prod_{i=1}^{M} x_i \text{ x } IRL_i \text{ x } \gamma_{Elec-i} + (1 - x_i) \quad (4\text{-}15)$$

$$f_{Heating} = \prod_{i=1}^{M} x_i \text{ x } IRL_i \text{ x } \gamma_{Heat-i} + (1 - x_i) \quad (4\text{-}16)$$

$$f_{Cooling} = \prod_{i=1}^{M} x_i \text{ x } IRL_i \text{ x } \gamma_{Cool-i} + (1 - x_i) \quad (4\text{-}17)$$

f_{Co2} is the greenhouse gases emission for a selected MEG entity

$$f_{co2} = [Energy_{Total} \text{ x } (1 - \alpha_1 \text{x } x_4)] \text{ x } \left[(1 - (x_1 + x_2)) \text{ x } \gamma_{Utility\ Co2} + x_1 \text{ x } \gamma_{Ren\ Co2} + x_2 \text{ x } \gamma_{Co-gen\ Co2}\right] \quad)4\text{-}18)$$

f_{OC} is the operation cost for the MEG

$$f_{OC} = [Energy_{Total} \text{ x } (1 - \alpha_2 * x_3)] * \left[(1 - (x_1 + x_2)) \text{ x } \gamma_{Utility\ buy} + x_1 \text{ x } \gamma_{Ren\ oper} + x_2 \text{ x } \gamma_{Co-gen\ oper}\right] \quad (4\text{-}19)$$

f_{CC} *is the capital cost for the MEG*

$$f_{CC} = Energy_{Total} \text{ x } \left[x_1 \text{ x } \gamma_{Ren\ capital} + x_2 \text{ x } \gamma_{Co-gen\ cpital}\right] + \left[x_3 \text{ x } \gamma_{Totsl\ cooling} \text{ x } \alpha_3 \text{ x } \gamma_{TES\ capital}\right] x\ [1 + \alpha_4 \text{ x } (x_4 + x_5 + x_6)] \quad)4\text{-}20)$$

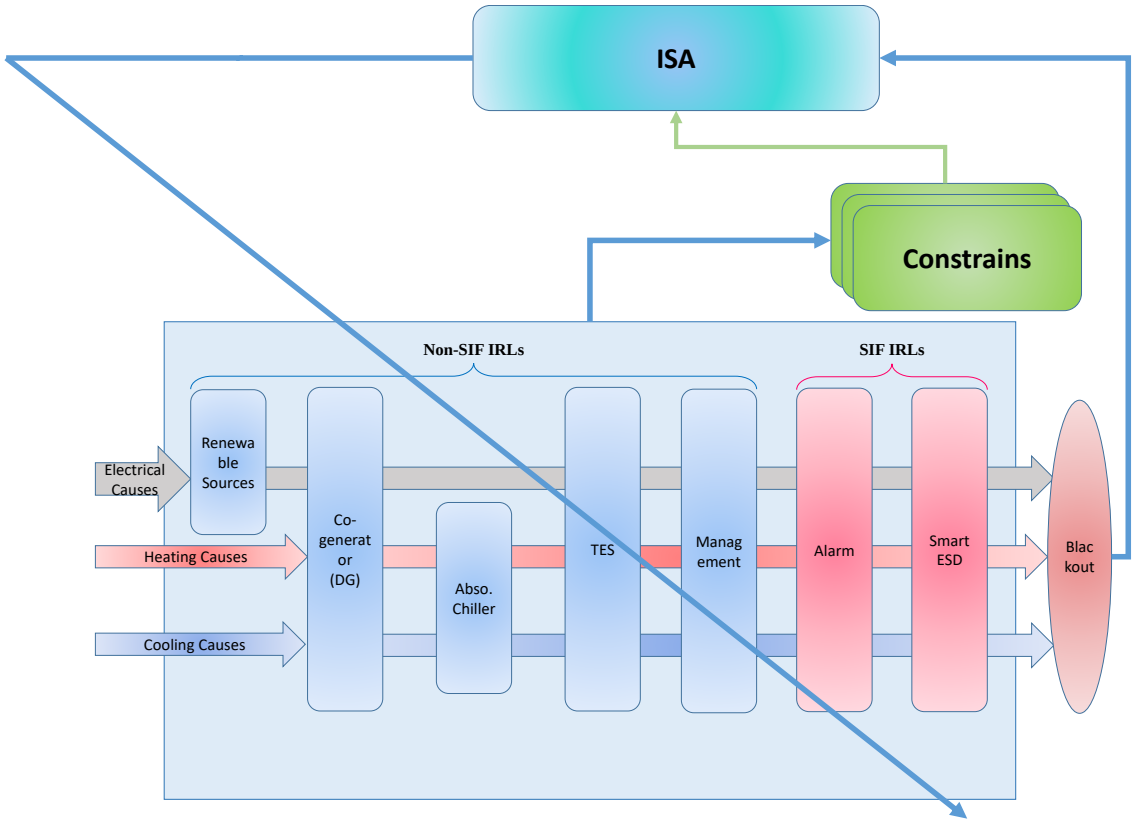

Fig. 4.10: *ISA based LORA structure*

The parameters of the proposed LORA-ISA model for design a resilient MEG are defined in ***Table 4-12***. The optimum set of the IRLs' contribution factors, x_i, are selected based on The minimum cost function in (4-13).

Table 4-12: *Constant value of specification*

Symbol	*Description*	*Value*	*Ref*
x_i	*Contribution factor for IRL*	*0-1*	*NA*
M	*Number of IRLs used for*	*6*	*NA*
γ_{Elec-i} γ_{Heat-i} γ_{Cool-i}	*The coefficient is 1 if the IRL has an impact on the energy stream*	*0 or 1*	*NA*

α_1	*C_{o2} reduction factor for utilizing advanced energy management*	*0.3*	*NA*
$\gamma_{Utility\ Co2}$	*The utility's greenhouse emission*	*865 kg/MWh*	[158]
$\gamma_{Ren\ Co2}$	*The renewable's greenhouse emission*	*0 kg/MWh*	[159]
$\gamma_{Co-gen\ Co2}$	*The co-gen's (Gas Turbine) greenhouse emission*	*570*	[160]
α_2	*Cost reduction factor for utilizing TES*	*0.2*	*NA*
$\gamma_{Utility\ buy}$	*Electricity purchasing average rate from utility*	*109.5 CAD$/MWh*	[161]
$\gamma_{Ren\ oper}$	*Renewable sources operation rate*	*10 CAD$/MWh*	[162]
$\gamma_{Co-gen\ oper}$	*Co-generator operation rate*	*110 CAD$/MWh*	[118]
$\gamma_{Ren\ capital}$	*Renewable sources capital rate*	*6700 CAD$/kWh*	[143]
$\gamma_{Co-gen\ cpital}$	*Co-generator capital rate*	*900 CAD$/MWh*	[159] [160]
$Energy_{Total}$	*Total MEG Energy demand in a week*	*19.42 MWh*	*NA*
α_3	*Cooling storage coefficient (7 days, 10 ten times for usage a day)*	*1/(7*10)*	[163]
α_4	*Budget rate for capital cost for the management, alarm and ESD systems respectively*	*0.1*	*NA*

μ_x	*The contribution parameter of each cost value*	*1, 10^{-8}, 10^{-8}*	*NA*

4.7.3 Constraints

In order to define the optimal selection of IRLs, the optimization algorithm should consider the components' limitation and the system constraints. The following constraints were selected based on experts knowledge, stakeholder(s) needs and manufacturer(s) recommendation.

$$0 \leq x_1 + x_2 \leq 1 \tag{4-21}$$

$$0 \leq x_i \leq 1 \quad i = 1, 2, \ldots 6 \tag{4-22}$$

$$Energy_{Total} \text{ x } (x_1 \text{x } \gamma_{Ren\ capital} - x_2 \text{ x } \gamma_{Co-gen\ cpital}) \geq 0 \tag{4-23}$$

The statistical results of the LORA-ISA are illustrated in ***Table 4-13***. With the selected six IRL elements the proposed procedure recognized the optimum value after about 10,000 structural analyses. The convergence trace of the results is illustrated in ***Fig. 4.11***.

Table 4-13: *Best solution of IRLs' contribution values*

IRL	Renewable x_1	Co-gen x_2	TES x_3	Management x_4	Alarm x_5	ESD x_6
Best value	0.212	0.788	0.590	0.999	0.984	0.999

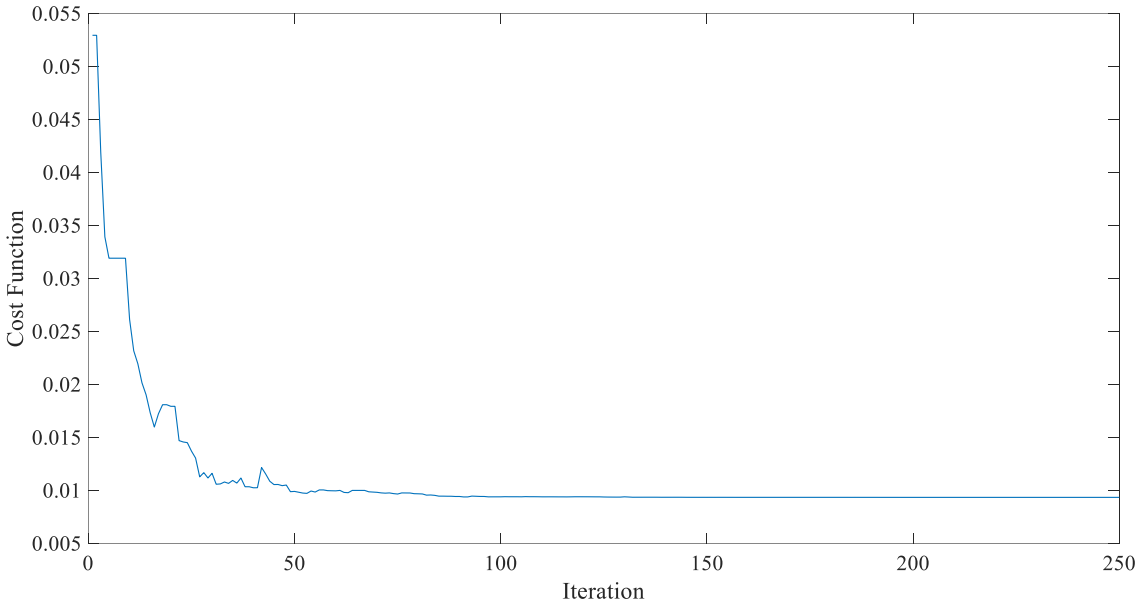

Fig. 4.11: *Convergence trace for a MEG consists six IRLs*

4.8 Chapter's Conclusions

In this chapter, a study of safety design and risk analysis for MEG was developed to achieve a resilient MEG design and implementation. Framework for the safety design methodology was presented and discussed. A developed resilience analysis algorithm for MEG was proposed to assist the decision-making team in prioritizing hazardous events. Afterward, advanced fault tree and proposed LORA were utilized to estimate the risk reduction value and the associated SIL of integrating a selected combination of IRLs in the MEG. Selected SIF and non-SIF IRLs were utilized to achieve a resilient MEG by increasing SIL. The extremely high hazards, that have low severity and low ecological risk with high class, hazards have high severity with low class and low ecological risk, and hazards have low severity and low class with high ecological risk, were eliminated to focus on the major effective hazards and propose suitable IRLs to prevent their consequences. The results showing that the proposed non-SIF IRLs reduce the risk of MEG blackout by 100 times and the proposed SIF IRLs offer another 1000 times reduction in the threaten risks of the base MEG. In light of the promising results in this research, it can be affirmed that the proposed methodology offers an effective safety tool for MEG design and

verification. The proposed tool can be widely utilized in design and verification of large complex systems.

The sensitivity analysis in Section 4.6.2 and Appendix II Sensitivity analysis for LORA assess the contribution of every IRLs on LORA and MEG's resilience level. The results show that number of cascaded IRLs used in MEG and the ratio of each IRL contribution has a direct impact on the MEG resilience. The SIL varies from SIL-0 for the base MEG to SIL-4 for the guarded MEG by six IRLs

It can be noticed that SIF IRLs are usually auxiliary systems that does not have direct effect on the operation cost and environment parameters of the energy system. However, SIF IRLs have significant effect on the systems' reliability. On the other hand, the non-SIF IRLs have direct effects on socio-econo-ecological parameters, where the type and capacity of the non-SIF IRL is able to improve the running cost, greenhouse gases emission and the overall system's reliability as illustrated in Section 7.2.

The novel combination of Interior search algorithm (ISA) and LORA was employed to support engineers on finding an optimal design for MEG's components. The proposed ISA structure takes in consideration the main constrains that facing resilient MEG design namely operation costs, greenhouse gases emission, capital cost and the system reliability. Results shows optimal values for IRLs for design a resilient MEG that considers risk calculation in the optimization cost function that. To the best of the author's knowledge, so far there is no other publication reporting design of resilient MEG based on LORA-ISA optimization algorithm.

CHAPTER 5 Resilient MEG Design using Proposed non-SIF IRL (Multi-Level Hierarchical Decision Making)

Effective design of fault-tolerant management system of a MEG realizes a full capability of resilient and eco-friendly energy production [164]. MEG comprises complex systems with dynamic response characteristics at various time-scales. Thus, a hierarchical pattern is recommended for the control of such complex systems [165]. It includes an overall supervisory control that determines the set point of critical performance parameters of the MEG based on the energy production and demand during the day course. For instance, the decision of which distributed energy resources (DERs) should be operating (on/off states), and at what conditions they must be operating (at energy levels, power level, temperatures, pressures, mass flow rates, and so on) [15].

A multi-level hierarchical decision making (MLHDM) is one of the IRLs that is proposed in this study as a non-SIF IRL. It enhances the self-healing characteristics of MEG against uncertainty hazards during the system operation. The structural design of MLHDM consists of three successive levels that functioning together to attain resilient operation.

5.1 ***Background***

Numerous control methodologies for MEG have been proposed and studied. The centralized, decentralized and multilevel hierarchical decision making of MEG have been discovered in previous theoretical and laboratory experimental studies [16][166][27][167]. The difference between these controls structures are shown in ***Fig. 5.1***, ***Fig. 5.2*** and ***Fig. 5.3***.

1- Decentralized control methodology of the MEG can be summarized as follows; the individual energy sources have the right to share the demand as per their specific capacity and local control characteristics. Those are fixed during installation and planning phases. Consequently, it is difficult to make any re-scheduling for Instantaneous energy production for each source to achieve optimum generation cost and emission conditions. This fact led to underutilize the energy sources, although they may have high efficiency and lower operating rates [168].

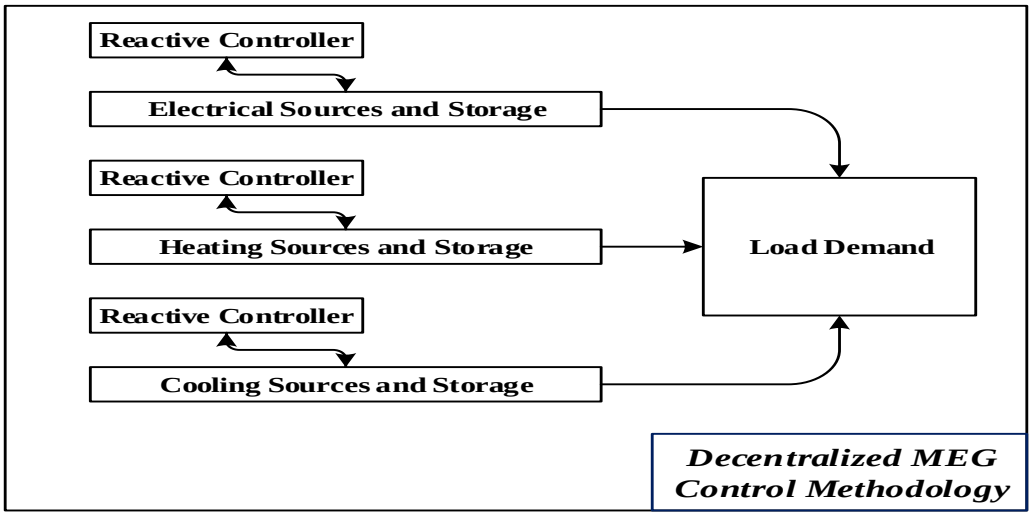

Fig. 5.1: *Decentralized MEG control methodology*

2- Centralized control methodology of the MEG mainly consists of a central control system for remote control all energy sources in the MEG boundary. Optimal performance can be achieved by using centralized control system, but it has a significant disadvantage on the reliability of energy system where if the central controller fails, most likely the overall energy system will collapse. The centralized control methodology is relying on the communication network, where the speed and reliability of the communication system have a direct impact on the MEG performance, reliability and resiliency.

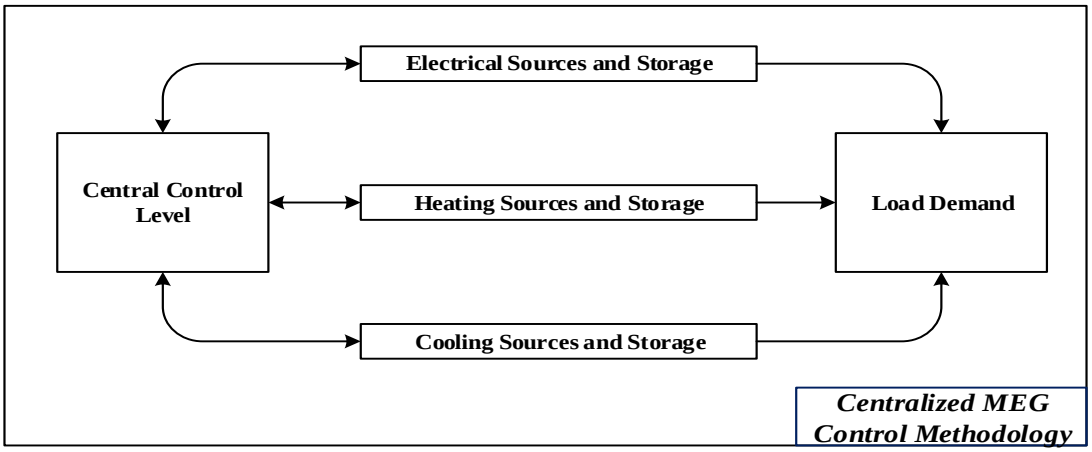

Fig. 5.2: *Centralized MEG control methodology*

3- A multilevel hierarchical decision making of the MEG provides a better methodology to overcome most of the obstacles accompanying centralized and decentralized control

methodologies [169]. This control type has a significant role in achieving an optimum operation of the MEG system similar to centralized control methodology but under lower speed and reliability level of the communication network requirements. However, the main challenge of hierarchical decision-making methodology is the necessity for clear boundaries of control range and domain based on control levels [170]. In the hierarchical decision making, the supervisory control and predictive control levels generally depend on the communication network to achieve the MEG system optimization operation same as a centralized methodology. But hierarchical has the advantage of decentralized methodology, where the reactive control level is not depending on the communication network. This feature immunizes the MEG from loss of operation once failure occurred in higher level control and/or network. Whilst the hierarchical may lose the optimal performance during such hazardous event.

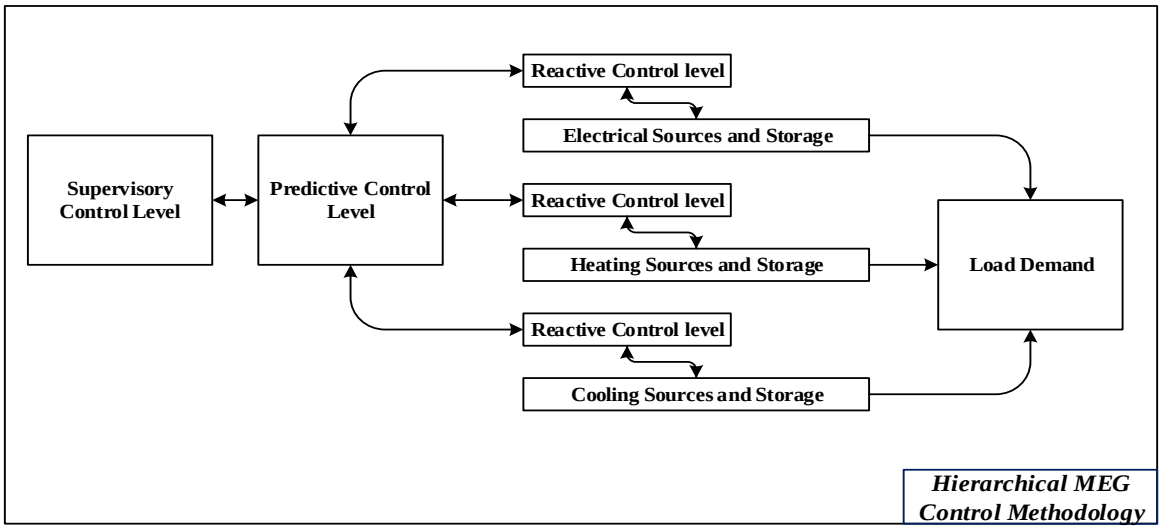

Fig. 5.3: *Hierarchical MEG decision making methodology*

The MEG performs dynamic control over energy sources, enabling autonomous and automatic self-healing operations. During normal or peak usage, or at times of the capital energy grid failure, a MEG can operate independently of the capital grid and isolate its generation nodes and energy loads from disturbance without affecting the capital grid's integrity [171].

This section proposes a MEG topology has the capability for self-sufficiency of electricity, cooling and heating demands majority of the year by utilizing co-generation unit (CG), solar power (PV), wind turbine farm (WT), heat recovery steam generator (HRSG), and district cooling units (DCUs) with thermal energy storage (TES). Also, it is supported by the supercapacitor bank for swift and dynamic power backup. A multi-level hierarchical decision making is proposed to provide autonomous self-healing supervisory and control for MEG. The control architecture consists of three levels working together to achieve the overall operational goal.

5.2 Hierarchical Decision Making Architecture

A hierarchical decision-making design is proposed and applied in order to manage the energy resources efficiently and effectively utilizes the MEG components. It comprises of three levels, including a self-ruling decision-making level, a predictive control level, and a reactive control level. Each level has its own local objective and they work together to realize a resilient operational performance. The higher level controller involves a fault tolerant control formulation, in order to deal with uncertainty hazardous conditions and to determine the best action for each subsystem. The predictive control level harnesses a pre-scheduled operational timing to manipulate the chiller units (DCUs) operation. The predictive control aims to operate the DCUs at off demand timing for charging the TES which required to cover an on-demand peak period. The lower level controller is a load following control for the demand that needs a fast response. ***Fig. 5.4*** shows the hierarchical decision making architecture.

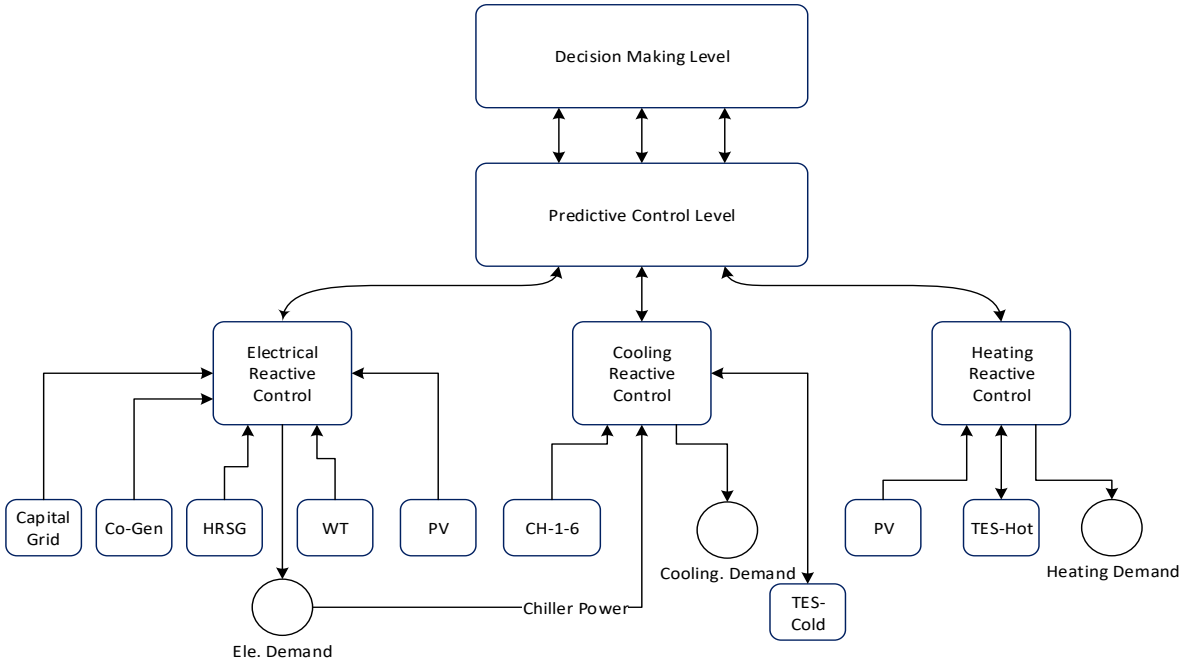

Fig. 5.4: *Hierarchical decision making architecture for MEG*

The efficiency of any control strategy depends on the selected performance parameters and the control structure [169]. A central decision-making control determines the control parameters based on the obtainable information collected by the subsystems. Nevertheless, the centralized method might be difficult to realize in large-scale systems, where the process of transmission and transformation of the information are more complex. Decentralization of the information and control structures is a feasible solution to overcome this dilemma. the decomposition of a large system into subsystems is mainly aimed to minimize the required computation process further to reduce the amount of information required for the decision-making level [172].

In the past, the MEG has been classified as either an islanded or a grid-connected mode. But the resilient energy grids demands for a flexible MEG that can operate in both grid-connected and islanded modes [173]. This system is open the door for great challenges, where establishing such systems requires for integrating different technologies of energy sources, energy storage, and energy management systems. In addition to, safety issues such as fault monitoring, predictive maintenance, or protection, which are fundamentals for MEGs with a high level of self-healing capability.

This chapter concerns on developing the decision-making and predictive control levels to manage the cooling demand and to minimize its negative impacts on the electrical energy system. Fuzzy (Sugeno) rules were implements for softening the conflict between pre-scheduled chiller units (DCUs) operation and reactive control response.

5.2.1 Design of adaptive neuro-fuzzy decision-making method

The fuzzy method is considered as a simple and tangible approach for solving dynamic nonlinear systems. Sugeno or Takagi-Sugeno-Kang fuzzy system was proposed in this study for its ability to provide a systematic method of producing fuzzy rules for definite input/output streams. The main difference between Mamdani and Sugeno is that the Sugeno output membership functions are either linear or constant.

Fig. 5.5 shows an adaptive-network-based fuzzy inference system (ANFIS) have an optimized structure of 5 layers organized as follow 2:10:25:25:1.

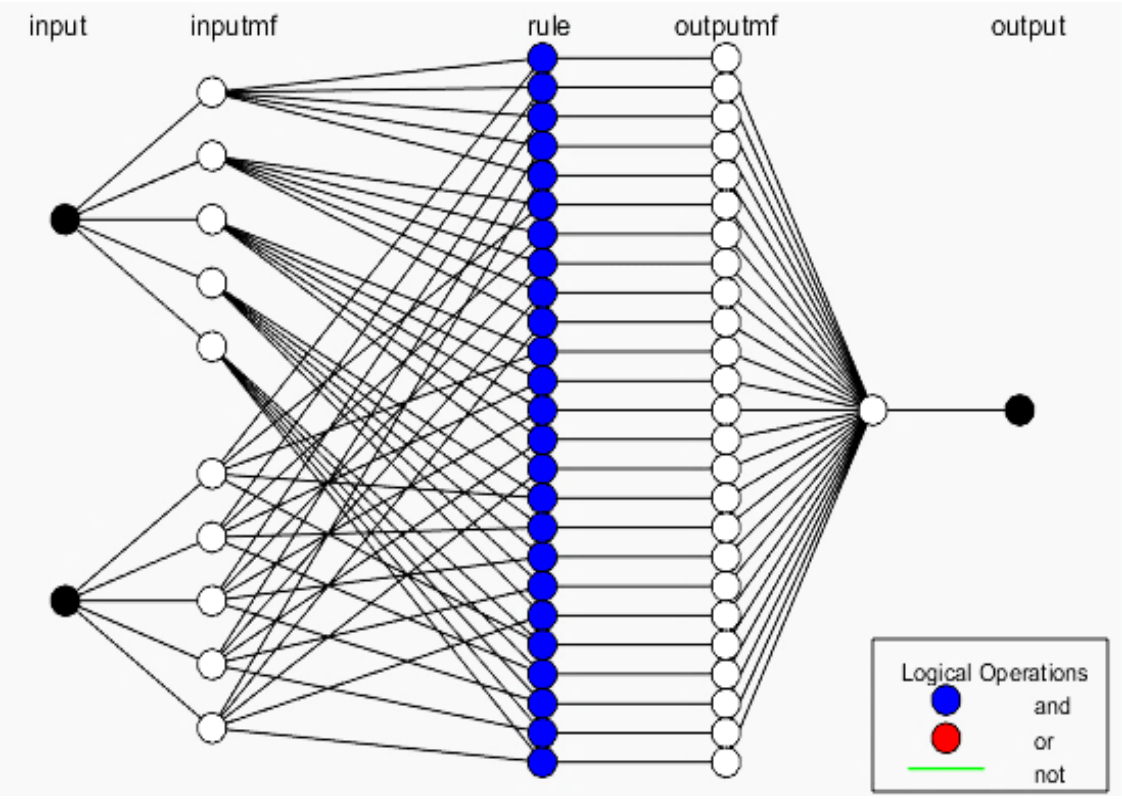

Fig. 5.5 *Optimized ANFIS architecture*

This structure was created from an initial data using MATLAB environment. Takagi-Sugeno-Kang fuzzy model-based ANFIS has been used with an architecture of two inputs

and one output, which is tuned online using a combination of least-squares estimation and back-propagation methods. The error between reference chillers operation and actual chillers operation is used to tune the neuro-fuzzy model parameters. Functions of each layer in the ANFIS architecture are formalized as follows [174]:

Layer 1: it is a fuzzification layer where each node is symbolized by a membership. Five Gaussian curve membership functions are designated to each input as shown in ***Fig. 5.5***, and its node equations are given as follows:

$$g(\xi; c, \sigma) = e^{-\frac{1}{2}\left(\frac{\xi - c}{\sigma}\right)^2} \tag{5-1}$$

where c is MF's center and σ is MF's width

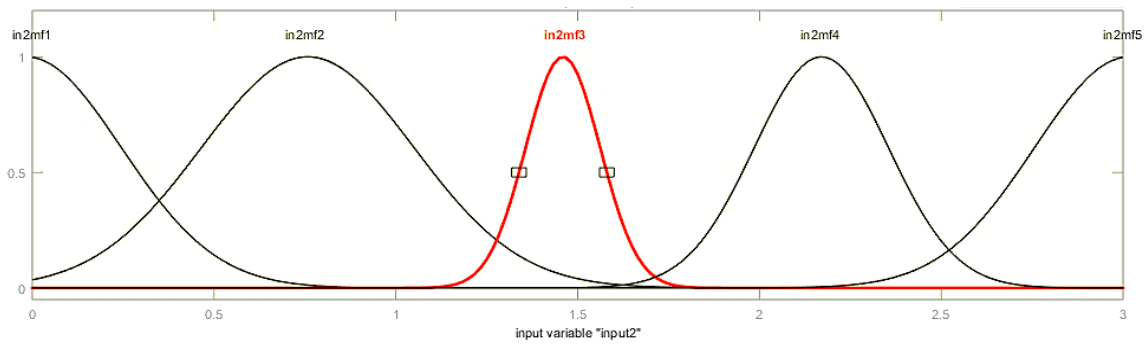

Fig. 5.6*: Gaussian curve fuzzy membership*

Layer 2: Each node in this layer is a multiplier which multiplies the input signals and forwards the result to the 3rd layer

$$\mu_{i,j} = \mu_{A_i(\xi_1)} . \mu_{B_j(\xi_2)} \ldots, i=j=1,2,3,4,5 \tag{5-2}$$

This equation characterizes the firing strength of a rule.

Layer 3: Each node in this layer calculates the normalized firing strength of each rule as given in the following:

$$\bar{\mu}_{i,j} = \frac{\mu_{i,j}}{\sum_{i=1}^{5}(\sum_{j=1}^{5}(\mu_{i,j}))} \tag{5-3}$$

Layer 4: in this layer, each node is multiplied by tuned variable weights $(a_0^{i,j}, a_1^{i,j})$ as shown in the following equation:

$$O_{i,j} = \bar{\mu}_{i,j} . f_{i,j} = \bar{\mu}_{i,j}\left(a_0^{i,j} + a_1^{i,j} . \xi\right), .. i, j = 1,2,3,4,5 \tag{5-4}$$

Layer 5: is the final output layer of the fuzzy system. The output of the system is the summation of all incoming signals from layer 3, computed as follows:

$$Y = \sum_{i=1}^{5}\left(\sum_{j=1}^{5}\left(O_{i,j}\right)\right), \ldots \quad i,j = 1,2,3,4,5 \tag{5-5}$$

5.2.2 Electrical and Cooling Energy System Procedure

Fig. 5.7 and ***Fig. 5.8*** are summarizing the general procedure of cooling and electrical systems at a resilient MEG, note that the heating system was not mentioned in this section because the heating demand is covered by the heating energy produced by the co-generator and HRSG.

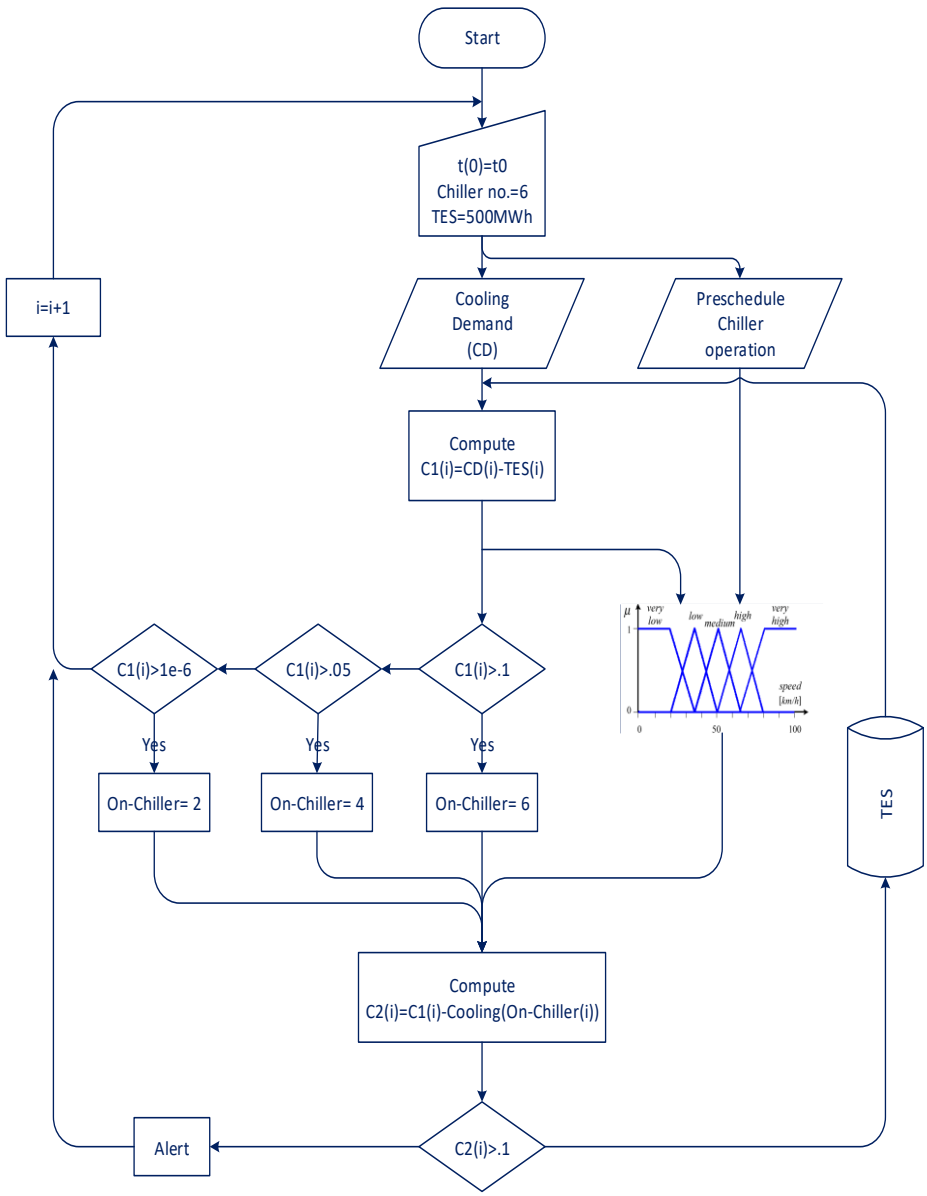

Fig. 5.7: *The MEG cooling system flowchart*

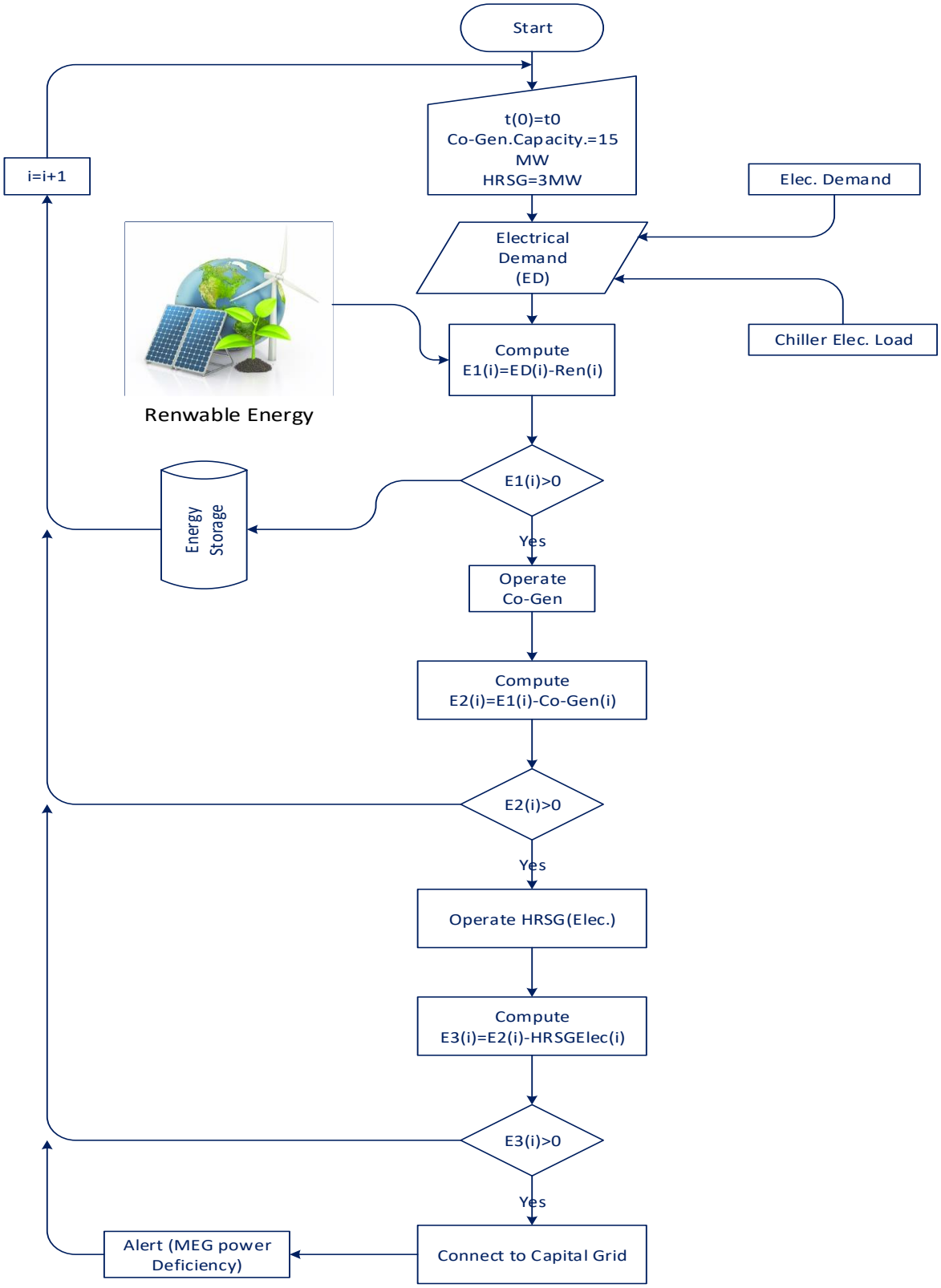

Fig. 5.8: The MEG electrical system flowchart

5.3 Case Study Simulation and Discussions

5.3.1 Simulation of a MEG with MLHDM

A case study for the proposed resilient MEG system is presented in this section using the Simulink environment. ***Fig. 5.9*** shows proposed resilient MEG has three IRLs including a hierarchical decision-making system. The proposed MEG system is implemented in the Simulink environment platform to study the system performance in different operational scenarios in order to examine the MEG system resilience for prescribed cooling, heating and electricity energy demands.

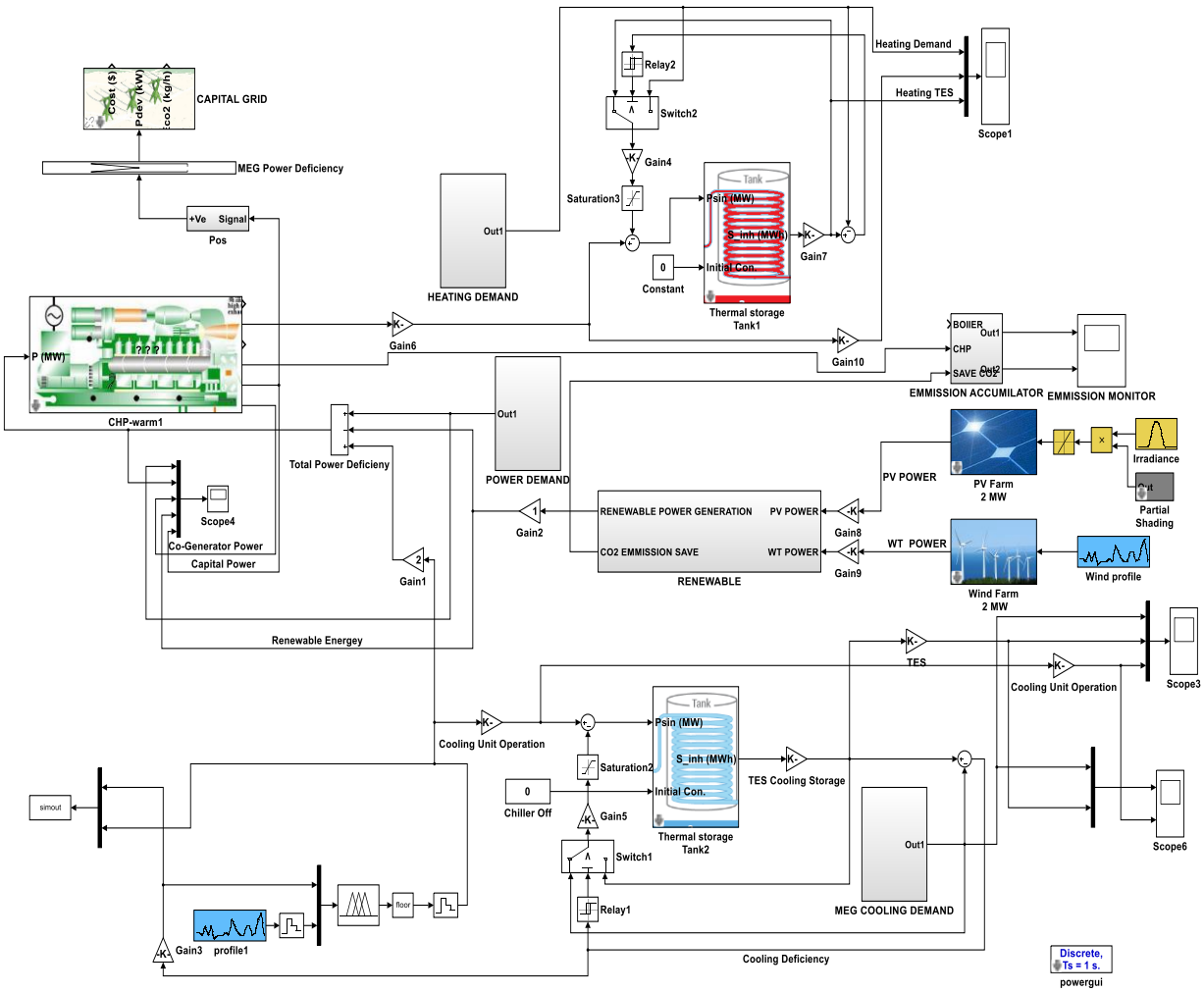

Fig. 5.9: *Simulink model for proposed MEG system*

Studying the following scenarios can realize a clear vision about the proposed IRLs performance and their effects on MEG resilience:

<u>Scenario1:</u> *Study the operation and performance of MEG (Co-generation with built-in reactive controllers)*

IRL-1 was applied in order to improve the MEG's resilience level by integrating a co-generator. The co-generator eliminates the renewable resources penetration and it covers around 60% of the energy demand requirements. In other words, this means a reduction of the severity risk of energy failure to 60% of the utility grid total failure multiplied by the PFD of the co-generator.

<u>Scenario-2:</u> *Study the operation and performance of MEG (TES and co-generation with built-in reactive controllers)*

This scenario illustrates IRL-2 capability on improving the MEG self-healing performance. IRL-2 shaves the peak demand at on-peak period by generating it at earlier off-peak periods. It can be shown that IRL-2 safeguards more than 17% of the total energy demand.

<u>Scenario-3:</u> *Study the operation and performance of MEG with TES, co-generation and a hierarchical decision-making system*

IRL-1, IRL-2 and IRL-3 were provided to the MEG in order to increase its capability and to make it operates in the islanded mode, which means IRL-3 is providing the remainder of the 23% of the total energy demand by manipulating the energy sources imports using a hierarchical decision-making approach in the MEG's structure.

<u>Scenario-4:</u> *Study the operation and performance of MEG with TES, co-generation and a hierarchical decision-making system during fault*

5.3.2 Results and discussion

In order to assess and evolve the MEG system operation, a data for a one week in summer with one-hour sampling time has been studied carefully. The interaction between co-generators, DCUs, TES storage, and the utility grid was developed by using MLHDM

to increase the MEG's level of safety, resilience, and self-healing. Three scenarios were examined in this section:

Scenario-1, one IRL, co-generation, was utilized

Scenario-2, two potentially valuable structures were utilized namely TES and co-generator.

Scenario-3, by using all the three IRLs namely, co-generator, TES and MLHDM during normal operation

Scenario-4, resilient MEG that comprises the three IRLs during fault event (four district cooling units are out of service).

The objective of the proposed strategies is to verify the performance of the proposed resilient MEG by utilizing a multi-level hierarchical decision making (MLHDM) with TES and Co-generator for the optimal reshaping of the energy demands. Hence, to propose a safety design approach that is able to reduce the impact of hazardous scenarios on the MEG's operational conditions. Performance indices of DERs, utility grid imports, and DCUs operation have been processed in order to achieve an optimum management of the electricity, heating and cooling energy profiles.

a) Scenario-1 Foundation MEG design with co-generation

Fig. 5.10 illustrates the power demand profile for a one week in summer for the original MEG structure with one IRL namely the co-generation. It can be noticed that the combination of DERs, i.e. Co-generator and RES were unable to satisfy the customer's power demand. Thus, the utility power handled the power deficiency.

The MEG cooling demand of a one week in summer is shown in ***Fig. 5.11***. The figure presents a high frequency of on-off operation of the DCUs. In every start-up the DCUs the inrush current crosses beyond a double of the unit's rated current, which increases the electricity demand due to the the high correlation between cooling and electricity demands.

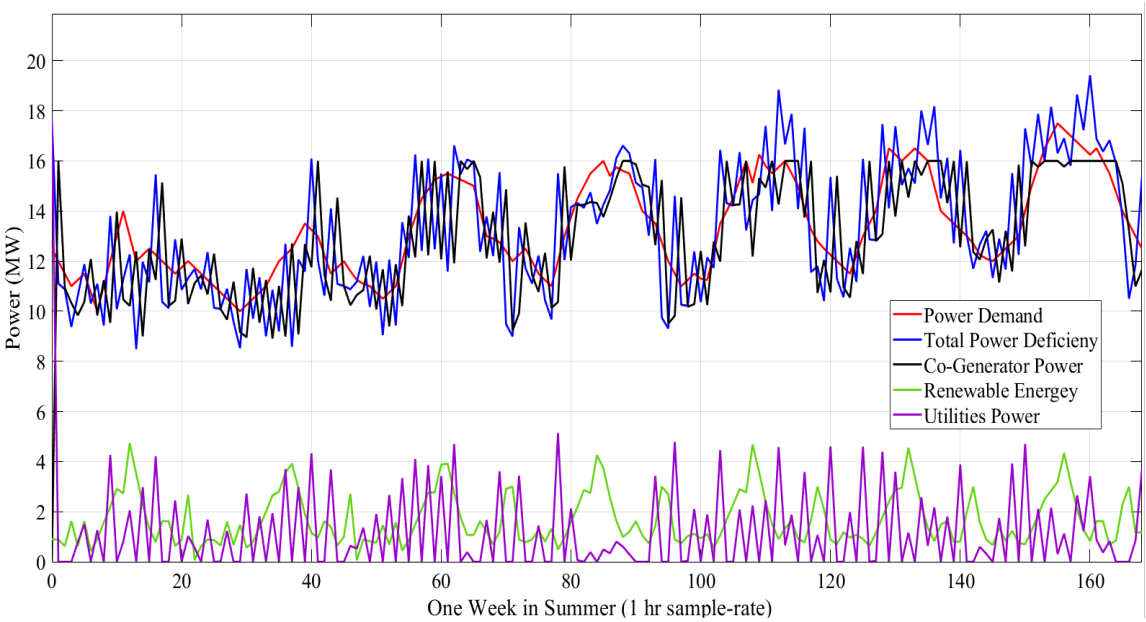

Fig. 5.10: *Power profile for foundation MEG*

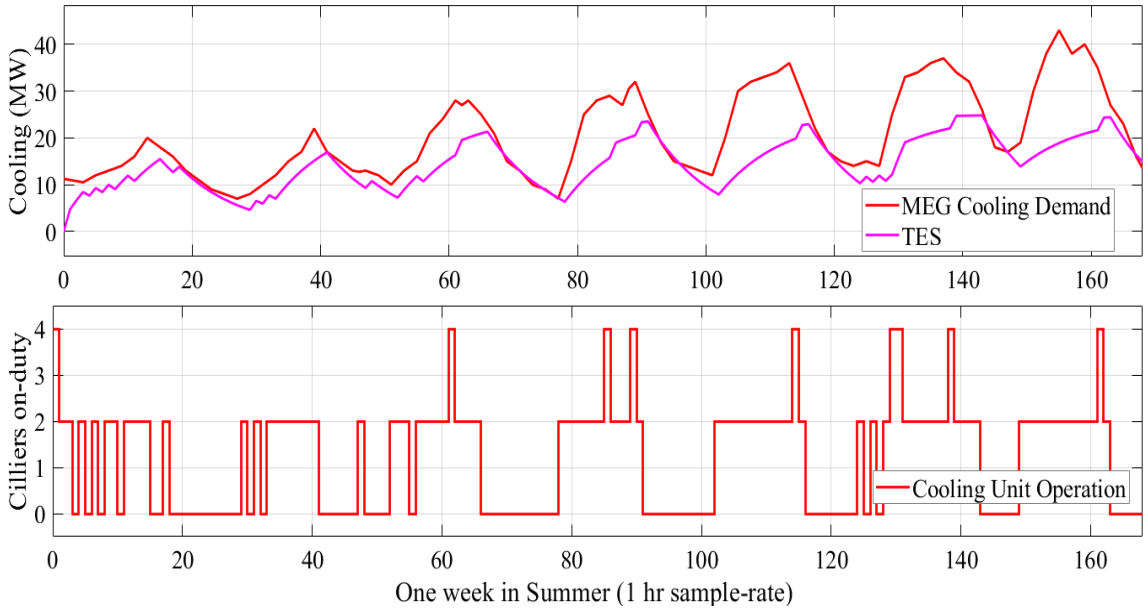

Fig. 5.11: *Cooling profile for foundation MEG*

b) *Scenario-2 Resilient MEG design comprises TES and cogeneration IRLs* with built-in reactive controllers

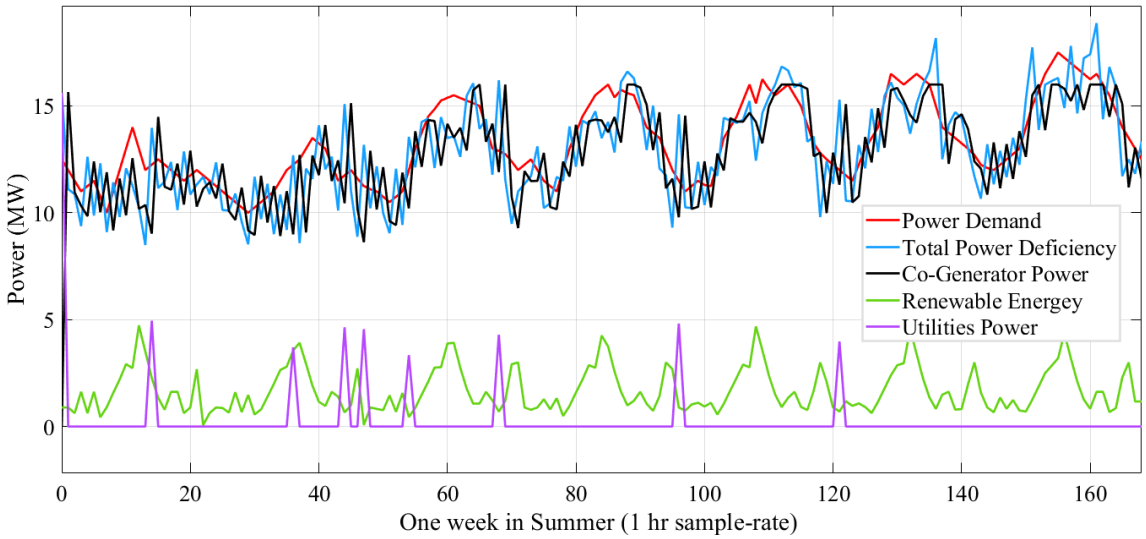

Fig. 5.12: *MEG power profile by utilizing co-generation and TES IRLs*

Fig. 5.12 presents the power demand profile for a one week in summer using co-generator and TES IRLs. The figure shows that the local DERs are not sufficient to cover the power demand during the course of the day, where the deficiency caused by a sudden rise in the power demand must be handled by the utility grid. The power deficiency occurred in two to four hours intervals a day with a maximum 8 MW while co-generator serves an average of 14 MW with a maximum production capacity of 18 MW.

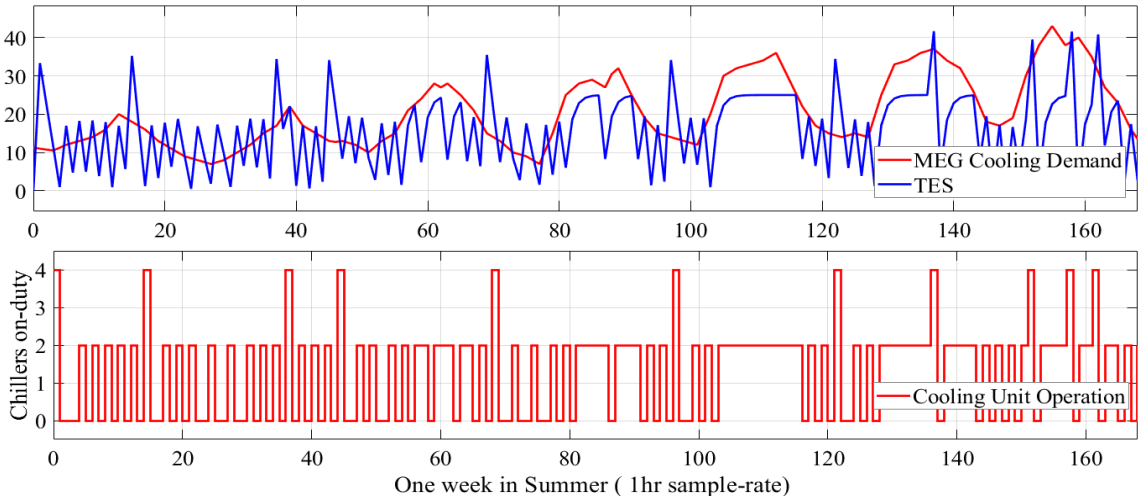

Fig. 5.13: *MEG cooling profile by utilizing co-generation and TES IRLs*

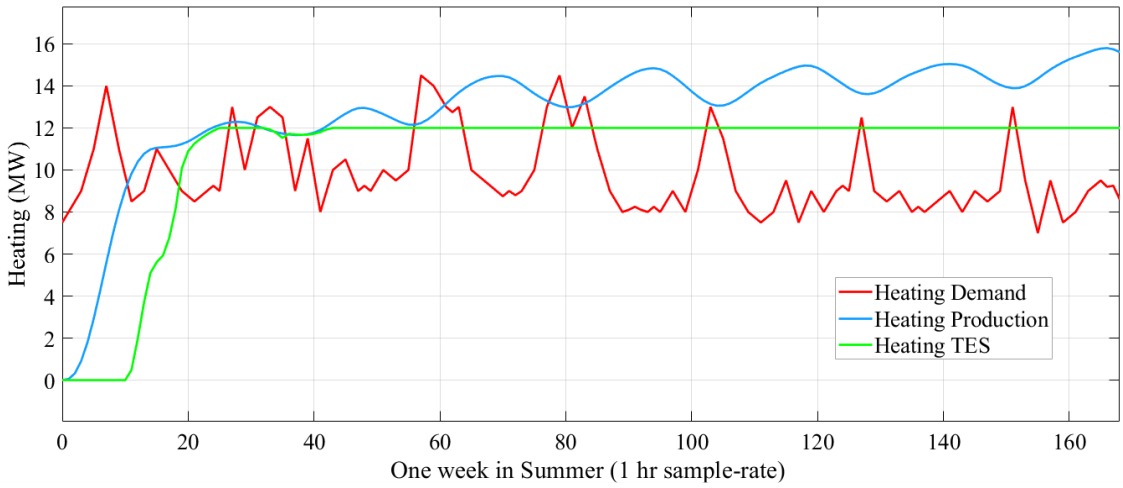

Fig. 5.14: *MEG heating profile by utilizing co-generation and TES IRLs*

Cooling profile in ***Fig. 5.13*** shows the MEG cooling demand for a one week in summer. Where the MEG is integrating a co-generator and TES. The figure illustrates that the TES improves the cooling production with less operational hours of the DCUs, regardless of the high correlation between the cooling and electricity demands.

Fig. 5.14 presents a sample of the heating demand profile for the same test week period. The figure shows that the heat generated by the co-generator was sufficient to meet the heating demand. Also, it can be noticed that there is a low correlation between electricity demand and heating demand during the summer season.

c) Scenario-3 Resilient MEG design comprises three IRLs namely, co-generator, TES and MLHDM during normal operation

Integrating the three IRLs have impressive results on the safety of a MEG, where it reduces the need for utility grid imports.

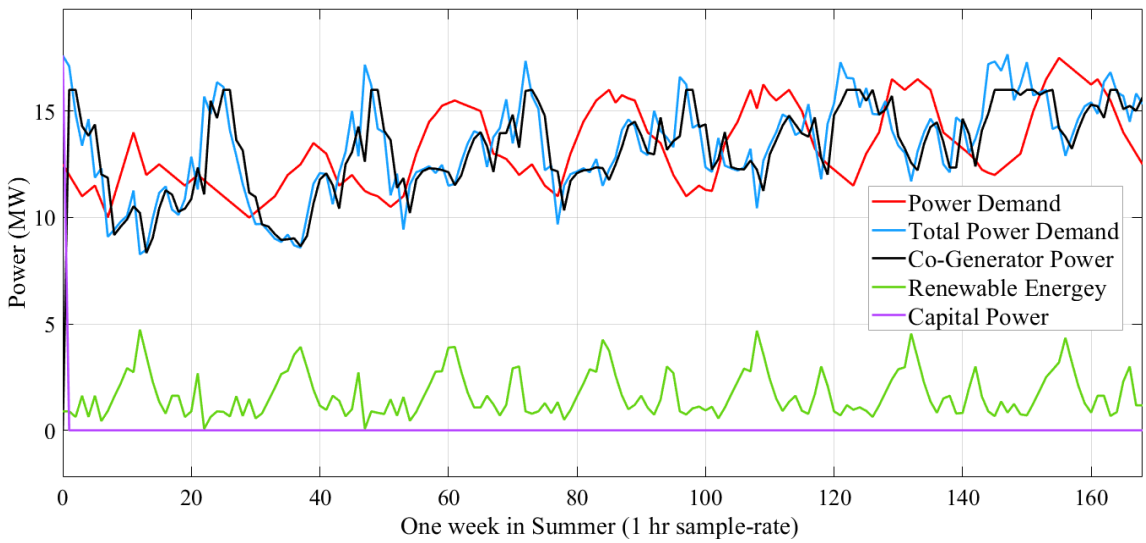

Fig. 5.15 shows more smooth power profile of the utility grid. The deficiency between total power demand and DERs production occurred on the first two days for a period of one hour in each. Mainly this happens due to the scheduled charging of the TES during the night. It can be clearly noticed that the proposed system succeeds in shifting the cooling demand power requirement to off-demand period. No power deficiency occurred during this period.

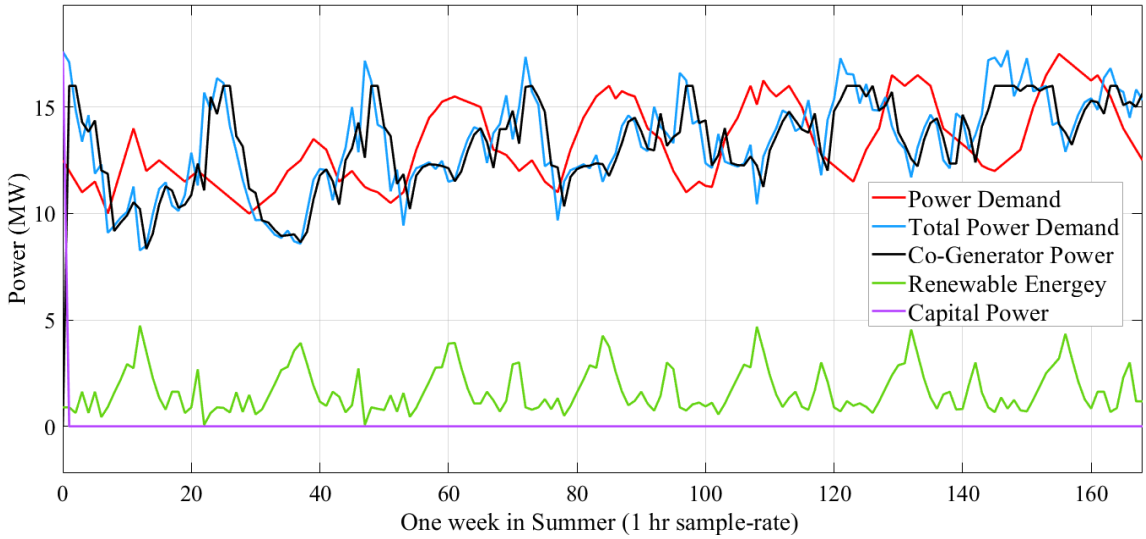

Fig. 5.15: *Power profile for a resilient MEG comprises IRL-1, IRL-2 and IRL3*

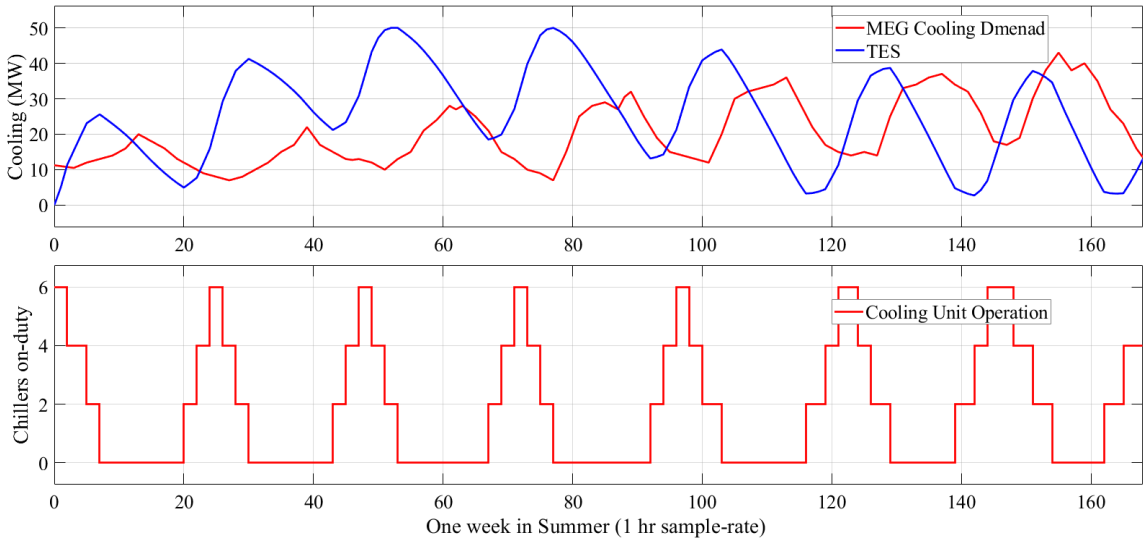

Fig. 5.16: *Cooling profile for a resilient MEG comprises IRL-1, IRL-2 and IRL3*

The cooling profile in ***Fig. 5.16*** shows an improvement in the thermal cooling units operations, where the on-peak cooling was shifted completely to the off-peak periods by using a hierarchical decision making and rescheduling the operation of the DCUs. The shifting of cooling on demand has a major positive impact on both power and cooling profiles. subsequently, it increases the MEG capability without additional upgradation of the physical hardware of the MEG infrastructure. Furthermore, it increases the MEG resilience and self-healing capability.

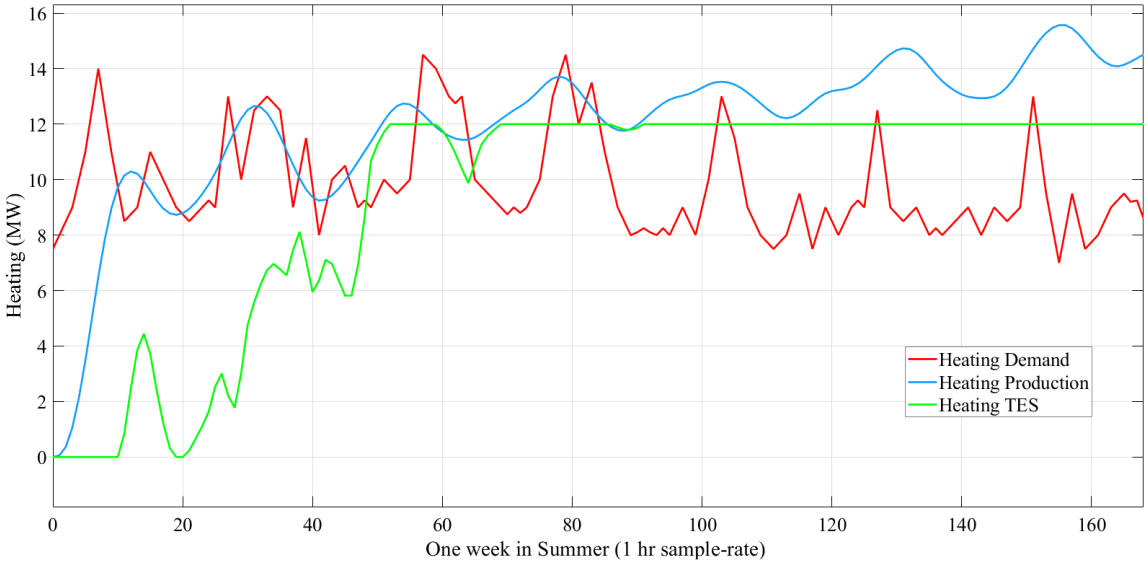

Fig. 5.17: *Heating profile for a resilient MEG comprises IRL-1, IRL-2 and IRL3*

A trial of the heating demand profile for one week in summer was presented in . Widespread coverage of the heating demand can be achieved by the heat generated from the co-generator unit. However, the figure demonstrates an exaggerated heating production by the co-generator with respect to the heating demand in summer.

d) Scenario-4 Resilient MEG that comprises three IRLs during a fault event

In order to examine the behavior of a hierarchical decision making on the MEG resilience four out of six DCUs were turned out of service to simulate a fault event in the cooling system. In this case, the pre-schedule chiller operation failed to produce the required cooling energy during the off demand period, therefore DCUs must operate during the on-demand period to cover the cooling demand shortage, as illustrated in ***Fig. 5.18***. The controller reaction helps to maintain serving cooling energy during a fault event occasion, as shown in the figure. Nevertheless, the MEG has lost the optimal flat profile for co-generator power production, it becomes following the energy demand profile, as shown in ***Fig. 5.19***.

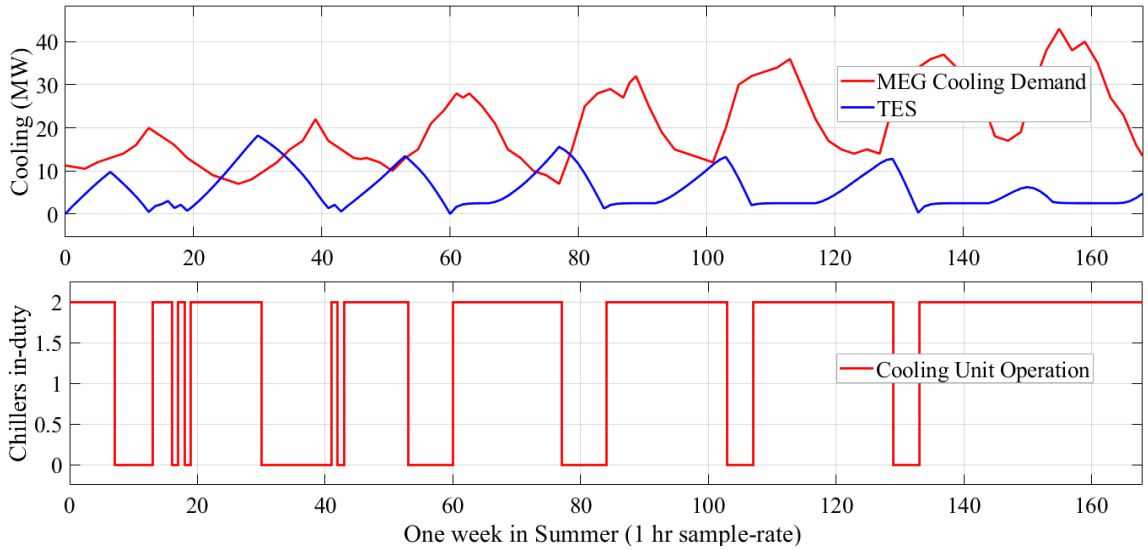

Fig. 5.18: *Cooling profile for a resilient MEG at hazard event*

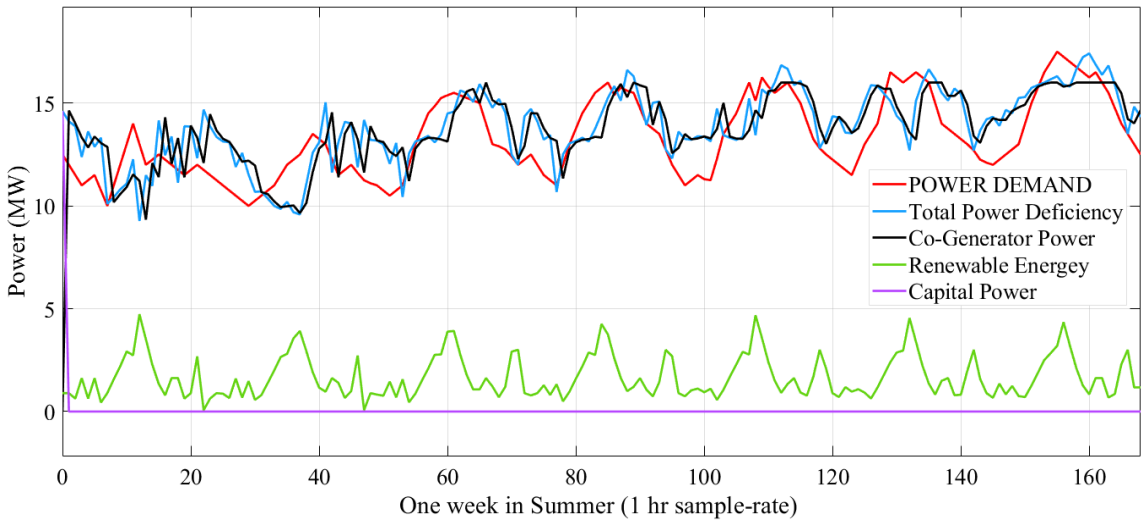

Fig. 5.19: *Power profile or a resilient MEG at hazard event*

5.4 Chapter's Conclusions

Operating during fault event is one of the challenges in MEG protection and control systems. The study presents a synthesis of safety control laws to a MEG system that composed various energy sources and storages. A proposal of non-SIF IRL namely hierarchical decision-making in three-level structure was implemented using an adaptive-network-based fuzzy inference. Coordination between control levels has been realized in order to achieve a higher resilience of the MEG and to optimize the energy production profile(s) based on the aggregated information that collected from local subsystems. This information determine some "directions" for the reactive and decision-making control levels, which refine the overall energy profiles.

Utilizing the proposed IRLs in the conventional MEG are improving the MEG's reliability to more than twice of its normal capacity, while the co-generator, TES, and MLHDM offer a significant reduction in the severity of the utility grid risk as discussed in CHAPTER 4. Subsequently, utilizing the IRLs improve the MEG performance with practical everyday considerations, such as equipment maintenance and variation in energy demand, that affect energy generation and distribution. Predicting future load profiles from historical data can provide a tolerable approximate tool for scheduling the dispatch of MEG

resources. The optimal energy imports can be achieved by using real-time energy dispatch control for effective management of MEG resources and energy flow mapping.

The case study scenarios show the different performance of the three control methodologies that discussed in 5.1. Hence, the second methodology, Centralized MEG Control, is not among these scenarios as it has a similar performance to the MLHDM, nevertheless it relies on the communication reliability. The statistical economical and ecological parameters for these operation types is illustrated in detail in CHAPTER 7.

CHAPTER 6 Proposed Intelligent Reasoning Framework for MEG Based on BBN-ANFIS (SIF-IRL)

By definition, MEG fault diagnosis is a differentiation of faults and abnormal conditions, e.g. intermittency and noncoincidence of RES, based on expert knowledge and/or historical data of MEG blackout [175]. Where the significant information of MEG's state can be extracted from sensors data [19]. Then artificial intelligence analysis, for this information, can diagnose symptoms [176].

Thus, fault diagnosis identifies fault root once it is detected. Usually, mapping the symptoms to faults in fault diagnosis procedure is a complex inference process. Generally, one fault may cause numerous symptoms, also different faults may cause similar symptoms. Fault diagnosis using rule-based method is common in fault diagnosis research. Where, rules are commonly established from expert knowledge, theoretical principles, or historical data. In the rule-based reasoning, a fault is diagnosed as soon as the corresponding rule is satisfied [177].

Bayesian belief network (BBN) was introduced earlier in Section 2.12. The BBN is vastly applied in fault diagnosis, probabilistic inference and knowledge discovery. The structure of BBN is a combination of combinatorial and probabilistic features, BBN is built over a directed acyclic graph (DAG) consist of a set of nodes linked via directional arcs [178]. Despite the BBN is guaranteed to be accurate for tree topologies, it is quite difficult to attain a full set of MEG's fault data.

6.1 Proposed fault analysis approach for MEG

The proposed approach in this study offers online fault analysis process of MEG that is considered a SIF-IRL for resilient MEG. The proposed approach is able to predict risks and diagnose faults based on Bayesian belief network (BBN). The main objective is to develop an advanced and more robust predictive/diagnosis techniques to improve the MEG condition monitoring and alarming systems. ***Fig. 6.1*** shows the flow scheme of BBN-based MEG's fault analysis approach. It consists a process of three stages, namely hazard analysis,

fault detection and BBN implementation, as well as fault prognostic and diagnostic processes.

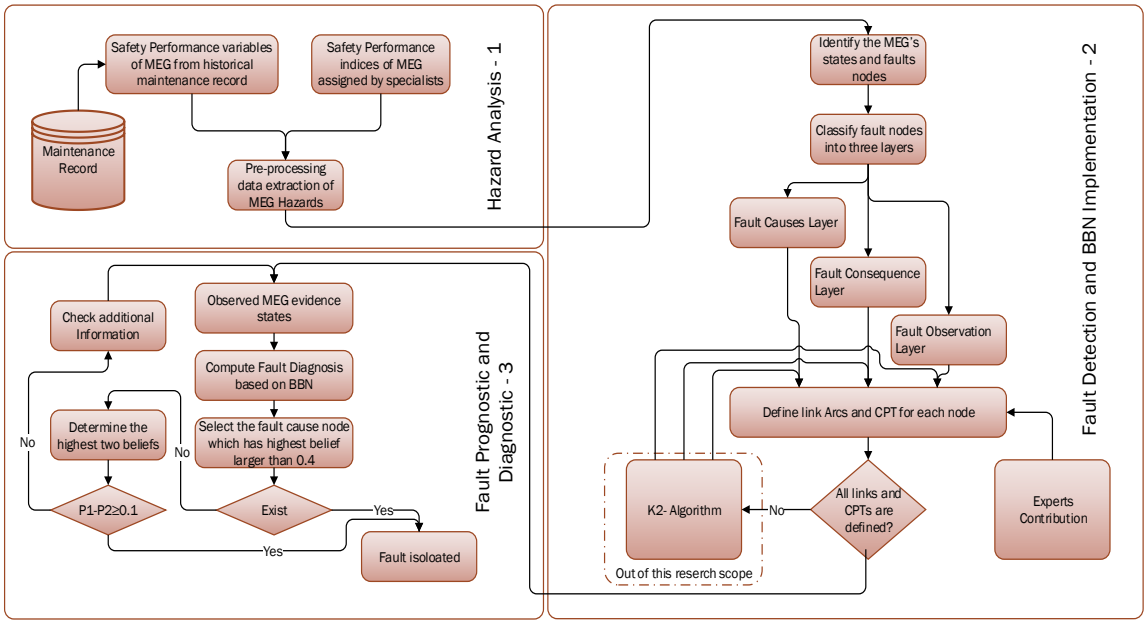

Fig. 6.1: *Flow scheme of the BBN-based MEG fault prognosis and diagnosis approach*

6.1.1 Hazard and Resilience Analysis

The MEG hazard and resilience analysis focus on determining safety performance indices. Typically, the safety indices are extracted from maintenance record and expert's knowledge. The MEG hazard analysis was discussed in detail in Section 4.2.

6.1.2 Fault Detection using BBN Implementation

In order to implement BBN structure for MEG fault detection purpose, the following steps should be considered.

Step-1: Identify the MEG's state and determine faulted nodes.

Step-2: Classify the nodes into three layers, i.e. causes, consequences and observation layers.

Step-3: Define links between parent nodes and descent nodes of successive layers then allocate the correspondent CPT of each node accordingly. The details are extensively discussed in Section 6.2.

6.1.3 Fault Prognosis and Diagnosis

Fault prognosis and diagnosis are the final product of the MEG fault analysis based-BBN approach. They provide the most realistic justification of the symptoms' inputs. The outputs are the prior and posterior probabilities respectively, as illustrated in ***Table 6-3*** and ***Table 6-5*** in section 6.4.

6.2 Bayesian Inference

The bayesian theorem is applied to define the conditional probability p(v|w), where *V* and *W* are random events. The following condition cases should be considered [179]:

1. If node W is a descendant of V $(W \in D(V))$ and $p(W) > 0$, then first Bayes' formula should be applied to reverse the direction, diagnosis query:

$$p(v|w) = \frac{p(w|v).p(v)}{p(w)} = \frac{p(v,w)}{p(w)} \tag{6-1}$$

Where *v* is a true variable of the random variable *V*, and *p(v,w)* is the joint probability. The right side term is prior probability, which is known in advance, and the left side term is the posterior probability that needs to be defined. In fact, the posterior probability is the essential concept of Bayesian inference

2. If node W is a parent of V, $(W \in C(V))$, then all other parent nodes should be identified and applying the following formula, predictive query:

$$p(v|w) = \sum_u p(v|u \wedge \ldots) \,.\, p(u \wedge \ldots |w) \tag{6-2}$$

3. If node *W* is neither a parent of *V* nor a descendant of V, $(W \in O(V))$ then there are two options:

   i. *If V* has no parents, then:

$$p(v|w) = p(v) \tag{6-3}$$

   ii. *If V* has parents, then:

$$p(v|w) = \sum_u p(v|u \wedge \ldots) \,.\, p(u \wedge \ldots |w) \tag{6-4}$$

The prior probability of the fault causes v, $p(v)$, and the conditional probability of the symptom w given v, $(p(w|v))$, can be determined based on the statistical features extracted from the historical maintenance records or assigned by specialists. Subsequently, the posterior probability $p(v|w)$ calculated by using (6-1. In general, BBN for MEG is complex as shown in ***Fig. 6.2***. There is a large number of related events of faults causes and symptoms observations, which can exponentially magnify the computation requirements of prior probabilities. BBN is offering an effective and powerful method to manage such difficulties effectively, further to its ability in interpolating the missing data of the BBN [180].

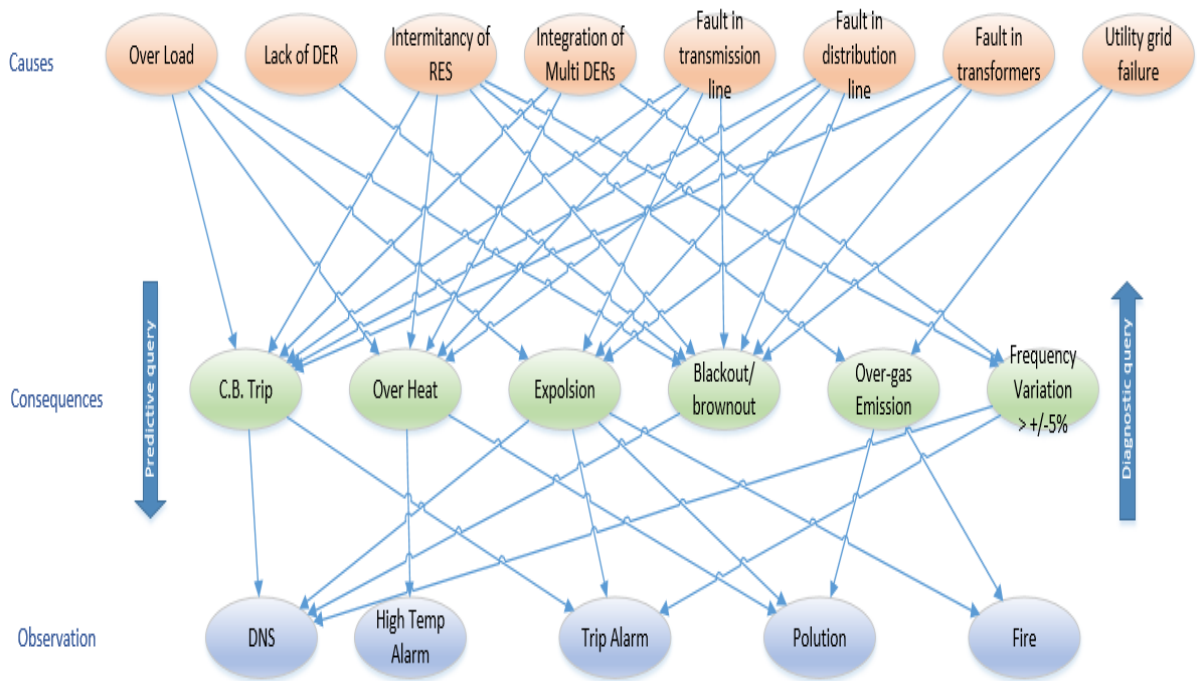

Fig. 6.2: *BBN structure of fault analysis of a MEG*

6.3 BBN Topology

In general, the BBN consists of two parts, namely the BBN structure and the nodes' parameters. The BBN structure is a graphical presentation of nodes' connections among successive layers. Node parameters are qualitative expositions of the probabilistic relationship among the model.

Table 6-1: *Node parameters in the fault causes layer*

	Node	Status	Prior probability	Hazard Event	Notes	Reference
A	Overload	Healthy	0.6014.		Feeder line section, main feeder (10km) or substation are overloaded ($\sum PFD_i$)	***Table 4-5***
		Risky	0.3986	The load demand is higher than the grid capability		
B	Lack of DER	Healthy	0.9811		The MEG has three DERs namely PV, WT and Co-gen ($\prod PFD_i$)	***Table 4-6***
		Risky	0.0189	One or more of DERs are out of service		
C	Intermittency of RES	Healthy	0.57635		Renewable sources energy production are sensitive to weather fluctuation during the day course [154]. *	
		Risky	0.42365	Unstable energy production by RES due to weather fluctuation		
D	Integration of multi DERs	False	0.9811		This MEG has three DERs namely PV, WT and Co-gen ($\prod PFD_i$)	***Table 4-6***
		True	0.0189	Negative impacts on grid parameters such as active power (P), reactive power (Q), voltage (V), phase shift (α) and frequency (f). On another word Bad Power Quality		
E	Transmission line	Healthy	0.9371		Failure rate is 0.065 ***Table 4-5***	[181][141]
		Risky	0.0629	Network congested		
F	Distribution line	Healthy	0.6703		Failure rate is 0.04/km for 10km in average, ***Table 4-5***	[141]
		Risky	0. 3297	DNS		
G	Transformers	Healthy	0.9851		Failure rate is 0.015 ***Table 4-5***	[181][141]
		Risky	0.0149	DNS		
H	Utility grid	Healthy	0.4856		Failure rate is 0.7224 ***Table 4-6***	[146]
		Risky	0.5144	DERs should cap the demand		

*by taking the MEG case study the total energy for RES is 284.6963 MWh per week, the average power production is 1.6946 MW . Thus the probability of availability is 0.42365

The BBN structure and node parameters can be determined by either expert knowledge or historical data or a mixture of both [175]. ***Table 6-1*** illustrates the prior probability of the nodes allocated in the layer of causes; these nodes are extracted from historical data provided in [182] and [183]. These nodes are root nodes as they do not have parents. On the other hand, child nodes have a conditional probability table (CPT) relied on parental probability values (e.g. ***Table 6-2*** for node "Fire" in the observation layer).

Several algorithms can be utilized for performing the inference. Mainly, the algorithms are classified into two categories as follows:

- Exact algorithms, such as the junction tree algorithm
- Approximate algorithms e.g. the weighting likelihood sampling and the Gibbs sampling algorithm.

In this study, the exact algorithm is used for the interest of accuracy.

Table 6-2: *Conditional probability table (CPT) for node "Fire" at 3rd layer in Fig. 6.2*

	Explosion	False		True	
	Over-gas emission	False	True	False	True
Fire	False	0.99	0.1	0.2	0.01
	True	0.01	0.9	0.8	0.99

The inference process is either a prediction query, when the fault causes are known, or diagnosis query, when certain observation symptoms are exist. Therefore, the BBN is utilized to provide the probability of observation symptoms and to evaluate the posterior probability of the fault roots subsequently.

6.3.1 BBN structure for MEG

The proposed BBN for MEG consists of three layers which are as follows: Fault causes - Layer 1, fault consequences – Layer 2 and fault observation – Layer 3

a) Fault causes – layer 1: This layer consists most of the potential failure hazards on MEG
b) Fault consequences – layer 2: This layer composes the direct consequences of the failure indicated in layer 1. These consequences can be determined by expertise or special measurement instruments
c) Failure observation – layer 3: This layer contains alarm indicators, performance indices and visible observation corresponding certain fault causes.

6.3.2 BBN node parameters

The node attributes for BBN can be categorized into two classes: prior probabilities for root nodes in the 1st layer, as shown in ***Table 6-1*** and conditional probabilities among rest of the nodes within the 2nd and 3rd layers, as illustrated in ***Table 6-2***.

6.4 Application Case Study of BBN Framework for MEG's Fault Diagnosis

The fault diagnosis BBN-based approach was conducted on the MEG case study described in CHAPTER 3.

The BBN is adapted to detect and diagnose faults based on expert knowledge and field operation team's feedback. The hazards matrix for a MEG case study is found in Section 4.2. This statistical data is utilized in BBN construction then the k_2 algorithm can be used to adapt the BBN structure and to adjust nodes probabilities [184]. Finally, the network query process can be done for selected shreds of evidence by utilizing the junction tree algorithm [185]. To the best of the author's knowledge, so far there is no other publication reporting MEG fault prognosis and diagnosis based on BBN.

6.4.1 BBN structure

The BBN structure is illustrated in ***Fig. 6.2***. Eight nodes comprise the fault causes layer. Each node has two states, e.g. healthy and risky, which indicate normal and faulty operation of node "overload" respectively. ***Table 6-1*** illustrates node parameters in the fault causes layer.

a) Fault Prognostic

Table 6-3 presents the conditional probability of fault prognostic in the observation query direction, it shows the observation probability for each node in the observation layer based on the assumption that one or two concurrent fault events is(are) occurring at the same time.

Table 6-3: *The conditional probability of fault prognostic for one and two combined fault causes of a MEG*

#	Fault causes Nodes	Fault Symptoms result				
		DNS	High Temp. Alarm	Trip Alarm	Pollution Alarm	Fire
		15	16	17	18	19
1	Overload	**0.8314**	0.5799	0.8000	0.6109	0.6708
2	Lack of DER	**0.6250**	0.3624	0.5904	0.4935	0.5952
3	Intermittency of RES	0.6283	0.4240	**0.7043**	0.5904	0.6970
4	Integration of multi DERs	0.6152	0.4296	**0.7602**	0.5130	0.5958
5	Fault in transmission line	**0.8430**	0.5575	0.8368	0.6192	0.6885
6	Fault in distribution line	0.8695	0.5263	**0.9068**	0.7688	0.8967
7	Fault in transformers	**0.8309**	0.3621	0.7970	0.5159	0.6229
8	Utility grid failure	0.6021	0.3646	0.5924	0.6158	**0.7540**
1-2	Overload-Lack of DER	**0.8682**	0.5799	0.8000	0.6109	0.6708
1-3	Overload-Intermittency of RES	0.8543	0.6253	**0.8551**	0.6938	0.7544
1-4	Overload-Integration of multi DERs	0.8437	0.6901	**0.8773**	0.6414	0.6716
1-5	Overload-Fault in transmission line	**0.9075**	0.7914	0.8902	0.7368	0.7687

1-6	Overload-Fault in distribution line	0.9370	0.7860	**0.9428**	0.8346	0.9143
1-7	Overload-Fault in transformers	**0.9118**	0.5799	0.8830	0.6134	0.6745
1-8	Overload-Utility grid failure	**0.8318**	0.5819	0.8006	0.7214	0.8010
2-3	Lack of DER-Intermittency of RES	0.6551	0.4240	**0.7043**	0.5904	0.6970
2-4	Lack of DER-Integration of multi DERs	0.6552	0.4296	**0.7602**	0.5130	0.5959
2-5	Lack of DER-Fault in transmission line	**0.8599**	0.5575	0.8368	0.6193	0.6886
2-6	Lack of DER-Fault in distribution line	0.8806	0.5263	**0.9068**	0.7688	0.8967
2-7	Lack of DER-Fault in transformers	**0.8412**	0.3621	0.7970	0.5159	0.6229
2-8	Lack of DER-Utility grid failure	0.6267	0.3646	0.5924	0.6158	**0.7540**
3-4	Intermittency of RES-Integration of multi DERs	0.6466	0.5027	**0.8093**	0.6122	0.6974
3-5	Intermittency of RES-Fault in transmission line	0.8551	0.5693	**0.8768**	0.6929	0.7678
3-6	Intermittency of RES-Fault in distribution line	0.8814	0.5495	**0.9303**	0.8291	0.9253
3-7	Intermittency of RES-Fault in transformers	0.8424	0.4236	**0.8451**	0.6108	0.7181
3-8	Intermittency of RES-Utility grid failure	0.6299	0.4267	0.7056	0.7249	**0.8716**
4-5	Integration of multi DERs-Fault in transmission line	0.8568	0.5779	**0.9042**	0.6245	0.6891

4-6	Integration of multi DERs-Fault in distribution line	0.8865	0.5664	**0.9464**	0.7773	0.8968
4-7	Integration of multi DERs-Fault in transformers	0.8419	0.4293	**0.8737**	0.5352	0.6236
4-8	Integration of multi DERs-Utility grid failure	0.6333	0.4321	**0.7613**	0.6344	0.7543
5-6	Fault in transmission line-Fault in distribution line	0.9007	0.6537	**0.9174**	0.8016	0.9051
5-7	Fault in transmission line-Fault in transformers	**0.8751**	0.5579	0.8351	0.6302	0.7057
5-8	Fault in transmission line-Utility grid failure	**0.8434**	0.5594	0.8372	0.7286	0.8121
6-7	Fault in distribution line-Fault in transformers	0.8984	0.5262	**0.9183**	0.7819	0.9135
6-8	Fault in distribution line-Utility grid failure	0.8696	0.5267	0.9070	0.8558	**0.9413**
7-8	Fault in transformers-Utility grid failure	**0.8314**	0.3642	0.7978	0.6360	0.7713

The fault consequence layer consists of six nodes, which account for major consequences of the failure due to faults stated in fault causes layer.

Five nodes form the observation layer, i.e. demand not served (DNS), High Temp Alarm, Trip Alarm, Pollution and Fire.

The observation or symptom nodes indicate the performance indices such as sensor instruments. The fault pattern for the selected fault detection approach is defined using arcs and parameters (CPT). Each node has two states i.e. Healthy/Risky, or True/False. It is useful to note that the nodes in the fault observation layer are mostly essential but not enough for detecting and diagnosing the faults in the fault causes layer, where other factors

may also lead to the same certain fault causes. ***Fig. 6.3*** and ***Table 6-4*** illustrates the fault observation frequency based on the fault causes combination shown in ***Table 6-3***. It is clear that "Trip Alarm" node has the highest frequency among all possible fault causes events with 70 % and then "DNS" 48 %. However, two other nodes namely " High Temp. Alarm" and "Pollution Alarm" are not the main reason for any of the case studies in ***Table 6-3*** but they have second and third highest probabilities for many cases in this table.

Table 6-4: *Fault observation frequency based on fault causes combination shown in Table 6-3*

Fault observation type	**DNS**	**High Temp. Alarm**	**Trip Alarm**	**Pollution Alarm**	**Fire**
Frequency Percent	48%	0%	70%	0%	15%

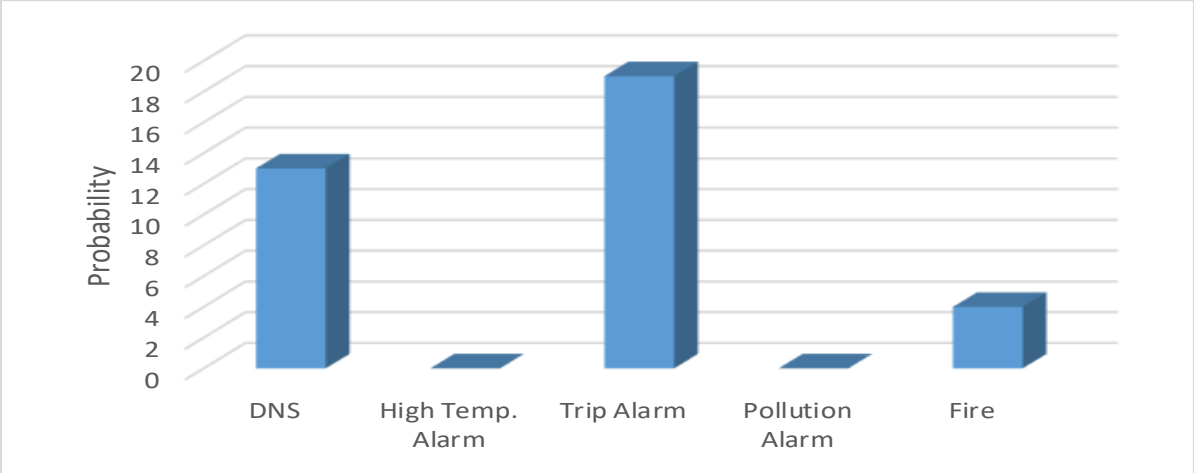

Fig. 6.3: *Fault observation frequency based on fault causes combination shown in Table 6-3*

b) Fault Diagnosis

The process direction of the fault diagnosis query is opposite to the prognostic query's direction, where information of observation layer status is known and the diagnostic probability of fault causes are required. In ***Table 6-5***, the diagnosis symptoms of one and two fault observation events are illustrated.

Table 6-5: *The conditional probability of fault diagnosis for one and two combined faults observation of a MEG*

Node #	**Fault observation nodes**	**Fault diagnosis result**							
		Overload	Lack of DER	Intermittency of RES	Integration of multi DERs	Fault in Transmission line	Fault in distribution line	Fault in transformer	Utility grid failure
		1	2	3	4	5	6	7	8
15	Demand not served (DNS)	**0.5716**	0.0203	0.4556	0.0200	0.0915	0.4970	0.0213	0.5276
16	High Temp. Alarm	**0.6411**	0.0189	0.4945	0.0225	0.0973	0.4838	0.0149	0.5139
17	Trip Alarm	**0.5430**	0.0189	0.5041	0.0244	0.0896	0.5117	0.0201	0.5124
18	Pollution Alarm	0.4960	0.0189	0.5056	0.0197	0.0794	0.519	0.0156	**0.6373**
19	Fire	0.4516	0.0189	0.4949	0.0190	0.0732	0.5019	0.0156	**0.6470**
15-16	Demand not served (DNS)-High Temp. Alarm	**0.7217**	0.0196	0.4795	0.0225	0.1111	0.5693	0.0173	0.5161
15-17	Demand not served (DNS)-Trip Alarm	**0.5965**	0.0195	0.4757	0.0218	0.0987	0.5755	0.0220	0.5134
15-18	Demand not served (DNS)-Pollution Alarm	0.5835	0.0195	0.4954	0.0202	0.0941	0.6199	0.0184	**0.6068**
15-19	Demand not served (DNS)-Fire	0.5517	0.0195	0.4842	0.0196	0.0898	**0.6192**	0.0190	0.6002

16-17	High Temp. Alarm-Trip Alarm	0.6929	0.0189	0.5040	0.0247	**0.1087**	0.5781	0.0168	0.5142
16-18	High Temp. Alarm-Pollution Alarm	0.6604	0.0189	0.5243	**0.0223**	0.1009	0.5750	0.0151	0.5865
16-19	High Temp. Alarm-Fire	0.6504	0.0189	0.5209	0.0218	**0.1001**	0.6132	0.0152	0.6020
17-18	Trip Alarm-Pollution Alarm	0.5599	0.0189	0.5201	0.0220	0.0918	**0.6255**	0.0177	0.6008
17-19	Trip Alarm-Fire	0.5303	0.0189	0.5121	0.0217	0.0878	**0.6239**	0.0182	0.5904
18-19	Pollution Alarm-Fire	0.4952	0.0189	0.5102	0.0194	0.0800	0.5655	0.0158	**0.6592**

Fig. 6.4 and ***Table 6-6*** illustrates the fault observation frequency based on the fault causes combination shown in ***Table 6-5***. It is clear that "Overload" and "Utility grid failure" nodes have the highest frequency among all possible fault causes events 33% and 27% respectively. However, three other nodes namely "Lack of DER", "Intermittency of RES" and "Fault in transformer" are not the main reason for any of the case studies in ***Table 6-5*** but they have second and third highest probabilities for many cases in this table.

Table 6-6: *Fault observation frequency based on fault causes combination shown in Table 6-3*

Fault observation type	Overload	Lack of DER	Intermittency of RES	Integration of multi DERs	Fault in Transmission	Fault in distribution	Fault in transformer	Utility grid failure
Frequency Percent	33%	0%	0%	7%	13%	20%	0%	27%

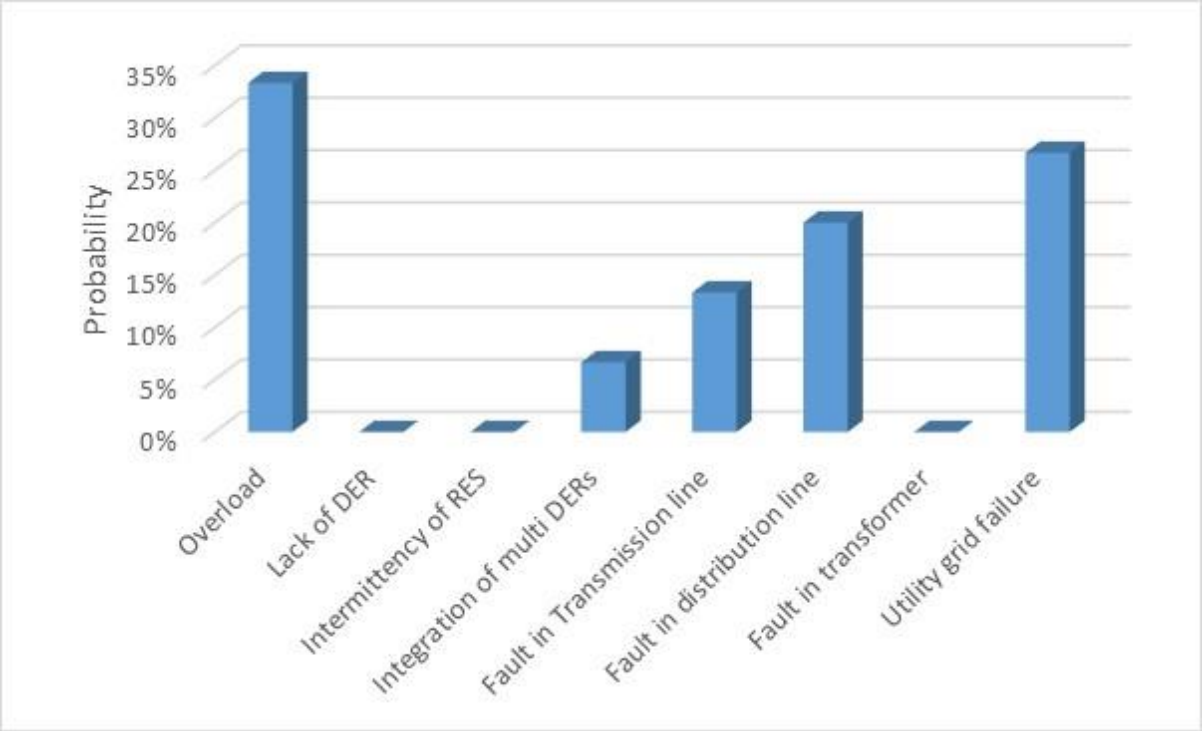

Fig. 6.4: *Fault observation frequency based on fault causes combination shown in Table 6-5*

6.4.2 Implementation of BBN-based MEG Fault Analysis using Matlab

The BBN-based fault analysis of MEG can be implemented using Matlab platform, as shown in ***Fig. 6.5***. BBN allows three types of inquiry process as follows:

1- Predictive query:

What is the probability of the cause of "Overload" lead to the observation of "DNS"?

P (15|1) = 16.86 % False

83.14 % True

2- Diagnosis query can be as follows:

What is the probability of observing "DNS" caused by the occurrence of "Overload"?

P(1|15) = 42.84 % False

57.16 % True

3- The intra-casual query can be as follows:

What is the probability of both causes “Overload” and “Intermittency of RES” lead to observe “DNS”?

P(15|1,3) = 14.57 % False

85.43 % True

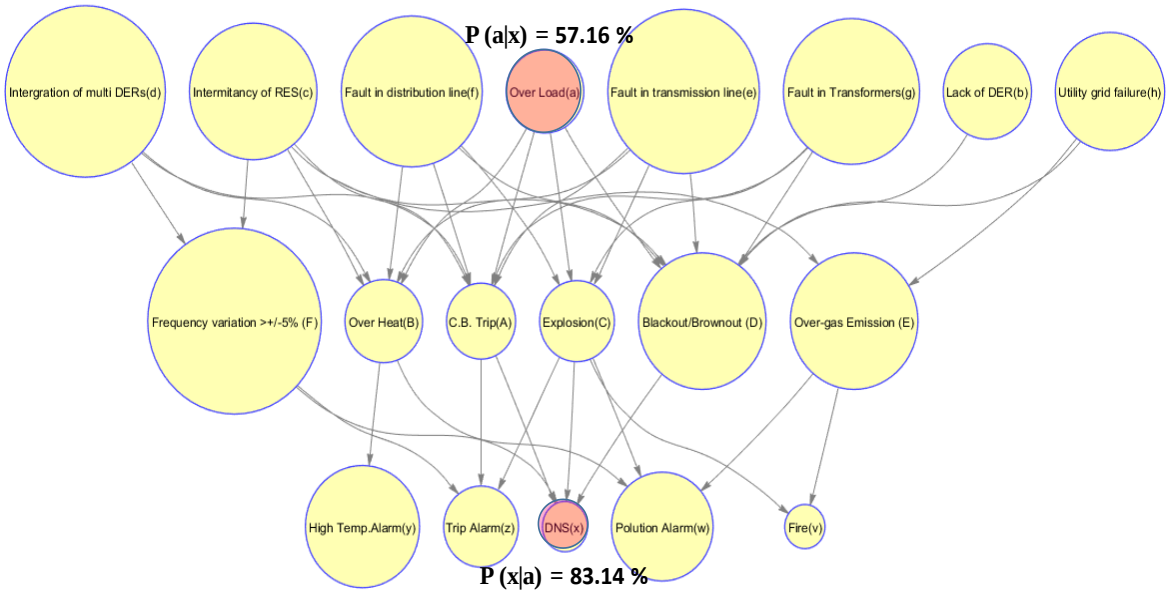

Fig. 6.5: *BBN implementation of MEG using Matlab platform*

6.5 Fault Diagnosis of Micro Energy Grids Using BBN and ANFIS

6.5.1 Introduction

The proposed MEG safety assessment approach in this section splits the analysis process into two main disciplines, i.e. Bayesian belief network (BBN) layer and adaptive-network-based fuzzy inference system (ANFIS) layer. The motivation of using ANFIS is to declare the ambiguous produced in the BBN output nodes and to incorporate the experts’ knowledge to the data collected from measurement instrumentation (I&C) in order to provide a more precise decision-making process.

The proposed hybrid technique considers the following data sets that are essential for safety analysis:

- Deterministic dataset of credible information such as system topology, operation parameters, units specification, etc.;
- Statistical data - historical observation of the system operation life cycle; and
- Linguistic data – defines the system behavior by expert's knowledge contribution.

The main challenges associated with MEG safety assessment are dealing with randomness, vagueness and uncertainties.

Many fuzzy models were presented to deal with vagueness [186] and many reasoning approaches were illustrated to deal with uncertainties [22]. However, integration of different safety assessment methods for complex systems is still in the early stages.

6.5.2 BBN-ANFIS Based Fault Diagnosis Model

The proposed approach consists of two cascaded layers i.e. BBN layer and ANFIS layer. Where the output of the BBN layer is the input to the ANFIS layer. Therefore, safety assessment process runs in consequence from top to bottom as given in ***Fig. 6.6***.

Deterministic data of MEG has sufficient information to create BBN qualitative structure for MEG diagnosis approach. The linguistic data is mainly used to build the ANFIS structure. The quantitative term of each node in the BBN and ANFIS structures can be illustrated from statistical data analysis, which is the conditional probability tables (CPT) and the membership function (MF) respectively [187].

The inputs to the BBN layer are MEG's condition measurements, which is extracted from the deterministic data of the MEG. ***Fig. 6.2*** illustrates the BBN structure of a MEG. The BBN consists of five parameters of condition measurements that form the observation level and the parameters are: demand not served (DNS), high-temperature alarm, trip alarm, pollution level and fire alarm. The BBN structure also consists of the output parameters which form the causes level and include: overload, lack of DER, intermittency of RES, integration of multi DERs, faults in the transmission line, faults in distribution line, faults in transformer and utility grid failure.

The main role of ANFIS layer is to process the BBN output values to provide an accurate decision of which parameter(s) is (are) causing the fault event.

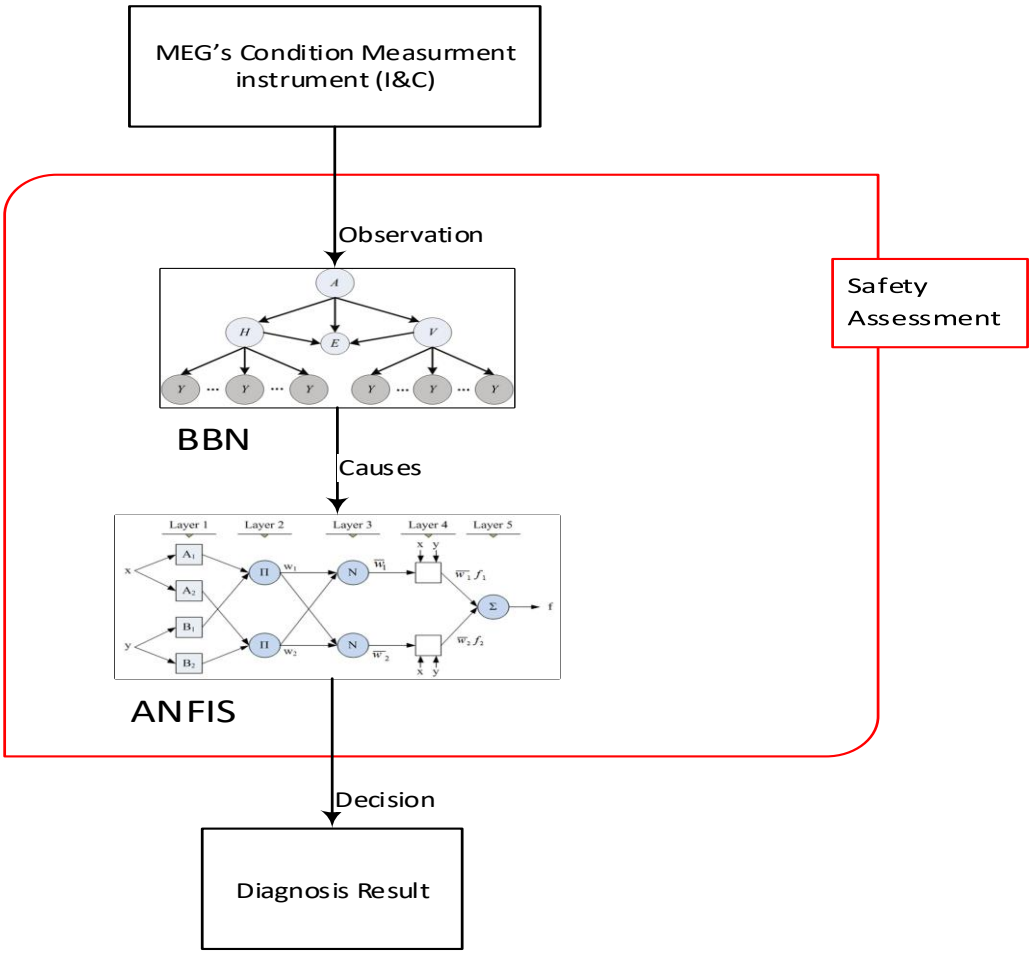

Fig. 6.6: *Hybrid MEG safety assessment approach*

6.5.3 Adaptive Neuro-Fuzzy interference system

The modern expert systems are utilizing fuzzy logic theory for reasoning the input data instead of Boolean logic [188]. The fuzzy expert system converts a set of user-supplied human language rules to their mathematical equivalents.

ANFIS is an integration of neural network (NN) and fuzzy logic (FL) [189]. Fuzzy logic has the capability to convert human knowledge and insights into a quantitative process and rules. Nevertheless, there is no defined rule governing the converting process of human knowledge to rule-based fuzzy inference system (FIS), further to a long process time to refine the shapes and ranges of the membership functions (MFs). The NN has a greater capability in the learning process. Thus, the NN was used to refine the MFs automatically [174].

6.5.4 Application of hybrid BBN-ANFIS for MEG Safety Assessment

In accordance with the literature, numerous faults may cause an energy blackout. The most common fault events and their observation parameters were presented in ref. [155]. The BBN structure in ***Fig. 6.2*** is proposed to reasoning links between fault observation and fault causes layers (diagnosis symptoms) as shown in ***Table 6-5***.

Fig. 6.7 shows an ANFIS structure of the MEG safety assessment decision-making stage. The ANFIS architecture consists of five main layers, each layer consists of a number of nodes distributed as follows: 8-112-14-141. The first and fourth layers consist of adaptive nodes while fixed nodes are used among the other layers.

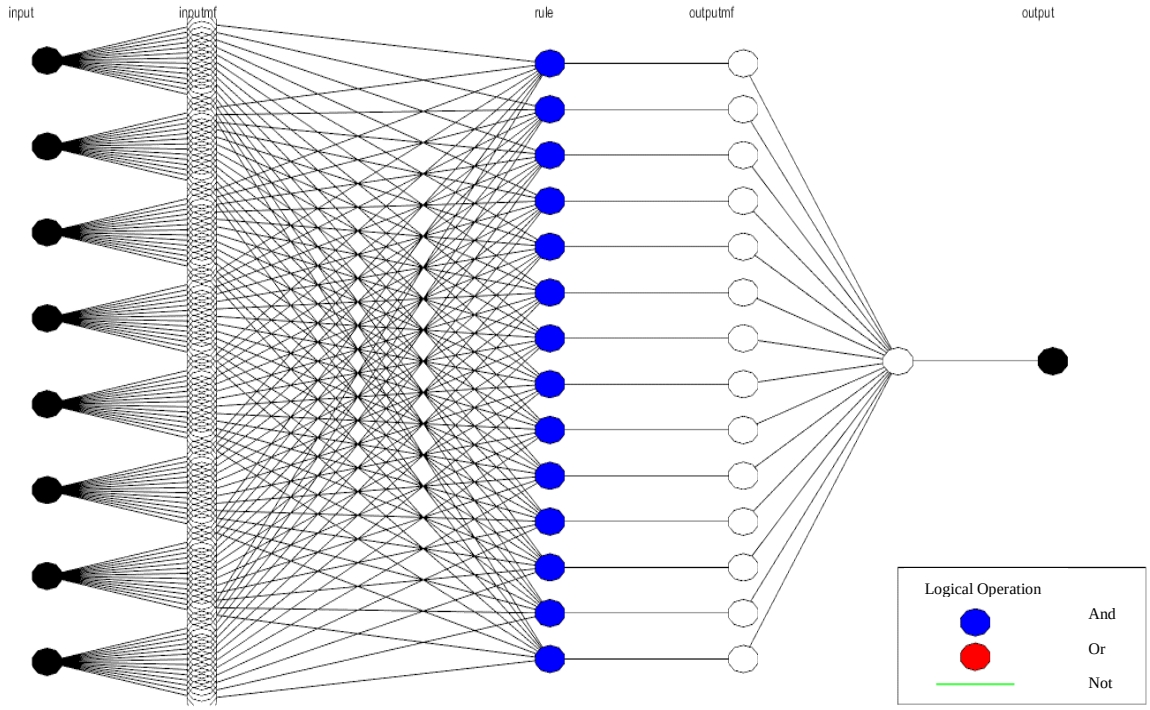

Fig. 6.7 : *The structure of adaptive neuro-fuzzy interference system*

The eight input nodes that form the first layer of ANFIS are the diagnosis symptoms of a MEG illustrated in ***Table 6-5*** and each node in this layer has three Gaussian membership functions

$$Gaussian(x, c, \sigma) = e^{\frac{1}{2}\left(\frac{x-c}{\sigma}\right)^2} \tag{6-5}$$

Where c is the center of the membership function and σ its width.

Unlikely, the output layer consists of one node that provides a decision of which input node(s) is (are) causing the hazardous event.

The scheme of fuzzy reasoning mechanism of ANFIS is illustrated in **Fig. 6.8**. Fourteen if-then rules are governing the process where the columns represent the eight inputs and one output data.

Fifteen cases with complete symptoms, see ***Table 6-5***, were utilized to evaluate the hybrid BBN-ANFIS performance for fault diagnosis of a MEG.

Fig. 6.8 illustrates the first case in ***Table 6-5***, where the symptom nodes states are medium, medium, medium, medium, medium, medium, medium and medium, respectively and the nodes summation is normalized. Based on this evidence, the posterior probability of each fault can be computed to obtain the most candidate fault among all, in this case, is the "Fault in transformer", with a probability of 98.31%.

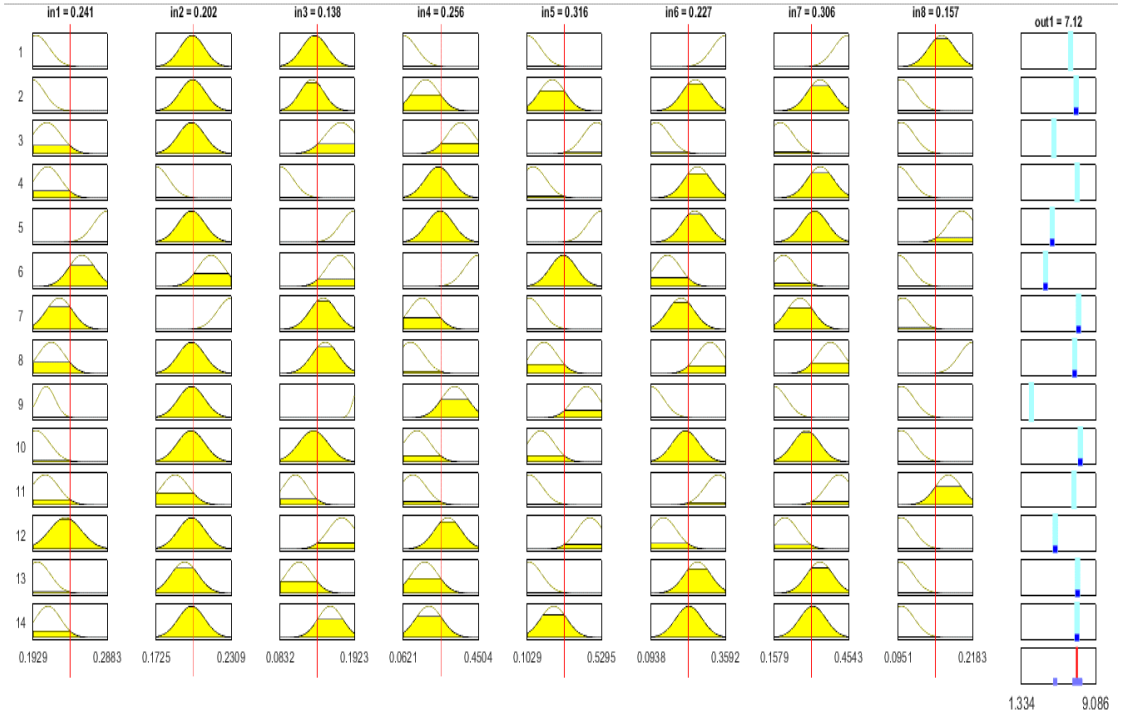

Fig. 6.8: *Fuzzy reasoning ANFIS scheme of MEG*

6.6 Chapter's Conclusions

The study in this chapter introduces a MEG SIF IRL namely MEG alarm system that using an intelligent reasoning framework based on BBN-ANFIS. The proposed BBN structural consists of three layers for MEG fault prognosis and diagnosis processes. The BBN is an accurate computation of the uncertainties occurrence in MEG fault analysis. Different sources of knowledge and information can be integrated to emulate the diagnostic thinking and diagnosis process of expert's knowledge. BBN can be utilized for instant fault prognosis process as well as it can be used for real-time fault diagnosis analysis. It is worth noticing that the more information involved in the BBN, the higher smartness it would be. Correspondingly, the more evidence included in the query process, the more precise the outcomes would be.

As exposed through the results, of the fault prognostic and diagnostic queries for MEG, the BBN approach performs properly for the uncertainties in MEG. The results in ***Table 6-3*** and ***Table 6-5*** came in line with the expectation shown in the hazard matrix of MEG [8] and the resilience matrix Appendix I, which based on experts' knowledge and field operation database.

Moreover, the BBN approach retains several other advantages. The BBN approach merges diagnostics and prognostics features effectively, as most of the potential hazard scenarios of MEG can be explicated in the BBN model. However, it is in a tentative way. The development of fault prognostic and diagnostic approaches are for the sake of MEG safety improvement during the engineering design stage and during the operation of MEG respectively.

A hybrid technique, using BBN and ANFIS based technologies, contributes an efficient tool for MEGs fault diagnosis. Where the results demonstrate that the hybrid BBN-ANFIS can perform fault diagnosis with complete or incomplete symptoms. The main strength of the proposed approach is due to its dependency on experts' knowledge than the data from measurement instrumentation (I&C) in its decision-making process. The results show a robust performance of the hybrid technique proposed for fault diagnosis of a MEG that

would potentially provide a solution to the reasoning problem of complex systems. This may be an interest of the authors for future works.

The proposed BBN-ANFIS based safety alarm system for MEG has no direct impact on the MEG performance as it is not part of the operation process however, it has a major advantage on the resilience of the MEG as it promote awareness about the system health status during the operation. The statistical economical, ecological and reliability parameters for these operation types will be illustrated in detail in CHAPTER 7.

CHAPTER 7 Validation of Data and Methodologies

This chapter aims to validate the data and methods used/proposed in this research. Three main items will be validated namely the simulation of MEG operation, LORA and BBN.

7.1 Validation of MEG Simulation

In order to validate the MEG operation that simulated in this study by using the Simulink platform, another software named optimization and management tool for complex multi-generation systems that implemented by the mean of XEMS13 software platform [190] will be utilized. XEMS13 is mainly for operational optimization using MILP approach. However, it will be utilized in this section to validate the simulation design for resilient MEG case study [191].

7.1.1 MEG system description

The inherent MEG system is shown in Fig. ***7.1*** has the ability for self-sufficiency for its electricity, cooling and heating demands most of the year by employing a on-site 13MW co-generation gas turbine (CGU) prime mover combined with auxiliary steam turbine of 3MW, 2 MW of solar power (PV) and 2 MW of wind turbines (WT) as renewable resources, in addition to six district cooling units (DC) of 2.1MW capacity and COP = 6.0 for each. Also, consist of two thermal energy storage (TES) tanks of capacity 25MWh and 200MWh for heating and cooling energy respectively. Further to a 2 MWh super-capacitor bank for instant and dynamic power backup.

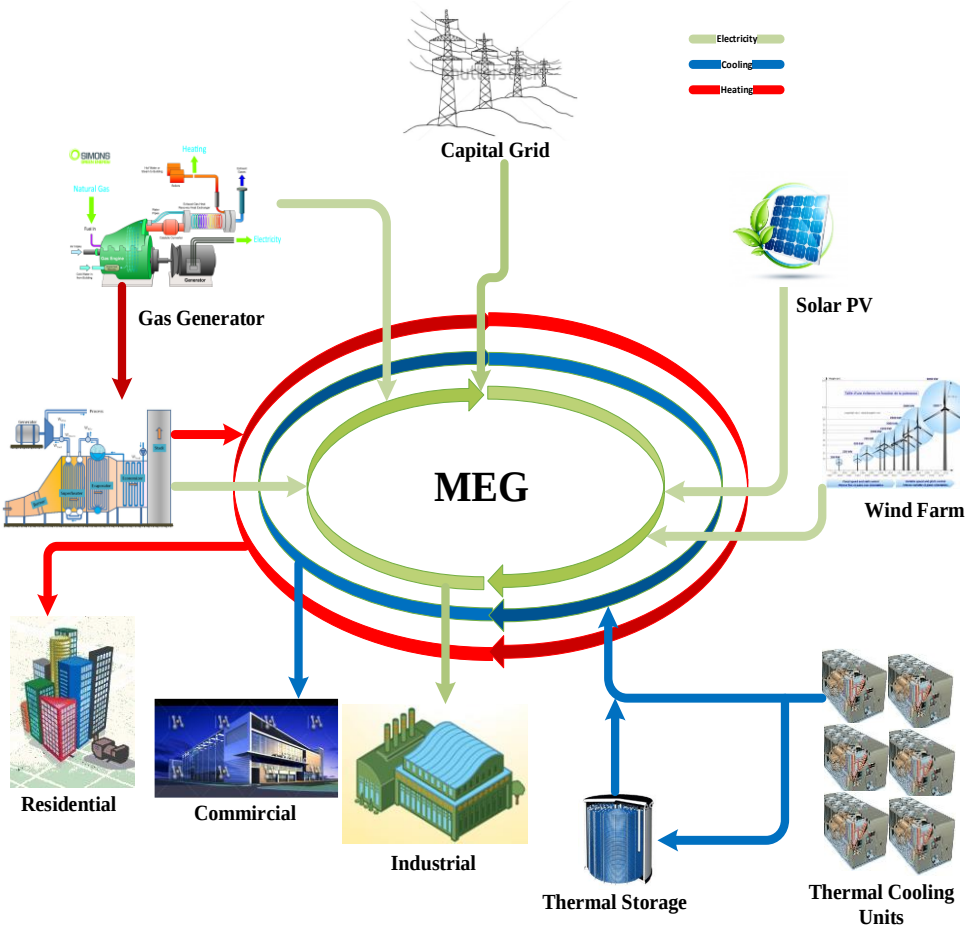

Fig. 7.1: *Proposed MEG configuration model*

In this case study, the MEG has the capability to switch to the grid-connected mode in the case of emergency. The CGU operates on NG to generate electricity and the consequential thermal energy is recovered via heat recovery steam generator to serve the heating demand, which found excessive in this case study. Therefore the absorption chiller is proposed to be utilized to convert the surplus heating to cooling energy, in order to avoid squandering of heating energy and to reduce electricity requirements for cooling.

In case of the power, production is more than the electricity demand, the surplus power can be sold to the utility grid. On the other hand, the lack of electricity production must be purchased from the utility grid. For the purposes of validation, a two different model for the MEG systems were established using static model for optimization algorithm XEMS13 software platform [190], and the dynamic one by using the Simulink platform [191].

7.1.2 Simulation results

The hourly electricity cost profile for one week in summer is shown in Fig. 7.2, based on actual energy prices in Ontario–Canada [192][161]. The selling price varies during the day due to several factors where it becomes negative in some interval when power generation is higher the demand. While the purchasing price is higher than selling as it is the nature of utility grid management and operation.

One week in summer was selected to test the operation of MEG in the harsh condition in term of heavy demands and weather conditions.

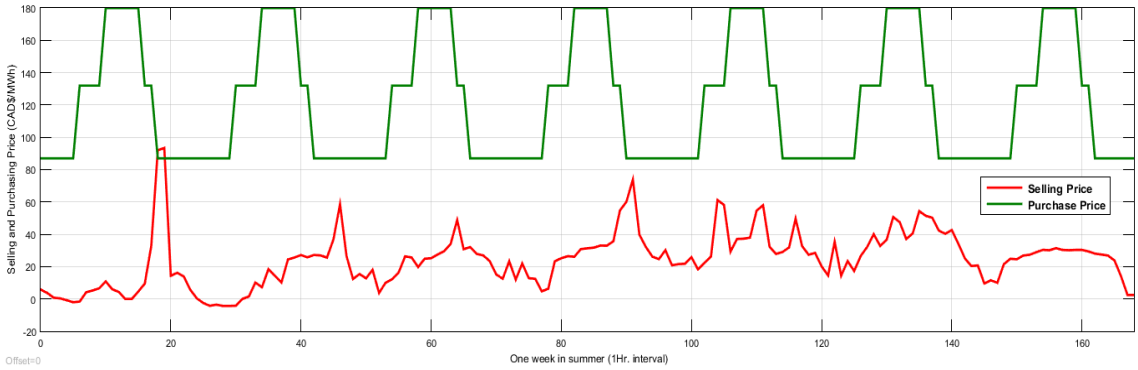

Fig. 7.2: *Selling and purchasing price of capital grid*

This study is to achieve the optimum operation cost for the MEG operation by efficient operation capacity and minimal numbers of the MEG devices operation. The operation cost for the inherent MEG system for one week in summer is 153,780 CAD$ with the operation profile shown in ***Fig. 7.3***, ***Fig. 7.4*** and ***Fig. 7.5***.

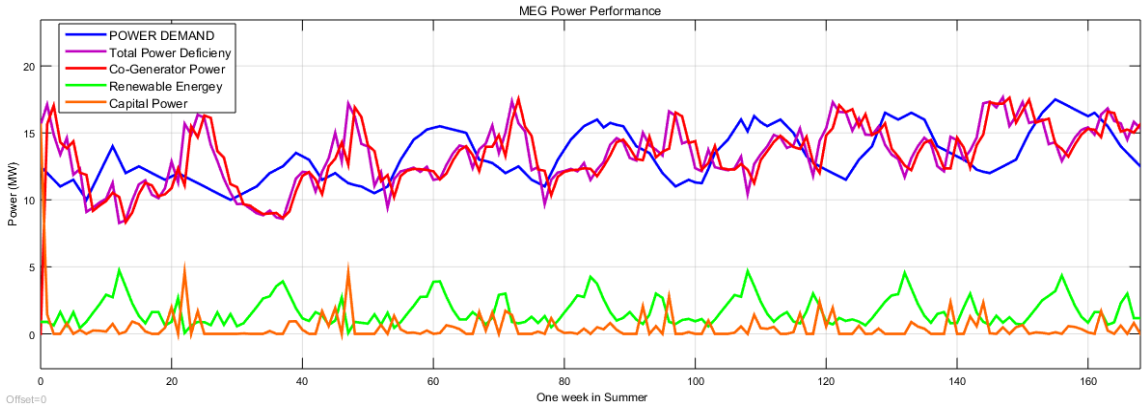

Fig. 7.3: *Power profile for the inherent MEG*

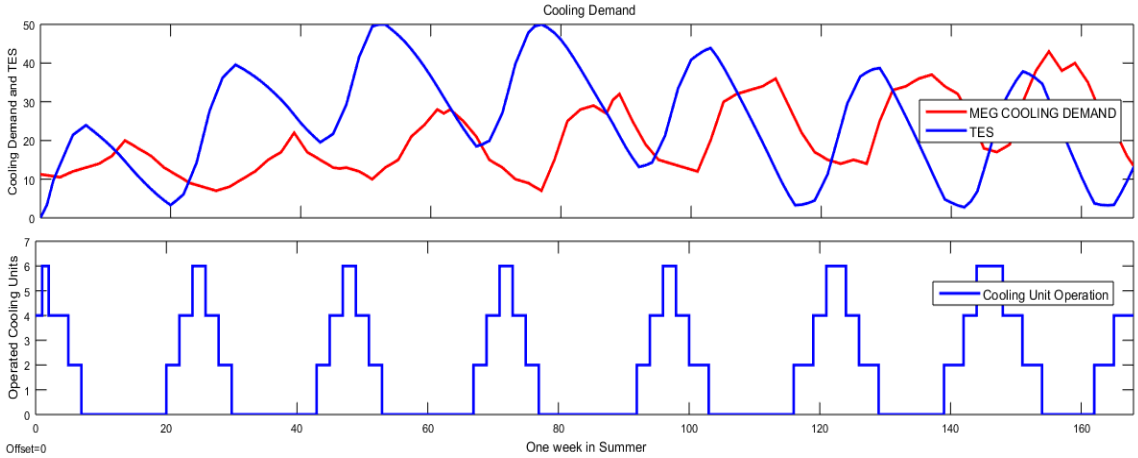

Fig. 7.4: *Cooling profile for the inherent MEG*

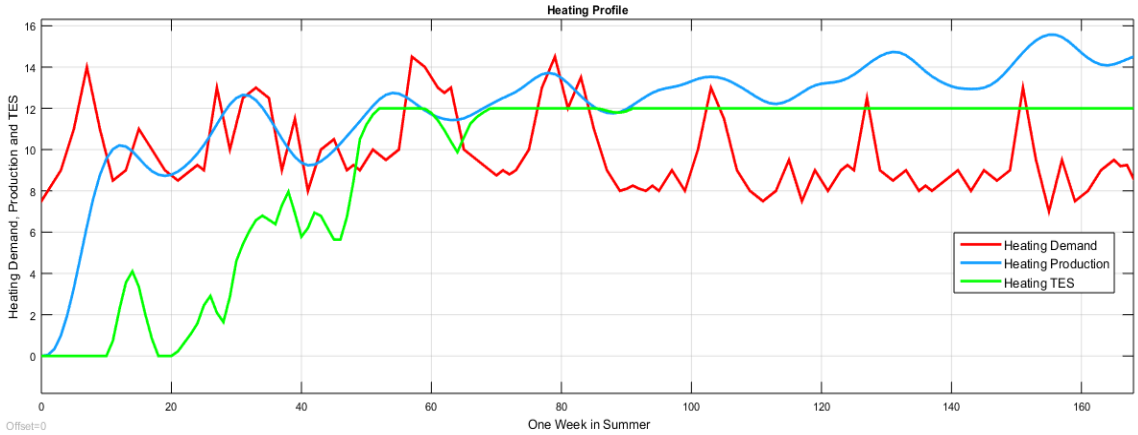

Fig. 7.5: *Heating profile for the inherent MEG*

From the figures above it can be defined that the co-generation unit working at an average of 75% of its capacity also the six district cooling chillers are working daily at off-peak interval to charge the TES with the required daily demand cooling energy. Further to squandering of the heating energy generated by the co-generation.

In order to mitigate the excessive loss in the heating energy, it is proposed to add an absorption chiller of 7 MW capacity and to remove the heating TES of 25 MWh.

The optimization technique for the static model of the new MEG structure, with absorption chiller of 7MW capacity, shows that the operation cost becomes 122,394 CAD$, with a cost reduction of more than 21% from the inherent MEG system operation cost. Furthermore, the optimization technique contributes impressive results as listed below:

1. The co-generation unit works at full capacity during the weekdays and at around 80% during the weekend, as shown in Fig. 7.6 and Fig. 7.7
2. The number of district cooling chillers required to run the MEG was reduced to three instead of six as it is the case in the inherent system as shown in Fig. 7.8 and Fig. 7.9
3. No squandering on heating energy by converting the surplus to cooling through the absorption chiller as illustrated in Fig. 7.10 and Fig. 7.11

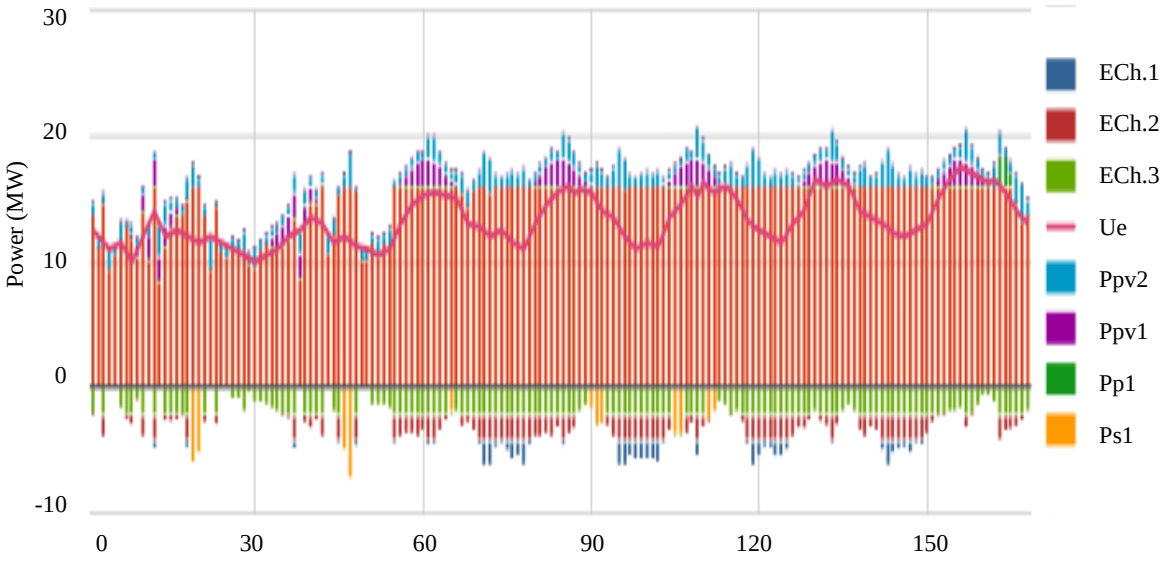

Fig. 7.6: *Hourly electricity profile for the MEG system in one week in summer (static module)*

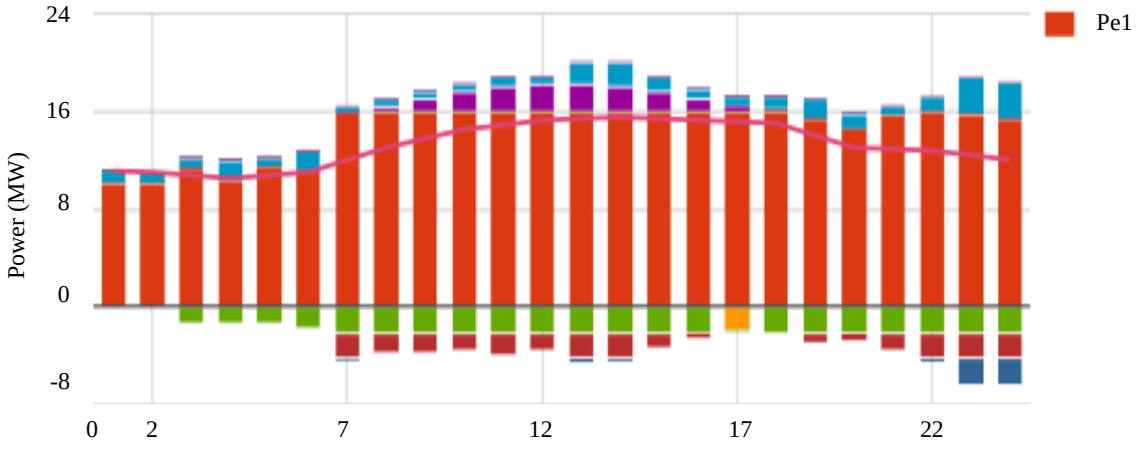

Fig. 7.7: *Hourly electricity profile for the MEG system in weekday profile (Monday) (static module)*

Fig. ***7.6*** and Fig. ***7.7*** demonstrations of the hourly power production profiles of the MEG system during one week in summer. Where EChill is the energy consumed by district cooling units (1, 2 and 3), Ue is the power demand Pv2 is the wind turbine generation, Pv1 is the Solar power contribution, Pp1 is the purchased power from the capital grid, Ps1 is the power sold to the capital grid and Pe1 is the cogeneration power contribution.

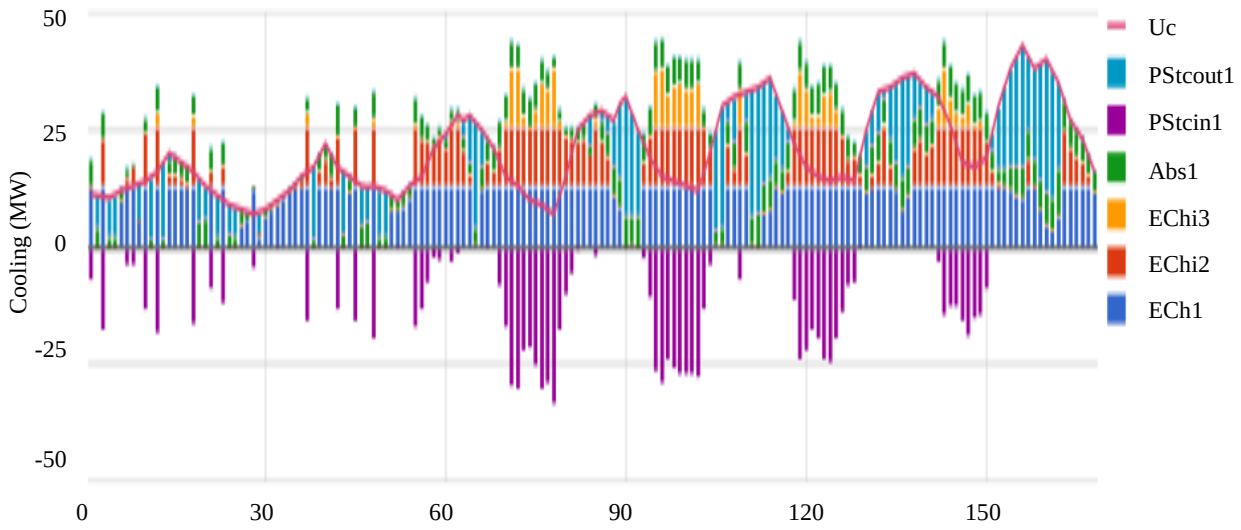

Fig. 7.8: *Hourly cooling energy profile (MWh) for the MEG system in one week in summer (static module)*

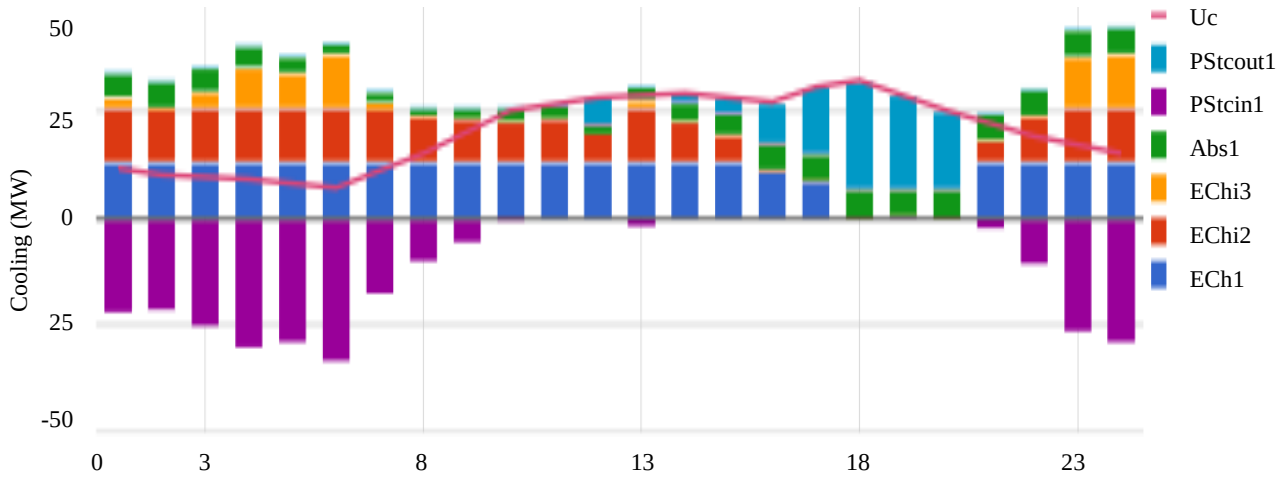

Fig. 7.9: *Hourly cooling energy profile for the MEG system in weekday profile (Monday) (static module)*

The optimization technique contributes an optimum operation for the district cooling units where only three units are sufficient to cover the cooling demand during the certain period, as shown in ***Fig. 7.8*** and ***Fig. 7.9***. Where U_c is the cooling demand, PStcount1 represents the TES discharging, PStcin1 is the TES charging, Abs1 is the cooling energy contributed from absorption chiller and EChi is the chillers energy production.

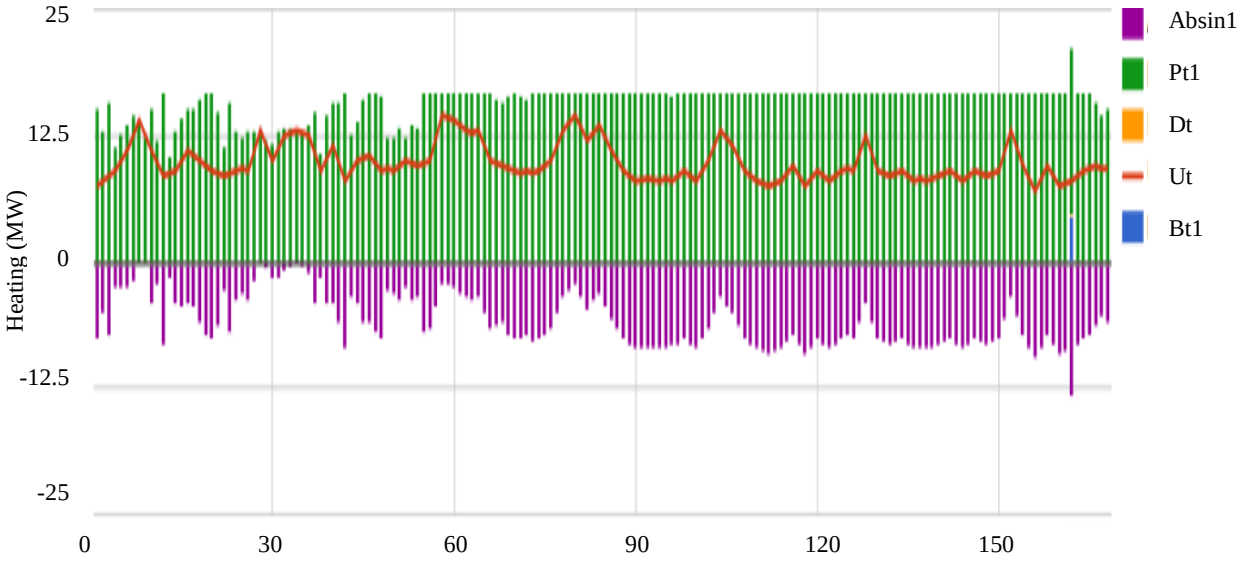

Fig. 7.10: *Hourly heating energy profile (MWh) for the MEG system in one week in summer (static module)*

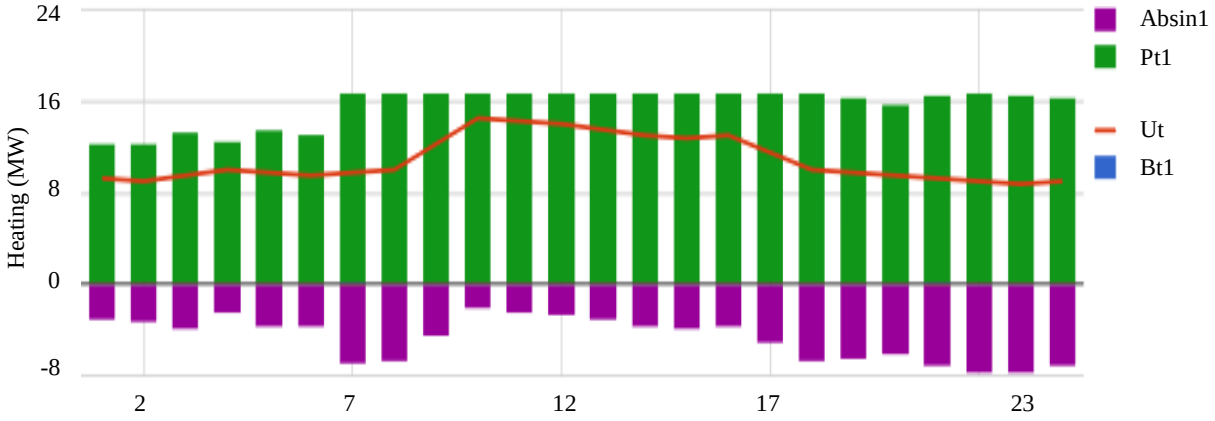

Fig. 7.11: *Hourly heating energy profile for the MEG system in weekday profile (Monday) (static module)*

The hourly heating energy profile for the MEG system was shown in ***Fig. 7.10*** and ***Fig. 7.11***. Where Absin1 is the input energy to the absorption chiller, Pt1 is the thermal

energy produced by the co-generation unit, Absin is the absorption power output and Ut is the heating demand. From the figures above it clearly defined that the heating energy produced by the co-generation excesses the heating demand and the surplus heating can be converted to cooling by utilizing the absorption chiller in order to achieve the maximum utilization of energy.

In order to validate the results given by the static MEG model, the optimized co-generation operation profile and the minimum district cooling chillers operation schedule were examined in the dynamic MEG model, shown in ***Fig. 7.13***. The operation cost of the dynamic model is 132,710 CAD$ and the energy profiles can be shown in ***Fig. 7.12-Fig. 7.16***.

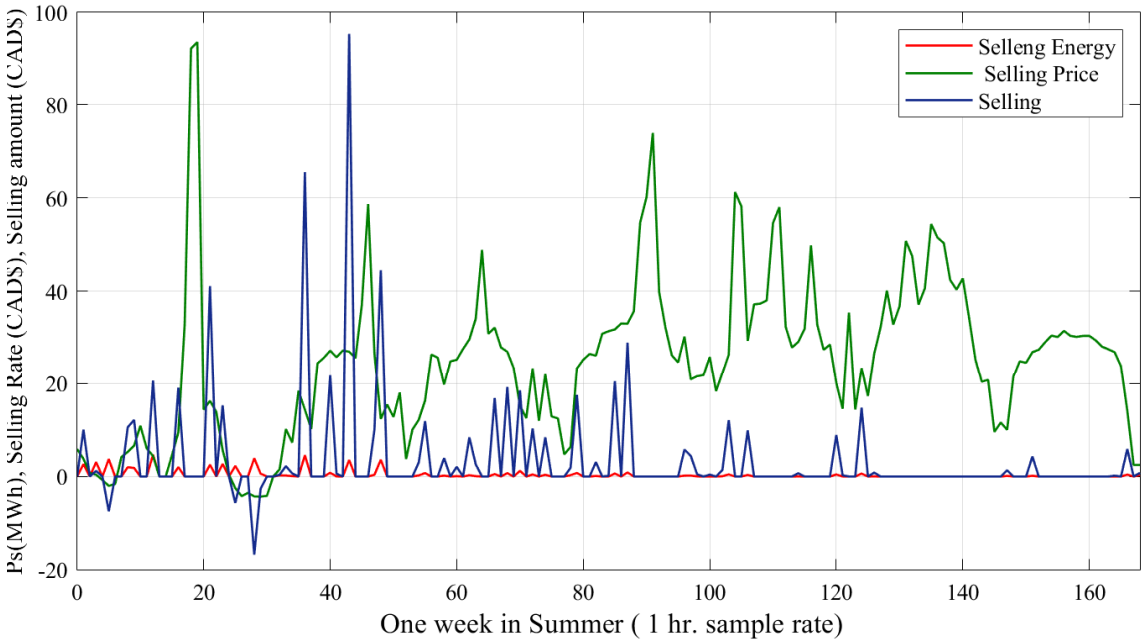

Fig. 7.12: *Grid selling energy, rate and total amount for the (dynamic model)*

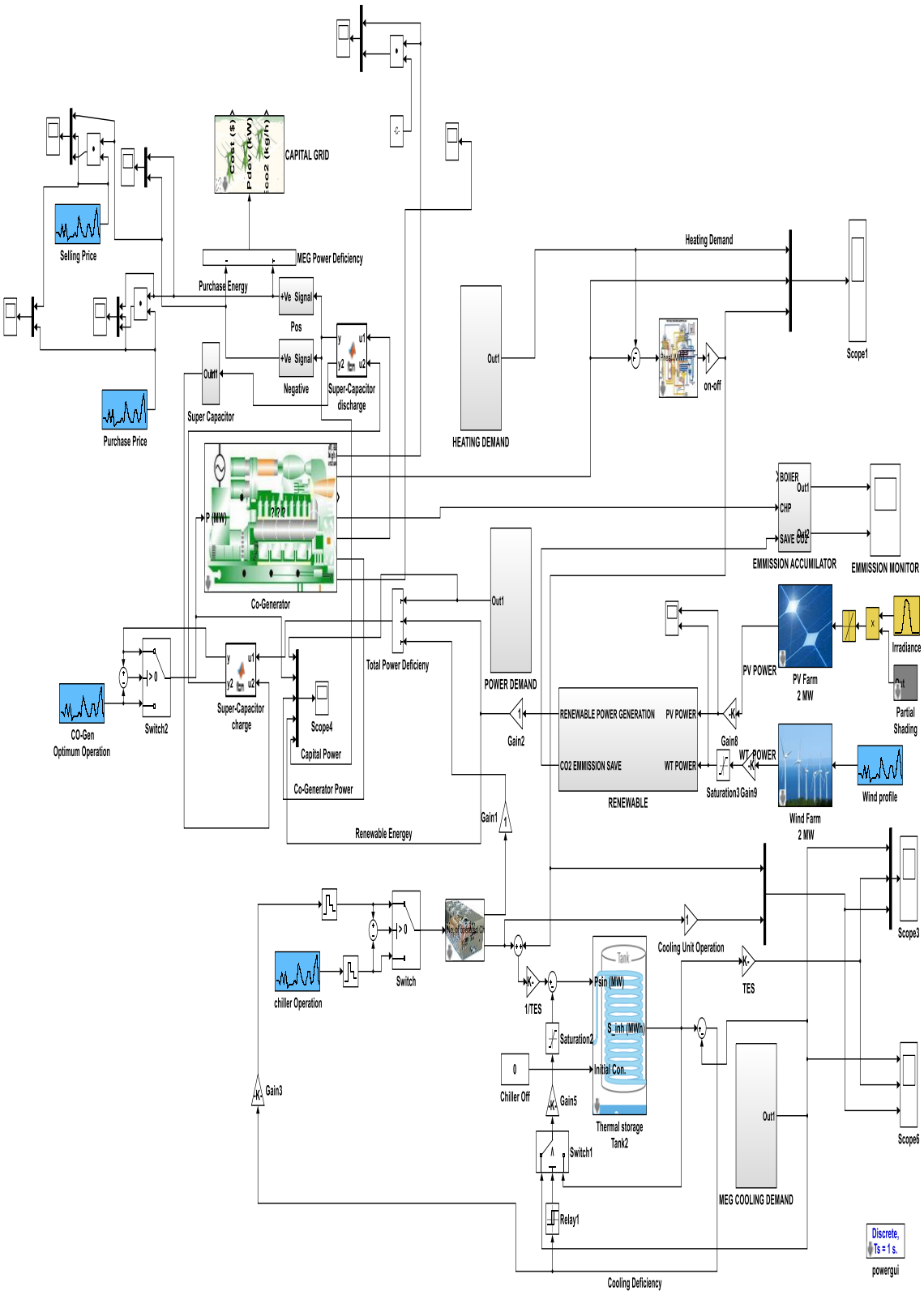

Fig. 7.13: *Optimal dynamic model for the MEG system*

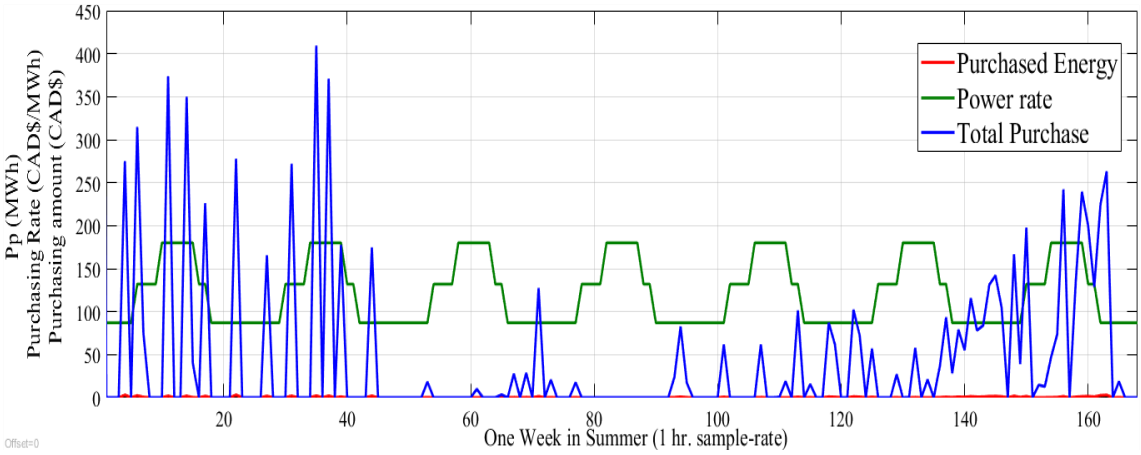

Fig. 7.14: *Grid purchasing energy, rate and total amount for the MEG (dynamic model)*

Fig. 7.12 demonstrates the hourly sold energy to the capital grid, selling rate and selling revenue CAD$/MWh for a period of one week in summer, also ***Fig. 7.14*** shows the hourly purchased energy from the capital grid, selling rate and selling revenue CAD$/MWh for the aforesaid period.

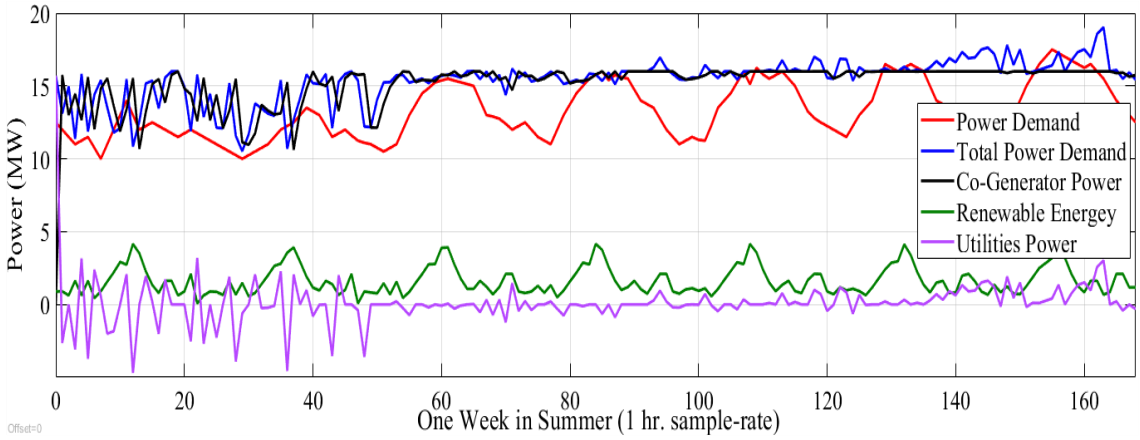

Fig. 7.15: *MEG power profile for one week in summer (dynamic model)*

The hourly power profile for the dynamic MEG model is shown in ***Fig. 7.15***, it can be clearly defined that the behavior of the dynamic model is similar to the static MEG shown in ***Fig. 7.6***. Hence, the interaction with the utility grid was reduced with respect to the profile of inherent MEG shown in ***Fig. 7.3***.

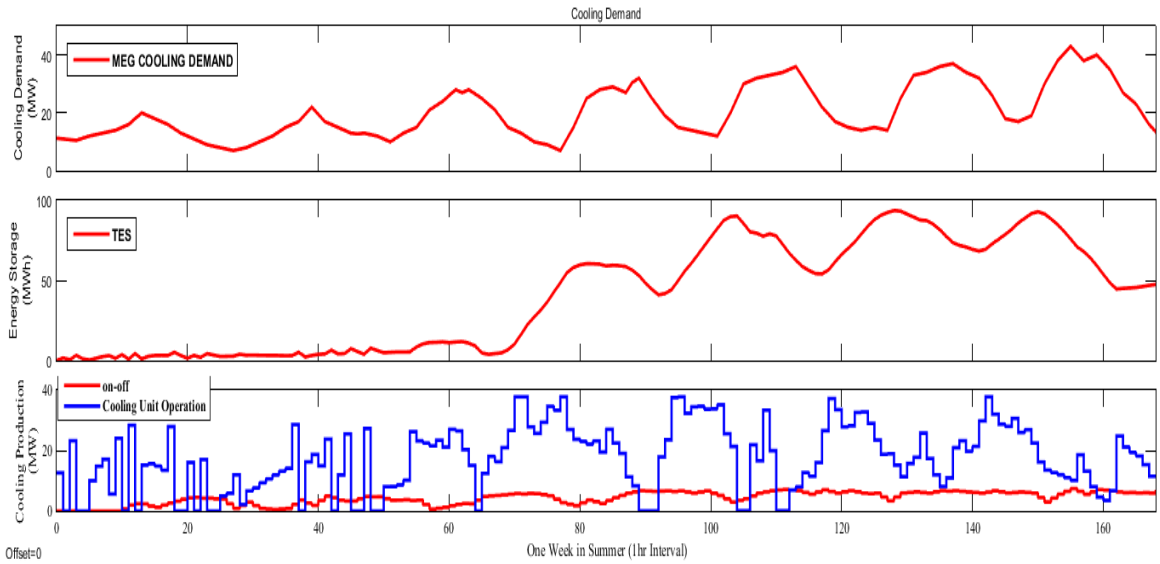

Fig. 7.16: *MEG colling energy profile for one week in summer (dynamic model)*

The results given by the dynamic MEG model (using Simulink) are quite similar to the one given by static MEG model (using XEMS13) as shown in ***Fig. 7.17***. The static comparison in ***Table 7-1*** shows minor varieties between Simulink and XEMS13 that can be caused by the different behavior of static and dynamic modules.

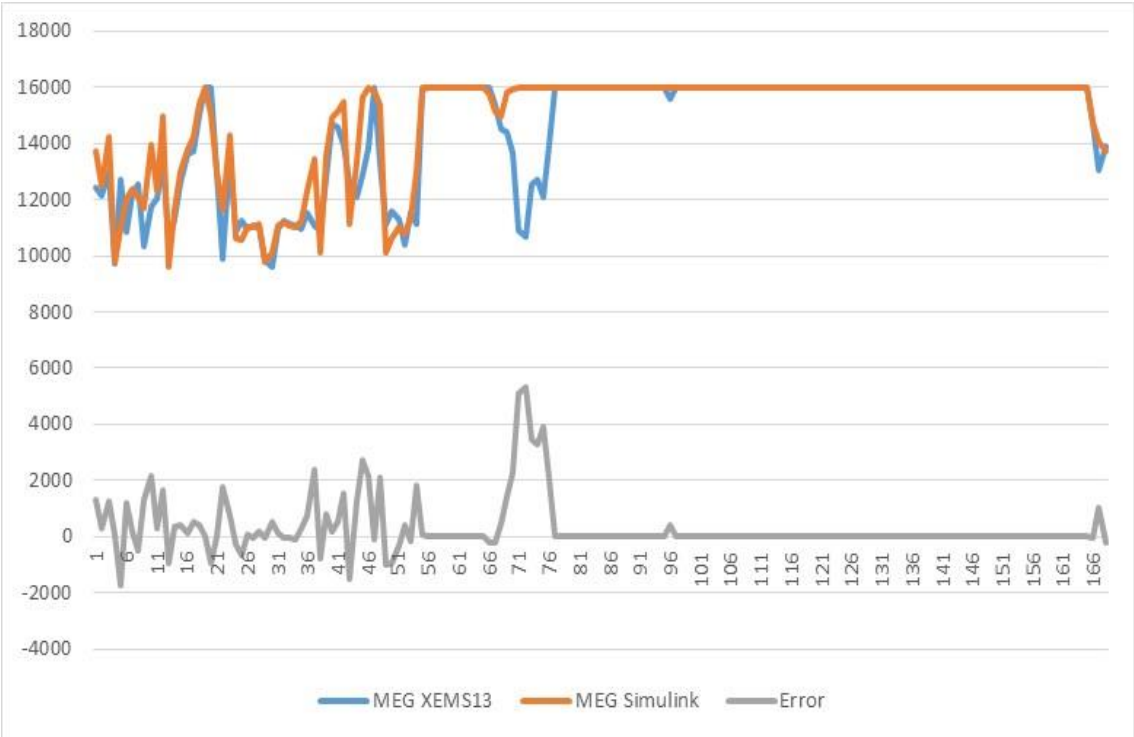

Fig. 7.17: *Power generation by the co-generator using Simulink and XEMS13 (kW)*

Table 7-1: *Statics comparison for power generation by the co-generator using Simulink and XEMS13 (kW)*

	MEG Simulink	**MEG XEMS13**	**Error (Simulink-XEMS13)**
Max.	16000 kW	16000 kW	15.74-33.19%
Min.	9598.9 kW	9633.2517 kW	0%
Median	15999.85 kW	16000 kW	0%
Average	14842.46 kW	14546.41 kW	1.99%
Operation Cost	132,710 CAD$	122,394 CAD$	7.77%

The 2% diversity in the Co-generation operation in ***Table 7-1*** is within the acceptable tolerance margin, however it causes around 7% difference in the operation cost between the foresaid models.

Sankey diagram provides a simple visualization tool for material or energy flows with proportional arrow magnitudes [193]. The energy statics data for the one week in summer of MEG operation can be illustrated in a Sankey diagram. The energy flow are converted through the MEG generation process, as obtained in Fig. ***7.18***.

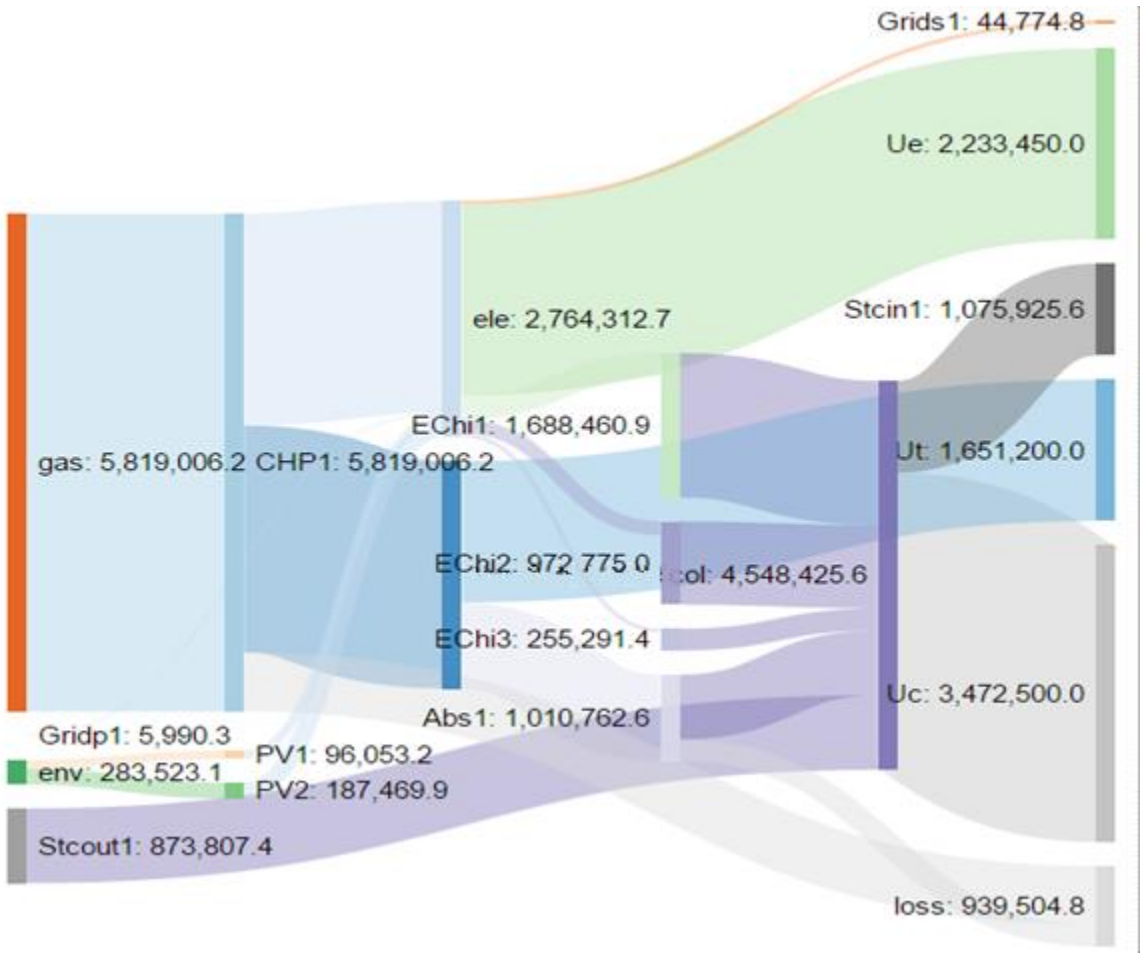

Fig. 7.18: *Sankey diagram for one summer week: on the left side the contributes of the primary energy and on the right side the final energy conversion (kWh)*

7.2 Validation of LORA

LORA is proposed to assess the resilience of MEG and to determine the impact, of adding/removing IRLs to the MEG entity, on the resilience of the energy service. In this section, validation of LORA can be done by implementing LORA for the MEG structures mentioned in Section 7.1. LORA for these structures are shown in ***Fig. 7.19*** and ***Fig. 7.20*** in order to visualize the difference in structure and risk attributes with the MEG case study-1 that described in Section 4.6.10.

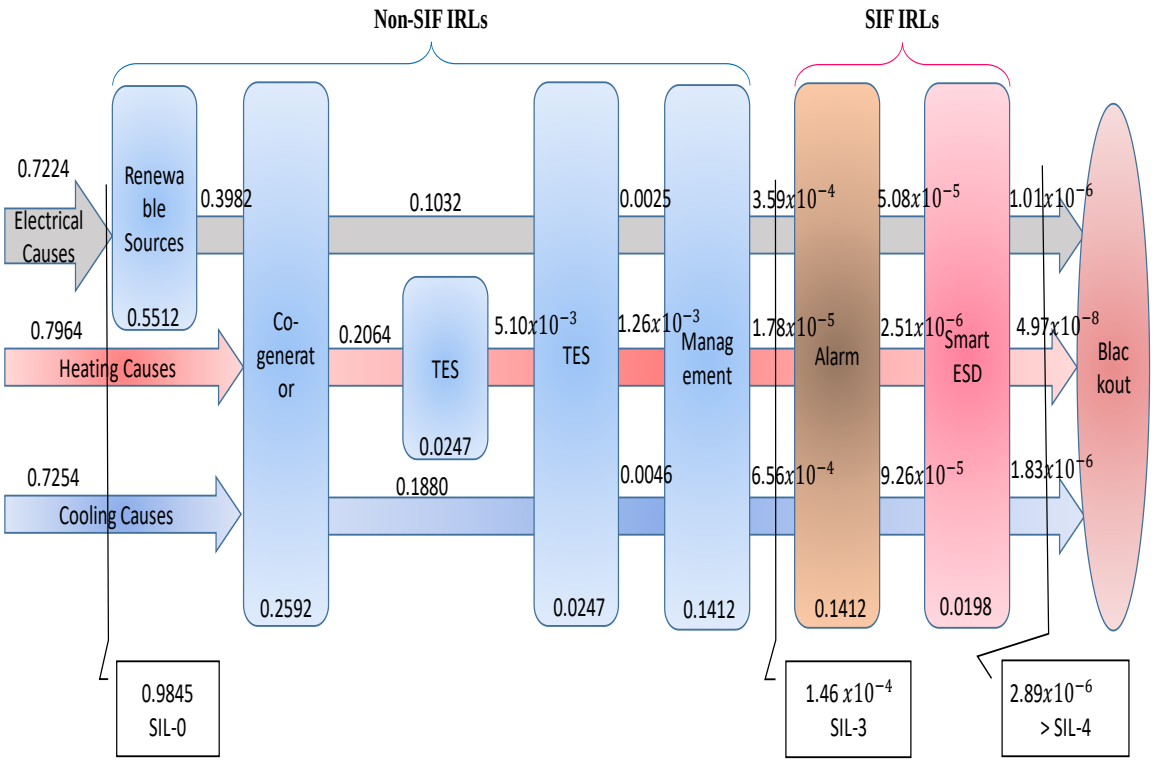

Fig. 7.19: *LORA path diagram for MEG case study-2*

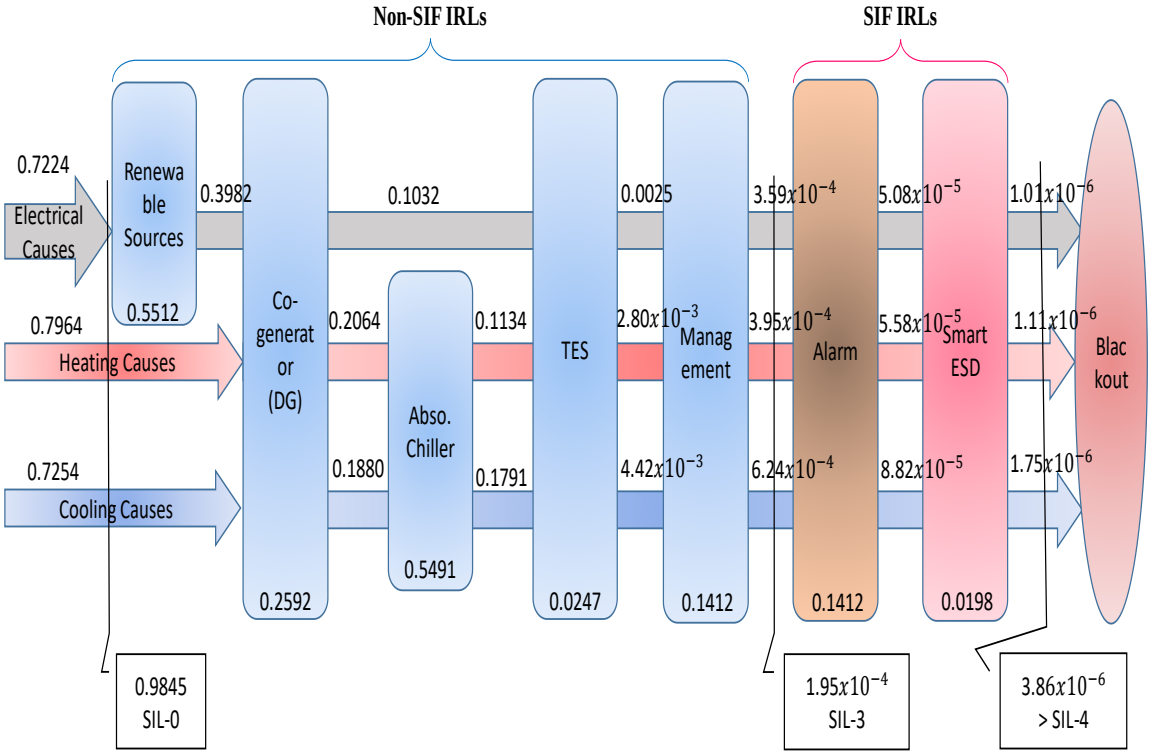

Fig. 7.20: *LORA path diagram for MEG case study-2plus*

Table 7-2 illustrates a comparison between three different MEG's structures that mentioned in the above. It shows that the more IRLs used in the MEG the lower value of LORA and the more resilience of the entire energy system. This conclusion comes in line with the operating performance that presented in different operational scenarios shown in CHAPTER 3 and CHAPTER 5.

On the other hand, the table illustrates that the three different MEG structures have different attributes' values. In addition, ***Table 7-2*** proofs that each IRL has a different effect on the three attributes. Nevertheless, the effect is not necessary to be the same on these attributes.

Table 7-2: *LORA comparison for the three case studies*

		MEGs with a GT prime mover								
		Case study-1			Case study-2			Using Case study-2plus		
No. #	IRL types	IRLs names	LORA (PFD)	Environment pollution (Ton CO_2/MWh)	IRLs names	LORA (PFD)	Environment pollution (Ton CO_2/MWh)	IRLs names	LORA (PFD)	Environment pollution (Ton CO_2/MWh)
1	Base MEG	N/A	0.9844	7,215.34 (1)	N/A	0.9844	7,215.34 (1)	N/A	0.9844	7,215.34 (1)
2	Non-SIF IRLs	RES	0.9662	6,970.1 (2)	RES	0.9662	6,970.1 (2)	RES	0.9662	6,970.1 (2)
		Operation Cost 373,890 CAD$ CO_2 6,970.1 Ton/Week PFD 0. 9662								
3		Co-gen.	0.4220	4,955.3 (3)	Co-gen.	0.4220	4,955.3 (3)	Co-gen.	0.4220	4,955.3 (3)
4					TES (heating)	0.2753	4,955.3 (3)	Abso. Chiller	0.3472	4,955.3 (3)
5		TES (cooling)	0.0122	4,955.3 (3)	TES (cooling)	7.30×10^{-3}	4,955.3 (3)	TES (cooling)	9.74×10^{-3}	4,955.3 (3)
6		Management	1.73×10^{-3}	4,955.3 (3)	Management	1.03×10^{-3}	4,556.3 (4)	Management	1.38×10^{-3}	3,322.0 (5)
		Operation Cost 154,440 CAD$ CO_2 4,955.3 Ton/Week PFD 1.73×10^{-3}			Operation Cost 153,780 CAD$ CO2 4,556.3 Ton/Week PFD 1.03×10^{-3}			Operation Cost 132,710 CAD$ CO_2 3,322.0 Ton/Week PFD 1.38×10^{-3}		
7	SIF IRLs	Alarm	2.45×10^{-4}	4,955.3 (3)	Alarm	1.46×10^{-4}	4,556.3 (4)	Alarm	1.95×10^{-4}	3,322.0 (5)
8		Smart ESD	4.85×10^{-6}	4,955.3 (3)	Smart ESD	2.89×10^{-6}	4,556.3 (4)	Smart ESD	3.86×10^{-6}	3,322.0 (5)

(#) Calculation of the step between brackets is shown in **Appendix III Data Validation**

Table 7-3 shows the effect of using different prime mover co-generation technology in the MEG case study-2plus. The economic and ecological attributes of different DERs technologies are illustrated in ***Table 7-4***. Further details on the calculation of the total attributes of each DERs in the MEG case study are illustrated in **Appendix III Data Validation**.

Table 7-3: *LORA comparison for different co-generator technology used in case-study2plus*

		MEGs with a GT prime mover			MEGs with a FC prime mover			MEGs with a MT prime mover			MEGs with a DE prime mover		
		Using Case study-2plus			Using Case study-2plus			Using Case study-2plus			Using Case study-2plus		
No. #	IRL types	IRLs names	LORA (PFD)	Environment pollution (Ton CO_2/MWh)	IRLs names	LORA (PFD)	Environment pollution (Ton CO_2/MWh)	IRLs names	LORA (PFD)	Environment pollution (Ton CO_2/MWh)	IRLs names	LORA (PFD)	Environment pollution (Ton CO_2/MWh)
1	Base MEG	N/A	0.9844	7,215.34 (1)	N/A	0.9844	7,215.34 (1)	N/A	0.9844	7,215.34 (1)	N/A	0.9844	7,215.34 (1)
2	Non-SIF IRLs	RES	0.9662	6,970.1 (2)	RES	0.9662	6,970.1 (2)	RES	0.9662	6,970.1 (2)	RES	0.9662	6,970.1 (2)
		Operation Cost 373,890 CAD$ CO_2 6,970.1 Ton/Week, PFD 0.9662											
3		Co-gen.	0.4220	4,955.3 (3)	Co-gen.	0.7629	4,566.0 (6)	Co-gen.	0.6599	5,843.2 (9)	Co-gen.	0.7704	5,549.5 (11)
4		Abso. Chiller	0.3472	4,955.3 (3)	Abso. Chiller	0.6447	4,566.0 (6)	Abso. Chiller	0.5514	5,843.2 (9)	Abso. Chiller *	0.6517	5,549.5 (11)
5		TES (cooling)	9.74 x10^{-3}	4,955.3 (3)	TES (cooling)	0.0213	4,566.0 (6)	TES (cooling)	0.0171	5,843.2 (9)	TES (cooling)	0.0216	5,549.5 (11)
6		Management	1.38 x10^{-3}	3,322.0 (5)	Management	3.0 x10^{-3}	2,990.3 (7)	Management	2.43 x10^{-3}	4,078.5 (10)	Management	3.06 x10^{-3}	3,828.3 (12)
		Operation Cost 132,710 CAD$, CO_2 3,322.0 Ton/Week PFD 1.38x10^{-3}			Operation Cost 183,000 CAD$, CO_2 2,990.3 Ton/Week (8) PFD 3.0 x10^{-3}			Operation Cost 108,380 CAD$, CO_2 4,078.5 Ton/Week (8) PFD 2.43 x10^{-3}			Operation Cost 190,900 CAD$, CO_2 3,828.3 Ton/Week (8) PFD 3.06 x10^{-3}		
7	SIF IRLs	Alarm	1.95 x10^{-4}	3,322.0 (5)	Alarm	4.26 x10^{-4}	2,990.3 (7)	Alarm	3.43 x10^{-4}	4,078.5 (10)	Alarm	4.33247 x10^{-4}	3,828.3 (12)
8		Smart ESD	3.86 x10^{-6}	3,322.0 (5)	Smart ESD	8.45 x10^{-6}	2,990.3 (7)	Smart ESD	6.80 x10^{-6}	4,078.5 (10)	Smart ESD	8.58 x10^{-6}	3,828.3 (12)

* Absorption chiller is not the optimum choice with DE prime mover since the DE's output is electricity only. Therefore, utilizing Abso. Chiller will not has an effect on the operation cost at the normal condition but it increases the MEG's reliability during partial DERs outage.

(#) Calculation of the step between brackets is shown in **Appendix III Data Validation**

Table 7-3 declares that each co-gen. technology has different effect on the three attributes (i.e. economical, ecological and reliability) which not necessary to be in the same direction and/or rate. ***Table 7-5*** summaries the performance of the MEG with different prime-mover in term of operation cost, greenhouse gas emission and reliability.

Table 7-4: *Economic and ecological attributes of different DERs technologies*

Attribute		DER Technologies						
		PV	WT	FC	MT	GT	DE	UG
Investment cost (CAD/kW) [159] [160]		7,800 (20yrs)	5,600 (25yrs)[143]	3,240 (10yrs)	1,380 (20yrs)	900 (25yrs)	420 (20yrs)	-
Maintenance cost (CAD/kW)		0.01 [162]	0.01 [162]	0.03 [162]	0.016 [162]	0.0275 [118]	0.055 [194]	Depends on the course time of the day ***Fig. 7.2*** [192][161]
Pollution emission (kg/MWh)	CO2	0 [159]	0 [159]	513 [195]	700 [160]	570 [160]	657 [142]	865 [158]
	NOx	0 [159]	0 [159]	0 [195]	0.068 [160]	0.4 [160]	6.69 [142]	-
	SO2	0 [159]	0 [159]	0 [195]	0.003 [160]	1.94e-03 [160]	0.359 [142]	-
	CO	0 [159]	0 [159]	0.0194 [195]	246.8	143.96	1275.1	-
	PM10	0 [159]	0 [159]	0	18.51	16.45	160.4	-
Noise (dB) [159]		0	84	46	60	70	75	-

(a) Photovoltaics (PV), wind turbines (WT), fuel cell (FC), micro-turbine (MT), gas turbines (GT), diesel engines (DE), utility grid (UG). (b) Noise emissions of DG units are measured at a distance of 3m.(c) 1 US$ ≈ 1.2 CAD$

Table 7-5: *Attributes comparison between the prime movers shown in* ***Table 6-3***

Prime-mover / Attributes	GT	FC	MT	DE
Economic	2	3	1	4
Ecological	2	1	4	3
Reliability	1	3	2	4

* 1 indicates the best performance among the other prime-movers in a selected attribute and 4 is the worst performance

Utilizing MT prime mover in the MEG has the best operation rate among the other prime movers used in

Table 7-3. However it is not the case for gas emission. On the other hand, utilizing FC prime mover has the best ecological attribute although it has bad attributes in operation rate and reliability. GT prime mover has moderate performance on the three attributes. Finally, the DE has the worst reliability and economic attributes in addition to high greenhouse gas emission. Therefore, choosing the best fit prime mover technology is challenging the design engineers under the restrictive standards that determine the acceptable range of the three attributes and which of these attributes has higher priority on the design criteria.

Table 7-2 and ***Table 7-3*** illustrate that utilizing SIF IRLs have major impact on systems reliability however there are no impact on the operation cost or environment parameters of the MEG. In contradiction, utilizing non-SIF IRLs have a direct effect on the three contributes. In addition, implementing the non-SIF IRLs in the MEG asset, normally takes time and affect the system operation during construction period, which not the case for incorporating the SIF IRLs in the MEG entity.

7.3 Validation of BBN

The BBN based intelligent reasoning for fault diagnosis of wind turbine gearbox that presented in [103] is implemented in order to validate the programming code for BBN that implemented in this research study to compute the BBN reasoning for MEG.

Fig. 7.21 shows the BBN structure for gearbox failure which presented in [103]. The comparison between the results in [103] and the model implemented in ***Fig. 7.22*** is shown in ***Table 7-6,*** which shows identical results between the two models.

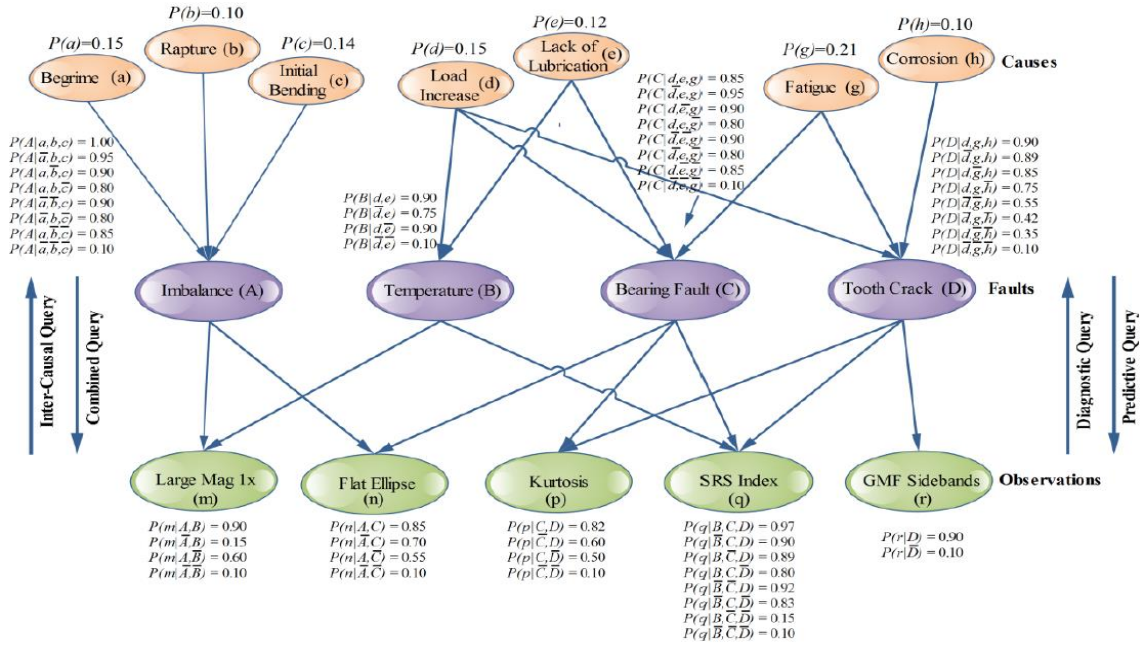

Fig. 7.21: *BBN for gearbox failure* [103]

Table 7-6: *Comparison between computation results in* [103] *and the BBN model implemented by using developed BBN program that used in this study*

No.#	Query	*P(A|B)* [103]	*P(A|B) this study*
1	**Diagnostic Query** *P(Begrime (a) | Large Mag 1x (m))*	18.91 % True 81.09 % False	18.91 % True 81.09 % False
2	**Predictive Query** *P(SRS index (q) | Lack of Lubrication (e))*	8.49 % True 91.51 % False	8.43 % True 91.57 % False
3	**Inter-causal Query** *P(Fatigue (g), Corrosion (h) | SRS Index (q))*	23.97 % True 76.03 % False	24.02 % True 75.98 % False

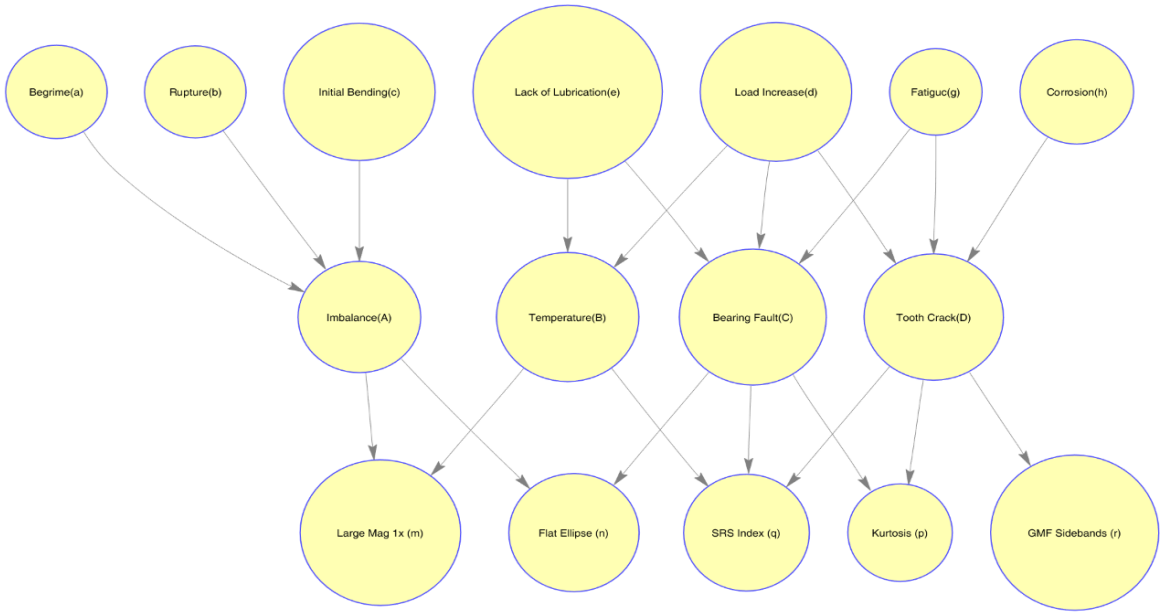

Fig. 7.22: *BBN Implementation of gearbox failure* [103] *using developed BBN program that used in this study*

CHAPTER 8 Conclusions and Recommendations

8.1 Summary

The consistent increase of deploying DERs, including renewable energy sources, for energy production requires better understanding of how stochastic power generation affects the stability of energy grids. The main objective of this research is to offer a sophisticated study on the design and implementation of a resilient MEG using safety analysis tools by developing advanced risk analysis approaches. Employing risk analysis in MEG design improves its resiliency and offers an effective safety tools for designing resilient MEGs. It is important to mention that the conclusions and recommendations of this thesis are depending on a MEG case study that was illustrated in CHAPTER 3, therefore the results may varies for other MEG structures, load types and location.

8.2 Conclusions

This dissertation describes a novel method for design resilient MEG infrastructure by using safety analysis tools. The proposed method came in five main stages as follows:

1. A resilience matrix (RM) and a resilience risk performance indicator (RRPI) were proposed in this work resilience MEG design. The RRPI consists information of socio-econo-ecological of each hazard event that provides informative knowledge that is useful and important for the design engineers and decision maker personnel.
2. Principles of two risk analysis models were developed to offer effective safety tools for MEGs' risk evaluation namely the developed fault tree analysis (FTA) and the proposed layer of resilience analysis (LORA). The proposed safety analysis tools were utilized for design a resilience MEG by estimating the risk level of LORA path and define the associated SIL for a MEG entity that consists selected combination of varies types and capacities of independent resilience layers (IRLs).
3. Numerous combination of IRLs (SIF and non-SIF) were proposed inorder to ensure achieving adequate level of MEG's resilience that predetermined by the engineers. Hence, the group of hazards that have low severity and low ecological risk with high class, hazards have high severity with low class and low ecological risk, and hazards

have low severity and low class with high ecological risk were eliminated to address the most effective hazards and propose suitable IRLs that precludes faults propagation. The results in CHAPTER 4 show that the selected non-SIF resilience layers reduced the risk of MEG blackout PFD by 10^{-3} while the selected SIF protection layers offer another 10^{-3} reduction of the risk of the original MEG. In addition, it can be noticed that SIF IRLs are usually auxiliary systems that does not have direct effect on the operation cost and environment parameters of the energy system. However, SIF IRLs have significant effect on the systems' reliability. In contrast, the non-SIF IRLs have direct effects on socio-econo-ecological parameters, where the type and capacity of the non-SIF IRL is able to improve the running cost, greenhouse gases emission and the overall system's reliability as illustrated in Section 7.2.

The novel combination of interior search algorithm (ISA) and LORA was employed to support engineers on finding an optimal design for MEG's components. The proposed ISA structure takes in consideration the main constrains that facing resilient MEG design namely operation costs, greenhouse gases emission, capital cost and the system reliability. Results shows optimal values for IRLs for design a resilient MEG that considers risk calculation in the optimization cost function that. To the best of the author's knowledge, so far there is no other publication reporting design of resilient MEG based on LORA-ISA optimization algorithm.

In light of the promising results of this research, it can be affirmed that the proposed methodology offers an effective safety analysis tool for resilient MEG design and validation. Therefore, the proposed risk modeling approaches can be extensively applied in designing and validation for similar mega systems.

4. A proposal of non-SIF IRL namely hierarchical decision making of three control levels was implemented in Simulink platform by using an adaptive-network-based fuzzy inference as demonstrated in CHAPTER 5. Collaboration between different control levels has been attained to improve MEG's resiliency and to achieve optimistic profiles of energy generation. This has been done by accumulating data from local subsystems that obtains directive information to the reactive controller level and to the decision-making controller level to plan the overall energy profile.

Utilizing the proposed IRLs into the conventional MEG improve the MEG's reliability to more than twice of its normal capacity, while the co-generator, TES, and hierarchical decision making offer a significant reduction in the severity of the utility grid risks. Subsequently, employing IRLs into MEG improve the performance with practical everyday considerations, such as equipment maintenance and variation in energy demand, that affect MEGs' energy generation and distribution. Predicting future load profiles from historical data can provide a tolerable approximate tool for scheduling the dispatch of MEG resources. The optimal energy imports can be achieved by using real-time energy dispatch control for effective management of MEG resources and energy flow mapping.

The results in CHAPTER 3 and CHAPTER 5 show a direct proportion relation between the sampling rate resolution and accurate performance of energy profiles.

5. A MEG's alarm system using intelligent reasoning model was proposed as a SIF-IRL to boost the resilience level for MEG. This model is based on BBN and ANFIS, where the BBN structure consists of three layers, for MEG fault prognosis and diagnosis process. BBN can be utilized for instant fault prognosis process as well as it can be used for real-time fault diagnosis analysis. It is worth to notice that the more information involved in the BBN, the higher smartness it would be. Subsequently, the more evidence involved in the query process, the more accurate results would be.

   Moreover, BBN approach retains several other advantages. The BBN approach merges diagnostics and prognostics features effectively, as most of the potential hazard scenarios of MEG can be explicated in BBN model. However, it is in a tentative way. The development of fault prognostic and diagnostic approaches are for the sake of MEG resilience improvement during engineering design stage and during the operation of MEG respectively.

   A hybrid technique, using BBN and ANFIS based technologies, contributes an efficient tool for MEGs fault diagnosis. Where the results demonstrate that the hybrid BBN-ANFIS can perform fault diagnosis with complete or incomplete symptoms. The main strength of the proposed approach is its dependency on experts' knowledge more than data from measurement instrumentation (I&C) in the decision-making process. The results show a robust performance of the hybrid technique proposed for fault

diagnosis of a MEG that would potentially provide a solution to the reasoning problem of complex systems.

On the other hand, the results show that the MEG's safety alarm system has no direct impact on MEG's performance, in term of operation cost and greenhouse gas emission, as it is not a part of the operation process nevertheless, it has positive impact on RRPI of the MEG as demonstrated in CHAPTER 7.

More applications for the proposed approach can be examined. In addition, it can be applied to build a dedicated BBN for fault prognosis and diagnosis for similar energy systems. Hence, minor modification may be required on the BBN structure and/or ANFIS to fit the specific needs of the system under investigation.

Finally, validation of the data and approaches that used/offered in this dissertation were performed in CHAPTER 7. Different techniques and case studies were utilized to ensure the proposed methods namely, the simulation of MEG operation, LORA and BBN, are accurate and used properly.

8.3 Innovative contributions in the research study

Risk analysis for complex systems like MEG that has interaction between numerous components and energy vectors is relatively a new topic that needs to be tackled by innovative and specific safety tools.

This study addresses most hazards that combining energy grid operation and analyses their consequences in what forms the resilience matrix (RM) of MEG.

The concept of independent resilience layer (IRL) is another contribution that was developed through the thesis and where the implementation is leading to an important contribution to achieve higher resilience of the MEG.

The FTA method was developed and LORA was proposed for MEGs safety analysis to assess the resilience level for the MEG. To the best of the author's knowledge, this is the first time the proposed safety analysis tools are suggested for design a resilience MEG by assessing the risk level of LORA path.

Intelligent reasoning methodologies exploiting neural networks and Bayesian analysis is a new approach that can translate the resilience matrix in an effective tool for increasing the MEG resiliency.

This research reveals numerous contributions in design and validation of resilient MEG. The key milestones that were achieved in this dissertation can be summarized as follows, see ***Fig. 8.1***:

1. Study hazards and resilience action for MEGs by proposing a resilience matrix framework for MEG and contribute an RRPI to measure the strength of MEG's resiliency
2. Develop safety analysis tools namely fault tree analysis (FTA) and propose LORA with IRLs for improving the MEG's resiliency
3. Implement non-SIF IRL namely multi-level hierarchical decision making to improve the resiliency of a MEG case study
4. Implement SIF IRL that is intelligent reasoning algorithm (Alarm system) by using BBN and ANFIS for safety analysis and fault diagnosis

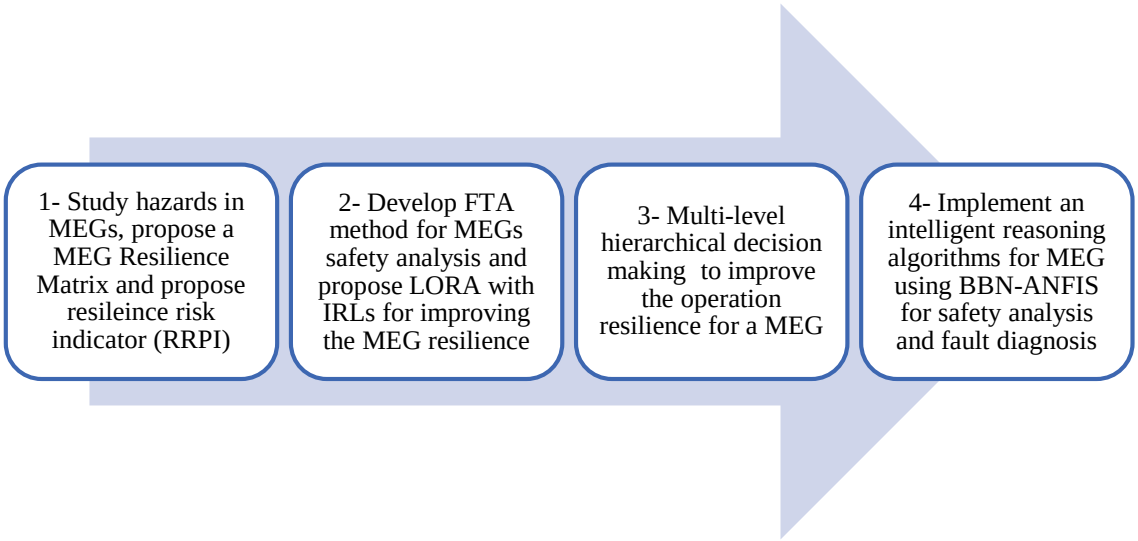

Fig. 8.1: *Contribution of this research study*

This research has seven academic publications presented in numerous high reputation publishers in a form of journal articles, conference papers and chapter-books.

The Most significant achievements of this study are listed as follows:

1- Article published in Elsevier-Sustainable cities and society **Impact Factor 3.160**
2- Article published in MDPI-Energies **Impact Factor 2.676**
3- **Best Paper Award** at IEEE-SEGE-2017

8.4 Future works

The main thrust of future development of MEG risk analysis will be in supporting the safety assessment tools development and potentially proposing numerous IRLs to study their impacts on MEG resiliency.

Another area for potential future work is to support implementing a real application of resilient MEG that serves varies load types such as factories, residential buildings.

The resilience matrix can be extended to cover more risk information, parameters and expertise's recommendation in order to improve the qualification and quantification of risk modeling tools for various types of MEG. More research can be conducted to develop the RRPI for more accurate evaluation of MEG resilience measurements.

Moreover, the proposed LORA can be developed and tested on numerous types of MEG for better evaluation risk modeling tool for optimal design of resilient MEG.

On other hand, K2- learning algorithm can be adopted in BBN structure to provide a more accurate nodes values for MEG's alarm system.

Finally, a recommendation to implement an actual resilient MEG that serving different load types such as factories or residential buildings is required in order to get a real data that can be compared with the design finding.

References

[1] C. B. Donadel, J. F. Fardin, and L. F. Encarnação, "Electrical distribution network operation with a presence of distributed generation units in a Pre Smart Grid environment using a clustering-based methodology," *Energy Syst.*, vol. 6, no. 4, pp. 455–477, Nov. 2015.

[2] Y. Levron, Y. Beck, L. Katzir, and J. M. Guerrero, "Real-time reactive power distribution in microgrids by dynamic programing," *IET Gener. Transm. Distrib.*, vol. 11, no. 2, pp. 530–539, Jan. 2017.

[3] A. Sheikhi, M. Rayati, and A. M. Ranjbar, "Demand side management for a residential customer in multi-energy systems," *Sustain. Cities Soc.*, vol. 22, pp. 63–77, 2016.

[4] Y. Koraz and H. A. Gabbar, "Hierarchical safety control for micro energy grids using adaptive neuro-fuzzy decision making method," in *IEEE International conference on Smart Energy Grid Engineering*, 2016, pp. 131–136.

[5] Z. Zhou, P. Liu, Z. Li, E. N. Pistikopoulos, and M. C. Georgiadis, "Impacts of equipment off-design characteristics on the optimal design and operation of combined cooling, heating and power systems," *Comput. Chem. Eng.*, vol. 48, pp. 40–47, Jan. 2013.

[6] M. Liu, "Energy efficient operation strategy design for the combined cooling, heating and power system," M.A. thesis, University of Victoria, 2012.

[7] X. Chen, G. Gong, Z. Wan, C. Zhang, and Z. Tu, "Performance study of a dual power source residential CCHP system based on PEMFC and PTSC," *Energy Convers. Manag.*, vol. 119, pp. 163–176, 2016.

[8] H. A. Gabbar and Y. Koraz, "Safety design of resilient micro energy grids," in *Smart Energy Grid Engineering*, 1st ed., Elsevier/Academic Press, 2017, pp. 101–150.

[9] A. Lawson, M. Goldstein, and C. J. Dent, "Bayesian framework for power network planning under uncertainty," *Sustain. Energy, Grids Networks*, vol. 7, pp. 47–57,

2016.

[10] B. Lin, “Optimization of building cooling heating and power,” M. A. thesis, Pennsylvania State University, USA, 2012.

[11] A. R. Abbasi and A. R. Seifi, “Considering cost and reliability in electrical and thermal distribution networks reinforcement planning,” *Energy*, vol. 84, pp. 25–35, 2015.

[12] J. G. Elerath and M. Pecht, “IEEE 1413: A standard for reliability predictions,” *IEEE Trans. Reliab.*, vol. 61, no. 1, pp. 125–129, 2012.

[13] H. Gabbar, “Design and planning support tool for interconnected micro energy grids,” *Br. J. Appl. Sci. Technol.*, vol. 12, no. 6, pp. 1–15, 2016.

[14] T. Ma, J. Wu, and L. Hao, “Energy flow modeling and optimal operation analysis of the micro energy grid based on energy hub,” *Energy Convers. Manag.*, vol. 133, pp. 292–306, 2017.

[15] V. Chandan *et al.*, “Modeling and optimization of a combined cooling, heating and power plant system,” in *2012 American Control Conference (ACC)*, 2012, pp. 3069–3074.

[16] K. Telecom and S. Korea, “Korea micro energy grid technology the use case of the first-town in Sejong,” *Netw. Oper. Manag. Symp. (APNOMS), 2013 15th Asia-Pacific*, 2013.

[17] D. McLarty, C. Civit Sabate, J. Brouwer, and F. Jabbari, “Micro-grid energy dispatch optimization and predictive control algorithms; A UC Irvine case study,” *Int. J. Electr. Power Energy Syst.*, vol. 65, pp. 179–190, 2014.

[18] D. Chan, M. Cameron, and Y. Yoon, “Implementation of micro energy grid: A case study of a sustainable community in China,” *Energy Build.*, vol. 139, pp. 719–731, 2017.

[19] E. Zio and L. R. Golea, “Analyzing the topological, electrical and reliability characteristics of a power transmission system for identifying its critical elements,” *Reliab. Eng. Syst. Saf.*, vol. 101, pp. 67–74, 2012.

[20] D. Gama Dessavre, J. E. Ramirez-Marquez, and K. Barker, “Multidimensional approach to complex system resilience analysis,” *Reliab. Eng. Syst. Saf.*, vol. 149, pp. 34–43, 2016.

[21] D. C. Montgomery, *Introduction to statistical quality control*. John Wiley, 2005.

[22] L. Yang and J. Lee, “Bayesian belief network-based approach for diagnostics and prognostics of semiconductor manufacturing systems,” *Robot. Comput. Integr. Manuf.*, vol. 28, no. 1, pp. 66–74, Feb. 2012.

[23] D. T. Ton and M. A. Smith, “The U.S. Department of Energy’s Microgrid Initiative,” *Electr. J.*, vol. 25, no. 8, pp. 84–94, Oct. 2012.

[24] R. H. Lasseter, “Smart distribution: Coupled microgrids,” *Proc. IEEE*, vol. 99, no. 6, pp. 1074–1082, 2011.

[25] C. Brandoni and M. Renzi, “Optimization of hybrid micro-CCHP systems in the day-ahead electricity market,” in *The 3rd edition of the International Conference on Microgeneration and Related Technologies*, 2013, p. 10.

[26] M. Z. Daud, A. Mohamed, and M. A. Hannan, “An improved control method of battery energy storage system for hourly dispatch of photovoltaic power sources,” *Energy Convers. Manag.*, vol. 73, pp. 256–270, Sep. 2013.

[27] H. A. Gabbar, L. Bower, D. Pandya, A. Agarwal, M. U. Tomal, and F. R. Islam, “Resilient micro energy grids with gas-power and renewable technologies,” *Proc. - ICPERE 2014 2nd IEEE Conf. Power Eng. Renew. Energy 2014*, pp. 1–6, 2014.

[28] A. K. Hueffed and P. J. Mago, “Influence of prime mover size and operational strategy on the,” *Proc. Inst. Mech. Eng. Sci. Database pg*, vol. 224, pp. 5–591, 2010.

[29] A. Arnauld and P. Nicole, *Logic or the Art of Thinking*, 5th ed. Cambridge: Cambridge University Press, 1996.

[30] J. Siefring, *The Oxford dictionary of idioms*. Oxford University Press, 2004.

[31] A. Chen and X. Su, “Knightian uncertainty and insurance regulation decision,”

Decis. Econ. Financ., vol. 32, no. 1, pp. 13–33, May 2009.

[32] M. J. Machina, "Risk, ambiguity, and the rank-dependence axioms," *Am. Econ. Assoc. Risk Am. Econ. Rev. Am. Econ. Rev.*, vol. 99, no. 1, pp. 385–392, 2009.

[33] H. Joffe, T. Rossetto, and J. Adams, Eds., *Cities at risk*, vol. 33. Dordrecht: Springer Netherlands, 2013.

[34] N. L. Erik Hollnagel, David D. Woods, "Resilience engineering: concepts and precepts," *Qual. Saf. Heal. Care*, vol. 15, no. 6, pp. 447–448, Dec. 2006.

[35] B. Ale, P. Burnap, and D. Slater, "On the origin of PCDS – (Probability consequence diagrams)," *Saf. Sci.*, vol. 72, pp. 229–239, Feb. 2015.

[36] F. Goerlandt and G. Reniers, "An approach for reconciling different perspectives and stakeholder views on risk ranking," *J. Clean. Prod.*, vol. 149, pp. 1219–1232, Apr. 2017.

[37] E. S. Levine, "Improving risk matrices: the advantages of logarithmically scaled axes," *J. Risk Res.*, vol. 15, no. 2, pp. 209–222, Feb. 2012.

[38] A. Pickering and S. Cowley, "Risk matrices: implied accuracy and false assumptions," *J. Heal. H Saf. reSearc H Pract.*, vol. 2, pp. 9–16, 2010.

[39] Y. Y. Haimes, *Risk modeling, assessment, and management*, 4th ed. John Wiley & Sons, Inc, 2015.

[40] A. T. Bahill, "Design and testing of an illuminance management system," *Int. Test Eval. Assoc.*, vol. 31, no. 1, pp. 63–89, 2010.

[41] J. Daniels, P. W. Werner, and a. T. Bahill, "Quantitative methods for tradeoff analyses," *Syst. Eng.*, vol. 4, no. 3, pp. 190–212, 2001.

[42] J. Cooper, "Soft mathematical aggregation in safety assessment and decision analysis," *Sandia*, no. SAN 009-1496C, p. 5, 1999.

[43] H. Kerzner, *Project management: a systems approach to planning, scheduling, and controlling.*, 11th ed. New York, NY: John Wiley & Sons, Inc, 2013.

[44] A. T. Bahill and J. Daniels, "Correction to quantitative methods for tradeoff

analyses," *Syst. Eng.*, vol. 8, no. 1, pp. 93–93, 2005.

[45] J. Z. Ben-Asher, "Development Program Risk Assessment Based on Utility Theory," *Risk Manag.*, vol. 10, no. 4, pp. 285–299, Oct. 2008.

[46] T. Carbone and D. Tippett, "Project risk management using the project risk FMEA," *J. Eng. Manag.*, vol. 16, no. 4, pp. 1–8, 2004.

[47] T. N. McManus, *Management of hazardous energy deactivation, de-energization, isolation, and lockout*, 1st ed. Boca Raton, Florida: CRC Press/Taylor & Francis Group, 2013.

[48] D. K. Pradhan, J. Mathew, and R. Shafik, *Energy-efficient fault-tolerant systems*. New York : Springer Publishing Company, Incorporated, 2014.

[49] Q. He and R. S. Blum, "Smart grid fault detection using locally optimum unknown or estimated direction hypothesis test," *Energy Procedia*, vol. 12, pp. 170–179, 2011.

[50] E. De Santis, L. Livi, A. Sadeghian, and A. Rizzi, "Modeling and recognition of smart grid faults by a combined approach of dissimilarity learning and one-class classification," *Neurocomputing*, vol. 170, pp. 368–383, 2015.

[51] M. Kezunovic, "Smart fault location for smart grids," *IEEE Trans. Smart Grid*, vol. 2, no. 1, pp. 11–22, 2011.

[52] M. J. B. Reddy, D. V. Rajesh, P. Gopakumar, and D. K. Mohanta, "Smart fault location for smart grid operation using RTUs and computational intelligence techniques," *IEEE Syst. J.*, vol. 8, no. 4, pp. 1260–1271, 2014.

[53] Z. Wu, F. Yang, and Q. Han, "A novel islanding fault detection for distributed generation systems," *Int. J. Robust Nonlinear Control*, vol. 18, no. October 2014, pp. 1431–1445, 2014.

[54] A. Zidan *et al.*, "Fault detection, isolation, and service restoration in distribution systems: state-of-the-art and future trends," *IEEE Trans. Smart Grid*, vol. PP, no. 99, pp. 1–16, 2016.

[55] K. M. Dowling, “Hardware-in-loop evaluation of microgrid protection schemes,” M.A. thesis, University of Tennessee, Knoxville, USA, 2014.

[56] A. A. Memon and K. Kauhaniemi, “A critical review of AC microgrid protection issues and available solutions,” *Electr. Power Syst. Res.*, vol. 129, pp. 23–31, 2015.

[57] H. Samet, “Evaluation of digital metering methods used in protection and reactive power compensation of micro-grids,” *Renew. Sustain. Energy Rev.*, vol. 62, pp. 260–279, 2016.

[58] J. Keller, *Understanding fault characteristics of inverter-based distributed energy resources (Technical Report)*. Golden, CO : National Renewable Energy Laboratory, 2010.

[59] S. Thale and V. Agarwal, “Controller area network (CAN) based smart protection scheme for Solar PV, fuel cell, ultra-capacitor and wind energy system based microgrid,” in *2012 38th IEEE Photovoltaic Specialists Conference*, 2012, pp. 000580–000585.

[60] N. Costantino *et al.*, “Design and test of an HV-CMOS intelligent power switch with integrated protections and self-diagnostic for harsh automotive applications,” *IEEE Trans. Ind. Electron.*, vol. 58, no. 7, pp. 2715–2727, 2011.

[61] W. Friedl, L. Fickert, E. Schmautzer, and C. Obkircher, “Safety and reliability for smart-, micro-and islanded grids,” in *CIRED Seminar 2008: SmartGrids for Distribution*, 2008, pp. 15–15.

[62] H. Nikkhajoei and R. H. Lasseter, “Microgrid protection,” in *2007 IEEE Power Engineering Society General Meeting*, 2007, pp. 1–6.

[63] W. Deng, W. Pei, Z. Shen, Z. Zhao, and H. Qu, “Adaptive micro-grid operation based on IEC 61850,” *Energies*, vol. 8, no. 5, pp. 4455–4475, 2015.

[64] H. J. Laaksonen, “Protection principles for future microgrids,” *IEEE Trans. Power Electron.*, vol. 25, no. 12, pp. 2910–2918, Dec. 2010.

[65] P. M. Twigg, M. Thomson, B. A. Majeed, and N. Ruck, “Fault detection of heat

exchanger fouling for combined heat and power units using statistical process control techniques," *Adv. Process Control*, vol. 4, pp. 23–30, 1995.

[66] M. Thomson, P. M. Twigg, B. a. Majeed, and N. Ruck, "Statistical process control based fault detection of CHP units," *Control Eng. Pract.*, vol. 8, no. 1, pp. 13–20, 2000.

[67] A. Lazzaretto and A. Toffolo, "A critical review of the thermoeconomic diagnosis methodologies for the location of causes of malfunctions in energy systems," *J. Energy Resour. Technol.*, vol. 128, no. 4, p. 335, Dec. 2006.

[68] T. Alemu Lemm and F. Mohd Hashi, "IFDD: Intelligent fault detection and diagnosis-application to a cogeneration and cooling plant," *Asian J. Sci. Res.*, vol. 6, no. 3, pp. 478–487, Mar. 2013.

[69] J. Schein, S. T. Bushby, N. S. Castro, and J. M. House, "A rule-based fault detection method for air handling units," *Energy Build.*, vol. 38, no. 12, pp. 1485–1492, 2006.

[70] G. Li *et al.*, "An improved fault detection method for incipient centrifugal chiller faults using the PCA-R-SVDD algorithm," *Energy Build.*, vol. 116, pp. 104–113, Mar. 2016.

[71] S. Simani and P. Castaldi, "Active actuator fault-tolerant control of a wind turbine benchmark model," *Int. J. Robust Nonlinear Control*, vol. 24, no. 8–9, pp. 1283–1303, May 2014.

[72] T. Knüppel *et al.*, "Fault diagnosis for electrical distribution systems using structural analysis," *Int. J. Robust Nonlinear Control*, vol. 18, no. October 2014, pp. 1446–1465, May 2014.

[73] H. Bevrani, A. Ghosh, and G. Ledwich, "Renewable energy sources and frequency regulation: survey and new perspectives," *IET Renew. Power Gener.*, vol. 4, no. 5, pp. 438–457, 2010.

[74] F. Tedesco and A. Casavola, "Fault-tolerant distributed load/frequency supervisory strategies for networked multi-area microgrids," *Int. J. Robust Nonlinear Control*,

vol. 24, no. 8–9, pp. 1380–1402, May 2014.

[75] C. Winzer, “Conceptualizing energy security,” *Energy Policy*, vol. 46, pp. 36–48, 2012.

[76] C. Böhringer and M. Bortolamedi, “Sense and no(n)-sense of energy security indicators,” *Ecol. Econ.*, vol. 119, pp. 359–371, Nov. 2015.

[77] J. Martchamadol and S. Kumar, “Thailand’s energy security indicators,” *Renew. Sustain. Energy Rev.*, vol. 16, no. 8, pp. 6103–6122, Oct. 2012.

[78] B. W. Ang, W. L. Choong, and T. S. Ng, “Energy security: Definitions, dimensions and indexes,” *Renew. Sustain. Energy Rev.*, vol. 42, pp. 1077–1093, Feb. 2015.

[79] W. M. Goble and H. Cheddie, *Safety instrumented systems verification: practical probabilistic calculations*. North Carolina: ISA-The Instrumentation, Systems and Automation Society, 2005.

[80] K. Wolter, *Stochastic models for fault tolerance: restart, rejuvenation and checkpointing*. Berlin, Germany: Springer Publishing Company, Incorporated, 2010.

[81] M. R. Islam and H. A. Gabbar, “Study of micro grid safety and protection strategies with control system infrastructures,” *Smart Grid Renew. Energy*, vol. 03, no. 01, pp. 1–9, Feb. 2012.

[82] A. Sharifi and Y. Yamagata, “Major principles and criteria for development of an urban resilience assessment index,” in *International Conference and Utliity Exhibition 2014*, 2014, no. March, pp. 19–21.

[83] A. Sharifi and Y. Yamagata, “Principles and criteria for assessing urban energy resilience: A literature review,” *Renew. Sustain. Energy Rev.*, vol. 60, pp. 1654–1677, 2016.

[84] G. Song, H. Chen, and B. Guo, “A layered fault tree model for reliability evaluation of smart grids,” *Energies*, vol. 7, no. 8, pp. 4835–4857, 2014.

[85] A. Chaves and A. Terry Bahill, “Comparison of risk analysis approaches and a case study of the risk of incorporating solar photovoltaic systems into a commercial electric power grid,” *Syst. Eng.*, vol. 17, no. 1, pp. 89–111, 2014.

[86] A. T. Bahill, “Diogenes, a process for identifying unintended consequences,” *Syst. Eng.*, vol. 15, no. 3, pp. 287–306, Sep. 2012.

[87] A. B. Agrawal, K. Barker, and Y. Y. Haimes, “Adaptive multiplayer approach for risk-based decision-making: 2006 Virginia Gubernatorial Inauguration,” *Syst. Eng.*, vol. 14, no. 4, pp. 455–470, Dec. 2011.

[88] A. T. Bahill and W. J. Karnavas, “Risk analysis of a pinewood derby: A case study,” *Syst. Eng.*, vol. 3, no. 3, pp. 143–155, 2000.

[89] Y. Zhao, S. Wang, and F. Xiao, “A statistical fault detection and diagnosis method for centrifugal chillers based on exponentially-weighted moving average control charts and support vector regression,” *Appl. Therm. Eng.*, vol. 51, no. 1, pp. 560–572, 2013.

[90] Y. Chen and L. Lan, “A fault detection technique for air-source heat pump water chiller/heaters,” *Energy Build.*, vol. 41, no. 8, pp. 881–887, 2009.

[91] Y. Zhao, F. Xiao, and S. Wang, “An intelligent chiller fault detection and diagnosis methodology using Bayesian belief network,” *Energy Build.*, vol. 57, pp. 278–288, 2013.

[92] S. Saponara, L. Fanucci, F. Bernardo, and A. Falciani, “Predictive diagnosis of high-power transformer faults by networking vibration measuring nodes with integrated signal processing,” *IEEE Trans. Instrum. Meas.*, vol. 65, no. 8, pp. 1749–1760, Aug. 2016.

[93] S. Saponara, “Distributed measuring system for predictive diagnosis of uninterruptible power supplies in safety-critical applications,” *Energies*, vol. 9, no. 5, p. 327, 2016.

[94] Y. Zhang, M. Zhao, S. Zhang, J. Wang, and Y. Zhang, “An integrated approach to estimate storage reliability with initial failures based on E-Bayesian estimates,”

Reliab. Eng. Syst. Saf., vol. 159, no. November 2016, pp. 24–36, 2017.

[95] J. Pearl, "Bayesian networks a model of self-activated memory for evidential reasoning," in *Proceedings of the 7th Conference of the Cognitive Science Society*, 1985, pp. 329–334.

[96] C. Kang, "A Bayesian belief network-based advisory system for operational availability focused diagnosis of complex nuclear power systems," *Expert Syst. Appl.*, vol. 17, no. 1, pp. 21–32, Jul. 1999.

[97] G. Kabir, R. Sadiq, and S. Tesfamariam, "A fuzzy Bayesian belief network for safety assessment of oil and gas pipelines," *Struct. Infrastruct. Eng.*, vol. 12, no. 8, pp. 874–889, 2016.

[98] G. Li and J. Shi, "Applications of Bayesian methods in wind energy conversion systems," *Renew. Energy*, vol. 43, pp. 1–8, Jul. 2012.

[99] P. Trucco, E. Cagno, F. Ruggeri, and O. Grande, "A Bayesian belief network modelling of organisational factors in risk analysis: a case study in maritime transportation," *Reliab. Eng. Syst. Saf.*, vol. 93, no. 6, pp. 845–856, Jun. 2008.

[100] C. Rojas-Guzman and M. A. Kramer, "Comparison of belief networks and rule-based expert systems for fault diagnosis of chemical processes," *Eng. Appl. Artif. Intell.*, vol. 6, no. 3, pp. 191–202, 1993.

[101] D. Malloy and C. Biegl, "Development of a real-time turbine engine diagnostic system," in *XIII International Symposium on Air Breathing Engines*, 2002.

[102] A. K. M. C. Romessis, A. Stamatis, "Setting up a belief network for turbofan diagnosis with the aid of an engine performance model," in *Laboratory of thermal turbomachine*, Zografou, Greece: National Technical University of Athens, 2001, p. 21.

[103] Hussain Sajid, "Intelligent fault diagnosis of gearboxes and its applications on wind turbines," Ph.D. thesis, University of Ontario Institute of Technology, Canada, 2013.

[104] Z. Liu, Y. Liu, D. Zhang, B. Cai, and C. Zheng, "Fault diagnosis for a solar

assisted heat pump system under incomplete data and expert knowledge," *Energy*, vol. 87, pp. 41–48, 2015.

[105] M. Borunda, O. A. Jaramillo, A. Reyes, and P. H. Ibarguengoytia, "Bayesian networks in renewable energy systems: A bibliographical survey," *Renew. Sustain. Energy Rev.*, vol. 62, pp. 32–45, 2016.

[106] B. G. Xu, "Intelligent fault inference for rotating flexible rotors using Bayesian belief network," *Expert Syst. Appl.*, vol. 39, no. 1, pp. 816–822, 2012.

[107] H. A. Gabbar, M. Isham, S. Hussain, and L. Zhang, "BBN-based reasoning approach for safety verification using FSN," *J. Chem. Eng. Japan*, vol. 48, no. 8, pp. 684–689, 2015.

[108] C.-C. Wang, Y. Kang, and C.-C. Liao, "Gear fault diagnosis in time domains via Bayesian networks," *Trans. Can. Soc. Mech. Eng.*, vol. 37, no. 3, 2013.

[109] J. Chen and G. Hao, "Research on the fault diagnosis of wind turbine gearbox based on Bayesian networks," in *Advances in Intelligent and Soft Computing*, 2011, vol. 124, pp. 217–223.

[110] J. Monteiro, J. Eduardo, P. J. S. Cardoso, and J. Semiao, "A distributed load scheduling mechanism for micro grids," *2014 IEEE Int. Conf. Smart Grid Commun. SmartGridComm 2014*, pp. 278–283, 2015.

[111] G. R. Aghajani, H. A. Shayanfar, and H. Shayeghi, "Presenting a multi-objective generation scheduling model for pricing demand response rate in micro-grid energy management," *Energy Convers. Manag.*, vol. 106, pp. 308–321, 2015.

[112] D. E. Olivares, "Trends in Microgrid control," *IEEE Trans. Smart Grid*, vol. 5, no. 4, 2014.

[113] A. Khodaei, "Provisional Microgrids," *IEEE Trans. Smart Grid*, vol. 6, no. 3, 2015.

[114] G. Hug, S. Kar, and C. Wu, "Consensus + Innovations approach for distributed multiagent coordination in a Microgrid," *IEEE Trans. Smart Grid*, vol. 6, no. 4, pp. 1893–1903, Jul. 2015.

[115] A. J. del Real, A. Arce, and C. Bordons, “Combined environmental and economic dispatch of smart grids using distributed model predictive control,” *Int. J. Electr. Power Energy Syst.*, vol. 54, pp. 65–76, Jan. 2014.

[116] L. Ji, D. X. Niu, M. Xu, and G. H. Huang, “An optimization model for regional micro-grid system management based on hybrid inexact stochastic-fuzzy chance-constrained programming,” *Int. J. Electr. Power Energy Syst.*, vol. 64, pp. 1025–1039, 2015.

[117] M. Ameri and Z. Besharati, “Optimal design and operation of district heating and cooling networks with CCHP systems in a residential complex,” *Energy Build.*, vol. 110, pp. 135–148, 2016.

[118] C. A. Hernandez-Aramburo, “Fuel consumption minimization of a Microgrid,” *Ind. Appl. IEEE Trans.*, vol. 41, no. 3, pp. 673–681, 2005.

[119] A. A. Girgis and S. Mathure, “Application of active power sensitivity to frequency and voltage variations on load shedding,” *Electr. Power Syst. Res.*, vol. 80, no. 3, pp. 306–310, 2010.

[120] P. Costamagna, L. Magistri, and a. F. Massardo, “Design and part-load performance of a hybrid system based on a solid oxide fuel cell reactor and a micro gas turbine,” *J. Power Sources*, vol. 96, no. 2, pp. 352–368, 2001.

[121] C. C. Schultz, “Closing the cogeneration gap,” *Engineered Systems Magazine*, BNP Media, pp. 38–43, 2010.

[122] J. H. Frankland, “A model-based feasibility study of combined heat and power systems for use in urban environments,” M. A. thesis, Georgia institute of technology, USA, 2013.

[123] S. M. Hosseinalipour, E. Abdolahi, and M. Razaghi, “Static and dynamic mathematical modeling of a Micro gas turbine,” *J. Mech.*, vol. 29, no. 02, pp. 327–335, 2013.

[124] A. Abobghala, “Modelling , simulation and optimisation for the operation of heat recovery steam generators,” M.Eng. report, University Of Huddersfield, UK, 2010.

[125] A. Ghaffari, A. Chaibakhsh, and S. Shahhoseini, “Neuro-Fuzzy modeling of heat recovery steam generator,” *Int. J. Mach. Learn. Comput.*, vol. 2, no. Icmlc, pp. 49–53, 2013.

[126] S. Turner, Wayne C; Doty, *Energy managment handbook*, 8th ed. The Fairmont Press, Inc., 2013.

[127] D. I. H. Rodríguez, “Development of a control strategy for mini CHP plants for an active voltage management in low voltage networks,” M.Sc. thesis, Technische Universitat Dortmund, Germany, 2011.

[128] K. S. Lee, *Underground thermal energy storage*. London: Springer London, 2013.

[129] N. Petchers, *Combined heating, cooling & power handbook: technologies & applications an integrated approach to energy resource optimization*. New York, NY: Fairmont Press, 2012.

[130] K. M. Powell and T. F. Edgar, “An adaptive-grid model for dynamic simulation of thermocline thermal energy storage systems,” *Energy Convers. Manag.*, vol. 76, pp. 865–873, 2013.

[131] D. I. Hidalgo Rodriguez, L. Spitalny, J. Myrzik, and M. Braun, “Development of a control strategy for mini CHP plants for an active voltage management in low voltage networks,” in *2012 3rd IEEE PES Innovative Smart Grid Technologies Europe (ISGT Europe)*, 2012, pp. 1–8.

[132] T. L. Bergman, F. P. Incropera, D. P. DeWitt, and A. S. Lavine, *Fundamentals of heat and mass transfer*. John Wiley & Sons, 2011.

[133] S. Tyler and M. Moench, “A framework for urban climate resilience,” *Clim. Dev.*, vol. 4, no. 4, pp. 311–326, Oct. 2012.

[134] D. Butler *et al.*, “Reliable, resilient and sustainable water management: the Safe & SuRe approach,” *Glob. Challenges*, vol. 1, no. 1, pp. 63–77, 2017.

[135] S. Jackson, “How resilience engineering maintains sustainable value,” *Insight*, vol. 19, no. 2, pp. 25–27, Jul. 2016.

[136] D. US Department of Defense, “Military standard 882B system safety program requirements (Report),” Washington DC, 1984.

[137] H. A. Gabbar and Y. Koraz, “Risk assessment of micro energy grid protection layers,” *Energies 2017*, vol. 10, no. 8, p. 1176, 2017.

[138] E. Piesik, M. Śliwiński, and T. Barnert, “Determining and verifying the safety integrity level of the safety instrumented systems with the uncertainty and security aspects,” *Reliab. Eng. Syst. Saf.*, vol. 152, pp. 259–272, Aug. 2016.

[139] E. Dubrova, *Fault-tolerant design*. New York, NY: Springer Science+Business Media, 2013.

[140] P. Baybutt, “Risk tolerance criteria and the IEC 61511/ISA 84 standard on safety instrumented systems,” *Process Saf. Prog.*, vol. 32, no. 3, pp. 307–310, Sep. 2013.

[141] R. N. Allan, R. Billinton, I. Sjarief, L. Goel, and K. S. So, “A reliability test system for educational purposes-basic distribution system data and results,” *IEEE Trans. Power Syst.*, vol. 6, no. 2, pp. 813–820, 1991.

[142] T. Adefarati and R. C. Bansal, “Reliability and economic assessment of a microgrid power system with the integration of renewable energy resources,” *Appl. Energy*, vol. 206, no. September, pp. 911–933, 2017.

[143] T. Adefarati and R. C. Bansal, “Reliability assessment of distribution system with the integration of renewable distributed generation,” *Appl. Energy*, vol. 185, pp. 158–171, 2017.

[144] J. Ribrant and L. M. Bertling, “Survey of failures in wind power systems with focus on Swedish wind power plants during 1997-2005,” *IEEE Trans. Energy Convers.*, vol. 22, no. 1, pp. 167–173, 2007.

[145] C. A. Smith, M. D. Donovan, and M. J. Bartos, “Reliability survey of 600- to 1800-kW diesel and gas-turbine generating units,” *IEEE Trans. Ind. Appl.*, vol. 26, no. 4, pp. 741–755, 1990.

[146] R. Billinton, “A test system for teaching overall power system reliability assessment,” *IEEE Trans. Power Syst.*, vol. 11, no. 4, pp. 1670–1676, 1996.

[147] Trane, “Trane® CenTraVac ™ Chillers The most efficient and reliable centrifugal chillers on the planet (white paper),” Dublin, Republic of Ireland, 2017.

[148] F. Dinter and D. M. Gonzalez, “Operability, reliability and economic benefits of CSP with thermal energy storage: First year of operation of ANDASOL 3,” *Energy Procedia*, vol. 49, pp. 2472–2481, 2013.

[149] R. Orumbayev, A. Kibarin, T. Khodanova, and M. Korobkov, “Economical and ecological assessment of hot-water boilers substitution or modernization within district heat supply systems across the Republic of Kazakhstan,” *Energy Procedia*, vol. 141, pp. 304–309, 2017.

[150] L. Fuji Electric Co., “Fuji electric review fuel cell power generation,” Tokyo, Japan, 2001.

[151] Capstone Turbine Corporation, “C200 Microturbine,” Van Nuys, CA, USA, 2008.

[152] N. Vedachalam and G. A. Ramadass, “Reliability assessment of multi-megawatt capacity offshore dynamic positioning systems,” *Appl. Ocean Res.*, vol. 63, pp. 251–261, 2017.

[153] H. Gunduz and D. Jayaweera, “Reliability assessment of a power system with cyber-physical interactive operation of photovoltaic systems,” *Int. J. Electr. Power Energy Syst.*, vol. 101, no. March, pp. 371–384, 2018.

[154] S. Deb, D. Ghosh, and D. K. Mohanta, “Reliability analysis of PV cell, wind turbine and diesel generator by using Bayesian network,” in *International Conference on Electrical, Electronics, and Optimization Techniques (ICEEOT) - 2016*, 2016, pp. 2714–2719.

[155] Y. Koraz and H. A. Gabbar, “Risk analysis and self-healing approach for resilient interconnect Micro energy grids,” *Sustain. Cities Soc.*, vol. 32, no. February, pp. 638–653, 2017.

[156] A. H. Gandomi and D. A. Roke, “Engineering optimization using interior search algorithm,” *IEEE SSCI 2014 - 2014 IEEE Symp. Ser. Comput. Intell. - SIS 2014 2014 IEEE Symp. Swarm Intell. Proc.*, pp. 20–26, 2015.

[157] A. H. Gandomi, “Interior search algorithm (ISA): A novel approach for global optimization,” *ISA Trans.*, vol. 53, no. 4, pp. 1168–1183, 2014.

[158] A. Natural Resources Canada, “Appendix B – CO2 emission factors | natural resources canada,” *Government of Cansda*. [Online]. Available: http://www.nrcan.gc.ca/energy/efficiency/industry/technical-info/benchmarking/canadian-steel-industry/5193. [Accessed: 27-Feb-2018].

[159] A. Zangeneh, S. Jadid, and A. Rahimi-Kian, “A hierarchical decision making model for the prioritization of distributed generation technologies: A case study for Iran,” *Energy Policy*, vol. 37, no. 12, pp. 5752–5763, 2009.

[160] C. Lo Prete *et al.*, “Sustainability and reliability assessment of microgrids in a regional electricity market,” *Energy*, vol. 41, no. 1, pp. 192–202, 2012.

[161] “IESO power data.” [Online]. Available: http://www.ieso.ca/pages/power-data/default.aspx#demand.

[162] X. Wu, X. Wang, S. Member, C. Qu, and S. Member, “A hierarchical framework for generation scheduling of Microgrids,” *IEEE Trans. Power Deliv.*, vol. 29, no. 6, pp. 2448–2457, 2014.

[163] A. Hauer, G. Simbolotti, G. Tosato, and D. Gielen, “Thermal energy storage (White paper),” 2013.

[164] United Technologies Research Center, “Micro-CHP systems for residential applications final report,” East Hartford, 2006.

[165] R. Garduno-ramirez and K. Y. Lee, “Multiobjective optimal power plant operation through coordinate control with pressure set point scheduling,” *IEEE Trans. Energy Convers.*, vol. 16, no. 2, pp. 115–122, 2001.

[166] T. Hwang, M. Choi, S. Kang, and I. Lee, “Design of application-level reference models for micro energy grid in IT Perspective,” *Int. Conf. Comput. Netw. Technol.*, 2012.

[167] M. U. Tomal and H. A. Gabbar, “Key performance assessment of fuel cell based distributed energy generation system in resilient micro energy grid,” *IEEE Int.*

Conf. Smart Energy Grid Eng., pp. 1–6, 2015.

[168] L. C. Lipan, L. Pislaru-Danescu, D. C. Dasu, L. Tomescu, I. Pisica, and G. Comanescu, "Design and implementation of a combined cooling, heating and power plant to support data centre supply reliability," in *47th International Universities Power Engineering Conference (UPEC)*, 2012, pp. 1–6.

[169] Y. Li and D. Mavris, "A hierarchical control architecture for resource allocation," in *12th International Conference on Control, Automation, Robotics & Vision*, 2012, pp. 955–959.

[170] R. G. Wandhare, S. Thale, and V. Agarwal, "Reconfigurable hierarchical control of a microgrid developed with PV, wind, micro-hydro, fuel cell and ultra-capacitor," in *Twenty-Eighth Annual IEEE Applied Power Electronics Conference and Exposition (APEC)*, 2013, pp. 2799–2806.

[171] O. Erdinc and M. Uzunoglu, "Optimum design of hybrid renewable energy systems: Overview of different approaches," *Renew. Sustain. Energy Rev.*, vol. 16, no. 3, pp. 1412–1425, 2012.

[172] Z. Duda, "Two-level hierarchical control in a large scale stochastic system," in *Proceedings of the European Control Conference*, 2001, pp. 2193–2197.

[173] J. M. Guerrero, J. C. Vasquez, J. Matas, L. G. De Vicuña, and M. Castilla, "Hierarchical control of droop-controlled AC and DC microgrids - A general approach toward standardization," *IEEE Trans. Ind. Electron.*, vol. 58, no. 1, pp. 158–172, 2011.

[174] M. Kurano, M. Yasuda, J. Nakagami, and Y. Yoshida, "A fuzzy approach to Markov decision processes with uncertain transition probabilities," *Fuzzy Sets Syst.*, vol. 157, no. 19, pp. 2674–2682, 2006.

[175] I. Lorencin and M. Pantoš, "Evaluating Generating Unit Unavailability Using Bayesian Power Priors," *IEEE Trans. Power Syst.*, vol. 32, no. 3, pp. 2315–2323, 2017.

[176] C. Bielza, G. Li, and P. Larrañaga, "Multi-dimensional classification with

Bayesian networks," *Int. J. Approx. Reason. Multi-dimensional Classif. with Bayesian networks*, vol. 52, pp. 705–727, 2011.

[177] D. Smith, B. Veitch, F. Khan, and R. Taylor, "Understanding industrial safety: Comparing fault tree, Bayesian network, and FRAM approaches," *J. Loss Prev. Process Ind.*, vol. 45, pp. 88–101, 2017.

[178] E. Roventa and T. Spircu, "Bayesian (belief) networks," in *Management of knowledge imperfection in building intelligent systems*, Berlin, Heidelberg, Heidelberg: Springer Berlin Heidelberg, 2009, pp. 133–152.

[179] M. Vileiniskis, R. Remenyte-Prescott, D. Rama, and J. Andrews, "Fault detection and diagnostics of a three-phase separator," *J. Loss Prev. Process Ind.*, vol. 41, pp. 215–230, 2016.

[180] Y. Zhao, J. Tong, L. Zhang, and Q. Zhang, "Pilot study of dynamic Bayesian networks approach for fault diagnostics and accident progression prediction in HTR-PM," *Nucl. Eng. Des.*, vol. 291, pp. 154–162, 2015.

[181] K. Zou, A. P. Agalgaonkar, K. M. Muttaqi, and S. Perera, "An analytical approach for reliability evaluation of distribution systems containing dispatchable and nondispatchable renewable DG units," *IEEE Trans. Smart Grid*, vol. 5, no. 6, pp. 2657–2665, Nov. 2014.

[182] H. Danesh, K.-Z. H., H. Daneshi, H. Khorashadi-Zadeh, H. Danesh, and K.-Z. H., "Microgrid energy management system : A study of reliability and economic issues," in *2012 IEEE Power and Energy Society General Meeting*, 2012, pp. 1–5.

[183] EEH Power Systems Laboratory, *Electrical power systems (Company's report)*. Berlin, 2007.

[184] G. F. Cooper and E. Herskovits, "A Bayesian method for the induction of probabilistic networks from data," *Mach. Learn.*, vol. 9, no. 4, pp. 309–347, Oct. 1992.

[185] A. L. Madsen and F. V. Jensen, "Lazy propagation: A junction tree inference algorithm based on lazy evaluation," *Artif. Intell.*, vol. 113, no. 1, pp. 203–245,

1999.

[186] J. Wang and O. Kieran, “Off shore safety assessment and safety-based decision-making-the current status and future aspects,” *J. Offshore Mech. Arct. Eng.*, vol. 122, no. 2, p. 93, 2000.

[187] Y. Koraz and H. A. Gabbar, “Fault diagnosis of micro energy grids using Bayesian belief network and adaptive neuro-fuzzy interference system,” in *2017 IEEE International Conference on Smart Energy Grid Engineering (SEGE)*, 2017, pp. 143–147.

[188] D. McNeill and P. Freiberger, *Fuzzy logic*. New York: Simon & Schuster, 1994.

[189] J.-S. R. Jang, “ANFIS: adaptive-network-based fuzzy inference system,” *IEEE Trans. Syst. Man. Cybern.*, vol. 23, no. 3, pp. 665–685, 1993.

[190] F. D ’urso *et al.*, “An optimization and management tool for complex multi-generation systems,” in *16th International Conference on Environment and Electrical Engineering (EEEIC)*, 2016, pp. 1–6.

[191] Y. Koraz and P. Lazzeroni, “Micro Energy Grid Optimal Design Using MILP Approach,” in *2018 IEEE Canadian Conference on Electrical & Computer Engineering (CCECE)*, 2018, pp. 1–4.

[192] “Ontario time-of-use electricity Rates.” [Online]. Available: http://www.ontario-hydro.com/current-rates.

[193] “SankeyMATIC (BETA): Build a diagram.” [Online]. Available: http://sankeymatic.com/build/.

[194] G. Specifications, “QSM11 marine propulsion and auxiliary engines for commercial and government applications (data sheet).”

[195] A. B. Stambouli and E. Traversa, “Solid oxide fuel cells (SOFCs): A review of an environmentally clean and efficient source of energy,” *Renew. Sustain. Energy Rev.*, vol. 6, no. 5, pp. 433–455, 2002.

[196] S. Burwood, “Methods of SIL determination,” in *IET Workshops and Seminar on*

Safety Integrity Levels - Challenges and Solutions, 2012, pp. 2–2.

[197] J. Pinto, "Wind energy projects integration in electricity grids portugal and med tso experiences," *https://www.slideshare.net/featured/category/technology*, 2013. [Online]. Available: https://www.slideshare.net/rcreee/wind-energy-projects-integration-in-electricity-grids-portugal-and-med-tso-experiences. [Accessed: 09-Jan-2018].

[198] POLLARA, "Electricity outage and reliability study September 2010 consumer component contents (report)," Toronto, Canada, 2010.

[199] POLLARA, "Electricity outage and reliability study September 2010 business component contents (report)," Toronto, Canada, 2010.

[200] Eaton, "Blackout tracker: United States annual report 2015 (Company's report)," Boulder, US, 2015.

[201] S. Lecturer and M. E. Student, "Development of an efficient load management system for improved health care delivery in Nigeria," *Int. J. Eng. Appl. Sci.*, vol. 5, no. 05, p. 8, 2014.

[202] A. A. Chowdhury and L. Bertling, "Distribution system in-depth causal reliability assessment," in *2006 International Conference on Probabilistic Methods Applied to Power Systems*, 2006, pp. 1–8.

[203] Bloomberg, "Profiling the risks in solar and wind: A case for new risk management approaches in the renewable energy sector (white paper)," Zurich, 2013.

[204] W. Gang, S. Wang, K. Shan, and D. Gao, "Impacts of cooling load calculation uncertainties on the design optimization of building cooling systems," *Energy Build.*, vol. 94, pp. 1–9, 2015.

[205] S. Kallio, "Modelling of a combined heat and power system," M.Sc. thesis, Tampereen Teknillinen Yliopisto, Finland, 2012.

[206] AUHSE Department, "AU general risk assessment (Report)," Aberystwyth, 2015.

[207] X. Shan, K. Liu, and P.-L. Sun, “Risk analysis on leakage failure of natural gas pipelines by Fuzzy Bayesian network with a bow-tie model,” *Sci. Program.*, vol. 2017, pp. 1–11, Feb. 2017.

[208] S. K. Korkua and K. Thinsurat, “A load prioritization model for a smart demand responsive energy management system in the residential sector,” *Walailak J. Sci. Technol.*, vol. 11, no. 1, pp. 7–18, Sep. 2013.

[209] D. Schlabe and J. Lienig, “Energy management of aircraft electrical systems - state of the art and further directions,” in *2012 Electrical Systems for Aircraft, Railway and Ship Propulsion*, 2012, pp. 1–6.

[210] Y. Wang, C. Chen, J. Wang, and R. Baldick, “Research on resilience of power systems under natural disasters - A review,” *IEEE Trans. Power Syst.*, vol. 31, no. 2, pp. 1604–1613, 2016.

[211] C. Fang, F. Marle, and M. Xie, “Applying importance measures to risk analysis in engineering project using a risk network model,” *IEEE Syst. J.*, vol. 11, no. 3, pp. 1–9, Sep. 2016.

[212] A. T. Bahill and E. D. Smith, “An Industry Standard Risk Analysis Technique,” *Eng. Manag. J.*, vol. 21, no. 4, 2009.

Appendix I Proposed Resilience Matrix for MEG

	1	2	3	4	5	6	7	8	9	10	11	12	13
SI	**Grid Type**	**Hazard Scenario Top Event**	**Hazard Event Initiator**	**Ref.**	**Likelihood** *(C)*	**Severity** *(S)*	**Ecological Risk Index** *(E)* [196]	**RRPI**	**Catastrophic Level**	**Resilience Risk Rank**	**Adverse Effects / Consequences**	**Action (remedial, prevention or mitigation)**	**Proposed solutions and IRLs**
			SCORE		*1= Very Low* *2= Low* *3= Moderate* *4= High* *5= Extremely High*	*1 = Negligible* *2 =Marginal* *3 =Moderate* *4=Critical* *5= Catastrophic*	*1= Negligible* *2 =Minor release* *3 = Local impact* *4 =Regional impact* *5=National impact*	*HL=C*S*E*	*Low: x<30* *Moderate: 60>x>30* *High: x>60*	*Higher rank means lower risk*	(1) On Society (2) On Economy (3) On Environment		
1	Electrical MEG	Power Blackout	Overload/Over demand (above the grid capability)	[40] [197] (R2) [198] [199] [200]	2 [198]	3 [197]	3	18	L	11	(1) Demand not Served (DNS) (2) Overheated transmission and distribution cables, Asset Damage, fire and power blackout (3) Fire causes CO2 Emission	1- Upgrade grid capacity 2- Shift on-peak power demand 3- dynamic grid mapping based on load demand and priority	1- Intelligent Energy Storage System(super capacitor, Fly Wheel, TES and pumped hydro, or hydrogen storage 2- Intelligent Fault Tolerant Controller 3- ranking the loads as per its prioritization level
2			MEG has lack of DER	[197] (R8) [199] [201]	3 [197]	5 [197]	4	60	H	2	(1) Interruption on service (2) Power interruption and/or blackout (3) Lack of DER= more demand on Fossil fuel generators which cause Emission	High dynamic performance from the distributed power and energy system by : • Store off-peak power production for using at on-peak demand • Utilize Gas Generator • Connect to Capital Grid (Utility)	1- Intelligent Energy Storage System (super capacitor, Fly Wheel, TES and pumped hydro, or hydrogen storage. 2- Load Following or dispatchable Generator (fuel cells, micro-gas turbines, and hybrid fuel cell gas turbine systems) 3- Higher level Self-Healing Management Controller
3			Intermittency of on site renewable sources	[40] [197] (R3)	4 [40]	3 [40]	4	48	M	4	(1) Disturbance on service (2) Intermittency and non-coincidence of power production		

											(3) Lack of DER= more demand on Fossil fuel generators		
4			Integration of multi sources DERs	[58] [197] (R7)	3 [197]	3	3	27	L	6	(1) Operation Failure of Sensitive Devices (2) Negative impacts on grid parameters such as active power (P), reactive power (Q), voltage (V), phase shift (α) and frequency (*f*). On other word Bad Power Quality (3) Excessive on Energy Resources and Emission	1- full utilization of DERs to increase energy efficiency 2- improve power quality 3- enhance system stability	1- Advanced D-FACTS system on AC/DC MEG to achieve resilient MEG 2- Create Robust KPI parameters able to optimize feedback control coefficients
5			Faults in the power systems (transmission or distribution systems)	[40] [198] [199] [200][202]	4 [199]	3	5	60	H	3	(1) Unsatisfied condition for customers (2) Power failure and/or outage may cause loss of business and production (3) Fire cause CO2 Emission	1- Isolate the minimal affected branch 2- Switch off and isolate the DERs allocated in the affected zone	1-Wide area Monitoring and Alarm systems 2- Utilizing numerical smart relays 3- Emergency Shutdown system ESD 4- Periodical testing and maintenance procedure
6			Utility grid failure (Loss of electricity)**	[40] [85] [198] [199] [200] [202]	1 [85]	5 [85]	4	20	L	8	(1) Unsatisfied condition for customers (2) Power failure and/or outage may cause loss of business and production (3) More demand on Fossil fuel generators	1- open the main switch gear (islanded mode) 2- standby all available DERs 3- reduce the load based on priority and power production availability	1-Monitoring and Alarm systems for Utility grid energy quality and status 2- Safety management controller dealing with hazards scenarios 3- Emergency Shutdown system ESD
7			Grid voltage exceeds +/-5% limits	[85]	2 [85]	1 [85]	2	4	L	29	(1) Operation Failure of Sensitive Devices (2) Negative impacts on grid parameters such as active power (P), reactive power (Q), voltage (V), phase shift (α) and frequency (*f*). On other word Bad Power Quality (3) Excessive on Energy Resources and Emission	1- full utilization of DERs to increase energy efficiency 2- improve power quality 3- enhance system stability	1- Advanced D-FACTS system on AC/DC MEG to achieve resilient MEG 2- Create Robust KPI parameters able to optimize feedback control coefficients
8			Grid frequency goes out of +/-0.5Hz limits	[85]	1 [85]	2 [85]	2	4	L	30			
9			Electric storage system fails	[85]	1 [85]	1 [85]	2	2	L	36			
10				[85]	1 [85]	1 [85]	3	3	L	35	(1) Interruption on service		

			Co-gen power generation is unavailable in a timely manner								(2) Power interruption and/or blackout	High dynamic performance from the distributed power and energy system by : • Store off-peak power production for using at on-peak demand • Utilize Gas Generator • Connect to Capital Grid (Utility)	1- Intelligent Energy Storage System (super capacitor, Fly Wheel, TES and pumped hydro, or hydrogen storage. 2- Load Following or dispatchable Generator (fuel cells, micro-gas turbines, and hybrid fuel cell gas turbine systems) 3- Higher level Self-Healing Management Controller
11		Solar Farm Outage [85]	Short-range weather prediction system fails	[85] [203]	1 [85]	2 [85]	2	4	L	31	(3) Lack of DER= more demand on Fossil fuel generators which cause Emission		
12			Solar Panel output drops by 60 MW in a 15 min.	[40] [85]	2 [85]	2 [85]	3	12	L	17	(1) Breakers could trip leaving customers without electric power. (2) Voltage on the grid could drop and frequency of main generators could change (3) Increase the demand on coal-fired generators	1- Store off-peak power production for using at on-peak demand 2- dynamic grid mapping based on load demand and priority	1- adopt an advanced power storage units such as super capacitor
13			Feeder circuit disconnects from substation	[40] [85] [202] [203]	3 [85]	1 [85]	2	6	L	24	(1) The customer can no longer sell electricity to utility grid (2) Feeder circuit voltage could get out of phase with the grid (3) Increase the demand on coal-fired generators	1- dynamic network based on load demand and priority 2- reduce the load based on priority and power production availability	1- Intelligent Alarm systems for panel power quality and status 2- Adopt SIS management dealing with hazards scenarios
14			Short to ground on distribution grid	[85]	1 [85]	2 [85]	1	2	L	37	(1) Unsatisfied condition for customers (2) Equipment could be damaged, particularly transformers and capacitor banks. (3) Increase the demand on coal-fired generators	1- dynamic network based on load demand and priority 2- reduce the load based on priority and power production availability	1- Intelligent Alarm systems for panel power quality and status 2- Adopt SIS management dealing with hazards scenarios
15			Failure of DC to AC inverters	[85]	3 [85]	1 [85]	2	6	L	25	(1) The customer can no longer sell electricity to utility grid	1- Isolate the minimal affected branches 2- Switch off and isolate the affected inverters	1- Utilizing numerical smart relays 2- Periodical testing and maintenance procedure
16			Transient local outages	[85]	2 [85]	1 [85]	1	2	L	38			

17			Solar panels accumulate layers of dust or other particles	[85]	1 [85]	2 [85]	2	4	L	32	(2) Power failure and/or outage may cause loss of business and production (3) Increase the demand on coal-fired generators		
18			Junction box fails	[85]	1 [85]	2 [85]	1	2	L	39			
19			PV module fails	[85]	1 [85]	2 [85]	2	4	L	33			
20	Cooling MEG	Cooling Outage	High correlation of cooling demand with electricity demand	[15]* [17]	4	4	4	64	H	1	(1) Demand not served (2) Increase on-peak electricity demand could cause interruption and/or blackout (3) Increase demand on Fossil Fuel generation	Shift on-peak cooling demand to off-peak demand	1- Utilize TES tanks 2- Predictive energy management 3- ranking the Cooling demand as per its prioritization level
21			MEG cooling contingency load with lack of Chiller units	[17] [15]*	1 [147]	4	4	16	L	14	(1) Uncomfortable condition for human (2) Can't meet the on-peak cooling demand (3) Reduces the cooling efficiency. Also, using individual A/C units lead to increase Global Worming	1- isolate the affected chiller unit from both electrical and cooling network 2- stand by all absorption chiller units for compensation purpose 3- update the management control to reschedule storage strategies by Store off-peak cooling production for using at on-peak demand	1- Utilize TES tanks 2- Intelligent contingency energy management (for emergency procedure) 3- Utilizing numerical smart valves
22			Faults in the Cooling system (Chiller, TES, Pumps or Pipes and valves) systems	[25]*	1 [148]	4	5	20	L	9	(1) Unsatisfied condition for customers (2) Cooling energy failure may cause loss of business and production (3) May cause pollution by liquid and gases spreads or by direct fire	1- Isolate the minimal affected branch 2- switch off and isolate the Cooling DERs allocated in the affected zone	1- Utilizing numerical smart meters 2- Emergency Shutdown system ESD 3- Periodical testing and maintenance procedure
23			Leak in the cooling pipe branch	[70]*	1	3	4	12	L	18			
24			Cooling Overload	[70] [204]*	2	3	4	24	L	7	(1) Uncomfortable condition for human (2) Can't meet the on-peak cooling demand (3) Reduces the cooling efficiency. Also, using	1- reduce the load as per priority index to match the production capacity 2- peak shave management for dispatchable loads to balance between power production and demand	1- Utilizing numerical smart meters 2- Emergency Shutdown system ESD 3- Utilize absorption chillers

											individual A/C units lead to increase Global Worming	3- Convert heating to cooling energy	
25	Heating MEG	Heating Outage	Irregular hot-water demand	[127][131]*	2 [127]	3	3	18	L	12	(1) Uncomfortable condition for human (2) Failure to meet the Hot water on-peak demand (3) Alternative heat sources like furnace produce emission	1- Store off-peak Hot water production for using at on-peak demand	1- Utilize TES tanks 2- Predictive energy management
26			Thermal overload	[127] [131] [205]*	1 [205]	3	2	6	L	26	(1) Uncomfortable condition for human (2) Failure to meet the Hot water on-peak demand (3) Alternative heat sources like furnace produce more emission	1- reduce the load as per priority index to match the production capacity 2- peak shave management for dispatchable loads to balance between power production and demand 3- discharge the thermal storage energy 4- switch off the absorption chillers	1- Utilizing numerical smart meters 2- Emergency Shutdown system ESD 3- Safety management controller dealing with hazards scenarios
27			Faults in the Heating system (Cogen, Boiler, TES, Pumps or Pipes and valves) systems	[68]*	1	4	5	20	L	10	(1) Unsatisfied condition for customers (2) Heating energy failure may cause loss of business and production (3) Fire cause CO2 Emission	1- isolate the minimal affected branch 2- switch off and isolate the thermal DERs allocated in the affected zone	1-Wide area Monitoring and Alarm systems 2- Emergency Shutdown system ESD 3- Periodical testing and maintenance procedure
28			Loss of electrical boiler	[206]	1 [206]	3 [206]	2	6	L	27	(1) Unsatisfied condition for customers (2) Heating energy failure may cause loss of business and production (3) Alternative heat sources like furnace produce emission	1- Isolate the Electrical boiler from power and thermal networks 2- Standby Co-gen and gas boiler to cover the thermal deficiency 3- Update the management control to reschedule storage strategies	1-Wide area Monitoring and Alarm systems 2- Emergency Shutdown system ESD 3- Periodical testing and maintenance procedure
29			Loss of gas boiler	[67][206]	1*	3	2	6	L	28	(1) Unsatisfied condition for customers (2) Heating energy failure may cause loss of business and production	1- Isolate the Electrical boiler from power and thermal networks 2- Standby Co-gen and electrical boiler to cover	1-Wide area Monitoring and Alarm systems 2- Emergency Shutdown system ESD

											(3) Alternative heat sources like furnace produce more emission	the thermal deficiency 3- Notify the control room to reschedule storage strategies	3- Periodical testing and maintenance procedure
30	Natural Gas	Natural Gas Outage	Gas Leak in Co-gen's feeder pipe	[205]	2*	3	3	18	L	13	(1) Loss of Life's , Injury and suffocation (2) Damage in assets and loss of business (3) toxic gases and CO2 Emission	1- Close the affected branch 2- switch off and isolate the Co-gen from electrical and heating networks 3- switch to grid connected mode to cover the lackage in power production 4- standby boiler furnace to serve the thermal demand	1-Wide area Monitoring and Alarm systems 2- Emergency Shutdown system ESD
31			Gas Leak in boiler's feeder pipe	[206]	1 [206]	3 [206]	3	9	L	22		1- Close the affected branch 2- switch off and isolate the gas boiler from gas and heating networks 3- standby electrical boiler to serve the thermal demand 4- switch to grid connected mode to cover the lackage in power production	
32			Gas Leak in the Main Pipes	[207]	1 [207]	4	4	16	L	15		1- Isolate the affected pipes 2- switch off all systems which feeded by the affected pipes	
33			Lack of fuel	[85]	1 [85]	2 [85]	2	4	L	34	(1) Unsatisfied condition for customers (2) Heating energy failure may cause loss of business and production (3) Alternative heat sources like furnace produce more emission	1- Isolate the Electrical boiler from power and thermal networks 2- Standby Co-gen and utility to cover the deficiency in energy 3- Notify the control room to reschedule storage strategies	1- Emergency Shutdown system ESD 2- Periodical testing and maintenance procedure
34	Transportation	Transportation Breakdown		[200] [208] [209] *	2 [200]	4	5	40	M	5	(1) Loss of Life's , Injury and delay	1- Achieve energy management balance	1- Energy Storage System (super capacitor, Fly

			Transportation energy demand contingency								(2) failure in energy threaten the safety for Properties and the public (3) Back-up Engines works using Fossil Fuel which increase Emission	between transportation units and MEG for more reliability and security enhancement, reduced emissions and improved energy quality.	Wheel, TES and pumped hydro, or hydrogen storage. 2- Following Generator (fuel cells, micro-gas turbines, and hybrid fuel cell gas turbine systems) 3- Intelligent management Controller
35	May affect all energy types	Natural Phenomenon	Violent storms / Tree failing	[85] [198] [199] [200] [202] [210]	3 [210]	3 [210]	1	9	L	23	(1) Loss of Life's , Injury and delay	Isolate the affected area from the service	1- Intelligent Management Controller 2- Smart Relays and metering
36			Earth Quake	[40] [210]	1 [210]	5 [210]	2	10	L	20	(2) failure in energy threaten the safety for properties and the public (3) Spreading the damages and may initiate new hazards		
37			Water Flood	[210]	1 [199]	5	2	10	L	21	(1) Loss of Life's , Injury and delay (2) failure in energy threaten the safety for properties and the public (3) Spreading the damages and may initiate new hazards	Isolate the affected area from the service	1- Intelligent Management Controller 2- Smart Relays and metering
38			Thunder Storm and lightning	[40] [85] [198] [200] [202]	4 [200]	2 [200]	2	16	L	16	(1) Loss of Life's , Injury and delay (2) Electrical devices might get damaged (3) Spreading the damages and may initiate new hazards	Isolate the affected area from the service	1- Intelligent Management Controller 2- Smart Relays and metering
39			Wild Fire	[210]	2 [210]	3 [210]	2	12	L	19	(1) Loss of Life's , Injury and delay (2) Electrical devices might get damaged (3) Spreading the damages and may initiate new hazards	Isolate the affected area from the service	1- Intelligent Management Controller 2- Smart Relays and metering

* The severity and likelihood values are estimated based on experts' knowledge and engineers

** Faulty Equipment / Human errors

8.5 Severity Value Computation Procedure

The calculation of severity risk values of a certain hazard event can be done by different techniques that are varies on the results but they are all common on the base as they are subject to previous project experience and experts' knowledge and judgement [45] [87] [110] [207] [211]. The following procedure is well known in the industry [212]:

1- The occurrence frequency is defined from maintenance historical data of similar projects.
2- Allocate the worst value S_{worst} to the most severe hazard event. This is the reference value to the other hazard events
3- Compare each hazard event to the most severe hazard event by assess how many of this hazard event (N_i) would be equal the impact of the worst event.
4- Calculate the severity of each hazard event by using the following equation: $S_i = {S_{worst}}/{N_i}$
5- Normalize the severity values to have similar range to the occurrence values

8.6 Electrical-MEG Hazards

The following points can summarize the main hazard events in electrical-MEG

1- *Overload (above the grid Capability):* the electrical demand could be increased suddenly for a short period due to different reasons such as extremely hot and cold weather that may lead to several negative impacts as follows:

I. Impacts on human: demand not served (DNS)

II. Impact on the facility: overheated transmission and distribution cables, Asset Damages, fire and power blackout.

III. Impacts on environment: fire causes CO_2 emission

This can be prevented by several remedial actions or IRLs such as:

	Remedial actions or IRLs	Requirements
1	Upgrade grid capacity	Consume time and cost much money
2	Shift on-peak power demand	By using Intelligent Energy Storage System such as super capacitor, Fly Wheel, TES and pumped hydro, or hydrogen storage.
3	Dynamic grid mapping based on load demands and priorities	Intelligent energy management

2- *Lack of DER:* DERs could be out of service due to scheduled routine maintenance or due to breakdown and failure. However, many negative consequences may occur due to this even as follows:

i. *On human:* interruption of service
ii. *On the facility:* could lead to risks of losing the electricity power of a wide region or general blackout.
iii. *On the environment:* lack of DER means increasing the demand on fossil fuel generators, which cause a dramatic increase in greenhouse gases emissions.

Preventing IRL action can be through high dynamic performance from the distributed power and energy system by:

Remedial actions or IRLs	Requirements
• Store off-peak power production for using at emergency or at on-peak demand,	TES, Super capacitor, hydro tanks

• Utilize backup Co-generator units,	Gas generators, fuel cell, gas-oil generators
• Connect to the Capital Grid (utility).	High dynamic controller

3- *Utilize of on-site renewable sources:* despite renewable resources are known as eco-friendly power sources, they have the accompanying hazard of intermittency and non-coincidence in electricity production, which may cause lack of power sufficiency. This can be prevented by utilizing the IRLs mentioned in point 2.

4- *Integration of multi-DERs:* has Negative impacts on the grid's vital parameters, such as active power (P), reactive power (Q), voltage (V), phase shift (α) and frequency (f). The following remedial actions and IRLs can be utilized:

Remedial actions or IRLs	Requirements
• Full utilization of DERs to increase energy efficiency,	Intelligent energy management and optimization
• Improve power quality,	Adding D-FACTS
• Enhance system stability.	Power factor correction system

8.7 Cooling-MEG Hazards

Cooling-MEG resilience could be affected by following hazards:

1- *High correlation between cooling demand and electricity demand:* this relation has negative effects on the MEG resilience as illustrated in the following points:

i. Impacts on humans: uncomfortable condition (temperature and humidity beyond convenient limits).

ii. Impacts on the facility: the on-peak demand for both electricity and cooling grids are accrued at the same time, and this subsequently leads to an increase in the actual electricity of on-peak demand, which might cause interruption and/or blackout for both services.

iii. Impacts on the environment: Increases the demand on Fossil Fuel generation, and its consequences on emissions.

This hazard can be avoided by shifting on-peak cooling demand to off-peak demand by utilizing TES and intelligent management control.

2- *MEG contingency with the lack of Chiller unit:* this may cause a major deficiency in the energy service. Thus, several undesirable influences may occur accordingly:

i. Impacts on humans: uncomfortable condition due to DNS
ii. Impacts on facility: shortage on cooling production leads to lack of service
iii. Impacts on the environment: individual A/C units are one of the solutions to overcome the lack of service. A/C unit usage has an impact on electricity demand and global warming.

This hazard can be evaded by storing off-peak cooling production for use at the on-peak demand by using TES and management control to ensure higher MEG reliability levels.

8.8 Thermal Heating-MEG Hazards

From the historical data on heating demand, it can be clearly defined that there is an irregular heating demand with a low correlation with electrical demand, which may lead to a failure to meet the on-peak heating demand. Consequently, several negative impacts may occur, such as the following:

i. Impacts on humans: uncomfortable condition (temperature and humidity).
ii. Impacts on the facility: failure to meet the heating on-peak demand.
iii. Impacts on the environment: increases the requirement for alternative heat sources such as furnaces, which increase the gases emissions.

To prevent the hazard of heating failure, a strategy to storing off-peak heating production should be utilized.

8.9 Transportation MEG Hazards

Transportation is a vital service for the society and the public; therefore, the energy demand conjugated with it is essential for its resiliency. Any interruption might have harmful impacts as follows:

i. Impacts on humans: loss of life, injury, and delay.
ii. Impact on the facility: failure in energy threaten the safety of properties and the public.
iii. Impacts on the environment: backup Engines work by using fossil fuel, which increases emissions.

Achieving an energy management balance between transportation units and MEG is one of the main solutions for more reliability, security enhancement, emissions reduction and energy quality improvement.

Appendix II Sensitivity analysis for LORA

Excerpts from sensitivity analysis table

	IRLs	Renewable (0.5512)	Co-gen (0.2592)	TES (0.0247)	Management (0.1412)	Alarm (0.1412)	ESD (0.0198)	
1	Contribution %	0%	0%	0%	0%	0%	0%	
	Failure rate (*f/yr.*) Electricity	0.7224	0.7224	0.7224	0.7224	0.7224	0.7224	
	Failure rate (*f/yr.*) Heating	0.7964	0.7964	0.7964	0.7964	0.7964	0.7964	
	Failure rate (*f/yr.*) Cooling	0.7245	0.7245	0.7245	0.7245	0.7245	0.7245	
	Risk level	0.984428916	0.984428916	0.984428916	0.984428916	0.984428916	0.984428916	0.984428916
2	Contribution %	25%	0%	0%	0%	0%	0%	
	Failure rate (*f/yr.*)	0.64134672	0.64134672	0.64134672	0.64134672	0.64134672	0.64134672	
	Failure rate (*f/yr.*) Heating	0.7964	0.7964	0.7964	0.7964	0.7964	0.7964	
	Failure rate (*f/yr.*) Cooling	0.7245	0.7245	0.7245	0.7245	0.7245	0.7245	
	Risk level	0.979882492	0.979882492	0.979882492	0.979882492	0.979882492	0.979882492	0.979882492
3	Contribution %	50%	0%	0%	0%	0%	0%	
	Failure rate (*f/yr.*)	0.56029344	0.56029344	0.56029344	0.56029344	0.56029344	0.56029344	
	Failure rate (*f/yr.*) Heating	0.7964	0.7964	0.7964	0.7964	0.7964	0.7964	
	Failure rate (*f/yr.*) Cooling	0.7245	0.7245	0.7245	0.7245	0.7245	0.7245	
	Risk level	0.975336068	0.975336068	0.975336068	0.975336068	0.975336068	0.975336068	0.975336068
4	Contribution %	75%	0%	0%	0%	0%	0%	
	Failure rate (*f/yr.*)	0.47924016	0.47924016	0.47924016	0.47924016	0.47924016	0.47924016	
	Failure rate (*f/yr.*) Heating	0.7964	0.7964	0.7964	0.7964	0.7964	0.7964	
	Failure rate (*f/yr.*) Cooling	0.7245	0.7245	0.7245	0.7245	0.7245	0.7245	
	Risk level	0.970789643	0.970789643	0.970789643	0.970789643	0.970789643	0.970789643	0.970789643
5	Contribution %	100%	0%	0%	0%	0%	0%	
	Failure rate (*f/yr.*)	0.39818688	0.39818688	0.39818688	0.39818688	0.39818688	0.39818688	

	Failure rate (*f/yr.*) Heating	0.7964	0.7964	0.7964	0.7964	0.7964	0.7964	
	Failure rate (*f/yr.*) Cooling	0.7245	0.7245	0.7245	0.7245	0.7245	0.7245	
	Risk level	0.966243219	0.966243219	0.966243219	0.966243219	0.966243219	0.966243219	0.966243219
6	Contribution %	0%	25%	0%	0%	0%	0%	
	Failure rate (*f/yr.*)	0.7224	0.58861152	0.58861152	0.58861152	0.58861152	0.58861152	
	Failure rate (*f/yr.*) Heating	0.7964	0.64890672	0.64890672	0.64890672	0.64890672	0.64890672	
	Failure rate (*f/yr.*) Cooling	0.7245	0.5903226	0.5903226	0.5903226	0.5903226	0.5903226	
	Risk level	0.984428916	0.940827945	0.940827945	0.940827945	0.940827945	0.940827945	0.940827945
7	Contribution %	25%	25%	0%	0%	0%	0%	
	Failure rate (*f/yr.*)	0.64134672	0.522569307	0.522569307	0.522569307	0.522569307	0.522569307	
	Failure rate (*f/yr.*) Heating	0.7964	0.64890672	0.64890672	0.64890672	0.64890672	0.64890672	
	Failure rate (*f/yr.*) Cooling	0.7245	0.5903226	0.5903226	0.5903226	0.5903226	0.5903226	
	Risk level	0.979882492	0.931328765	0.931328765	0.931328765	0.931328765	0.931328765	0.931328765
8	Contribution %	50%	25%	0%	0%	0%	0%	
	Failure rate (*f/yr.*)	0.56029344	0.456527095	0.456527095	0.456527095	0.456527095	0.456527095	
	Failure rate (*f/yr.*) Heating	0.7964	0.64890672	0.64890672	0.64890672	0.64890672	0.64890672	
	Failure rate (*f/yr.*) Cooling	0.7245	0.5903226	0.5903226	0.5903226	0.5903226	0.5903226	
	Risk level	0.975336068	0.921829584	0.921829584	0.921829584	0.921829584	0.921829584	0.921829584
9	Contribution %	75%	25%	0%	0%	0%	0%	
	Failure rate (*f/yr.*)	0.47924016	0.390484882	0.390484882	0.390484882	0.390484882	0.390484882	
	Failure rate (*f/yr.*) Heating	0.7964	0.64890672	0.64890672	0.64890672	0.64890672	0.64890672	
	Failure rate (*f/yr.*) Cooling	0.7245	0.5903226	0.5903226	0.5903226	0.5903226	0.5903226	
	Risk level	0.970789643	0.912330404	0.912330404	0.912330404	0.912330404	0.912330404	0.912330404
10	Contribution %	100%	25%	0%	0%	0%	0%	
	Failure rate (*f/yr.*)	0.39818688	0.32444267	0.32444267	0.32444267	0.32444267	0.32444267	

	Failure rate (*f/yr.*) Heating	0.7964	0.64890672	0.64890672	0.64890672	0.64890672	0.64890672	
	Failure rate (*f/yr.*) Cooling	0.7245	0.5903226	0.5903226	0.5903226	0.5903226	0.5903226	
	Risk level	0.966243219	0.902831224	0.902831224	0.902831224	0.902831224	0.902831224	0.902831224
11	Contribution %	0%	50%	0%	0%	0%	0%	
	Failure rate (*f/yr.*)	0.7224	0.45482304	0.45482304	0.45482304	0.45482304	0.45482304	
	Failure rate (*f/yr.*) Heating	0.7964	0.50141344	0.50141344	0.50141344	0.50141344	0.50141344	
	Failure rate (*f/yr.*) Cooling	0.7245	0.4561452	0.4561452	0.4561452	0.4561452	0.4561452	
	Risk level	0.984428916	0.852170528	0.852170528	0.852170528	0.852170528	0.852170528	0.852170528
12	Contribution %	25%	50%	0%	0%	0%	0%	
	Failure rate (*f/yr.*)	0.64134672	0.403791895	0.403791895	0.403791895	0.403791895	0.403791895	
	Failure rate (*f/yr.*) Heating	0.7964	0.50141344	0.50141344	0.50141344	0.50141344	0.50141344	
	Failure rate (*f/yr.*) Cooling	0.7245	0.4561452	0.4561452	0.4561452	0.4561452	0.4561452	
	Risk level	0.979882492	0.838332989	0.838332989	0.838332989	0.838332989	0.838332989	0.838332989
13	Contribution %	50%	50%	0%	0%	0%	0%	
	Failure rate (*f/yr.*)	0.56029344	0.35276075	0.35276075	0.35276075	0.35276075	0.35276075	
	Failure rate (*f/yr.*) Heating	0.7964	0.50141344	0.50141344	0.50141344	0.50141344	0.50141344	
	Failure rate (*f/yr.*) Cooling	0.7245	0.4561452	0.4561452	0.4561452	0.4561452	0.4561452	
	Risk level	0.975336068	0.82449545	0.82449545	0.82449545	0.82449545	0.82449545	0.82449545
14	Contribution %	75%	50%	0%	0%	0%	0%	
	Failure rate (*f/yr.*)	0.47924016	0.301729605	0.301729605	0.301729605	0.301729605	0.301729605	
	Failure rate (*f/yr.*) Heating	0.7964	0.50141344	0.50141344	0.50141344	0.50141344	0.50141344	
	Failure rate (*f/yr.*) Cooling	0.7245	0.4561452	0.4561452	0.4561452	0.4561452	0.4561452	
	Risk level	0.970789643	0.810657912	0.810657912	0.810657912	0.810657912	0.810657912	0.810657912
15	Contribution %	100%	50%	0%	0%	0%	0%	
	Failure rate (*f/yr.*)	0.39818688	0.25069846	0.25069846	0.25069846	0.25069846	0.25069846	

	Failure rate (*f/yr.*) Heating	0.7964	0.50141344	0.50141344	0.50141344	0.50141344	0.50141344	
	Failure rate (*f/yr.*) Cooling	0.7245	0.4561452	0.4561452	0.4561452	0.4561452	0.4561452	
	Risk level	0.966243219	0.796820373	0.796820373	0.796820373	0.796820373	0.796820373	0.796820373
16	Contribution %	0%	75%	0%	0%	0%	0%	
	Failure rate (*f/yr.*)	0.7224	0.32103456	0.32103456	0.32103456	0.32103456	0.32103456	
	Failure rate (*f/yr.*) Heating	0.7964	0.35392016	0.35392016	0.35392016	0.35392016	0.35392016	
	Failure rate (*f/yr.*) Cooling	0.7245	0.3219678	0.3219678	0.3219678	0.3219678	0.3219678	
	Risk level	0.984428916	0.702570406	0.702570406	0.702570406	0.702570406	0.702570406	0.702570406
17	Contribution %	25%	75%	0%	0%	0%	0%	
	Failure rate (*f/yr.*)	0.64134672	0.285014482	0.285014482	0.285014482	0.285014482	0.285014482	
	Failure rate (*f/yr.*) Heating	0.7964	0.35392016	0.35392016	0.35392016	0.35392016	0.35392016	
	Failure rate (*f/yr.*) Cooling	0.7245	0.3219678	0.3219678	0.3219678	0.3219678	0.3219678	
	Risk level	0.979882492	0.686791345	0.686791345	0.686791345	0.686791345	0.686791345	0.686791345
18	Contribution %	50%	75%	0%	0%	0%	0%	
	Failure rate (*f/yr.*)	0.56029344	0.248994405	0.248994405	0.248994405	0.248994405	0.248994405	
	Failure rate (*f/yr.*) Heating	0.7964	0.35392016	0.35392016	0.35392016	0.35392016	0.35392016	
	Failure rate (*f/yr.*) Cooling	0.7245	0.3219678	0.3219678	0.3219678	0.3219678	0.3219678	
	Risk level	0.975336068	0.671012285	0.671012285	0.671012285	0.671012285	0.671012285	0.671012285
19	Contribution %	75%	75%	0%	0%	0%	0%	
	Failure rate (*f/yr.*)	0.47924016	0.212974327	0.212974327	0.212974327	0.212974327	0.212974327	
	Failure rate (*f/yr.*) Heating	0.7964	0.35392016	0.35392016	0.35392016	0.35392016	0.35392016	
	Failure rate (*f/yr.*) Cooling	0.7245	0.3219678	0.3219678	0.3219678	0.3219678	0.3219678	
	Risk level	0.970789643	0.655233224	0.655233224	0.655233224	0.655233224	0.655233224	0.655233224
20	Contribution %	100%	75%	0%	0%	0%	0%	
	Failure rate (*f/yr.*)	0.39818688	0.176954249	0.176954249	0.176954249	0.176954249	0.176954249	

	Failure rate (*f/yr.*) Heating	0.7964	0.35392016	0.35392016	0.35392016	0.35392016	0.35392016	
	Failure rate (*f/yr.*) Cooling	0.7245	0.3219678	0.3219678	0.3219678	0.3219678	0.3219678	
	Risk level	0.966243219	0.639454163	0.639454163	0.639454163	0.639454163	0.639454163	0.639454163
21	Contribution %	0%	100%	0%	0%	0%	0%	
	Failure rate (*f/yr.*)	0.7224	0.18724608	0.18724608	0.18724608	0.18724608	0.18724608	
	Failure rate (*f/yr.*) Heating	0.7964	0.20642688	0.20642688	0.20642688	0.20642688	0.20642688	
	Failure rate (*f/yr.*) Cooling	0.7245	0.1877904	0.1877904	0.1877904	0.1877904	0.1877904	
	Risk level	0.984428916	0.476141325	0.476141325	0.476141325	0.476141325	0.476141325	0.476141325
22	Contribution %	25%	100%	0%	0%	0%	0%	
	Failure rate (*f/yr.*)	0.64134672	0.16623707	0.16623707	0.16623707	0.16623707	0.16623707	
	Failure rate (*f/yr.*) Heating	0.7964	0.20642688	0.20642688	0.20642688	0.20642688	0.20642688	
	Failure rate (*f/yr.*) Cooling	0.7245	0.1877904	0.1877904	0.1877904	0.1877904	0.1877904	
	Risk level	0.979882492	0.462600016	0.462600016	0.462600016	0.462600016	0.462600016	0.462600016
23	Contribution %	50%	100%	0%	0%	0%	0%	
	Failure rate (*f/yr.*)	0.56029344	0.14522806	0.14522806	0.14522806	0.14522806	0.14522806	
	Failure rate (*f/yr.*) Heating	0.7964	0.20642688	0.20642688	0.20642688	0.20642688	0.20642688	
	Failure rate (*f/yr.*) Cooling	0.7245	0.1877904	0.1877904	0.1877904	0.1877904	0.1877904	
	Risk level	0.975336068	0.449058706	0.449058706	0.449058706	0.449058706	0.449058706	0.449058706
24	Contribution %	75%	100%	0%	0%	0%	0%	
	Failure rate (*f/yr.*)	0.47924016	0.124219049	0.124219049	0.124219049	0.124219049	0.124219049	
	Failure rate (*f/yr.*) Heating	0.7964	0.20642688	0.20642688	0.20642688	0.20642688	0.20642688	
	Failure rate (*f/yr.*) Cooling	0.7245	0.1877904	0.1877904	0.1877904	0.1877904	0.1877904	
	Risk level	0.970789643	0.435517397	0.435517397	0.435517397	0.435517397	0.435517397	0.435517397
25	Contribution %	100%	100%	0%	0%	0%	0%	
	Failure rate (*f/yr.*)	0.39818688	0.103210039	0.103210039	0.103210039	0.103210039	0.103210039	

	Failure rate (*f/yr.*) Heating	0.7964	0.20642688	0.20642688	0.20642688	0.20642688	0.20642688	
	Failure rate (*f/yr.*) Cooling	0.7245	0.1877904	0.1877904	0.1877904	0.1877904	0.1877904	
	Risk level	0.966243219	0.421976088	0.421976088	0.421976088	0.421976088	0.421976088	0.421976088
26	Contribution %	0%	0%	25%	0%	0%	0%	
	Failure rate (*f/yr.*)	0.7224	0.7224	0.54626082	0.54626082	0.54626082	0.54626082	
	Failure rate (*f/yr.*) Heating	0.7964	0.7964	0.60221777	0.60221777	0.60221777	0.60221777	
	Failure rate (*f/yr.*) Cooling	0.7245	0.7245	0.547848788	0.547848788	0.547848788	0.547848788	
	Risk level	0.984428916	0.984428916	0.918391507	0.918391507	0.918391507	0.918391507	0.918391507
27	Contribution %	25%	0%	25%	0%	0%	0%	
	Failure rate (*f/yr.*)	0.64134672	0.64134672	0.484970356	0.484970356	0.484970356	0.484970356	
	Failure rate (*f/yr.*) Heating	0.7964	0.7964	0.60221777	0.60221777	0.60221777	0.60221777	
	Failure rate (*f/yr.*) Cooling	0.7245	0.7245	0.547848788	0.547848788	0.547848788	0.547848788	
	Risk level	0.979882492	0.979882492	0.907367944	0.907367944	0.907367944	0.907367944	0.907367944
28	Contribution %	50%	0%	25%	0%	0%	0%	
	Failure rate (*f/yr.*)	0.56029344	0.56029344	0.423679892	0.423679892	0.423679892	0.423679892	
	Failure rate (*f/yr.*) Heating	0.7964	0.7964	0.60221777	0.60221777	0.60221777	0.60221777	
	Failure rate (*f/yr.*) Cooling	0.7245	0.7245	0.547848788	0.547848788	0.547848788	0.547848788	
	Risk level	0.975336068	0.975336068	0.896344381	0.896344381	0.896344381	0.896344381	0.896344381
29	Contribution %	75%	0%	25%	0%	0%	0%	
	Failure rate (*f/yr.*)	0.47924016	0.47924016	0.362389428	0.362389428	0.362389428	0.362389428	
	Failure rate (*f/yr.*) Heating	0.7964	0.7964	0.60221777	0.60221777	0.60221777	0.60221777	
	Failure rate (*f/yr.*) Cooling	0.7245	0.7245	0.547848788	0.547848788	0.547848788	0.547848788	
	Risk level	0.970789643	0.970789643	0.885320818	0.885320818	0.885320818	0.885320818	0.885320818
30	Contribution %	100%	0%	25%	0%	0%	0%	
	Failure rate (*f/yr.*)	0.39818688	0.39818688	0.301098964	0.301098964	0.301098964	0.301098964	

	Failure rate (*f/yr.*) Heating	0.7964	0.7964	0.60221777	0.60221777	0.60221777	0.60221777	
	Failure rate (*f/yr.*) Cooling	0.7245	0.7245	0.547848788	0.547848788	0.547848788	0.547848788	
	Risk level	0.966243219	0.966243219	0.874297255	0.874297255	0.874297255	0.874297255	0.874297255
31	Contribution %	0%	25%	25%	0%	0%	0%	
	Failure rate (*f/yr.*)	0.7224	0.58861152	0.445093316	0.445093316	0.445093316	0.445093316	
	Failure rate (*f/yr.*) Heating	0.7964	0.64890672	0.490687039	0.490687039	0.490687039	0.490687039	
	Failure rate (*f/yr.*) Cooling	0.7245	0.5903226	0.446387192	0.446387192	0.446387192	0.446387192	
	Risk level	0.984428916	0.940827945	0.843537303	0.843537303	0.843537303	0.843537303	0.843537303
32	Contribution %	25%	25%	25%	0%	0%	0%	
	Failure rate (*f/yr.*)	0.64134672	0.522569307	0.395153846	0.395153846	0.395153846	0.395153846	
	Failure rate (*f/yr.*) Heating	0.7964	0.64890672	0.490687039	0.490687039	0.490687039	0.490687039	
	Failure rate (*f/yr.*) Cooling	0.7245	0.5903226	0.446387192	0.446387192	0.446387192	0.446387192	
	Risk level	0.979882492	0.931328765	0.829456261	0.829456261	0.829456261	0.829456261	0.829456261
33	Contribution %	50%	25%	25%	0%	0%	0%	
	Failure rate (*f/yr.*)	0.56029344	0.456527095	0.345214376	0.345214376	0.345214376	0.345214376	
	Failure rate (*f/yr.*) Heating	0.7964	0.64890672	0.490687039	0.490687039	0.490687039	0.490687039	
	Failure rate (*f/yr.*) Cooling	0.7245	0.5903226	0.446387192	0.446387192	0.446387192	0.446387192	
	Risk level	0.975336068	0.921829584	0.815375219	0.815375219	0.815375219	0.815375219	0.815375219
34	Contribution %	75%	25%	25%	0%	0%	0%	
	Failure rate (*f/yr.*)	0.47924016	0.390484882	0.295274906	0.295274906	0.295274906	0.295274906	
	Failure rate (*f/yr.*) Heating	0.7964	0.64890672	0.490687039	0.490687039	0.490687039	0.490687039	
	Failure rate (*f/yr.*) Cooling	0.7245	0.5903226	0.446387192	0.446387192	0.446387192	0.446387192	
	Risk level	0.970789643	0.912330404	0.801294177	0.801294177	0.801294177	0.801294177	0.801294177
35	Contribution %	100%	25%	25%	0%	0%	0%	
	Failure rate (*f/yr.*)	0.39818688	0.32444267	0.245335436	0.245335436	0.245335436	0.245335436	

	Failure rate (*f/yr.*) Heating	0.7964	0.64890672	0.490687039	0.490687039	0.490687039	0.490687039	
	Failure rate (*f/yr.*) Cooling	0.7245	0.5903226	0.446387192	0.446387192	0.446387192	0.446387192	
	Risk level	0.966243219	0.902831224	0.787213135	0.787213135	0.787213135	0.787213135	0.787213135
36	Contribution %	0%	50%	25%	0%	0%	0%	
	Failure rate (*f/yr.*)	0.7224	0.45482304	0.343925812	0.343925812	0.343925812	0.343925812	
	Failure rate (*f/yr.*) Heating	0.7964	0.50141344	0.379156308	0.379156308	0.379156308	0.379156308	
	Failure rate (*f/yr.*) Cooling	0.7245	0.4561452	0.344925597	0.344925597	0.344925597	0.344925597	
	Risk level	0.984428916	0.852170528	0.733175408	0.733175408	0.733175408	0.733175408	0.733175408
37	Contribution %	25%	50%	25%	0%	0%	0%	
	Failure rate (*f/yr.*)	0.64134672	0.403791895	0.305337336	0.305337336	0.305337336	0.305337336	
	Failure rate (*f/yr.*) Heating	0.7964	0.50141344	0.379156308	0.379156308	0.379156308	0.379156308	
	Failure rate (*f/yr.*) Cooling	0.7245	0.4561452	0.344925597	0.344925597	0.344925597	0.344925597	
	Risk level	0.979882492	0.838332989	0.71748152	0.71748152	0.71748152	0.71748152	0.71748152
38	Contribution %	50%	50%	25%	0%	0%	0%	
	Failure rate (*f/yr.*)	0.56029344	0.35276075	0.26674886	0.26674886	0.26674886	0.26674886	
	Failure rate (*f/yr.*) Heating	0.7964	0.50141344	0.379156308	0.379156308	0.379156308	0.379156308	
	Failure rate (*f/yr.*) Cooling	0.7245	0.4561452	0.344925597	0.344925597	0.344925597	0.344925597	
	Risk level	0.975336068	0.82449545	0.701787633	0.701787633	0.701787633	0.701787633	0.701787633
39	Contribution %	75%	50%	25%	0%	0%	0%	
	Failure rate (*f/yr.*)	0.47924016	0.301729605	0.228160384	0.228160384	0.228160384	0.228160384	
	Failure rate (*f/yr.*) Heating	0.7964	0.50141344	0.379156308	0.379156308	0.379156308	0.379156308	
	Failure rate (*f/yr.*) Cooling	0.7245	0.4561452	0.344925597	0.344925597	0.344925597	0.344925597	
	Risk level	0.970789643	0.810657912	0.686093746	0.686093746	0.686093746	0.686093746	0.686093746
40	Contribution %	100%	50%	25%	0%	0%	0%	
	Failure rate (*f/yr.*)	0.39818688	0.25069846	0.189571908	0.189571908	0.189571908	0.189571908	

	Failure rate (*f/yr.*) Heating	0.7964	0.50141344	0.379156308	0.379156308	0.379156308	0.379156308	
	Failure rate (*f/yr.*) Cooling	0.7245	0.4561452	0.344925597	0.344925597	0.344925597	0.344925597	
	Risk level	0.966243219	0.796820373	0.670399858	0.670399858	0.670399858	0.670399858	0.670399858
41	Contribution %	0%	75%	25%	0%	0%	0%	
	Failure rate (*f/yr.*)	0.7224	0.32103456	0.242758308	0.242758308	0.242758308	0.242758308	
	Failure rate (*f/yr.*) Heating	0.7964	0.35392016	0.267625577	0.267625577	0.267625577	0.267625577	
	Failure rate (*f/yr.*) Cooling	0.7245	0.3219678	0.243464001	0.243464001	0.243464001	0.243464001	
	Risk level	0.984428916	0.702570406	0.580436901	0.580436901	0.580436901	0.580436901	0.580436901
42	Contribution %	25%	75%	25%	0%	0%	0%	
	Failure rate (*f/yr.*)	0.64134672	0.285014482	0.215520826	0.215520826	0.215520826	0.215520826	
	Failure rate (*f/yr.*) Heating	0.7964	0.35392016	0.267625577	0.267625577	0.267625577	0.267625577	
	Failure rate (*f/yr.*) Cooling	0.7245	0.3219678	0.243464001	0.243464001	0.243464001	0.243464001	
	Risk level	0.979882492	0.686791345	0.565345495	0.565345495	0.565345495	0.565345495	0.565345495
43	Contribution %	50%	75%	25%	0%	0%	0%	
	Failure rate (*f/yr.*)	0.56029344	0.248994405	0.188283344	0.188283344	0.188283344	0.188283344	
	Failure rate (*f/yr.*) Heating	0.7964	0.35392016	0.267625577	0.267625577	0.267625577	0.267625577	
	Failure rate (*f/yr.*) Cooling	0.7245	0.3219678	0.243464001	0.243464001	0.243464001	0.243464001	
	Risk level	0.975336068	0.671012285	0.550254088	0.550254088	0.550254088	0.550254088	0.550254088
44	Contribution %	75%	75%	25%	0%	0%	0%	
	Failure rate (*f/yr.*)	0.47924016	0.212974327	0.161045862	0.161045862	0.161045862	0.161045862	
	Failure rate (*f/yr.*) Heating	0.7964	0.35392016	0.267625577	0.267625577	0.267625577	0.267625577	
	Failure rate (*f/yr.*) Cooling	0.7245	0.3219678	0.243464001	0.243464001	0.243464001	0.243464001	
	Risk level	0.970789643	0.655233224	0.535162681	0.535162681	0.535162681	0.535162681	0.535162681
45	Contribution %	100%	75%	25%	0%	0%	0%	
	Failure rate (*f/yr.*)	0.39818688	0.176954249	0.13380838	0.13380838	0.13380838	0.13380838	

	Failure rate (*f/yr.*) Heating	0.7964	0.35392016	0.267625577	0.267625577	0.267625577	0.267625577	
	Failure rate (*f/yr.*) Cooling	0.7245	0.3219678	0.243464001	0.243464001	0.243464001	0.243464001	
	Risk level	0.966243219	0.639454163	0.520071274	0.520071274	0.520071274	0.520071274	0.520071274
46	Contribution %	0%	100%	25%	0%	0%	0%	
	Failure rate (*f/yr.*)	0.7224	0.18724608	0.141590805	0.141590805	0.141590805	0.141590805	
	Failure rate (*f/yr.*) Heating	0.7964	0.20642688	0.156094846	0.156094846	0.156094846	0.156094846	
	Failure rate (*f/yr.*) Cooling	0.7245	0.1877904	0.142002406	0.142002406	0.142002406	0.142002406	
	Risk level	0.984428916	0.476141325	0.378452863	0.378452863	0.378452863	0.378452863	0.378452863
47	Contribution %	25%	100%	25%	0%	0%	0%	
	Failure rate (*f/yr.*)	0.64134672	0.16623707	0.125704316	0.125704316	0.125704316	0.125704316	
	Failure rate (*f/yr.*) Heating	0.7964	0.20642688	0.156094846	0.156094846	0.156094846	0.156094846	
	Failure rate (*f/yr.*) Cooling	0.7245	0.1877904	0.142002406	0.142002406	0.142002406	0.142002406	
	Risk level	0.979882492	0.462600016	0.366949955	0.366949955	0.366949955	0.366949955	0.366949955
48	Contribution %	50%	100%	25%	0%	0%	0%	
	Failure rate (*f/yr.*)	0.56029344	0.14522806	0.109817828	0.109817828	0.109817828	0.109817828	
	Failure rate (*f/yr.*) Heating	0.7964	0.20642688	0.156094846	0.156094846	0.156094846	0.156094846	
	Failure rate (*f/yr.*) Cooling	0.7245	0.1877904	0.142002406	0.142002406	0.142002406	0.142002406	
	Risk level	0.975336068	0.449058706	0.355447048	0.355447048	0.355447048	0.355447048	0.355447048
49	Contribution %	75%	100%	25%	0%	0%	0%	
	Failure rate (*f/yr.*)	0.47924016	0.124219049	0.09393134	0.09393134	0.09393134	0.09393134	
	Failure rate (*f/yr.*) Heating	0.7964	0.20642688	0.156094846	0.156094846	0.156094846	0.156094846	
	Failure rate (*f/yr.*) Cooling	0.7245	0.1877904	0.142002406	0.142002406	0.142002406	0.142002406	
	Risk level	0.970789643	0.435517397	0.343944141	0.343944141	0.343944141	0.343944141	0.343944141
50	Contribution %	100%	100%	25%	0%	0%	0%	
	Failure rate (*f/yr.*)	0.39818688	0.103210039	0.078044851	0.078044851	0.078044851	0.078044851	

	Failure rate (*f/yr.*) Heating	0.7964	0.20642688	0.156094846	0.156094846	0.156094846	0.156094846	
	Failure rate (*f/yr.*) Cooling	0.7245	0.1877904	0.142002406	0.142002406	0.142002406	0.142002406	
	Risk level	0.966243219	0.421976088	0.332441234	0.332441234	0.332441234	0.332441234	0.332441234
51	Contribution %	0%	0%	50%	0%	0%	0%	
	Failure rate (*f/yr.*)	0.7224	0.7224	0.37012164	0.37012164	0.37012164	0.37012164	
	Failure rate (*f/yr.*) Heating	0.7964	0.7964	0.40803554	0.40803554	0.40803554	0.40803554	
	Failure rate (*f/yr.*) Cooling	0.7245	0.7245	0.371197575	0.371197575	0.371197575	0.371197575	
	Risk level	0.984428916	0.984428916	0.765541204	0.765541204	0.765541204	0.765541204	0.765541204
52	Contribution %	25%	0%	50%	0%	0%	0%	
	Failure rate (*f/yr.*)	0.64134672	0.64134672	0.328593992	0.328593992	0.328593992	0.328593992	
	Failure rate (*f/yr.*) Heating	0.7964	0.7964	0.40803554	0.40803554	0.40803554	0.40803554	
	Failure rate (*f/yr.*) Cooling	0.7245	0.7245	0.371197575	0.371197575	0.371197575	0.371197575	
	Risk level	0.979882492	0.979882492	0.750083423	0.750083423	0.750083423	0.750083423	0.750083423
53	Contribution %	50%	0%	50%	0%	0%	0%	
	Failure rate (*f/yr.*)	0.56029344	0.56029344	0.287066344	0.287066344	0.287066344	0.287066344	
	Failure rate (*f/yr.*) Heating	0.7964	0.7964	0.40803554	0.40803554	0.40803554	0.40803554	
	Failure rate (*f/yr.*) Cooling	0.7245	0.7245	0.371197575	0.371197575	0.371197575	0.371197575	
	Risk level	0.975336068	0.975336068	0.734625641	0.734625641	0.734625641	0.734625641	0.734625641
54	Contribution %	75%	0%	50%	0%	0%	0%	
	Failure rate (*f/yr.*)	0.47924016	0.47924016	0.245538696	0.245538696	0.245538696	0.245538696	
	Failure rate (*f/yr.*) Heating	0.7964	0.7964	0.40803554	0.40803554	0.40803554	0.40803554	
	Failure rate (*f/yr.*) Cooling	0.7245	0.7245	0.371197575	0.371197575	0.371197575	0.371197575	
	Risk level	0.970789643	0.970789643	0.719167859	0.719167859	0.719167859	0.719167859	0.719167859
55	Contribution %	100%	0%	50%	0%	0%	0%	
	Failure rate (*f/yr.*)	0.39818688	0.39818688	0.204011048	0.204011048	0.204011048	0.204011048	

	Failure rate (*f/yr.*) Heating	0.7964	0.7964	0.40803554	0.40803554	0.40803554	0.40803554	
	Failure rate (*f/yr.*) Cooling	0.7245	0.7245	0.371197575	0.371197575	0.371197575	0.371197575	
	Risk level	0.966243219	0.966243219	0.703710077	0.703710077	0.703710077	0.703710077	0.703710077
56	Contribution %	0%	25%	50%	0%	0%	0%	
	Failure rate (*f/yr.*)	0.7224	0.58861152	0.301575112	0.301575112	0.301575112	0.301575112	
	Failure rate (*f/yr.*) Heating	0.7964	0.64890672	0.332467358	0.332467358	0.332467358	0.332467358	
	Failure rate (*f/yr.*) Cooling	0.7245	0.5903226	0.302451784	0.302451784	0.302451784	0.302451784	
	Risk level	0.984428916	0.940827945	0.674788087	0.674788087	0.674788087	0.674788087	0.674788087
57	Contribution %	25%	25%	50%	0%	0%	0%	
	Failure rate (*f/yr.*)	0.64134672	0.522569307	0.267738385	0.267738385	0.267738385	0.267738385	
	Failure rate (*f/yr.*) Heating	0.7964	0.64890672	0.332467358	0.332467358	0.332467358	0.332467358	
	Failure rate (*f/yr.*) Cooling	0.7245	0.5903226	0.302451784	0.302451784	0.302451784	0.302451784	
	Risk level	0.979882492	0.931328765	0.659032481	0.659032481	0.659032481	0.659032481	0.659032481
58	Contribution %	50%	25%	50%	0%	0%	0%	
	Failure rate (*f/yr.*)	0.56029344	0.456527095	0.233901657	0.233901657	0.233901657	0.233901657	
	Failure rate (*f/yr.*) Heating	0.7964	0.64890672	0.332467358	0.332467358	0.332467358	0.332467358	
	Failure rate (*f/yr.*) Cooling	0.7245	0.5903226	0.302451784	0.302451784	0.302451784	0.302451784	
	Risk level	0.975336068	0.921829584	0.643276876	0.643276876	0.643276876	0.643276876	0.643276876
59	Contribution %	75%	25%	50%	0%	0%	0%	
	Failure rate (*f/yr.*)	0.47924016	0.390484882	0.200064929	0.200064929	0.200064929	0.200064929	
	Failure rate (*f/yr.*) Heating	0.7964	0.64890672	0.332467358	0.332467358	0.332467358	0.332467358	
	Failure rate (*f/yr.*) Cooling	0.7245	0.5903226	0.302451784	0.302451784	0.302451784	0.302451784	
	Risk level	0.970789643	0.912330404	0.627521271	0.627521271	0.627521271	0.627521271	0.627521271
60	Contribution %	100%	25%	50%	0%	0%	0%	
	Failure rate (*f/yr.*)	0.39818688	0.32444267	0.166228202	0.166228202	0.166228202	0.166228202	

	Failure rate (*f/yr.*) Heating	0.7964	0.64890672	0.332467358	0.332467358	0.332467358	0.332467358	
	Failure rate (*f/yr.*) Cooling	0.7245	0.5903226	0.302451784	0.302451784	0.302451784	0.302451784	
	Risk level	0.966243219	0.902831224	0.611765665	0.611765665	0.611765665	0.611765665	0.611765665
61	Contribution %	0%	50%	50%	0%	0%	0%	
	Failure rate (*f/yr.*)	0.7224	0.45482304	0.233028585	0.233028585	0.233028585	0.233028585	
	Failure rate (*f/yr.*) Heating	0.7964	0.50141344	0.256899176	0.256899176	0.256899176	0.256899176	
	Failure rate (*f/yr.*) Cooling	0.7245	0.4561452	0.233705993	0.233705993	0.233705993	0.233705993	
	Risk level	0.984428916	0.852170528	0.563260623	0.563260623	0.563260623	0.563260623	0.563260623
62	Contribution %	25%	50%	50%	0%	0%	0%	
	Failure rate (*f/yr.*)	0.64134672	0.403791895	0.206882777	0.206882777	0.206882777	0.206882777	
	Failure rate (*f/yr.*) Heating	0.7964	0.50141344	0.256899176	0.256899176	0.256899176	0.256899176	
	Failure rate (*f/yr.*) Cooling	0.7245	0.4561452	0.233705993	0.233705993	0.233705993	0.233705993	
	Risk level	0.979882492	0.838332989	0.548372319	0.548372319	0.548372319	0.548372319	0.548372319
63	Contribution %	50%	50%	50%	0%	0%	0%	
	Failure rate (*f/yr.*)	0.56029344	0.35276075	0.18073697	0.18073697	0.18073697	0.18073697	
	Failure rate (*f/yr.*) Heating	0.7964	0.50141344	0.256899176	0.256899176	0.256899176	0.256899176	
	Failure rate (*f/yr.*) Cooling	0.7245	0.4561452	0.233705993	0.233705993	0.233705993	0.233705993	
	Risk level	0.975336068	0.82449545	0.533484015	0.533484015	0.533484015	0.533484015	0.533484015
64	Contribution %	75%	50%	50%	0%	0%	0%	
	Failure rate (*f/yr.*)	0.47924016	0.301729605	0.154591163	0.154591163	0.154591163	0.154591163	
	Failure rate (*f/yr.*) Heating	0.7964	0.50141344	0.256899176	0.256899176	0.256899176	0.256899176	
	Failure rate (*f/yr.*) Cooling	0.7245	0.4561452	0.233705993	0.233705993	0.233705993	0.233705993	
	Risk level	0.970789643	0.810657912	0.518595711	0.518595711	0.518595711	0.518595711	0.518595711
65	Contribution %	100%	50%	50%	0%	0%	0%	
	Failure rate (*f/yr.*)	0.39818688	0.25069846	0.128445356	0.128445356	0.128445356	0.128445356	

	Failure rate (*f/yr.*) Heating	0.7964	0.50141344	0.256899176	0.256899176	0.256899176	0.256899176	
	Failure rate (*f/yr.*) Cooling	0.7245	0.4561452	0.233705993	0.233705993	0.233705993	0.233705993	
	Risk level	0.966243219	0.796820373	0.503707407	0.503707407	0.503707407	0.503707407	0.503707407
66	Contribution %	0%	75%	50%	0%	0%	0%	
	Failure rate (*f/yr.*)	0.7224	0.32103456	0.164482057	0.164482057	0.164482057	0.164482057	
	Failure rate (*f/yr.*) Heating	0.7964	0.35392016	0.181330994	0.181330994	0.181330994	0.181330994	
	Failure rate (*f/yr.*) Cooling	0.7245	0.3219678	0.164960202	0.164960202	0.164960202	0.164960202	
	Risk level	0.984428916	0.702570406	0.42882222	0.42882222	0.42882222	0.42882222	0.42882222
67	Contribution %	25%	75%	50%	0%	0%	0%	
	Failure rate (*f/yr.*)	0.64134672	0.285014482	0.14602717	0.14602717	0.14602717	0.14602717	
	Failure rate (*f/yr.*) Heating	0.7964	0.35392016	0.181330994	0.181330994	0.181330994	0.181330994	
	Failure rate (*f/yr.*) Cooling	0.7245	0.3219678	0.164960202	0.164960202	0.164960202	0.164960202	
	Risk level	0.979882492	0.686791345	0.416206068	0.416206068	0.416206068	0.416206068	0.416206068
68	Contribution %	50%	75%	50%	0%	0%	0%	
	Failure rate (*f/yr.*)	0.56029344	0.248994405	0.127572283	0.127572283	0.127572283	0.127572283	
	Failure rate (*f/yr.*) Heating	0.7964	0.35392016	0.181330994	0.181330994	0.181330994	0.181330994	
	Failure rate (*f/yr.*) Cooling	0.7245	0.3219678	0.164960202	0.164960202	0.164960202	0.164960202	
	Risk level	0.975336068	0.671012285	0.403589916	0.403589916	0.403589916	0.403589916	0.403589916
69	Contribution %	75%	75%	50%	0%	0%	0%	
	Failure rate (*f/yr.*)	0.47924016	0.212974327	0.109117396	0.109117396	0.109117396	0.109117396	
	Failure rate (*f/yr.*) Heating	0.7964	0.35392016	0.181330994	0.181330994	0.181330994	0.181330994	
	Failure rate (*f/yr.*) Cooling	0.7245	0.3219678	0.164960202	0.164960202	0.164960202	0.164960202	
	Risk level	0.970789643	0.655233224	0.390973765	0.390973765	0.390973765	0.390973765	0.390973765
70	Contribution %	100%	75%	50%	0%	0%	0%	
	Failure rate (*f/yr.*)	0.39818688	0.176954249	0.09066251	0.09066251	0.09066251	0.09066251	

	Failure rate (*f/yr.*) Heating	0.7964	0.35392016	0.181330994	0.181330994	0.181330994	0.181330994	
	Failure rate (*f/yr.*) Cooling	0.7245	0.3219678	0.164960202	0.164960202	0.164960202	0.164960202	
	Risk level	0.966243219	0.639454163	0.378357613	0.378357613	0.378357613	0.378357613	0.378357613
71	Contribution %	0%	100%	50%	0%	0%	0%	
	Failure rate (*f/yr.*)	0.7224	0.18724608	0.095935529	0.095935529	0.095935529	0.095935529	
	Failure rate (*f/yr.*) Heating	0.7964	0.20642688	0.105762812	0.105762812	0.105762812	0.105762812	
	Failure rate (*f/yr.*) Cooling	0.7245	0.1877904	0.096214411	0.096214411	0.096214411	0.096214411	
	Risk level	0.984428916	0.476141325	0.269336285	0.269336285	0.269336285	0.269336285	0.269336285
72	Contribution %	25%	100%	50%	0%	0%	0%	
	Failure rate (*f/yr.*)	0.64134672	0.16623707	0.085171563	0.085171563	0.085171563	0.085171563	
	Failure rate (*f/yr.*) Heating	0.7964	0.20642688	0.105762812	0.105762812	0.105762812	0.105762812	
	Failure rate (*f/yr.*) Cooling	0.7245	0.1877904	0.096214411	0.096214411	0.096214411	0.096214411	
	Risk level	0.979882492	0.462600016	0.260636862	0.260636862	0.260636862	0.260636862	0.260636862
73	Contribution %	50%	100%	50%	0%	0%	0%	
	Failure rate (*f/yr.*)	0.56029344	0.14522806	0.074407596	0.074407596	0.074407596	0.074407596	
	Failure rate (*f/yr.*) Heating	0.7964	0.20642688	0.105762812	0.105762812	0.105762812	0.105762812	
	Failure rate (*f/yr.*) Cooling	0.7245	0.1877904	0.096214411	0.096214411	0.096214411	0.096214411	
	Risk level	0.975336068	0.449058706	0.251937438	0.251937438	0.251937438	0.251937438	0.251937438
74	Contribution %	75%	100%	50%	0%	0%	0%	
	Failure rate (*f/yr.*)	0.47924016	0.124219049	0.06364363	0.06364363	0.06364363	0.06364363	
	Failure rate (*f/yr.*) Heating	0.7964	0.20642688	0.105762812	0.105762812	0.105762812	0.105762812	
	Failure rate (*f/yr.*) Cooling	0.7245	0.1877904	0.096214411	0.096214411	0.096214411	0.096214411	
	Risk level	0.970789643	0.435517397	0.243238015	0.243238015	0.243238015	0.243238015	0.243238015
75	Contribution %	100%	100%	50%	0%	0%	0%	
	Failure rate (*f/yr.*)	0.39818688	0.103210039	0.052879664	0.052879664	0.052879664	0.052879664	

	Failure rate (*f/yr.*) Heating	0.7964	0.20642688	0.105762812	0.105762812	0.105762812	0.105762812	
	Failure rate (*f/yr.*) Cooling	0.7245	0.1877904	0.096214411	0.096214411	0.096214411	0.096214411	
	Risk level	0.966243219	0.421976088	0.234538591	0.234538591	0.234538591	0.234538591	0.234538591
76	Contribution %	0%	0%	75%	0%	0%	0%	
	Failure rate (*f/yr.*)	0.7224	0.7224	0.19398246	0.19398246	0.19398246	0.19398246	
	Failure rate (*f/yr.*) Heating	0.7964	0.7964	0.21385331	0.21385331	0.21385331	0.21385331	
	Failure rate (*f/yr.*) Cooling	0.7245	0.7245	0.194546363	0.194546363	0.194546363	0.194546363	
	Risk level	0.984428916	0.984428916	0.489625896	0.489625896	0.489625896	0.489625896	0.489625896
77	Contribution %	25%	0%	75%	0%	0%	0%	
	Failure rate (*f/yr.*)	0.64134672	0.64134672	0.172217628	0.172217628	0.172217628	0.172217628	
	Failure rate (*f/yr.*) Heating	0.7964	0.7964	0.21385331	0.21385331	0.21385331	0.21385331	
	Failure rate (*f/yr.*) Cooling	0.7245	0.7245	0.194546363	0.194546363	0.194546363	0.194546363	
	Risk level	0.979882492	0.979882492	0.475844302	0.475844302	0.475844302	0.475844302	0.475844302
78	Contribution %	50%	0%	75%	0%	0%	0%	
	Failure rate (*f/yr.*)	0.56029344	0.56029344	0.150452796	0.150452796	0.150452796	0.150452796	
	Failure rate (*f/yr.*) Heating	0.7964	0.7964	0.21385331	0.21385331	0.21385331	0.21385331	
	Failure rate (*f/yr.*) Cooling	0.7245	0.7245	0.194546363	0.194546363	0.194546363	0.194546363	
	Risk level	0.975336068	0.975336068	0.462062708	0.462062708	0.462062708	0.462062708	0.462062708
79	Contribution %	75%	0%	75%	0%	0%	0%	
	Failure rate (*f/yr.*)	0.47924016	0.47924016	0.128687964	0.128687964	0.128687964	0.128687964	
	Failure rate (*f/yr.*) Heating	0.7964	0.7964	0.21385331	0.21385331	0.21385331	0.21385331	
	Failure rate (*f/yr.*) Cooling	0.7245	0.7245	0.194546363	0.194546363	0.194546363	0.194546363	
	Risk level	0.970789643	0.970789643	0.448281114	0.448281114	0.448281114	0.448281114	0.448281114
80	Contribution %	100%	0%	75%	0%	0%	0%	
	Failure rate (*f/yr.*)	0.39818688	0.39818688	0.106923132	0.106923132	0.106923132	0.106923132	

	Failure rate (*f/yr.*) Heating	0.7964	0.7964	0.21385331	0.21385331	0.21385331	0.21385331	
	Failure rate (*f/yr.*) Cooling	0.7245	0.7245	0.194546363	0.194546363	0.194546363	0.194546363	
	Risk level	0.966243219	0.966243219	0.43449952	0.43449952	0.43449952	0.43449952	0.43449952
81	Contribution %	0%	25%	75%	0%	0%	0%	
	Failure rate (*f/yr.*)	0.7224	0.58861152	0.158056908	0.158056908	0.158056908	0.158056908	
	Failure rate (*f/yr.*) Heating	0.7964	0.64890672	0.174247677	0.174247677	0.174247677	0.174247677	
	Failure rate (*f/yr.*) Cooling	0.7245	0.5903226	0.158516376	0.158516376	0.158516376	0.158516376	
	Risk level	0.984428916	0.940827945	0.414969901	0.414969901	0.414969901	0.414969901	0.414969901
82	Contribution %	25%	25%	75%	0%	0%	0%	
	Failure rate (*f/yr.*)	0.64134672	0.522569307	0.140322923	0.140322923	0.140322923	0.140322923	
	Failure rate (*f/yr.*) Heating	0.7964	0.64890672	0.174247677	0.174247677	0.174247677	0.174247677	
	Failure rate (*f/yr.*) Cooling	0.7245	0.5903226	0.158516376	0.158516376	0.158516376	0.158516376	
	Risk level	0.979882492	0.931328765	0.402647316	0.402647316	0.402647316	0.402647316	0.402647316
83	Contribution %	50%	25%	75%	0%	0%	0%	
	Failure rate (*f/yr.*)	0.56029344	0.456527095	0.122588938	0.122588938	0.122588938	0.122588938	
	Failure rate (*f/yr.*) Heating	0.7964	0.64890672	0.174247677	0.174247677	0.174247677	0.174247677	
	Failure rate (*f/yr.*) Cooling	0.7245	0.5903226	0.158516376	0.158516376	0.158516376	0.158516376	
	Risk level	0.975336068	0.921829584	0.390324732	0.390324732	0.390324732	0.390324732	0.390324732
84	Contribution %	75%	25%	75%	0%	0%	0%	
	Failure rate (*f/yr.*)	0.47924016	0.390484882	0.104854953	0.104854953	0.104854953	0.104854953	
	Failure rate (*f/yr.*) Heating	0.7964	0.64890672	0.174247677	0.174247677	0.174247677	0.174247677	
	Failure rate (*f/yr.*) Cooling	0.7245	0.5903226	0.158516376	0.158516376	0.158516376	0.158516376	
	Risk level	0.970789643	0.912330404	0.378002147	0.378002147	0.378002147	0.378002147	0.378002147
85	Contribution %	100%	25%	75%	0%	0%	0%	
	Failure rate (*f/yr.*)	0.39818688	0.32444267	0.087120968	0.087120968	0.087120968	0.087120968	

	Failure rate (*f/yr.*) Heating	0.7964	0.64890672	0.174247677	0.174247677	0.174247677	0.174247677	
	Failure rate (*f/yr.*) Cooling	0.7245	0.5903226	0.158516376	0.158516376	0.158516376	0.158516376	
	Risk level	0.966243219	0.902831224	0.365679562	0.365679562	0.365679562	0.365679562	0.365679562
86	Contribution %	0%	50%	75%	0%	0%	0%	
	Failure rate (*f/yr.*)	0.7224	0.45482304	0.122131357	0.122131357	0.122131357	0.122131357	
	Failure rate (*f/yr.*) Heating	0.7964	0.50141344	0.134642044	0.134642044	0.134642044	0.134642044	
	Failure rate (*f/yr.*) Cooling	0.7245	0.4561452	0.12248639	0.12248639	0.12248639	0.12248639	
	Risk level	0.984428916	0.852170528	0.333378696	0.333378696	0.333378696	0.333378696	0.333378696
87	Contribution %	25%	50%	75%	0%	0%	0%	
	Failure rate (*f/yr.*)	0.64134672	0.403791895	0.108428219	0.108428219	0.108428219	0.108428219	
	Failure rate (*f/yr.*) Heating	0.7964	0.50141344	0.134642044	0.134642044	0.134642044	0.134642044	
	Failure rate (*f/yr.*) Cooling	0.7245	0.4561452	0.12248639	0.12248639	0.12248639	0.12248639	
	Risk level	0.979882492	0.838332989	0.322973035	0.322973035	0.322973035	0.322973035	0.322973035
88	Contribution %	50%	50%	75%	0%	0%	0%	
	Failure rate (*f/yr.*)	0.56029344	0.35276075	0.09472508	0.09472508	0.09472508	0.09472508	
	Failure rate (*f/yr.*) Heating	0.7964	0.50141344	0.134642044	0.134642044	0.134642044	0.134642044	
	Failure rate (*f/yr.*) Cooling	0.7245	0.4561452	0.12248639	0.12248639	0.12248639	0.12248639	
	Risk level	0.975336068	0.82449545	0.312567373	0.312567373	0.312567373	0.312567373	0.312567373
89	Contribution %	75%	50%	75%	0%	0%	0%	
	Failure rate (*f/yr.*)	0.47924016	0.301729605	0.081021942	0.081021942	0.081021942	0.081021942	
	Failure rate (*f/yr.*) Heating	0.7964	0.50141344	0.134642044	0.134642044	0.134642044	0.134642044	
	Failure rate (*f/yr.*) Cooling	0.7245	0.4561452	0.12248639	0.12248639	0.12248639	0.12248639	
	Risk level	0.970789643	0.810657912	0.302161712	0.302161712	0.302161712	0.302161712	0.302161712
90	Contribution %	100%	50%	75%	0%	0%	0%	
	Failure rate (*f/yr.*)	0.39818688	0.25069846	0.067318804	0.067318804	0.067318804	0.067318804	

	Failure rate (*f/yr.*) Heating	0.7964	0.50141344	0.134642044	0.134642044	0.134642044	0.134642044	
	Failure rate (*f/yr.*) Cooling	0.7245	0.4561452	0.12248639	0.12248639	0.12248639	0.12248639	
	Risk level	0.966243219	0.796820373	0.291756051	0.291756051	0.291756051	0.291756051	0.291756051
91	Contribution %	0%	75%	75%	0%	0%	0%	
	Failure rate (*f/yr.*)	0.7224	0.32103456	0.086205805	0.086205805	0.086205805	0.086205805	
	Failure rate (*f/yr.*) Heating	0.7964	0.35392016	0.095036411	0.095036411	0.095036411	0.095036411	
	Failure rate (*f/yr.*) Cooling	0.7245	0.3219678	0.086456403	0.086456403	0.086456403	0.086456403	
	Risk level	0.984428916	0.702570406	0.24454469	0.24454469	0.24454469	0.24454469	0.24454469
92	Contribution %	25%	75%	75%	0%	0%	0%	
	Failure rate (*f/yr.*)	0.64134672	0.285014482	0.076533514	0.076533514	0.076533514	0.076533514	
	Failure rate (*f/yr.*) Heating	0.7964	0.35392016	0.095036411	0.095036411	0.095036411	0.095036411	
	Failure rate (*f/yr.*) Cooling	0.7245	0.3219678	0.086456403	0.086456403	0.086456403	0.086456403	
	Risk level	0.979882492	0.686791345	0.236548377	0.236548377	0.236548377	0.236548377	0.236548377
93	Contribution %	50%	75%	75%	0%	0%	0%	
	Failure rate (*f/yr.*)	0.56029344	0.248994405	0.066861223	0.066861223	0.066861223	0.066861223	
	Failure rate (*f/yr.*) Heating	0.7964	0.35392016	0.095036411	0.095036411	0.095036411	0.095036411	
	Failure rate (*f/yr.*) Cooling	0.7245	0.3219678	0.086456403	0.086456403	0.086456403	0.086456403	
	Risk level	0.975336068	0.671012285	0.228552065	0.228552065	0.228552065	0.228552065	0.228552065
94	Contribution %	75%	75%	75%	0%	0%	0%	
	Failure rate (*f/yr.*)	0.47924016	0.212974327	0.057188931	0.057188931	0.057188931	0.057188931	
	Failure rate (*f/yr.*) Heating	0.7964	0.35392016	0.095036411	0.095036411	0.095036411	0.095036411	
	Failure rate (*f/yr.*) Cooling	0.7245	0.3219678	0.086456403	0.086456403	0.086456403	0.086456403	
	Risk level	0.970789643	0.655233224	0.220555752	0.220555752	0.220555752	0.220555752	0.220555752
95	Contribution %	100%	75%	75%	0%	0%	0%	
	Failure rate (*f/yr.*)	0.39818688	0.176954249	0.04751664	0.04751664	0.04751664	0.04751664	

	Failure rate (*f/yr.*) Heating	0.7964	0.35392016	0.095036411	0.095036411	0.095036411	0.095036411	
	Failure rate (*f/yr.*) Cooling	0.7245	0.3219678	0.086456403	0.086456403	0.086456403	0.086456403	
	Risk level	0.966243219	0.639454163	0.21255944	0.21255944	0.21255944	0.21255944	0.21255944
96	Contribution %	0%	100%	75%	0%	0%	0%	
	Failure rate (*f/yr.*)	0.7224	0.18724608	0.050280254	0.050280254	0.050280254	0.050280254	
	Failure rate (*f/yr.*) Heating	0.7964	0.20642688	0.055430778	0.055430778	0.055430778	0.055430778	
	Failure rate (*f/yr.*) Cooling	0.7245	0.1877904	0.050426417	0.050426417	0.050426417	0.050426417	
	Risk level	0.984428916	0.476141325	0.148160289	0.148160289	0.148160289	0.148160289	0.148160289
97	Contribution %	25%	100%	75%	0%	0%	0%	
	Failure rate (*f/yr.*)	0.64134672	0.16623707	0.044638809	0.044638809	0.044638809	0.044638809	
	Failure rate (*f/yr.*) Heating	0.7964	0.20642688	0.055430778	0.055430778	0.055430778	0.055430778	
	Failure rate (*f/yr.*) Cooling	0.7245	0.1877904	0.050426417	0.050426417	0.050426417	0.050426417	
	Risk level	0.979882492	0.462600016	0.143100263	0.143100263	0.143100263	0.143100263	0.143100263
98	Contribution %	50%	100%	75%	0%	0%	0%	
	Failure rate (*f/yr.*)	0.56029344	0.14522806	0.038997365	0.038997365	0.038997365	0.038997365	
	Failure rate (*f/yr.*) Heating	0.7964	0.20642688	0.055430778	0.055430778	0.055430778	0.055430778	
	Failure rate (*f/yr.*) Cooling	0.7245	0.1877904	0.050426417	0.050426417	0.050426417	0.050426417	
	Risk level	0.975336068	0.449058706	0.138040237	0.138040237	0.138040237	0.138040237	0.138040237
99	Contribution %	75%	100%	75%	0%	0%	0%	
	Failure rate (*f/yr.*)	0.47924016	0.124219049	0.03335592	0.03335592	0.03335592	0.03335592	
	Failure rate (*f/yr.*) Heating	0.7964	0.20642688	0.055430778	0.055430778	0.055430778	0.055430778	
	Failure rate (*f/yr.*) Cooling	0.7245	0.1877904	0.050426417	0.050426417	0.050426417	0.050426417	
	Risk level	0.970789643	0.435517397	0.132980211	0.132980211	0.132980211	0.132980211	0.132980211
100	Contribution %	100%	100%	75%	0%	0%	0%	
	Failure rate (*f/yr.*)	0.39818688	0.103210039	0.027714476	0.027714476	0.027714476	0.027714476	

	Failure rate (*f/yr.*) Heating	0.7964	0.20642688	0.055430778	0.055430778	0.055430778	0.055430778	
	Failure rate (*f/yr.*) Cooling	0.7245	0.1877904	0.050426417	0.050426417	0.050426417	0.050426417	
	Risk level	0.966243219	0.421976088	0.127920186	0.127920186	0.127920186	0.127920186	0.127920186
101	Contribution %	0%	0%	100%	0%	0%	0%	
	Failure rate (*f/yr.*)	0.7224	0.7224	0.01784328	0.01784328	0.01784328	0.01784328	
	Failure rate (*f/yr.*) Heating	0.7964	0.7964	0.01967108	0.01967108	0.01967108	0.01967108	
	Failure rate (*f/yr.*) Cooling	0.7245	0.7245	0.01789515	0.01789515	0.01789515	0.01789515	
	Risk level	0.984428916	0.984428916	0.054393469	0.054393469	0.054393469	0.054393469	0.054393469
102	Contribution %	25%	0%	100%	0%	0%	0%	
	Failure rate (*f/yr.*)	0.64134672	0.64134672	0.015841264	0.015841264	0.015841264	0.015841264	
	Failure rate (*f/yr.*) Heating	0.7964	0.7964	0.01967108	0.01967108	0.01967108	0.01967108	
	Failure rate (*f/yr.*) Cooling	0.7245	0.7245	0.01789515	0.01789515	0.01789515	0.01789515	
	Risk level	0.979882492	0.979882492	0.052465957	0.052465957	0.052465957	0.052465957	0.052465957
103	Contribution %	50%	0%	100%	0%	0%	0%	
	Failure rate (*f/yr.*)	0.56029344	0.56029344	0.013839248	0.013839248	0.013839248	0.013839248	
	Failure rate (*f/yr.*) Heating	0.7964	0.7964	0.01967108	0.01967108	0.01967108	0.01967108	
	Failure rate (*f/yr.*) Cooling	0.7245	0.7245	0.01789515	0.01789515	0.01789515	0.01789515	
	Risk level	0.975336068	0.975336068	0.050538444	0.050538444	0.050538444	0.050538444	0.050538444
104	Contribution %	75%	0%	100%	0%	0%	0%	
	Failure rate (*f/yr.*)	0.47924016	0.47924016	0.011837232	0.011837232	0.011837232	0.011837232	
	Failure rate (*f/yr.*) Heating	0.7964	0.7964	0.01967108	0.01967108	0.01967108	0.01967108	
	Failure rate (*f/yr.*) Cooling	0.7245	0.7245	0.01789515	0.01789515	0.01789515	0.01789515	
	Risk level	0.970789643	0.970789643	0.048610932	0.048610932	0.048610932	0.048610932	0.048610932
105	Contribution %	100%	0%	100%	0%	0%	0%	
	Failure rate (*f/yr.*)	0.39818688	0.39818688	0.009835216	0.009835216	0.009835216	0.009835216	

	Failure rate (*f/yr.*) Heating	0.7964	0.7964	0.01967108	0.01967108	0.01967108	0.01967108	
	Failure rate (*f/yr.*) Cooling	0.7245	0.7245	0.01789515	0.01789515	0.01789515	0.01789515	
	Risk level	0.966243219	0.966243219	0.046683419	0.046683419	0.046683419	0.046683419	0.046683419
106	Contribution %	0%	25%	100%	0%	0%	0%	
	Failure rate (*f/yr.*)	0.7224	0.58861152	0.014538705	0.014538705	0.014538705	0.014538705	
	Failure rate (*f/yr.*) Heating	0.7964	0.64890672	0.016027996	0.016027996	0.016027996	0.016027996	
	Failure rate (*f/yr.*) Cooling	0.7245	0.5903226	0.014580968	0.014580968	0.014580968	0.014580968	
	Risk level	0.984428916	0.940827945	0.044472348	0.044472348	0.044472348	0.044472348	0.044472348
107	Contribution %	25%	25%	100%	0%	0%	0%	
	Failure rate (*f/yr.*)	0.64134672	0.522569307	0.012907462	0.012907462	0.012907462	0.012907462	
	Failure rate (*f/yr.*) Heating	0.7964	0.64890672	0.016027996	0.016027996	0.016027996	0.016027996	
	Failure rate (*f/yr.*) Cooling	0.7245	0.5903226	0.014580968	0.014580968	0.014580968	0.014580968	
	Risk level	0.979882492	0.931328765	0.042890655	0.042890655	0.042890655	0.042890655	0.042890655
108	Contribution %	50%	25%	100%	0%	0%	0%	
	Failure rate (*f/yr.*)	0.56029344	0.456527095	0.011276219	0.011276219	0.011276219	0.011276219	
	Failure rate (*f/yr.*) Heating	0.7964	0.64890672	0.016027996	0.016027996	0.016027996	0.016027996	
	Failure rate (*f/yr.*) Cooling	0.7245	0.5903226	0.014580968	0.014580968	0.014580968	0.014580968	
	Risk level	0.975336068	0.921829584	0.041308962	0.041308962	0.041308962	0.041308962	0.041308962
109	Contribution %	75%	25%	100%	0%	0%	0%	
	Failure rate (*f/yr.*)	0.47924016	0.390484882	0.009644977	0.009644977	0.009644977	0.009644977	
	Failure rate (*f/yr.*) Heating	0.7964	0.64890672	0.016027996	0.016027996	0.016027996	0.016027996	
	Failure rate (*f/yr.*) Cooling	0.7245	0.5903226	0.014580968	0.014580968	0.014580968	0.014580968	
	Risk level	0.970789643	0.912330404	0.039727268	0.039727268	0.039727268	0.039727268	0.039727268
110	Contribution %	100%	25%	100%	0%	0%	0%	
	Failure rate (*f/yr.*)	0.39818688	0.32444267	0.008013734	0.008013734	0.008013734	0.008013734	

	Failure rate (*f/yr.*) Heating	0.7964	0.64890672	0.016027996	0.016027996	0.016027996	0.016027996	
	Failure rate (*f/yr.*) Cooling	0.7245	0.5903226	0.014580968	0.014580968	0.014580968	0.014580968	
	Risk level	0.966243219	0.902831224	0.038145575	0.038145575	0.038145575	0.038145575	0.038145575
111	Contribution %	0%	50%	100%	0%	0%	0%	
	Failure rate (*f/yr.*)	0.7224	0.45482304	0.011234129	0.011234129	0.011234129	0.011234129	
	Failure rate (*f/yr.*) Heating	0.7964	0.50141344	0.012384912	0.012384912	0.012384912	0.012384912	
	Failure rate (*f/yr.*) Cooling	0.7245	0.4561452	0.011266786	0.011266786	0.011266786	0.011266786	
	Risk level	0.984428916	0.852170528	0.034482151	0.034482151	0.034482151	0.034482151	0.034482151
112	Contribution %	25%	50%	100%	0%	0%	0%	
	Failure rate (*f/yr.*)	0.64134672	0.403791895	0.00997366	0.00997366	0.00997366	0.00997366	
	Failure rate (*f/yr.*) Heating	0.7964	0.50141344	0.012384912	0.012384912	0.012384912	0.012384912	
	Failure rate (*f/yr.*) Cooling	0.7245	0.4561452	0.011266786	0.011266786	0.011266786	0.011266786	
	Risk level	0.979882492	0.838332989	0.033251318	0.033251318	0.033251318	0.033251318	0.033251318
113	Contribution %	50%	50%	100%	0%	0%	0%	
	Failure rate (*f/yr.*)	0.56029344	0.35276075	0.008713191	0.008713191	0.008713191	0.008713191	
	Failure rate (*f/yr.*) Heating	0.7964	0.50141344	0.012384912	0.012384912	0.012384912	0.012384912	
	Failure rate (*f/yr.*) Cooling	0.7245	0.4561452	0.011266786	0.011266786	0.011266786	0.011266786	
	Risk level	0.975336068	0.82449545	0.032020485	0.032020485	0.032020485	0.032020485	0.032020485
114	Contribution %	75%	50%	100%	0%	0%	0%	
	Failure rate (*f/yr.*)	0.47924016	0.301729605	0.007452721	0.007452721	0.007452721	0.007452721	
	Failure rate (*f/yr.*) Heating	0.7964	0.50141344	0.012384912	0.012384912	0.012384912	0.012384912	
	Failure rate (*f/yr.*) Cooling	0.7245	0.4561452	0.011266786	0.011266786	0.011266786	0.011266786	
	Risk level	0.970789643	0.810657912	0.030789652	0.030789652	0.030789652	0.030789652	0.030789652
115	Contribution %	100%	50%	100%	0%	0%	0%	
	Failure rate (*f/yr.*)	0.39818688	0.25069846	0.006192252	0.006192252	0.006192252	0.006192252	

	Failure rate (*f/yr.*) Heating	0.7964	0.50141344	0.012384912	0.012384912	0.012384912	0.012384912	
	Failure rate (*f/yr.*) Cooling	0.7245	0.4561452	0.011266786	0.011266786	0.011266786	0.011266786	
	Risk level	0.966243219	0.796820373	0.029558819	0.029558819	0.029558819	0.029558819	0.029558819
116	Contribution %	0%	75%	100%	0%	0%	0%	
	Failure rate (*f/yr.*)	0.7224	0.32103456	0.007929554	0.007929554	0.007929554	0.007929554	
	Failure rate (*f/yr.*) Heating	0.7964	0.35392016	0.008741828	0.008741828	0.008741828	0.008741828	
	Failure rate (*f/yr.*) Cooling	0.7245	0.3219678	0.007952605	0.007952605	0.007952605	0.007952605	
	Risk level	0.984428916	0.702570406	0.024422638	0.024422638	0.024422638	0.024422638	0.024422638
117	Contribution %	25%	75%	100%	0%	0%	0%	
	Failure rate (*f/yr.*)	0.64134672	0.285014482	0.007039858	0.007039858	0.007039858	0.007039858	
	Failure rate (*f/yr.*) Heating	0.7964	0.35392016	0.008741828	0.008741828	0.008741828	0.008741828	
	Failure rate (*f/yr.*) Cooling	0.7245	0.3219678	0.007952605	0.007952605	0.007952605	0.007952605	
	Risk level	0.979882492	0.686791345	0.023547733	0.023547733	0.023547733	0.023547733	0.023547733
118	Contribution %	50%	75%	100%	0%	0%	0%	
	Failure rate (*f/yr.*)	0.56029344	0.248994405	0.006150162	0.006150162	0.006150162	0.006150162	
	Failure rate (*f/yr.*) Heating	0.7964	0.35392016	0.008741828	0.008741828	0.008741828	0.008741828	
	Failure rate (*f/yr.*) Cooling	0.7245	0.3219678	0.007952605	0.007952605	0.007952605	0.007952605	
	Risk level	0.975336068	0.671012285	0.022672828	0.022672828	0.022672828	0.022672828	0.022672828
119	Contribution %	75%	75%	100%	0%	0%	0%	
	Failure rate (*f/yr.*)	0.47924016	0.212974327	0.005260466	0.005260466	0.005260466	0.005260466	
	Failure rate (*f/yr.*) Heating	0.7964	0.35392016	0.008741828	0.008741828	0.008741828	0.008741828	
	Failure rate (*f/yr.*) Cooling	0.7245	0.3219678	0.007952605	0.007952605	0.007952605	0.007952605	
	Risk level	0.970789643	0.655233224	0.021797923	0.021797923	0.021797923	0.021797923	0.021797923
120	Contribution %	100%	75%	100%	0%	0%	0%	
	Failure rate (*f/yr.*)	0.39818688	0.176954249	0.00437077	0.00437077	0.00437077	0.00437077	

	Failure rate (*f/yr.*) Heating	0.7964	0.35392016	0.008741828	0.008741828	0.008741828	0.008741828	
	Failure rate (*f/yr.*) Cooling	0.7245	0.3219678	0.007952605	0.007952605	0.007952605	0.007952605	
	Risk level	0.966243219	0.639454163	0.020923019	0.020923019	0.020923019	0.020923019	0.020923019
121	Contribution %	0%	100%	100%	0%	0%	0%	
	Failure rate (*f/yr.*)	0.7224	0.18724608	0.004624978	0.004624978	0.004624978	0.004624978	
	Failure rate (*f/yr.*) Heating	0.7964	0.20642688	0.005098744	0.005098744	0.005098744	0.005098744	
	Failure rate (*f/yr.*) Cooling	0.7245	0.1877904	0.004638423	0.004638423	0.004638423	0.004638423	
	Risk level	0.984428916	0.476141325	0.01429357	0.01429357	0.01429357	0.01429357	0.01429357
122	Contribution %	25%	100%	100%	0%	0%	0%	
	Failure rate (*f/yr.*)	0.64134672	0.16623707	0.004106056	0.004106056	0.004106056	0.004106056	
	Failure rate (*f/yr.*) Heating	0.7964	0.20642688	0.005098744	0.005098744	0.005098744	0.005098744	
	Failure rate (*f/yr.*) Cooling	0.7245	0.1877904	0.004638423	0.004638423	0.004638423	0.004638423	
	Risk level	0.979882492	0.462600016	0.013779688	0.013779688	0.013779688	0.013779688	0.013779688
123	Contribution %	50%	100%	100%	0%	0%	0%	
	Failure rate (*f/yr.*)	0.56029344	0.14522806	0.003587133	0.003587133	0.003587133	0.003587133	
	Failure rate (*f/yr.*) Heating	0.7964	0.20642688	0.005098744	0.005098744	0.005098744	0.005098744	
	Failure rate (*f/yr.*) Cooling	0.7245	0.1877904	0.004638423	0.004638423	0.004638423	0.004638423	
	Risk level	0.975336068	0.449058706	0.013265806	0.013265806	0.013265806	0.013265806	0.013265806
124	Contribution %	75%	100%	100%	0%	0%	0%	
	Failure rate (*f/yr.*)	0.47924016	0.124219049	0.003068211	0.003068211	0.003068211	0.003068211	
	Failure rate (*f/yr.*) Heating	0.7964	0.20642688	0.005098744	0.005098744	0.005098744	0.005098744	
	Failure rate (*f/yr.*) Cooling	0.7245	0.1877904	0.004638423	0.004638423	0.004638423	0.004638423	
	Risk level	0.970789643	0.435517397	0.012751924	0.012751924	0.012751924	0.012751924	0.012751924
125	Contribution %	100%	100%	100%	0%	0%	0%	
	Failure rate (*f/yr.*)	0.39818688	0.103210039	0.002549288	0.002549288	0.002549288	0.002549288	

	Failure rate (*f/yr.*) Heating	0.7964	0.20642688	0.005098744	0.005098744	0.005098744	0.005098744	
	Failure rate (*f/yr.*) Cooling	0.7245	0.1877904	0.004638423	0.004638423	0.004638423	0.004638423	
	Risk level	0.966243219	0.421976088	0.012238042	0.012238042	0.012238042	0.012238042	0.012238042
126	Contribution %	0%	0%	0%	25%	0%	0%	
	Failure rate (*f/yr.*)	0.7224	0.7224	0.7224	0.56730072	0.56730072	0.56730072	
	Failure rate (*f/yr.*) Heating	0.7964	0.7964	0.7964	0.62541292	0.62541292	0.62541292	
	Failure rate (*f/yr.*) Cooling	0.7245	0.7245	0.7245	0.56894985	0.56894985	0.56894985	
	Risk level	0.984428916	0.984428916	0.984428916	0.930133857	0.930133857	0.930133857	0.930133857
127	Contribution %	25%	0%	0%	25%	0%	0%	
	Failure rate (*f/yr.*)	0.64134672	0.64134672	0.64134672	0.503649579	0.503649579	0.503649579	
	Failure rate (*f/yr.*) Heating	0.7964	0.7964	0.7964	0.62541292	0.62541292	0.62541292	
	Failure rate (*f/yr.*) Cooling	0.7245	0.7245	0.7245	0.56894985	0.56894985	0.56894985	
	Risk level	0.979882492	0.979882492	0.979882492	0.919856374	0.919856374	0.919856374	0.919856374
128	Contribution %	50%	0%	0%	25%	0%	0%	
	Failure rate (*f/yr.*)	0.56029344	0.56029344	0.56029344	0.439998438	0.439998438	0.439998438	
	Failure rate (*f/yr.*) Heating	0.7964	0.7964	0.7964	0.62541292	0.62541292	0.62541292	
	Failure rate (*f/yr.*) Cooling	0.7245	0.7245	0.7245	0.56894985	0.56894985	0.56894985	
	Risk level	0.975336068	0.975336068	0.975336068	0.90957889	0.90957889	0.90957889	0.90957889
129	Contribution %	75%	0%	0%	25%	0%	0%	
	Failure rate (*f/yr.*)	0.47924016	0.47924016	0.47924016	0.376347298	0.376347298	0.376347298	
	Failure rate (*f/yr.*) Heating	0.7964	0.7964	0.7964	0.62541292	0.62541292	0.62541292	
	Failure rate (*f/yr.*) Cooling	0.7245	0.7245	0.7245	0.56894985	0.56894985	0.56894985	
	RISK LEVEL	0.970789643	0.970789643	0.970789643	0.899301407	0.899301407	0.899301407	0.899301407
130	Contribution %	100%	0%	0%	25%	0%	0%	
	Failure rate (*f/yr.*)	0.39818688	0.39818688	0.39818688	0.312696157	0.312696157	0.312696157	

	Failure rate (*f/yr.*) Heating	0.7964	0.7964	0.7964	0.62541292	0.62541292	0.62541292	
	Failure rate (*f/yr.*) Cooling	0.7245	0.7245	0.7245	0.56894985	0.56894985	0.56894985	
	RISK LEVEL	0.966243219	0.966243219	0.966243219	0.889023923	0.889023923	0.889023923	0.889023923
131	Contribution %	0%	25%	0%	25%	0%	0%	
	Failure rate (*f/yr.*)	0.7224	0.58861152	0.58861152	0.462236627	0.462236627	0.462236627	
	Failure rate (*f/yr.*) Heating	0.7964	0.64890672	0.64890672	0.509586447	0.509586447	0.509586447	
	Failure rate (*f/yr.*) Cooling	0.7245	0.5903226	0.5903226	0.463580338	0.463580338	0.463580338	
	RISK LEVEL	0.984428916	0.940827945	0.940827945	0.858531949	0.858531949	0.858531949	0.858531949
132	Contribution %	25%	25%	0%	25%	0%	0%	
	Failure rate (*f/yr.*)	0.64134672	0.522569307	0.522569307	0.410373677	0.410373677	0.410373677	
	Failure rate (*f/yr.*) Heating	0.7964	0.64890672	0.64890672	0.509586447	0.509586447	0.509586447	
	Failure rate (*f/yr.*) Cooling	0.7245	0.5903226	0.5903226	0.463580338	0.463580338	0.463580338	
	RISK LEVEL	0.979882492	0.931328765	0.931328765	0.844888494	0.844888494	0.844888494	0.844888494
133	Contribution %	50%	25%	0%	25%	0%	0%	
	Failure rate (*f/yr.*)	0.56029344	0.456527095	0.456527095	0.358510728	0.358510728	0.358510728	
	Failure rate (*f/yr.*) Heating	0.7964	0.64890672	0.64890672	0.509586447	0.509586447	0.509586447	
	Failure rate (*f/yr.*) Cooling	0.7245	0.5903226	0.5903226	0.463580338	0.463580338	0.463580338	
	RISK LEVEL	0.975336068	0.921829584	0.921829584	0.831245039	0.831245039	0.831245039	0.831245039
134	Contribution %	75%	25%	0%	25%	0%	0%	
	Failure rate (*f/yr.*)	0.47924016	0.390484882	0.390484882	0.306647778	0.306647778	0.306647778	
	Failure rate (*f/yr.*) Heating	0.7964	0.64890672	0.64890672	0.509586447	0.509586447	0.509586447	
	Failure rate (*f/yr.*) Cooling	0.7245	0.5903226	0.5903226	0.463580338	0.463580338	0.463580338	
	RISK LEVEL	0.970789643	0.912330404	0.912330404	0.817601584	0.817601584	0.817601584	0.817601584
135	Contribution %	100%	25%	0%	25%	0%	0%	
	Failure rate (*f/yr.*)	0.39818688	0.32444267	0.32444267	0.254784829	0.254784829	0.254784829	

	Failure rate (*f/yr.*) Heating	0.7964	0.64890672	0.64890672	0.509586447	0.509586447	0.509586447	
	Failure rate (*f/yr.*) Cooling	0.7245	0.5903226	0.5903226	0.463580338	0.463580338	0.463580338	
	RISK LEVEL	0.966243219	0.902831224	0.902831224	0.803958129	0.803958129	0.803958129	0.803958129
136	Contribution %	0%	50%	0%	25%	0%	0%	
	Failure rate (*f/yr.*)	0.7224	0.45482304	0.45482304	0.357172533	0.357172533	0.357172533	
	Failure rate (*f/yr.*) Heating	0.7964	0.50141344	0.50141344	0.393759974	0.393759974	0.393759974	
	Failure rate (*f/yr.*) Cooling	0.7245	0.4561452	0.4561452	0.358210826	0.358210826	0.358210826	
	RISK LEVEL	0.984428916	0.852170528	0.852170528	0.749889791	0.749889791	0.749889791	0.749889791
137	Contribution %	25%	50%	0%	25%	0%	0%	
	Failure rate (*f/yr.*)	0.64134672	0.403791895	0.403791895	0.317097775	0.317097775	0.317097775	
	Failure rate (*f/yr.*) Heating	0.7964	0.50141344	0.50141344	0.393759974	0.393759974	0.393759974	
	Failure rate (*f/yr.*) Cooling	0.7245	0.4561452	0.4561452	0.358210826	0.358210826	0.358210826	
	RISK LEVEL	0.979882492	0.838332989	0.838332989	0.734297573	0.734297573	0.734297573	0.734297573
138	Contribution %	50%	50%	0%	25%	0%	0%	
	Failure rate (*f/yr.*)	0.56029344	0.35276075	0.35276075	0.277023017	0.277023017	0.277023017	
	Failure rate (*f/yr.*) Heating	0.7964	0.50141344	0.50141344	0.393759974	0.393759974	0.393759974	
	Failure rate (*f/yr.*) Cooling	0.7245	0.4561452	0.4561452	0.358210826	0.358210826	0.358210826	
	RISK LEVEL	0.975336068	0.82449545	0.82449545	0.718705355	0.718705355	0.718705355	0.718705355
139	Contribution %	75%	50%	0%	25%	0%	0%	
	Failure rate (*f/yr.*)	0.47924016	0.301729605	0.301729605	0.236948259	0.236948259	0.236948259	
	Failure rate (*f/yr.*) Heating	0.7964	0.50141344	0.50141344	0.393759974	0.393759974	0.393759974	
	Failure rate (*f/yr.*) Cooling	0.7245	0.4561452	0.4561452	0.358210826	0.358210826	0.358210826	
	RISK LEVEL	0.970789643	0.810657912	0.810657912	0.703113137	0.703113137	0.703113137	0.703113137
140	Contribution %	100%	50%	0%	25%	0%	0%	
	Failure rate (*f/yr.*)	0.39818688	0.25069846	0.25069846	0.1968735	0.1968735	0.1968735	

	Failure rate (*f/yr.*) Heating	0.7964	0.50141344	0.50141344	0.393759974	0.393759974	0.393759974	
	Failure rate (*f/yr.*) Cooling	0.7245	0.4561452	0.4561452	0.358210826	0.358210826	0.358210826	
	RISK LEVEL	0.966243219	0.796820373	0.796820373	0.687520918	0.687520918	0.687520918	0.687520918
141	Contribution %	0%	75%	0%	25%	0%	0%	
	Failure rate (*f/yr.*)	0.7224	0.32103456	0.32103456	0.25210844	0.25210844	0.25210844	
	Failure rate (*f/yr.*) Heating	0.7964	0.35392016	0.35392016	0.277933502	0.277933502	0.277933502	
	Failure rate (*f/yr.*) Cooling	0.7245	0.3219678	0.3219678	0.252841313	0.252841313	0.252841313	
	RISK LEVEL	0.984428916	0.702570406	0.702570406	0.596513807	0.596513807	0.596513807	0.596513807
142	Contribution %	25%	75%	0%	25%	0%	0%	
	Failure rate (*f/yr.*)	0.64134672	0.285014482	0.285014482	0.223821873	0.223821873	0.223821873	
	Failure rate (*f/yr.*) Heating	0.7964	0.35392016	0.35392016	0.277933502	0.277933502	0.277933502	
	Failure rate (*f/yr.*) Cooling	0.7245	0.3219678	0.3219678	0.252841313	0.252841313	0.252841313	
	RISK LEVEL	0.979882492	0.686791345	0.686791345	0.581253254	0.581253254	0.581253254	0.581253254
143	Contribution %	50%	75%	0%	25%	0%	0%	
	Failure rate (*f/yr.*)	0.56029344	0.248994405	0.248994405	0.195535306	0.195535306	0.195535306	
	Failure rate (*f/yr.*) Heating	0.7964	0.35392016	0.35392016	0.277933502	0.277933502	0.277933502	
	Failure rate (*f/yr.*) Cooling	0.7245	0.3219678	0.3219678	0.252841313	0.252841313	0.252841313	
	RISK LEVEL	0.975336068	0.671012285	0.671012285	0.5659927	0.5659927	0.5659927	0.5659927
144	Contribution %	75%	75%	0%	25%	0%	0%	
	Failure rate (*f/yr.*)	0.47924016	0.212974327	0.212974327	0.167248739	0.167248739	0.167248739	
	Failure rate (*f/yr.*) Heating	0.7964	0.35392016	0.35392016	0.277933502	0.277933502	0.277933502	
	Failure rate (*f/yr.*) Cooling	0.7245	0.3219678	0.3219678	0.252841313	0.252841313	0.252841313	
	RISK LEVEL	0.970789643	0.655233224	0.655233224	0.550732147	0.550732147	0.550732147	0.550732147
145	Contribution %	100%	75%	0%	25%	0%	0%	
	Failure rate (*f/yr.*)	0.39818688	0.176954249	0.176954249	0.138962172	0.138962172	0.138962172	

	Failure rate (*f/yr.*) Heating	0.7964	0.35392016	0.35392016	0.277933502	0.277933502	0.277933502	
	Failure rate (*f/yr.*) Cooling	0.7245	0.3219678	0.3219678	0.252841313	0.252841313	0.252841313	
	RISK LEVEL	0.966243219	0.639454163	0.639454163	0.535471593	0.535471593	0.535471593	0.535471593
146	Contribution %	0%	100%	0%	25%	0%	0%	
	Failure rate (*f/yr.*)	0.7224	0.18724608	0.18724608	0.147044347	0.147044347	0.147044347	
	Failure rate (*f/yr.*) Heating	0.7964	0.20642688	0.20642688	0.162107029	0.162107029	0.162107029	
	Failure rate (*f/yr.*) Cooling	0.7245	0.1877904	0.1877904	0.147471801	0.147471801	0.147471801	
	RISK LEVEL	0.984428916	0.476141325	0.476141325	0.390710418	0.390710418	0.390710418	0.390710418
147	Contribution %	25%	100%	0%	25%	0%	0%	
	Failure rate (*f/yr.*)	0.64134672	0.16623707	0.16623707	0.130545971	0.130545971	0.130545971	
	Failure rate (*f/yr.*) Heating	0.7964	0.20642688	0.20642688	0.162107029	0.162107029	0.162107029	
	Failure rate (*f/yr.*) Cooling	0.7245	0.1877904	0.1877904	0.147471801	0.147471801	0.147471801	
	RISK LEVEL	0.979882492	0.462600016	0.462600016	0.378925177	0.378925177	0.378925177	0.378925177
148	Contribution %	50%	100%	0%	25%	0%	0%	
	Failure rate (*f/yr.*)	0.56029344	0.14522806	0.14522806	0.114047595	0.114047595	0.114047595	
	Failure rate (*f/yr.*) Heating	0.7964	0.20642688	0.20642688	0.162107029	0.162107029	0.162107029	
	Failure rate (*f/yr.*) Cooling	0.7245	0.1877904	0.1877904	0.147471801	0.147471801	0.147471801	
	RISK LEVEL	0.975336068	0.449058706	0.449058706	0.367139935	0.367139935	0.367139935	0.367139935
149	Contribution %	75%	100%	0%	25%	0%	0%	
	Failure rate (*f/yr.*)	0.47924016	0.124219049	0.124219049	0.09754922	0.09754922	0.09754922	
	Failure rate (*f/yr.*) Heating	0.7964	0.20642688	0.20642688	0.162107029	0.162107029	0.162107029	
	Failure rate (*f/yr.*) Cooling	0.7245	0.1877904	0.1877904	0.147471801	0.147471801	0.147471801	
	RISK LEVEL	0.970789643	0.435517397	0.435517397	0.355354693	0.355354693	0.355354693	0.355354693
150	Contribution %	100%	100%	0%	25%	0%	0%	
	Failure rate (*f/yr.*)	0.39818688	0.103210039	0.103210039	0.081050844	0.081050844	0.081050844	

	Failure rate (*f/yr.*) Heating	0.7964	0.20642688	0.20642688	0.162107029	0.162107029	0.162107029	
	Failure rate (*f/yr.*) Cooling	0.7245	0.1877904	0.1877904	0.147471801	0.147471801	0.147471801	
	RISK LEVEL	0.966243219	0.421976088	0.421976088	0.343569452	0.343569452	0.343569452	0.343569452
151	Contribution %	0%	0%	25%	25%	0%	0%	
	Failure rate (*f/yr.*)	0.7224	0.7224	0.54626082	0.428978622	0.428978622	0.428978622	
	Failure rate (*f/yr.*) Heating	0.7964	0.7964	0.60221777	0.472921615	0.472921615	0.472921615	
	Failure rate (*f/yr.*) Cooling	0.7245	0.7245	0.547848788	0.430225653	0.430225653	0.430225653	
	RISK LEVEL	0.984428916	0.984428916	0.918391507	0.828513291	0.828513291	0.828513291	0.828513291
152	Contribution %	25%	0%	25%	25%	0%	0%	
	Failure rate (*f/yr.*)	0.64134672	0.64134672	0.484970356	0.380847221	0.380847221	0.380847221	
	Failure rate (*f/yr.*) Heating	0.7964	0.7964	0.60221777	0.472921615	0.472921615	0.472921615	
	Failure rate (*f/yr.*) Cooling	0.7245	0.7245	0.547848788	0.430225653	0.430225653	0.430225653	
	RISK LEVEL	0.979882492	0.979882492	0.907367944	0.814058673	0.814058673	0.814058673	0.814058673
153	Contribution %	50%	0%	25%	25%	0%	0%	
	Failure rate (*f/yr.*)	0.56029344	0.56029344	0.423679892	0.332715819	0.332715819	0.332715819	
	Failure rate (*f/yr.*) Heating	0.7964	0.7964	0.60221777	0.472921615	0.472921615	0.472921615	
	Failure rate (*f/yr.*) Cooling	0.7245	0.7245	0.547848788	0.430225653	0.430225653	0.430225653	
	RISK LEVEL	0.975336068	0.975336068	0.896344381	0.799604056	0.799604056	0.799604056	0.799604056
154	Contribution %	75%	0%	25%	25%	0%	0%	
	Failure rate (*f/yr.*)	0.47924016	0.47924016	0.362389428	0.284584418	0.284584418	0.284584418	
	Failure rate (*f/yr.*) Heating	0.7964	0.7964	0.60221777	0.472921615	0.472921615	0.472921615	
	Failure rate (*f/yr.*) Cooling	0.7245	0.7245	0.547848788	0.430225653	0.430225653	0.430225653	
	RISK LEVEL	0.970789643	0.970789643	0.885320818	0.785149438	0.785149438	0.785149438	0.785149438
155	Contribution %	100%	0%	25%	25%	0%	0%	
	Failure rate (*f/yr.*)	0.39818688	0.39818688	0.301098964	0.236453016	0.236453016	0.236453016	

	Failure rate (*f/yr.*) Heating	0.7964	0.7964	0.60221777	0.472921615	0.472921615	0.472921615	
	Failure rate (*f/yr.*) Cooling	0.7245	0.7245	0.547848788	0.430225653	0.430225653	0.430225653	
	RISK LEVEL	0.966243219	0.966243219	0.874297255	0.77069482	0.77069482	0.77069482	0.77069482
156	Contribution %	0%	25%	25%	25%	0%	0%	
	Failure rate (*f/yr.*)	0.7224	0.58861152	0.445093316	0.349531781	0.349531781	0.349531781	
	Failure rate (*f/yr.*) Heating	0.7964	0.64890672	0.490687039	0.385336532	0.385336532	0.385336532	
	Failure rate (*f/yr.*) Cooling	0.7245	0.5903226	0.446387192	0.350547862	0.350547862	0.350547862	
	RISK LEVEL	0.984428916	0.940827945	0.843537303	0.740336662	0.740336662	0.740336662	0.740336662
157	Contribution %	25%	25%	25%	25%	0%	0%	
	Failure rate (*f/yr.*)	0.64134672	0.522569307	0.395153846	0.310314315	0.310314315	0.310314315	
	Failure rate (*f/yr.*) Heating	0.7964	0.64890672	0.490687039	0.385336532	0.385336532	0.385336532	
	Failure rate (*f/yr.*) Cooling	0.7245	0.5903226	0.446387192	0.350547862	0.350547862	0.350547862	
	RISK LEVEL	0.979882492	0.931328765	0.829456261	0.724681265	0.724681265	0.724681265	0.724681265

Appendix III Data Validation

The Environment pollution parameters shown in ***Table 7-2*** and

Table 7-3 were calculated using the following steps:

The total energy demand for one week in summer is 8,341.43 MWh

1- The total CO_2 pollution in case of the source of energy is the utility 8,341.43*865= 7,215.34 Ton CO_2
2- The RES energy production is 283.5231 MWh with zero emission of CO_2 subsequently the total CO_2 pollution will be reduced to 8,057.91*865+283.5231*0= 6,970.1 Ton CO_2
3- The GT Co-gen. energy production is (5,819.0026 + 1,010.762) MWh and the CO_2 emission is 570 kg/MWh. Therefore, the total CO_2 emission is: Utility emission + RES emission + Co-gen. emission = 1,228.15*865+283.5231*0+6,829.76*570= 4,955.3 Ton CO_2
4- The GT Co-gen. energy production is (5,819.0026 + 310.762) MWh and the CO_2 emission is 570 kg/MWh. Therefore, the total CO_2 emission is: Utility emission + RES emission + Co-gen. emission = 1,228.15*865+283.5231*0+6,129.76*570= 4,556.3 Ton CO_2
5- The GT Co-gen. energy production reduced to 5,819.0026 MWh and the CO_2 emission is 570 kg/MWh. Therefore, the total CO_2 emission is: Utility emission + RES emission + Co-gen, emission = 5.99*865+283.5231*0+5,819.0026*570= 3,322.0 Ton CO_2
6- The FC Co-gen. energy production is (5,819.0026 + 1,010.762) MWh and the CO_2 emission is 513 kg/MWh. Therefore, the total CO_2 emission is: Utility emission + RES emission + Co-gen, emission = 1,228.15*865+283.5231*0+6,829.76*513= 4,566.0 Ton CO_2
7- The FC Co-gen. energy production reduced to 5,819.0026 MWh and the CO_2 emission is 513 kg/MWh. Therefore, the total CO_2 emission is: Utility emission + RES emission + Co-gen, emission = 5.99*865+283.5231*0+5,819.0026*513= 2,990.3 Ton CO_2

8- Operation price for GT: 5,819.0026 MWh *10+x=132,710 CAD$, the operation cost is 10CAD/MWh, x=74,520

   Operation price for FC: 5,819.0026 MWh *10*(0.03/0.0275) +74,520= 183,000 CAD$

   Operation price for MT: 5,819.0026 MWh *10*(0.016/0.0275) +74,520= 108,380 CAD$

   Operation price for DE: 5,819.0026 MWh *10*(0.055/0.0275) +74,520= 190,900 CAD$

9- The MT Co-gen. energy production is (5,819.0026 + 1,010.762) MWh and the CO_2 emission is 700 kg/MWh. Therefore the total CO_2 emission is: Utility emission + RES emission + Co-gen, emission = 1,228.15*865+283.5231*0+6,829.76*700= 5,843.2 Ton CO_2

10- The MT Co-gen. energy production reduced to 5,819.0026 MWh and the CO_2 emission is 700 kg/MWh. Therefore, the total CO_2 emission is: Utility emission + RES emission + Co-gen, emission = 5.99*865+283.5231*0+5,819.0026*700= 4,078.5 Ton CO_2

11- The DE Co-gen. energy production increased to (5,819.0026 + 1,010.762) MWh and the CO_2 emission is 657 kg/MWh. Therefore, the total CO_2 emission is: Utility emission (for heat and electricity generation) + RES emission + Co-gen, emission = 1,228.15*865+283.5231*0+6,829.76*657= 5,549.5 Ton CO_2

12- The DE Co-gen. energy production reduced to 5,819.0026 MWh and the CO_2 emission is 657 kg/MWh. Therefore, the total CO_2 emission is: Utility emission + RES emission + Co-gen, emission = 5.99*865+283.5231*0+5,819.0026*657= 3,828.3 Ton CO_2